UNDERSTANDING THE IMPACT OF REACTION PARAMETERS ON MACROMOLECULAR STRUCTURE, AND THE BINDING AND TRANSPORT PROPERTIES OF IMPRINTED CROSSLINKED POLYMERS

by

Vishal D. Salian

A dissertation submitted to the Graduate Faculty of
Auburn University
in partial fulfillment of the
requirements for the Degree of
Doctor of Philosophy

Auburn, Alabama
May 7, 2012

Keywords: living radical polymerization, molecular imprinting, controlled drug delivery, polymer hydrogels, recognitive polymers, iniferter mediated polymerization

Approved by

Dr. Mark E. Byrne, Chair, Daniel F. & Josephine Breeden Associate Professor of Chemical Engineering
Dr. Christopher B. Roberts, Uthlaut Professor of Chemical Engineering
Dr. Ram B. Gupta, Walt & Virginia Woltosz Professor of Chemical Engineering
Dr. Edward W. Davis, Lecturer of Polymer and Fiber Engineering

ABSTRACT

Molecular imprinting is the design and synthesis of polymer networks that can recognize a template molecule and bind it preferentially in solution. Selective binding of template combined with stability and cost effectiveness make them attractive for a wide variety of applications. In this work, molecularly imprinted, crosslinked poly(methacrylic acid-co-ethylene glycol dimethacrylate) or poly(MAA-co-EGDMA) and poly(hydroxyethyl methacrylate-co-diethylaminoethyl methacrylate-co-poly(ethyleneglycol200) dimethacrylate) or poly(HEMA-co-DEAEM-co-PEG200DMA) networks were synthesized and characterized to better understand the effect of various reaction parameters on their macromolecular structure and subsequently their binding and transport properties. Conventional free radical polymerization (FRP) as well as iniferter mediated living radical polymerization (LRP) was used for polymer synthesis.

LRP offers the ability to create improved imprinted polymers with more homogeneous networks and, as a result, better binding parameters. The use of LRP resulted in quadrupling of the number of binding sites in highly crosslinked imprinted poly(MAA-co-EGDMA) polymers; and a tripling of the number of binding sites in weakly crosslinked imprinted poly(MAA-co-EGDMA) gels. Analysis of the polymerization reaction revealed that the observed increase in binding parameters of the polymers could be explained by the extension of the reaction-controlled regime during propagation. LRP was shown to have extended propagation in polymerization reactions which subsequently resulted in more monodisperse polymer chains and more homogenous imprinted polymer networks with better template binding characteristics.

Weakly crosslinked poly(HEMA-co-DEAEM-co-PEG200DMA) gels imprinted with diclofenac sodium, an anti-inflammatory drug, and prepared via LRP demonstrated significantly higher drug binding as well as slower drug release rates as compared to corresponding gels prepared via FRP. In addition, the effects of varying reaction parameters, such as, template concentration, functional monomer concentration, presence of solvent, and degree and length of crosslinking, on the template binding and transport properties of the imprinted polymer gels was examined. Varying the reaction parameters had diverse effects on the polymer properties. For example, an increase in template concentration was shown to result in increased template binding and slower template release rates while an increase in the degree of crosslinking resulted in decreased template binding and template release rates. It was also shown that the use of LRP had a more significant impact than any other reaction parameter. Finally, the use of LRP in the formation of molecularly imprinted polymers was shown to result in significant improvements in the template binding and transport properties of the resulting polymers due to the improved network architecture of the molecularly imprinted polymers. In addition the ability to create imprinted polymer gels with high drug binding capacity and extended, tailorable and controlled drug release by combining LRP with variations in other reaction parameters was demonstrated.

ACKNOWLEDGEMENTS

At the outset, I want to thank my advisor, Dr. Mark Byrne for allowing me the opportunity to pursue my doctoral research work under his auspices as well as being a source of knowledge, encouragement and inspiration. I especially want to thank him for pushing me to excel and for believing in me when I found it difficult to do so myself. I also want to extend my heartfelt gratitude to my committee, Dr. Christopher Roberts, Dr. Ram Gupta, Dr. Edward Davis, and my outside reader, Dr. Jacek Wower, for their extraordinary patience and support. I would also like to acknowledge the support of the National Science Foundation in funding this research via a grant (NSF-CBET-0730903, Grant G00003191).

I would like to thank all the members of the Byrne Group that I have had the pleasure of working alongside as well as others who preceded me, Dr. Siddarth Venkatesh, Matthew Eggert, Amanda Paine, Matthew McBride, Kayla Pate, James Kacsmarek, Daniel Pulliam and Dr. Asa Vaughan, for his work which provided a basis for my own doctoral research. I especially want to thank Arianna Tieppo, Charles White and Padma Priya Mohana Sundaram for making labwork a joy. I will miss the camaraderie and the banter. I would also like to thank Urvi Kothari and Amogh Karwa for their friendship, laughter and for being my support structure in Auburn.

Finally, I want to thank my parents, Lajvanti and Damodar Salian. I cannot possibly thank you enough for all the sacrifices you have made to allow me to be in this position. This is as much your achievement as it is mine and this work is dedicated to you. Lastly, I want to thank my brother Purvang for being the ideal kid brother.

TABLE OF CONTENTS

LIST OF TABLES

LIST OF FIGURES

LIST OF ABBREVIATIONS

DEAEM	Diethylaminoethyl methacrylate
DI	Deionized (water)
DS	Diclofenac sodium
EA9A	Ethyl adenine-9-acetate
EGDMA	Ethylene glycol dimethacrylate
FRP	Conventional free radical polymerization
HEMA	2-hydroxyethyl methacrylate
LRP	Living radical polymerization
MAA	Methacrylic acid
MIP	Molecularly imprinted polymers
PEG	Poly(ethylene glycol)
PEG200DMA	Poly(ethylene glycol(200)dimethacrylate)
PEG400DMA	Poly(ethylene glycol(400)dimethacrylate)
RAFT	Reversible addition-fragmentation chain transfer reaction

CHAPTER 1: INTRODUCTION

Molecular imprinting is the creation of macromolecular memory in a polymer for a template molecule. A wide range of molecules can serve as templates, including nucleosides, analgesics, pesticides, carbohydrates, and steroids [1-3]. Molecularly imprinting is known for its synthetic efficiency and versatility [4]. Additionally, molecularly imprinted polymers (MIP) are more stable than biological receptors which are sensitive to changes in their environment and can be easily deactivated [5-7]. Selective binding of template molecules combined with stability and cost effectiveness make MIPs attractive for many analytical applications, including catalysis, sensing, solid-phase extraction, chromatography, and binding assays [8-11]. A relatively new area of application of MIPs is in the field of drug delivery. The potential for enhanced drug loading and controlled drug release from polymeric materials makes them ideal for drug delivery applications [12-14].

1.1 Motivation and Significance of Synthesizing Molecularly Imprinted Polymers via Living Radical Polymerization

Despite the many attractive attributes of MIPs, wide use of these materials has not been realized. This is primarily because of deficiencies in their binding properties. MIPs, in general, have low average binding affinities and a high degree of binding site heterogeneity. Improvement in template binding combined with decreased binding site heterogeneity would make them more attractive for a variety of applications. Living polymerization techniques offer the ability to create better polymer networks with more homogeneous network structures [15-16]

and, as a result, better binding parameters [17-22]. In addition, using living radical polymerization can lead to more control over network structures and a better understanding of their structure-property relationships; however, these reactions are relatively new to the imprinting field and have not been used extensively in molecular imprinting. This work demonstrates the potential of MIPs prepared via living radical polymerization, specifically in the field of drug delivery, by analyzing the impact of living radical polymerization on the network morphology of imprinted polymer networks. This knowledge is then used to achieve better control over the drug binding and transport properties of imprinted polymers prepared via living radical polymerization by adjusting specific reaction parameters. Chapter 2 offers an overview of molecularly imprinted polymers and their current applications as well as potential applications that could be developed in the future. Chapter 3 gives a detailed description for characterizing the structure as well as template binding and transport properties of imprinted polymer gels. Chapter 4 describes the use of living polymerization techniques to control the network morphology of crosslinked polymer networks. It also describes the impact of other non-reacting molecules (solvents, salts, template molecules) on the formation of the polymer network. Chapter 5 analyzes the effect of living radical polymerization on the network morphology of molecularly imprinted polymer networks with varying extents of crosslinking, and the subsequent impact on their template binding properties. Chapter 6 describes methods to enhance loading and control release of diclofenac sodium, an anti-inflammatory drug, from a weakly crosslinked imprinted polymer gel prepared via LRP by varying the strength and degree of non-covalent, ionic interaction between a drug molecule and the polymer chains froming the imprinted network. Chapter 7 describes the effect of variation in length and extent of

crosslinking monomers on network morphology, drug loading, and drug release from MIPs prepared via LRP.

A thorough understanding of the complex and interrelated effects of combining LRP with a variation of specific reaction parameters on the network structure of the imprinted polymers formed should lead to the rational design of imprinted polymer networks for not just drug delivery but for a wide variety of other applications.

1.2 References

1. Byrne ME, Park K, Peppas NA. Molecular imprinting within hydrogels. Adv. Drug Deliv. Rev. 2002, 54, 149-161.
2. Ye L, Mosbach K. Molecular imprinting: Synthetic materials as substitutes for biological antibodies and receptors. Chem. Mater. 2008, 20, 859-868.
3. Wulff G. Enzyme-like catalysis by molecularly imprinted polymers. Chem. Rev. 2002, 102, 1-27.
4. Ekberg B, Mosbach K. Molecular Imprinting: A Technique for producing Specific Separation Materials. Trends in Biotechnology. 1989, 7, 92-96.
5. Sellergren B. Noncovalent Molecular Imprinting: Antibody-like Molecular Recognition in Polymeric Network Materials. TrAC Trends in Analytical Chemistry. 1997, 16, 6, 310-320.
6. Wulff G. Molecular Imprinting in Cross-Linked Materials with the Aid of Molecular Templates - A Way towards Artificial Antibodies. Angewandte Chemie International Edition in English. 1995, 34, 17, 1812-1832.
7. Hedin-Dahlstrom J, Rosengren-Holmberg J P, Legrand S, Wikman S, Nicholls IA. A Class II Aldolase Mimic J. Org. Chem. 2006, 71, 13, 4845-4853.
8. Maier NM, Lindner W. Chiral recognition applications of molecularly imprinted polymers: a critical review. Anal. Bioanal. Chem. 2007, 389, 377-397.
9. Haupt K, Mosbach K. Molecularly imprinted polymers and their use in biomimetic sensors. Chemical review. 2000, 100, 2495-2504.
10. He Q, Chang X, Wu Q, Huang X, Hu Z, Zhai Y. Synthesis and Applications of Surface-grafted Th(IV)-imprinted Polymers for Selective Solid-phase Extraction of Thorium(IV). Analytica Chimica Acta. 2007, 605, 2, 192-197.

11. Davis ME, Katz A, Ahmad WR. Rational catalyst design via imprinted nanostructured materials. Chem. Mater. 1996, 8, 1820-1839.
12. Hilt JZ, Byrne ME. Configurational Biomimesis in Drug delivery: Molecular Imprinting of Biologically Significant Molecules. Advanced Drug Delivery Reviews. 2004, 56, 11, 1599-1620.
13. Byrne ME, Salian V. Molecular imprinting within hydrogels. II. Progress and analysis of the field. Int. J. Pharm. 2008, 364, 188–212.
14. . Byrne ME, Hilt JZ, Peppas NA. Recognitive biomimetic networks with moiety imprinting for intelligent drug delivery. J. Biomed. Mater. Res., Part A. 2008, 84A, 137-147.
15. Anandkumar KR, Anderson KJ, Anseth JW, Bowman CN. Use of "living" radical polymerizations to study the structural evolution and properties of highly crosslinked polymer networks. J. Polym. Sci., Part B: Polym. Phys. 1997, 35, 2297 -2307.
16. Anandkumar KR, Anseth JW, Bowman CN. A study of the evolution of mechanical properties and structural heterogeneity of polymer networks formed by photopolymerizations of multifunctional (meth)acrylates. Polymer. 1998, 39, 12, 2507-2513.
17. Boonpangrak S, Whitcombe MJ, Prachayasittikul V, Mosbach K, Ye L. Preparation of molecularly imprinted polymers using nitroxide-mediated living radical polymerization. Biosens Bioelectron. 2006, 22, 349–354.
18. Vaughan AD, Byrne ME. Optimizing recognition characteristics of biomimetic polymer gels via polymerization reaction and crosslinking density analysis. ACS PMSE Preprints. 2006, 94, 762–763.

19. Vaughan AD, Sizemore SP, Byrne ME. Enhancing molecularly imprinted polymer binding properties via living radical polymerization and reaction analysis. Polymer. 2007, 48, 74-81.
20. Vaughan AD, Zhang JB, Byrne ME. Enhancing Therapeutic Loading and Delaying Transport via Molecular Imprinting and Living/Controlled Polymerization. AIChE Journal. 2010, 56, 1, 268-279.
21. Pan G, Zu B, Guo X, Zhang Y, Li C, Zhang H. Preparation of molecularly imprinted polymer microspheres via reversible addition–fragmentation chain transfer precipitation polymerization. Polymer. 2009, 50, 2819–2825.
22. Pan G, Zhang Y, Guo X, Li C, Zhang H. An efficient approach to obtaining water-compatible and stimuli-responsive molecularly imprinted polymers by the facile surface-grafting of functional polymer brushes via RAFT polymerization. Biosens Bioelectron. 2010, 26, 3, 976-982.

CHAPTER 2: OVERVIEW OF MOLECULARLY IMPRINTED POLYMERS AND APPLICATIONS

The concept of molecular imprinting involves the creation of macromolecular memory for a template molecule within a polymer network. There have been many excellent reviews on the topic and we direct the reader to more traditional imprinting strategy reviews [1-8], and reviews focusing on imprinting biological molecules, therapeutics, proteins, macromolecules, and cells [9-18]. Most important to the non-covalent technique is the inclusion of a template molecule that the polymer must form around that is not covalently incorporated in the polymeric structure. Effective self-assembly of the functional monomer(s)-template complex is crucial toward imprinting efficacy. Macromolecular memory is primarily due to two synergistic effects: (i) shape specific cavities that match the template molecule, which provide stabilization of the chemistry in a crosslinked matrix, and (ii) chemical groups oriented to form multiple non-covalent complexation points with the template (Figure 2.1 A). Since gel structures can have significant flexibility in the polymer chains as well as collapsible and expansive structures, it is very suitable to use the term macromolecular memory or structural plasticity of polymer chains when describing molecular imprinting in gels. This term is much more appropriate in weakly crosslinked imprinted networks as compared to highly crosslinked networks.

The majority of imprinted polymers produced to date have been highly crosslinked in efforts to limit the flexibility of the associated binding cavities produced between polymer chains. Thus, the idea of the technique translating to polymeric networks with significant flexibility within

their polymer chains was highly suspect. It was assumed that flexibility of polymeric chains would lead to fatal deficiencies in the metrics by which imprinted structures are defined, namely template binding affinity, capacity, and selectivity. However, experimental work in the last decade has proven that this is not the case [19-31]. A certain degree of flexibility can also be seen in nature, where recognition occurs in a polar, protic, aqueous environment due to a diverse group of multiple non-covalent interactions. In most cases, biomolecular recognition, as exhibited by biological macromolecular structures, involves (i) a highly specific recognition event where strong non-covalent bonding is due to the structural orientation of multiple differing chemical functional groups, complementarity, and configuration; and (ii) a recognition event where recognition is usually a constitutive element of a complex functional mechanism that involves the conformational reorganization or flexibility of macromolecular counterparts [32-35]. Examples of the functional roles of flexibility in protein systems are induced fit mechanisms and regulation of enzyme activity via allosteric mechanisms, in which a molecule binds to a regulation site and subsequent reorganization results in controlled substrate binding at the substrate site. It can also include coupling of protein function by flexible linkage of domains (e.g., immunoglobulins can functionally adapt to the variation of antigenic sites on surfaces) [33]. Therefore, it is highly probable that the most specific recognition in nature occurs through the ordering of structures that have certain degrees of flexibility.

Much of the theoretical basis of the conformational memory of biological macromolecules and designed heteropolymers [32-43] can be applied to the concept of molecular imprinting. Macromolecular memory is favored by heteropolymer systems. Typically, one type of functional monomer will not provide optimal interactions between the polymer chains and the template (i.e., depending on the chemistry of the template molecule, each functional monomer will have

preferred and more energetically favorable interactions with certain chemical groups on the template). Imprinting can organize the incorporation of monomers within the growing polymer chains in a low energy state conformation that favors multiple point complexation with the template. During network formation, increasing the potential for growing polymer chains with template binding complexes to reach a global energy minimum will lead to increased memorization of the chain conformation and enhance template binding parameters in both highly and weakly crosslinked polymers. Frustrations between the template and polymer chains in forming complexes, as highlighted by Tanaka and coworkers [44-45], can be minimized by molecular imprinting.

Demchenko outlines some general principles of recognition between flexible structures, which include: (i) a reaction of complex formation which includes the diffusional formation of an encounter pair and, (ii) a sequential selection isomerization with kinetic proofreading or consecutive elementary steps of stochastic bond-making and breaking events of the encounter pair into a stable complex [32]. Systems with flexible conformations create configurational complementarity with an ordering process by many trial and error steps until the proper ligand-receptor interaction is reinforced by the ordering of short-range covalent bonds [33]. This process within the imprinting mechanism is important to produce effective macromolecular memory.

2.1 Imprinting Parameters for Polymer Networks

Successful imprinting in a polymer network depends on structural considerations and the underlying flexibility of polymer chains, limiting the expansion or collapse of polymer chains due to solvation or desolvation forces. It also depends on the number of template molecules in relation to the number of functional monomeric species, the level of diversity of functional

monomeric species that interact with the template, the strength of the monomer template interactions and the polymerization reaction.

2.1.1 Stability of Monomer-Template Complex

The strength of the monomer-template non-covalent interaction is paramount to a successful imprinting strategy. As the polymer is forming, any cross interaction between the solvent and the intended functional monomer-template non-covalent bonding will lead to decreased macromolecular memory. This depends on the strength of the intended non-covalent interactions (i.e., ionic, hydrogen bonding, hydrophobic interactions, pi-pi orbital interactions, and Van der Waals forces). For example, ionic non-covalent bonds are the strongest non-covalent bonds, with bond strengths of 5-35 kcal/mol, approaching a third of covalent bond strength [46-47]. Hydrogen bonding decreases and hydrophobic forces increase as the temperature increases. Thus, a strong interaction between functional monomer and the template is needed. Highly crosslinked imprinted polymers typically employ solvents as porogens [48], in the absence of which template diffusion out of the rigid structure of the highly crosslinked gel is severely limited. However, very high template removal can be achieved in hydrogels which have low crosslinking densities.

The relative amount of functional monomers and template is also very important to imprinting efficacy. The functional monomer to template (M/T) ratio is a major variable in effective design. There is considerable evidence of an optimal M/T ratio within highly crosslinked imprinted structures. There is also an optimum in weakly crosslinked structures, and the work of Alvarez-Lorenzo and coworkers has been noteworthy [22, 49]. In non-covalent systems, usually an excess of functional monomer is needed to push the reversible template-functional monomer interaction to the complexed state. Therefore, M/T ratios are usually much

higher than unity and are not commonly in stoichiometric amounts based on the functionality of the template. This optimum can be distinctively seen by looking at two extreme cases. At a very large M/T ratio, the memorized configuration of monomer within the polymer chains is very small compared to the randomly incorporated monomer, and there is no difference between the non-imprinted and imprinted gels. At very small M/T ratios, there are not effective multiple monomer interactions with the template, resulting in no recognition.

A diversity of functional monomers has also been demonstrated to increase binding parameters of imprinted hydrogels [19, 50]. Single non-covalent bond energies are much less than single covalent bond energies and they are slightly higher than the average kinetic energy of molecules at room temperature. Thus, many molecules almost possess sufficient kinetic energy to break their non-covalent bonds. However, when multiple non-covalent bonds exist, they produce very stable binding complexes, such as those found in proteins and receptor ligand binding pockets [46-47]. It has been demonstrated that at a fixed M/T ratio partitioning of drug into networks synthesized from multiple functional monomers (four different monomers) was 8 times greater than networks synthesized from single monomers [19]. To date, there is not much diversity in the choice of functional monomers and most synthetic gels use one or at the most two different monomeric units (not counting the crosslinking monomer) to interact with the template. Depending on the reaction and the interactions between monomers, integration of multiple monomeric species into the polymer gel is sometimes difficult to achieve.

Cross interaction and reactivity between the functional monomers must also be avoided [51]. With a cocktail of functional monomers, if they prefer to associate with each other or other monomers or are energetically more favored to have self- or other monomer-association rather than with the template, less effective recognition will occur. In many respects, this lack of

diversity and difficulties associated with the use of multiple monomers has not furthered the field.

2.1.2 Template Size, Chemical Functionality and Mobility

Just as a more diverse group of functional monomers increases imprinting effectiveness, templates with more chemical functionality and diverse chemical functionality are, in theory, easier to imprint. Of course as the size of the template increases, a determination of the hydrodynamic radius is needed to ascertain the template's ability to diffuse within the spaces between the polymer chains. Thus, the size of the template may impose structural considerations that must be reflected in the choice of crosslinking monomer size and concentration, which will affect the mesh size of the network. For example, a monomeric human growth hormone imprinted gel, which bound approximately seventy times more template than the non-imprinted gel, has been shown to bind approximately four and twenty-three times more template than the dimeric and trimeric forms, respectively [26].

Recently, moiety molecular imprinting techniques [23] have been developed for the preparation of polymer networks that can recognize a general moiety, D-glucose, and the novel evaluation of loading and release of a larger molecule with glucose as an integral part of its structure (i.e., fluorescently tagged glucose). Poly(acrylamide-co-poly(ethylene glycol)dimethacrylate) networks with varying crosslinking monomer percentages (80, 67, and 30%) and crosslinker lengths (average number of ethylene glycol units of 1, 4, and 14) were prepared and characterized using fluorescent microscopy, which allowed for micro scale observation of the dynamic binding and release within the polymer film. Experimental results indicate that tighter mesh-sized networks had increased affinity and capacity towards the glucose functionalized molecule as well as increased diffusional transport times, indicating the strong

potential to load significantly higher amounts of therapeutic within intelligent carriers as well as control and extend the rate of release via macromolecular structure.

The imprinting of hydrophobic templates in gels has not received much attention due to problems such as template/monomer mutual solubility and, if solvent is used, finding a suitable solvent to dissolve the water-soluble monomers and the hydrophobic template. These networks require the presence of hydrophilic backbone monomers since recognition will occur in aqueous solutions. Spizzirri and Peppas [52] describe a network where cholesterol, a largely hydrophobic molecule, is used as template, and mutual solubility during the polymerization is achieved by the use of two solvents of significantly differing polarity. This provides a dual benefit of countering the hydrophobicity of cholesterol as well as providing a means to make the hydrogel more porous to improve the transport of the large cholesterol molecule.

2.1.3 Controlling the Architecture of Polymer Chains

One of the most important considerations in effective template recognition is to maintain the binding cavity produced via differing polymer chains close to the state when the original imprint was formed (i.e., close to the relaxed state of the polymer). In other words, the swollen or collapsed polymer volume at equilibrium must not be too different from the relaxed polymer volume fraction. The thermodynamic compatibility of the polymer chains and solvent as well as the number of crosslinking points within the network determines the nature and extent of this transition. At a given crosslinking density in aqueous solvent, an imprinted network that contains more hydrophilic moieties along the polymer backbone will tend to swell or expand more than gels containing hydrophobic groups, which will try to minimize their exposure to aqueous solvent. The expansion of polymer chains increases the free volume available for template transport, but it can decrease the effectiveness of the imprinting site created by multiple polymer

chains. Equilibrium is reached when the swelling force is counterbalanced by the restrictive force due to crosslinking points in the network structure. In gels where significant collapse of the structure can occur (e.g. the gel is put in a thermodynamically non-compatible solvent), template transport may be significantly reduced and the binding cavity may be significantly altered in a collapsed state.

It is important to note that this does not dictate that gels prepared in the absence of solvent (in these cases, the largest monomer component is the solvent) and subsequently bind template in solvent have been unsuccessful. Typically, these systems have demonstrated higher affinity and capacity [19-22] compared to non-imprinted gels in aqueous solvents. In these cases, the largest component in the formulation was a hydrophilic monomer.

2.1.3.1 Solvent Effects

If the network is prepared in solvent, the growing polymer chains are solvated by the solvent and polymer must form around the solvent molecules. Depending on the amount of solvent in the formulation, the gel may have varying levels of porosity. Figure 2.2 highlights the classification of spaces within a hydrogel polymer. Hydrogels can be classified as macroporous, microporous, and nanoporous. As one approaches the nanoscale, the mesh size or the free-volume available between the polymer chains is reached. If this nanoporous mesh structure is in a collapsed state and the network is not formed in solvent, the polymer can be quite non-porous and significantly limit the transport of solutes. Critical point drying with transmission electron microscopy [53] and fluorescent and confocal imaging [23, 31, 54] have been used to view the imprinted nanocavities or to visualize [31] and quantify [23, 54] the template bound within the gel. Fluorescent spectroscopic methods allow the study of the local environment around the chromophore [55]. These studies offer evidence as to the size of the imprinted cavities, template

binding distribution within sections of the gel, as well as their potential within micro- and nano-biotechnology [56]. Section 3.3 presents these concepts further with discussion of structural and transport considerations of imprinted gels.

In addition, the polar and non-polar nature of the solvent has an effect upon the non-covalent bonding between the template molecule and functional monomer. A solvent with more hydrogen bonding capability has been shown to reduce the affinity and the selectivity of the recognitive polymer networks [57]. Solvents with an aprotic nature have shown results that recognitive systems made with the aprotic solvents have greater selectivity and a higher affinity [58].

2.1.3.2 Density and Flexibility of Crosslinking Points

Variations in network structure itself have been demonstrated to influence template binding and control the size of the imprinted cavities [23, 29, 52, 59-61]. Not surprisingly, crosslinking strategies have primarily included covalent crosslinks with very little work exploiting other methods. Imprinted networks linked by non-covalent interactions or permanent physical entanglements have not been explored while interpenetrating [28, 61-62] and semi-crystalline and crystalline imprinted networks [63-65] have received little attention (Figure 2.3). Typically, the low mechanical strength of gels and increased flexibility of the network can be overcome by increasing and controlling the junction points. If the junction points are reversible, binding, release, or other functions of the gel could be modulated.

For covalent crosslinks, the crosslinker length (i.e., linear size), concentration (i.e., the percent of crosslinking monomer reacted in network or degree of crosslinking), and crosslinker double bond functionality (i.e., two or more double bonds) influence imprinting effectiveness

(Figure 2.4). Covalent crosslinking can be classified by two distinct approaches, which depend on the monomer or polymer building blocks.

With additive polymerization, such as the case with free radical polymerizations, the double bond of a vinyl monomer will open and begin to build linear chains. Thus, the first approach involves a bifunctional or divinyl crosslinker being added to the growing polymer chain and serving as a bridge to link two distinctive chains (Figure 2.4A). The crosslink bridge is usually much smaller in molecular weight than the chains between two consecutive crosslinks and is sometimes represented in a similar manner as Flory, as a volume less point in respect to the rest of the polymer chains. In reality, the crosslinking structure is far from ideal and can have a number of defects, which may or may not participate in template recognition depending on the accessibility of the binding cavity and flexibility of the chains that comprise the binding cavity. The formation of primary loops, secondary loops, entanglements, and dangling ends can also occur within a crosslinked network.

The second covalent crosslinking approach is to start with oligomers or polymer chains with double bonds or suitable chemistry along the polymer chain, either along the polymer chain or branched pendant groups, that can be covalently reacted to different chains. A few groups have used this approach in imprinting, namely the use of oligomers with functional groups that complex with the template and then are covalently bonded into a growing network structure [27, 29-30, 66-73]. Recently, this has been demonstrated using a polyvinyl alcohol backbone oligomer functionalized with double bonds and pyridyl groups, which were randomly distributed with 3-5 per chain [67].

This is an exciting transition in the field, but more experimental work is needed with controlled studies that vary degrees of substitution, chain length, chain flexibility, and the diversity of functional chemistry in the chain that will interact with the template. Thus, it is expected that in the near future there will be more work creating oligomers with varying distributions of two types of chain functionality, one that promotes covalent linking into a network or onto a surface and one that non-covalently interacts with the template. This will lead to a better understanding of the imprinting process and the building of chains from monomeric units as in conventional methods, but it may also lead to more control of the imprinted network structure and lead to enhanced template binding parameters. However, this depends on efficient integration of the oligomer chain into the network structure with the binding site able to reach an energy minimum.

2.1.4 Polymerization Reaction

Since template binding properties are strongly dependent on the network structure, it is important to study the details of the reaction. For example, network structure of free radical polymerizations of multifunctional monomers depends upon monomer/macromer size, flexibility, functionality, the amount of solvent and concentration of monomers and initiators, initiation methods and initiation rate, as well as diffusional reaction constraints of propagating polymer chains. For example, monomer double bonds may possess different reactivities that are influenced by conversion (i.e., pendant double bonds typically have reduced reactivity) and significantly affect structural characteristics of the polymer network. It is in this reason why most synthetic polymers do not typically consist of a large diversity of monomers. Questions arise on the equal or equivalent incorporation of the monomers within the polymer chains. These are very real concerns and difficulties especially when imprinting to achieve well-functionalized, diverse

binding cavities. However, these issues can be overcome by proper understanding and study of monomer reactivities and reactivity ratios, the interaction between various monomers in the formulation, and the imprinting polymerization reaction itself.

The study of the imprinting polymerization reaction has been virtually unexplored and little effort has been expended in trying to understand the imprinting process on mechanistic or a basic molecular level. There have been a number of computational studies, but most groups have primarily focused on studying the pre-polymerization template-functional monomer-complex in the pre-polymerization solution [5, 74]. Only recently have researchers begun to analyze larger polymer chains and the polymerization process [75-77]. For example, a method simulating the formation of densely crosslinked networks was recently developed incorporating intra- and intermolecular interactions. An all-atom kinetic gelation simulation technique utilizing an off-lattice approach tracked the position and interaction of all atoms during imprinted polymer formation [76]. This type of work will lead to much insight into the mechanism of imprinted polymer formation.

Conventional free radical polymerization is highly non-ideal and differences in theory and experimental data indicate heterogeneity within the network structure [77]. Research work on non-imprinted structures has involved the examination of major variables that control crosslinking polymerization rate, conversions, and final cross-link density. While a lower concentration of crosslinking monomer and lower final conversion will produce less densely crosslinked networks, other factors, such as the pendant double bond reactivity which is based upon monomer size, monomer stiffness, comonomer ratio, and solvent concentration [78], significantly affect the structure and heterogeneity of the resulting polymeric network. Three types of cycles can form in a polymer network when a pendant double bond reacts with a free

radical. Typically, a pendant double bond is formed when one end of a crosslinking agent reacts in a polymer chain leaving the other reactive end dangling from the polymer chain and free to react. Primary cyclization or loops (where a radical reacts with the radical on its own propagating chain) will reduce the crosslinking density. Primary and secondary cycles or loops (where a radical reacts with the radical on secondary chain) do not contribute as crosslinks to the overall structure of the polymer (Figure 2.5). These lead to more heterogeneously crosslinked imprinted networks, which may negatively impact binding effectiveness, decrease the overall material strength, and alter template transport.

Reaction conditions such as the type of free radical initiation mechanism and the polymerization temperature have been explored, but more analysis is needed. Reactions that have controlled temperature have been demonstrated to lead to better imprinted structures and free radical, UV-initiated imprinted polymerizations have been demonstrated to lead to better binding parameters compared to thermally initiated polymerizations due to lower temperatures of polymerization [57, 79-81]. However, the benefits of reduced temperatures gained in the stability of the monomer-template complex [82] can negatively influence the structure of the network since reduced temperatures will decrease reaction rates and monomer conversion.

Imprinted polymer reaction analysis and living radical polymerization for the synthesis of imprinted polymers are other areas that have not received much attention. Recently, our group was the first to demonstrate that reaction analysis of a typical highly crosslinked poly(methacrylic acid-co-ethylene glycol dimethacrylate) molecularly imprinted network revealed low double bond conversion (35 +/- 2.3% at 0°C to 54 +/- 1.9% at 50°C) which was due to severely constrained network formation [83]. This work highlighted that the final composition of imprinted polymers does not represent the initial formulation when using significant amounts

of short bifunctional crosslinking monomer. Also, living radical polymerization with a reversible termination reaction can provide much more control over the network structure. It increased the potential for the growing polymer network and template binding complexes to reach a global energy minimum and led to further memorization of the chain conformation. Compared to conventional techniques, living radical polymerization resulted in a 63% increase in the number of binding sites at approximately equivalent average binding affinity while retaining selectivity for the template. This was hypothesized to be attributed to a decrease in kinetic chain length and/or a more narrow dispersity of kinetic chains which leads to increased structural homogeneity with more stability and integrity of more appropriately sized binding sites.

2.2 Emerging and Future Translational Applications of Imprinted Gels

Imprinted gels are currently being used to create functional materials in controlled and modulated drug delivery, sensors and diagnostics, membrane separation, and solid phase extraction. In these fields, they are leading to significant solutions and the development of new materials. Future applications of imprinted gels include tissue engineering, fluidic valves and actuators, as well as coatings for a number of drug delivery carriers and medical devices.

2.2.1 Responsive Intelligent Imprinted Gels

Stimuli-sensitive hydrogels that respond to changes in the external environment have been the subject of much research and have been demonstrated in a wide variety of hydrogel systems [84-85]. To date, molecularly imprinted responsive networks have been demonstrated with triggers such as pH [22, 68-69, 86], temperature [55, 86-89], light [90-91], and salt concentration [87] for templates such as ions [45, 92-94], low to moderate molecular weight molecules [44, 95-96], and proteins [87] (Table 2.1). Of course, flexible polymer chains with considerable mobility such as those found in hydrogel networks can expand and collapse depending on the solvent and

the interaction between the solvent and the polymer chains. Therefore, imprinted hydrogels can also alter binding differences in response to changes in the solvent (i.e., introducing a better or worse solvent which affect the solvation of polymer chains).

It is no surprise that molecular imprinting strategies have been used in the development of intelligent, recognitive, heteropolymer networks that contain stimuli sensitive moieties within the polymer chains. The first paper from Watanabe and coworkers in the field was classical molecular imprinting [95], but this type of work primarily began by using variations of the molecular imprinting technique (i.e., using templating of charged molecules (e.g., anionic small molecules and ions) with post-crosslinking [44, 83, 94] and acrylated multiple-functionality inclusion complexes [69]. Work has now progressed to include a much wider variety of molecules of increasing functionality and molecular size exploiting more non-covalent interactions with comparable synthesis techniques that match traditional molecular imprinting strategies.

On-demand or triggered release, where a stimulus invokes a reversible alteration of the template binding memory site leading to a decrease in template affinity and subsequent template release, has been demonstrated via two mechanisms (Figure 2.6). Primarily, it has been demonstrated to occur via changes in the chemistry along the main polymer chains which leads to the movement of the backbone chain and thereby, in a secondary way, disrupting the orientation of the chemistry that makes up the binding cavity. To a much lesser extent, template release has also involved only the disruption of the chemistry that makes up the binding site. This has been accomplished via alteration of the functional monomer(s) charge within the binding site or charges on the template, such as a pH change [86] or changing the conformation of the functional monomer, such as using photoswitchable azobenzene chromophores [91],

which undergo cis-trans isomerization. Of course, decrease in template affinity has also been demonstrated in a variety of highly crosslinked imprinted polymers by knocking out hydrogen bonding between the template and binding site chemistry with increased temperatures or using a solvent that competes or interferes with the binding site non-covalent interactions.

Modulatory mechanisms, or turning binding and release on and off through various cycles has been demonstrated in a number of systems with the successful reorientation of the binding site after the removal of the stimulus. However, in most systems to date the number of cycles has been relatively low, approaching approximately 3-4 cycles, with the sustainability of the binding mechanism decreasing slightly.

Comparing to conventional, intelligent hydrogels without imprinting mechanisms, Gong and coworkers [90] are correct when they say "molecularly imprinted responsive materials are able to provide additional degrees of control over the transfer of targeted substrates". The rational design and engineering of intelligent hydrogels using imprinting mechanisms will lead to greater control of the diffusional transport of template in these systems, and may solve some of the limitations of conventional systems, such as drug release or leaking in the collapsed state.

Before 1998, there were no papers discussing the incorporation of stimuli responsive monomers in the design of molecularly imprinted gels. The first paper in the field from Watanabe and coworkers demonstrated recognition of template during the shrunken state of a temperature-sensitive polymer with a volume change in response to the template [95]. Subsequent work began by elucidating the memory of conformations in heteropolymer systems exploiting previous work using statistical mechanics to understand macromolecular recognition. Tanaka and coworkers [97] demonstrated that a target molecule could be captured by multiple-

point electrostatic adsorption of flexible polymer chains and have differing affinity for the target. By varying polymer conformation and concentration, polymer gels demonstrated reversible thermosensitive affinity for target molecules by two or three orders of magnitude. Ionic recognition of Pyranine with 3 or 4 negative charges was proven in high salt concentration thereby limiting a mechanism based on Donnan potential. It is important to note that these gels were not polymerized in the presence of the template molecule as is the case with molecular imprinting. Nonetheless, this work outlined the strong possibilities of controlling and modulating target molecule affinity by the concentration and conformation of chemical groups along the polymer chain. The proximity of these groups and subsequent recognition was controlled by the reversible phase transition of groups along the polymer chains. This involved one monomer with non-covalent interaction with the target and another monomer that would undergo a transition.

Shortly afterward, three papers by Tanaka and coworkers were published that utilized molecular imprinting concepts in the creation of weakly crosslinked gels with reversible thermosensitive affinity [44-45, 94]. The first published paper utilized the same target, Pyranine tri- and tetrasulfonic sodium salt with 3 or 4 negative charges, and involved a post-crosslinking thiol reaction in the presence of the target as template. This was the earliest attempt in these systems to fix the conformation of polymer chains in a global energy minimum to impart memory within the flexible polymer network chains. However, templating was accomplished after the network was polymerized and was limited by not allowing a preferred, templated sequence of monomers. The other two papers included the molecular imprinting concept using a template (lead and calcium ions) in the polymerization reaction, which is more consistent with conventional molecular imprinting techniques [45, 94]. This is the first evidence of the use of molecular imprinting beginning with functional monomeric units demonstrating recognition

responsiveness to capture template ions. Later work by some of the authors included concurrent multiple point adsorption of two oppositely charged ions and a reversible crosslinker to further ascertain an enhancement of the imprinting technique [92-93]. A physical theory has been suggested for adsorption of templates to random heteropolymer gels, which were modeled as a set of adsorbing monomers connected by Gaussian chains to fixed crosslinking points [98]. Recently, Basavaraja and colleagues presented a self-oscillating imprinted hydrogel depending on the oxidation state of a metal catalyst group contained in the polymer chains [99]. The oscillation is induced by redox change of the covalently bound catalyst, which alters the hydrophilicity of the polymer chains leading to swelling and less effective recognition of ions.

Stimuli-responsive lysozyme imprinted polymers were demonstrated to respond to temperature and salt concentration, but also to the template proteins producing significant volume shrinking [87]. The polymer gel decreased in volume and the volume fraction in the swollen state increased as template protein increased. At concentration of lysozyme greater than 1 mg/mL, the polymer reached a limit of 85% of original volume. A small decrease was apparent using the template as well as bovine serum albumin with the non-imprinted system. Temperature-sensitive imprinted polymers for larger molecules have also been demonstrated using N-isopropylacrylamide as temperature sensitive monomer along with functional monomers that interact with the template. This has been shown for L-pyrogluamic acid [88] and 4-aminopyridine templates [89] using methacrylic acid as functional monomer with ethylene glycol dimethacrylate as crosslinking monomer. It is notable that reference [88] demonstrates the reusability of these gels showing four loading/release cycles with similar template loading and release amounts. Light responsiveness has also been demonstrated. The first paper in the field demonstrating photoresponsive imprinting had caffeine as template [91]. Recently, a molecularly

imprinted polymer has been synthesized with photoregulated affinity for paracetamol. Irradiation at 440 nm resulted in binding and irradiation at 353nm resulted in release. The polymer contained 4-[(4-methacryloyloxy)phenylazo] benzenesulfonic acid (MAPASA) that undergoes trans-cis photoisomerization within a polyacrylamide hydrogel. Non-imprinted gels did not demonstrate photoregulated release and two structural analogs had significantly less photoregulated uptake and release. Three uptake and release cycles were demonstrated with the reduction in the template bound and released hypothesized to be due to a gradual deformation of the imprinted receptor sites [90].

Another interesting notion is the movement of flexible polymer chains in the assisted assembly of template guided by multiple complexation points. Recently, exciting work has demonstrated that an imprinted polymer for native lysozyme promoted the folding of chemically denatured lysozyme [100]. At protein concentrations of 0.125 mg/mL with refolding yield measure by enzymatic activity, imprinted structures demonstrated substantially higher refolding yields as compared to non-imprinted polymers, which did not demonstrate template refolding. The authors also compared the refolding of lysozyme in a cytochrome c imprinted polymer (i.e., a similarly sized protein), and found the correct pore size alone did not lead to folding. The mechanism of molecularly imprinted assisted folding and the potential of an "induced fit mechanism" is convincing and plausible, but more details of the mechanism are needed. It is important to note that the poly(acrylamide-co-2-(dimethylamino)ethyl methacrylate –co-methacrylic acid-co- N,N'-methylenebisacrylamide) hydrogel network had multiple complexation points with the template.

Recently, interpenetrating polymers of poly(acrylic acid) and poly(vinyl alcohol) were imprinted for 1-(4-methoxyphenyl)-5-methyl-1,2,3-triazol-4-carboxylic acid (MMTCA) [62].

The imprinted interpenetrating network (IPN) exhibited higher binding capacity than the non-imprinted IPN and networks of either polymer alone. Work has also included the imprinting of metal ions [61] and hemoglobin [28] via interpenetrating networks. Exciting progress has been made in small molecule and protein-sensitive gels, where the template either alters the water solvation of polymer chains or results in effective crosslinks in the gel.

In the last few years, there has been a considerable increase in the number of imprinted gels with responsive mechanisms. As with conventional intelligent hydrogels, the number of responsive mechanisms will increase (e.g, there are no magnetic or electric field responsive imprinted gels to date) and the type of networks will expand to include more multiple-responsive mechanisms. Considerable effort will also be put forward to increase the dynamics associated with the recognition/release cycle. This will be obtained by carefully controlling network structure and the size of the gel. Maintaining cycles without reduction in binding/affinity is not a significant problem to overcome, but significant response lifetimes have not been demonstrated. We highlight some of our envisioned intelligent imprinted systems of the future in Figure 2.7.

2.2.2 Controlled and Modulated Therapeutic Delivery

Controlled drug release from hydrogels has been extensively studied for the past three decades. Molecular design and control of the network architecture are driving new developments in the field. Only recently has molecular imprinting been applied to drug delivery, which is highlighted in the following reviews [9-10, 101-104].

In order to emphasize the significance imprinting may have on drug delivery, it is best to highlight the past. Langer and coworkers [105] studied the interconnected pore network structures formed when proteins were included within the creation of normally non-porous

polymers. The study of the voids left behind or the amount of protein trapped within the structure led to the rational development of formulations to extend or delay the transport of the therapeutic protein from the polymer structure. These early studies indicated how the nature of embedded molecule and the concentration and size of these molecules influenced the underlying porosity of the resulting polymer, and subsequent release.

Other than highlighting non-specific interactions between the drug and polymer such as hydrophobicity affecting drug transport, the field has done very little to understand the influence of the molecule on the organization of the chemical functionality and orientation of polymer chains when it is included in the polymerization process. To be clear, this is exactly where molecular imprinting is gaining a new role in drug delivery. Imprinted network formation, with a proper optimization of drug affinity relating to number and strength of functional monomer interactions, crosslinking structure, and mobility of polymer chains, has a strong potential to influence a number of hydrogel carriers and add to the variables one can alter to tune the release profile. Imprinting can lead to delayed transport of therapeutic.

Two schemes are typically used to load therapeutics into hydrogels – produce the gel in the presence of drug or synthesize the gel and then load drug into the gel via equilibrium partitioning. It is common knowledge that preparation conditions of hydrogels can lead to significant changes in the network structure and resulting properties. Surprisingly, no work has addressed the potential impact of the inclusion of drug and its affect on the organization of polymer chains. Only recently has work addressed the potential to extend or optimize controlled release by tailored drug-polymer chain interactions, such as those produced by molecular imprinting and there have not been many drug release studies conducted on weakly crosslinked

imprinted structures or hydrogels. Recently, we have proven that imprinting leads to delayed template transport and it is not due to differing mesh structures or porosity [50].

To further clarify the role of imprinting in controlled release, one must first look at mechanisms of drug release from hydrogel structures. We direct the reader to the following references [106-109]. Molecular imprinting can provide control of the drug release profile in swollen networks, dynamically swelling or swelling-controlled networks (i.e., drug-loaded networks going from a dry to a swollen state), and responsive-swollen networks (i.e., a swollen gel that undergoes a reversible volume transition based on a stimulus such as pH, temperature, ionic strength, etc.). Responsive hydrogels can be engineered to change network structure in response to a stimulus due to the presence of specific chemical/biological species along their backbone polymer chains.

For swelling-controlled release from hydrogels, if there is a constant rate of solvent front penetration which is much smaller than the drug diffusion rate in the swollen gel, a constant drug release rate, or zero-order release, arises [107]. Imprinting may aid this process in swelling-controlled gels, decreasing the drug diffusion rate. If the polymer relaxation rate is high and the drug diffusion is rate-limiting, this results in the drug release rate being proportional to the concentration gradient between the drug source and the surroundings (i.e., a Fickian drug release profile). In this situation, a number of strategies have been attempted to achieve an extended zero-order release such as bioerodible and biodegradable systems with solvent penetration fronts moving with similar velocities as the outer eroding front [110], hydrogels with rate controlling-barriers such as higher crosslinked outer edges [111], and non-uniform drug distribution [112].

Molecular imprinting has led to the development of extended drug releasing contact lenses, which cannot use conventional strategies to delay drug transport from the equilibrium swollen polymer network [19-22, 49, 113]. Recently, dynamic, *in vitro* drug release studies from imprinted hydrogel contact lenses within a novel microfluidic device that simulated the volumetric flow rate, tear volume, and composition of the eye resulted in a constant, zero order release [114]. Imprinting delays transport from the polymer chains, and a tumbling hypothesis was recently proposed analyzing one-dimensional template transport [50]. We direct the reader to the following articles discussing the impact of such systems in ocular drug delivery [115-116].

Recently, multi-nuclear heteroneuclear correlation solid state NMR spectroscopy has been used to provide evidence of monomer-drug interactions leading to sustained release [117], but it is important to note that hydrophobic effects dominated the drug release profile of the imprinted porous gels prepared in ethanol/water [118]. Hydrophobic interaction with the drug retarded the drugs dissolution or release kinetics and the hydrophobicity of the gel reduced water diffusion in the pores. However, studies such as these will lead to validation of imprinting mechanisms delaying transport.

Further control of transport at decreasing thicknesses will be paramount for the success of micro- and nanoscale drug delivery carriers. Imprinted drug delivery networks will be especially important is situations where the carrier or film must be limited in volume or extended release is needed from thin layers.

Work has also included transdermal drug delivery [103, 119], solid-phase extraction [120-121], and membrane separation [121-122]; however, most of these networks are not flexible gels. Recently, selective enrichment has been demonstrated [70], and dopamine-imprinted,

temperature-sensitive polymer gels have been used for selective separation [120]. Imprinted, temperature-sensitive networks have also been grafted on non-woven polypropylene films [123], where separation of heavy metal ions by temperature swing adsorption has been demonstrated with ion adsorption/desorption kinetics [123-124]. Also, enantioselective-controlled delivery was investigated by Suedee et al. [119, 125], where they applied imprinted networks as enantioselective excipients and transdermal systems. Composite membranes for transdermal delivery of S-propranolol have been developed using pore functionalization via imprinting with selective transport of the enantiomer [119]. Also, an enantioselective membrane for L-phenyalanine (template) over d-phenylalanine was prepared by sol-gel process [126]. Hybrid membranes of chitosan and γ-glycidoxypropyltrimethoxysilane with varying degrees of crosslinking demonstrated increase in enantiomeric selectivity factor as membrane swelling decreased or the crosslinking content increased. The imprinted gels had higher template binding and decreased template permeation.

Combining imprinted poly(acrylamide-co-N,N'-methylene-bis-acrylamide) gels with electrophoresis has created an exciting, powerful analytical tool to selectively separate protein [127], virus (Semliki Forest Virus, diameter 70 nm) [128], and E. coli bacteria (rod shape, 1-2μm in length, 0.1-0.5 μm in diameter) [129]. The artificial gels can sense the difference between the template virus and a mutant virus which only differs by three amino acids in one of the three proteins on the surface of the virus particle [128]. Neutral imprinted gel particles migrated in the electric field when complexed with charged virus, protein [127], or cells [129].

Imprinted hydrogels have also performed catalysis with pH sensitivity decreasing the activity, as demonstrated by Karmalkar [130]. This work highlights the proximity of active functional groups by imprinting and demonstrates on-off release of catalyzed molecule. Coating

silica beads with imprinted hydrogels have been used to bind and detect lysozyme [131], and imprinted calcium alginate gel microspheres have been prepared with recognition for albumin [132].

2.2.3 Sensor Substrates, Diagnostics, and Biomarker Detection

Molecularly imprinted hydrogels are gaining popularity as recognition elements due to their ability to translate analyte binding event into a mechanical or chemical signal. Imprinted polymers are more robust than biological sensing elements and have economic advantage in terms of raw material price as well as manufacturability. Recently, Lotierzo et al. [133] showed that imprinted polymers outperformed monoclonal antibody natural receptors with a wide detection range and long stability. These studies are prompting the transition of imprinted networks toward point-of-care diagnostics, sensors that must work in areas outside the controlled environment of the laboratory. The main problem associated with large molecules is decreased transport through gels, which increases response time. However, with the use of extremely thin films satisfactory results can be achieved [56, 59]. We direct the reader to the following reviews of imprinted sensors [134-135]. A selection of papers that utilize imprinted hydrogels is highlighted in the following paragraphs.

Lavine and coworkers [136] describe molecularly imprinted, temperature-sensitive nanogel particles which selectively bind theophylline template. The binding event increases the phase transition temperature of the gel, and the increased hydrophilicity results in volume swelling of the gel. The volume transition decreases the refractive index which is used to quantify the amount of theophylline bound using surface plasmon resonance spectroscopy. Theophylline concentration values as low as 10^{-6} M were detected using the sensor. In addition, caffeine,

which is similar in structure to theophylline, does not cause a volume transition in the particles even at values as high as 10^{-2} M.

Results have also been very encouraging with large molecules such as proteins, viruses, and DNA. Miyata and coworkers used imprinted hydrogels to recognize tumor marker glycoproteins by lectin and antibody ligands [137]. Lectin (Con-A) and antibodies (polyclonal anti-AFP) were first functionalized with vinyl groups using N-succinimidylacrylate and then a copolymer of Con A and acrylamide was prepared. Then poly(acrylamide-g-Con-A) was copolymerized with acrylamide with N,N`-methylenebisacrylamide as crosslinker in the presence of the template, a-fetoprotein (AFP). AFP is a glycoprotein widely used for the serum diagnosis of primary hepatoma. AFP provides a recognition link between the Con-A and the antibody, which are on different polymer chains. Thus, when free AFP is present, Con-A and anti-AFP are bound together by AFP which leads to shrinking of the gel. The work also demonstrates selectivity for AFP over ovalbumin, another glycoprotein with a saccharide chain similar to AFP but with a different peptide chain. This work promises an intensive application for cancer detection.

Recently, a three-dimensional highly ordered macroporous structure was produced using silica colloidal crystal templating [138]. In this highly innovative work, an albumin imprinted hydrogel was polymerized within the void spaces of a silica colloidal crystal array. When the silica and protein was removed, a surface imprinted macroporous gel was produced. Selective protein binding and subsequent hydrogel swelling was determined optically via color change of the imprinted film without the use of a transducer. This system was fast (i.e., on order of minutes) and very sensitive with a 1 ng/mL concentration of albumin detected. Recently, this same technique was used to produce selective theophylline and ephedrine photonic-imprinted hydrogels [139]. Biosensing via optical detection of molecule-sensitive hydrogels is very

promising, demonstrated by using bioconjugated hydrogels as microlenses [140]. Upon recognition of molecules and loss of effective crosslinks within the gel, swelling occurs and allows a pattern on the substrate to be visualized. It is important to note that this work [140] did not exploit imprinting strategies; however, it is evident that molecular imprinting will be very beneficial in the transition of these devices to market and the generalization of these systems.

In conclusion, it is easy to imagine imprinted hydrogel films/coatings on medical devices, polymer carriers, and drug particles. Imprinted films would provide an additional level of control in these decreased length scale applications where delayed release of therapeutic is imperative and other mechanisms cannot be used. Recent progress in the field of imprinted hydrogels is leading to exciting developments. The field of hydrogel imprinting did not exist ten years ago and has seen significant growth with the realization of large molecule imprinting within flexible structures. The field has transitioned to protein and larger particle imprinting and has begun to confirm selectivity of imprinted gels. Also, responsive gels have exploded in both the number of modulatory mechanisms to bind or release template and in the control of such mechanisms. The future is indeed bright, and the next few years will see unprecedented progress in the control and fabrication of such systems and the translational application of these intelligent structures at all length scales within pharmacy, medicine, tissue engineering, sensors and diagnostics, micro and nanodevices, and separation processes.

2.3 References

1. Ye L, Mosbach K. Molecular imprinting: Synthetic materials as substitutes for biological antibodies and receptors. Chem. Mater. 2008, 20, 859-868.
2. Wulff G. Enzyme-like catalysis by molecularly imprinted polymers. Chem. Rev. 2002, 102, 1-27.
3. Mayes AG, Whitcombe MJ. Synthetic strategies for the generation of molecularly imprinted organic polymers. Adv. Drug Deliv. Rev. 2005, 57, 1742-1778.
4. Cormack PAG, Mosbach K. Molecular imprinting: recent developments and the road ahead. React. Funct. Polym. 1999, 41, 115-124.
5. Wei S, Mizaikoff B. Recent advances on noncovalent molecular imprints for affinity separations. J. Sep. Sci. 2007, 30, 1794-1805.
6. Whitcombe MJ, Vulfson EN. Imprinted polymers. Adv. Mater. 2001, 13, 467-478.
7. Alexander C, Andersson HS, Andersson LI, Ansell RJ, Kirsch N, Nicholls IA, O'Mahony J, Whitcombe MJ. Molecular imprinting science and technology: a survey of the literature for the years up to and including 2003. J. Mol. Recognit. 2006, 19, 106-180.
8. Davis ME, Katz A, Ahmad WR. Rational catalyst design via imprinted nanostructured materials. Chem. Mater. 1996, 8, 1820-1839.
9. Byrne ME, Park K, Peppas NA. Molecular imprinting within hydrogels. Adv. Drug Deliv. Rev. 2002, 54, 149-161.
10. Hilt JZ, Byrne ME. Configurational biomimesis in drug delivery: molecular imprinting of biologically significant molecules. Adv. Drug Deliv. Rev. 2004, 56, 1599-1620.
11. Ge Y, Turner AP. Too large to fit? Recent developments in macromolecular imprinting. Trends Biotechnol. 2008, 26, 218-224.

12. Hillberg AL, Tabrizian M. Biomolecule imprinting: Developments in mimicking dynamic natural recognition systems. ITBM-RBM. 2008, 29, 89-104.
13. Bergmann NM, Peppas NA. Molecularly imprinted polymers with specific recognition for macromolecules and proteins. Prog. Polym. Sci. 2008, 33, 271-288.
14. Wei ST, Jakusch M, Mizaikoff B. Capturing molecules with templated materials - Analysis and rational design of molecularly imprinted polymers. Anal. Chim. Acta. 2006, 578, 50-58.
15. Zhang HQ, Ye L, Mosbach K. Non-covalent molecular imprinting with emphasis on its application in separation and drug development. J. Mol. Recognit. 2006, 19, 248-259.
16. Janiak DS, Kofinas P. Molecular imprinting of peptides and proteins in aqueous media. Anal. Bioanal. Chem. 2007, 389, 399-404.
17. Bossi A, Bonini F, Turner APF, Piletsky SA. Molecularly imprinted polymers for the recognition of proteins: the state of the art. Biosens. Bioelectron. 2007, 22, 1131–1137.
18. Turner NW, Jeans CW, Brain KR, Allender CJ, Hlady V, Britt DW. From 3D to 2D: A review of the molecular imprinting of proteins. Biotechnol. Prog. 2006, 22, 1474–1489.
19. Venkatesh S, Sizemore SP, Byrne ME. Biomimetic hydrogels for enhanced loading and extended release of ocular therapeutics. Biomaterials. 2007, 28, 717-724.
20. Alvarez-Lorenzo C, Hiratani H, Gomez-Amoza JL, Martinez-Pacheco R, Souto C, Concheiro A. Soft contact lenses capable of sustained delivery of timolol. J. Pharm. Sci. 2002, 91, 2182-2192.
21. Venkatesh S, Sizemore SP, Zhang JB, Byrne ME. Therapeutic contact lenses: A biomimetic approach towards tailored ophthalmic extended delivery. Abstr. Pap. Am. Chem. Soc. 2006, 231.

22. Alvarez-Lorenzo C, Yanez F, Barreiro-Iglesias R, Concheiro A. Imprinted soft contact lenses as norfloxacin delivery systems. J. Controlled Release. 2006, 113, 236-244.
23. Byrne ME, Hilt JZ, Peppas NA. Recognitive biomimetic networks with moiety imprinting for intelligent drug delivery. J. Biomed. Mater. Res. 2008, Part A, 84A, 137-147.
24. Hawkins DM, Stevenson D, Reddy SM. Investigation of protein imprinting in hydrogel-based molecularly imprinted polymers (HydroMIPs). Anal. Chim. Acta. 2005, 542, 61-65.
25. Kimhi O, Bianco-Peled H. Study of the interactions between protein-imprinted hydrogels and their templates. Langmuir. 2007, 23, 6329-6335.
26. Kublickas R, Werner C, Jariene G, Voit B, Lasas L. Polyacrylamide gels containing ionized functional groups for the molecular imprinting of human growth hormone. Polym. Bull. 2007, 58, 611-617.
27. Parmpi P, Kofinas P. Biomimetic glucose recognition using molecularly imprinted polymer hydrogels. Biomaterials. 2004, 25, 1969-1973.
28. Xia YQ, Guo TY, Song MD, Zhang BH, Zhang BL. Hemoglobin recognition by imprinting in semi-interpenetrating polymer network hydrogel based on polyacrylamide and chitosan. Biomacromolecules. 2005, 6, 2601-2606.
29. Espinosa-Garcia BM, Argelles-Monal WM, Hernandez J, Felix-Valenzuela L, Acosta N, Goycoolea FM. Molecularly imprinted chitosan-genipin hydrogels with recognition capacity toward o-xylene. Biomacromolecules. 2007, 8(11), 3355-3364.
30. Wizeman WJ, Kofinas P. Molecularly imprinted polymer hydrogels displaying isomerically resolved glucose binding. Biomaterials. 2001, 22, 1485–91.

31. Hawkins DM, Trache A, Ellis EA, Stevenson D, Holzenburg A, Meininger GA, Reddy SM. Quantification and confocal imaging of protein specific molecularly imprinted polymers. Biomacromolecules. 2006, 7, 2560-2564.
32. Demchenko AP. Recognition between flexible protein molecules: induced and assisted folding. J. Mol. Recognit. 2001, 14, 42-61.
33. Huber R, Bennett WS. Functional significance of flexibility in proteins. Biopolymers. 1983, 22, 261-279.
34. Blackburne BP, Hirst J.D. Evolution of functional model proteins. J. Chem. Phys. 2001, 115, 1935-1942.
35. Lemieux RU. How water provides the impetus for molecular recognition in aqueous solution. Acc. Chem. Res. 1996, 29, 373-380.
36. De Gennes PG. Pattern Recognition by Flexible Coils. In: Grinstein, G., Mazenko, G. (Eds.), Directions in Condensed Matter Physics. 1986, World Scientific, Singapore, 83-99.
37. Bryngelson JD, Wolynes PG. Spin Glasses and the statistical mechanics of protein folding. Proc. Natl. Acad. Sci. U.S.A. 1987, 84, 7524-7528.
38. Pande VS, Grosberg AY, Tanaka T. Folding thermodynamics and kinetics of imprinted renaturable heteropolymers, J. Chem. Phys. 1994, 101, 8246-8257.
39. Pande VS, Grosberg AY, Tanaka TA. Thermodynamic procedure to synthesize heteropolymers that can renature to recognize a given target molecule. Proc. Natl. Acad. Sci. U.S.A. 1994, 91, 12976-12979.
40. Pande VS, Grosberg AY, Tanaka TA. Statistical mechanics of simple models of protein folding and design. Biophys. J. 1997, 73, 3192-3210.

41. Pande VS, Grosberg AY, Tanaka TA. Heteropolymer freezing and design: Towards physical models of protein folding. Rev. Mod. Phys. 2000, 72, 259-314.
42. Jozefowicz M, Jozefonvicz J. Randomness and biospecificity: random copolymers are capable of biospecific molecular recognition in living systems. Biomaterials. 1997, 18, 1633-1644.
43. Peppas NA, Huang Y. Polymers and gels as molecular recognition agents. Pharm. Res. 2002, 19, 578-587.
44. Enoki T, Tanaka K, Watanabe T, Oya T, Sakiyama T, Takeoka Y, Ito K, Wang G, Annaka M, Hara H, Du R, Chuang J, Wasserman K, Grosberg AY, Masamune S, Tanaka T. Frustrations in polymer conformation in gels and their minimization through molecular imprinting. Phys. Rev. Lett. 2000, 85, 5000-5003.
45. C. Alvarez-Lorenzo C, Guney O, Oya T, Sakai Y, Kobayashi M, Enoki T, Takeoka Y, Ishibashi T, Kuroda K, Tanaka K, Wang G, Grosberg AY, Masamune S, Tanaka, T. Polymer gels that memorize elements of molecular conformation. Macromolecules. 2000, 33, 8693-8697.
46. Meot-Ner M. The ionic hydrogen bond. Chem. Rev. 2005, 105, 213-284.
47. Lodish H, Berk A, Zipursky LS, Matsudaira P, Baltimore D, Darnell J. Molecular Cell Biology, Section 2.2 Noncovalent Bonds. 2000, W.H. Freeman and Co., New York, NY.
48. Umpleby II RJ, Bode M, Shimizu KD. Measurement of the continuous distribution of binding sites in molecularly imprinted polymers. Analyst. 2000, 125(7), 1261-1265.
49. Hiratani H, Mizutani Y, Alvarez-Lorenzo C. Controlling drug release from imprinted hydrogels by modifying the characteristics of the imprinted cavities. Macromol. Biosci. 2005, 5, 728-733.

50. Venkatesh S, Saha J, Pass S, Byrne ME. Transport and structural analysis of molecularly imprinted hydrogels for controlled drug delivery. Eur. J. Pharm. Biopharm. 2008, 69, 852-860.
51. Lubke C, Lubke M, Whitcombe MJ, Vulfson EN. Imprinted polymers prepared with stoichiometric template-monomer complexes: efficient binding of ampicillin from aqueous solutions, Macromolecules. 2000, 33, 5098-5105.
52. Spizzirri UG, Peppas NA. Structural analysis and diffusional behavior of molecularly imprinted polymer networks for cholesterol recognition. Chem. Mater. 2005, 17, 6719-6727.
53. Hawkins DM, Ellis EA, Stevenson D, Holzenburg A, Reddy SM. Novel critical point drying (CPD) based preparation and transmission electron microscopy (TEM) imaging of protein specific molecularly imprinted polymers, J. Mater. Sci. 2007, 42, 9465-9468.
54. Byrne ME, Oral E, Hilt JZ, Peppas NA. Networks for the recognition of biomolecules: molecular imprinting and micropatterning poly(ethylene glycol)-containing films, Polym. Adv. Technol. 2002, 13, 798-816.
55. Aburto J, Le Borgne S. Selective adsorption of dibenzothiophene sulfone by an imprinted and stimuli-responsive chitosan hydrogel, Macromolecules. 2004, 37, 2938-2943.
56. Hilt JZ, Byrne ME, Peppas NA. Microfabrication of intelligent biomimetic networks for recognition of glucose, Chem. Mater. 2006, 18, 5869-5875.
57. Spivak D, Gilmore MA, Shea KD. Evaluation of binding and origins of specificity of 9-ethyladenine imprinted polymers, J. Am. Chem. Soc. 1997, 119, 4388–4393.

58. Wu Liqing, Kuaichang Zhu, Meiping Zhao, Yuanzong Li. Theoretical and Experimental Study of Nicotinamide Molecularly Imprinted Polymers with Different Porogens, Analytica Chimica Acta. 2005, 549, 39-44.
59. Noss KR, Vaughan AD, Byrne ME. Tailored binding and transport parameters of molecularly imprinted films via macromolecular structure: The rational design of recognitive polymers. J. Appl. Polym. Sci. 2008, 107, 3435-3441.
60. Djourelov N, Ates Z, Guven O, Misheva M, Suzuki T. Positron annihilation lifetime spectroscopy of molecularly imprinted hydroxyelthyl methacrylate based polymers, Polymer. 2007, 48, 2692-2699.
61. Yamashita K, Nishimura T, Ohashi K, Ohkouchi H, Nango M. Two-step Imprinting Procedure of Inter-penetrating Polymer Network-Type Stimuli-Responsive Hydrogel Adsorbents, Polym. J. 2003, 35, 545-550.
62. Wang B, Liu MZ, Liang R, Ding SL, Chen ZB, Chen SL, Jin SP. MMTCA Recognition by molecular imprinting in interpenetrating polymer network hydrogels based on poly(acrylic acid) and poly(vinyl alcohol), Macromol. Biosci. 2008, 8, 417-425.
63. Binet C, Ferrere S, Lattes A, Laurent E, Marty JD, Mauzac M, Mingotaud AF, Palaprat G, Weyland M. Benefit of liquid crystal moieties in the MIP technique, Anal. Chim. Acta. 2007, 591, 1-6.
64. Marty JD, Tizra M, Mauzac M, Rico-Lattes I, Lattes A. New molecular imprinting materials: Liquid crystalline networks, Macromolecules. 1999, 32, 8674-8677.
65. Palaprat G, Weyland M, Phou T, Binet C, Marty JD, Mingotaud AF, Mauzac M. Introduction of unusual properties into polymers by the use of liquid-crystalline moieties, Polym. Int. 2006, 55, 1191-1198.

66. Bolisay LD, Culver JN, Kofinas P. Molecularly imprinted polymers for tobacco mosaic virus recognition, Biomaterials. 2006, 27(22), 4165-4168.

67. Guo MJ, Zhao Z, Fan YG, Wang CH, Shi LQ, Xia JJ, Long Y, Mi HF. Protein-imprinted polymer with immobilized assistant recognition polymer chains, Biomaterials. 2006, 27, 4381-4387.

68. Kanekiyo Y, Naganawa R, Tao H. Molecular imprinting of bisphenol A and alkylphenols using amylose as a host matrix, Chem. Commun. 2002, 2698-2699.

69. Kanekiyo Y, Naganawa R, Tao H. pH-responsive molecularly imprinted polymers. Angew, Chem., Int. Ed. 2003, 42, 3014-3016.

70. Zhao Z, Wang CH, Guo MJ, Shi LQ, Fan YG, Long Y, Mi HF. Molecular imprinted polymer with cloned bacterial protein template enriches authentic target in cell extract, Febs. Lett. 2006, 580, 2750-2754.

71. Moritani T, Alvarez-Lorenzo C. Conformational imprinting effect on stimuli-sensitive gels made with an "Imprinter" monomer, Macromolecules. 2001, 34, 7796-7803.

72. Jacob R, Tate M, Banti Y, Rix C, Mainwaring DE. Synthesis, characterization, and ab initio theoretical study of a molecularly imprinted polymer selective for biosensor materials, J. Phys. Chem. A. 2008, 112, 322-331.

73. Silvestri D, Cristallini C, Ciardelli G, Giusti P, Barbani N. Molecularly imprinted bioartifical membranes for the selective recognition of biological molecules. Part 2: Release of components and thermal analysis, J. Biomater. Sci. Polymer Edn. 2005, 16, 3, 397-410.

74. Chianella I, Karim K, Piletska EV, Preston C, Piletsky SA. Computational design and synthesis of molecularly imprinted polymers with high binding capacity for

pharmaceutical applications-model case: Adsorbent for abacavir, Anal. Chim. Acta. 2006, 559, 73-78.

75. Pavel D, Lagowski J. Computationally designed monomers and polymers for molecular imprinting of theophylline - part II, Polymer. 2005, 46, 7543-7556.
76. Henthorn DB, Peppas NA. Molecular simulations of recognitive behavior of molecularly imprinted intelligent polymeric networks, Ind. Eng. Chem. Res. 2007, 46, 6084-6091.
77. Monti S, Cappelli C, Bronco S, Giusti P, Ciardelli G. Towards the design of highly selective recognition sites into molecular imprinting polymers: A computational approach. Biosens, Bioelectron. 2006, 22, 153-163.
78. Elliott JE, Bowman CN. Monomer functionality and polymer network formation, Macromolecules. 2001, 34, 4642-4649.
79. Spivak DA, Shea KJ. Investigation into the Scope and Limitations of Molecular Imprinting with DNA Molecules, Analytica Chimica Acta. 2001, 435, 65-74.
80. Piletsky SA, Mijangos I, Guerreiro A, Piletska EV, Chianella I, Karim K, Turner APF. Polymer Cookery: Influence of Polymerization Time and Different Initiation Conditions on Performance of Molecularly Imprinted Polymers, Macromolecules. 2005, 38, 1410-1414.
81. Rampey AM, Umpleby RJ, Rushton GT, Iseman JC, Shah RN, Shimizu KD. Characterization of the imprint effect and the influence of imprinting conditions on affinity, capacity, and heterogeneity in molecularly imprinted polymers using the freundlich isotherm-affinity distribution analysis, Anal. Chem. 2004, 76, 4, 1123-1133.

82. O'Shannessy DJ, Ekberg B, Mosbach K. Molecular imprinting of amino-acid derivatives at low temperature using photolytic homolysis of azobisnitriles, Anal. Biochem. 1989, 177, 144-149.

83. Vaughan AD, Byrne ME. Optimizing Recognition Characteristics of Biomimetic Polymer Gels via Polymerization Reaction and Crosslinking Density Analysis. PMSE Preprints. 2006, 94, 762-763.

84. Peppas NA, Hilt JZ, Khademhosseini A, Langer R. Hydrogels in biology and medicine: From molecular principles to bionanotechnology, Advanced Materials. 2006, 18, 11, 1345-1360.

85. Ulijn RV, Bibi N, Jayawarna V, Thornton PD, Todd SJ, Mart RJ, Smith AM, Gough JE. Bioresponsive hydrogels, Materials Today. 2007, 10, 4, 40-48.

86. Demirel G, Ozcetin G, Turan E, Caykara T. pH/temperature-sensitive imprinted ionic poly (N-tert-butylacrylamide-co-acrylamide/maleic acid) hydrogels for bovine serum albumin. Macromolecular Bioscience. 2005, 5, 1032-1037.

87. Chen ZY, Hua ZD, Xu L, Huang Y, Zhao MP, Li YZ. Protein-responsive imprinted polymers with specific shrinking and rebinding. J. Mol. Recognit. 2008, 21, 71-77.

88. Liu XY, Guan Y, Ding XB, Peng YX, Long XP, Wang XC, Chang K. Design of temperature sensitive imprinted polymer hydrogels based on multiple-point hydrogen bonding. Macromol. Biosci. 2004, 4, 680-684.

89. Liu XY, Ding XB, Guan Y, Peng YX, Long XP, Wang XC, Chang K, Zhang Y. Fabrication of temperature-sensitive imprinted polymer hydrogel. Macromol. Biosci. 2004, 4, 412-415.

90. Gong CB, Wong KL, Lam MHW. Photoresponsive molecularly imprinted hydrogels for the photoregulated release and uptake of pharmaceuticals in the aqueous media. Chem. Mater. 2008, 20, 1353-1358.
91. Gong CB, Lam MHW, Yu HX. The fabrication of a photoresponsive molecularly imprinted polymer for the photoregulated uptake and release of caffeine. Adv. Funct. Mater. 2006, 16, 1759-1767.
92. Alvarez-Lorenzo C, Hiratani H, Tanaka K, Stancil K, Grosberg AY, Tanaka T. Simultaneous multiple-point adsorption of aluminum ions and charged molecules a polyampholyte thermosensitive gel: Controlling frustrations in a heteropolymer gel. Langmuir. 2001, 17, 3616-3622.
93. Hiratani H, Alvarez-Lorenzo C, Chuang J, Guney O, Grosberg AY, Tanaka T. Effect of reversible cross-linker, N,N '-bis(acryloyl)cystamine, on calcium ion adsorption by imprinted gels. Langmuir. 2001, 17, 4431-4436.
94. Alvarez-Lorenzo C, Guney O, Oya T, Sakai Y, Kobayashi M, Enoki T, Takeoka Y, Ishibashi T, Kuroda K, Tanaka K, Wang GQ, Grosberg AY, Masamune S, Tanaka T. Reversible adsorption of calcium ions by imprinted temperature sensitive gels. J. Chem. Phys. 2001, 114, 2812-2816.
95. Watanabe M, Akahoshi T, Tabata Y, Nakayama D. Molecular specific swelling change of hydrogels in accordance with the concentration of guest molecules. J. Am. Chem. Soc. 1998, 120, 5577-5578.
96. Watanabe T, Ito K, Alvarez-Lorenzo C, Grosberg AY, Tanaka T. Salt effects on multiple-point adsorption of target molecules by heteropolymer gel. J. Chem. Phys. 2001, 115, 1596-1600.

97. Oya T, Enoki T, Grosberg AY, Masamune S, Sakiyama T, Takeoka Y, Tanaka, K, Wang G, Yilmaz Y, Feld MS, Dasari R, Tanaka T. Reversible molecular adsorption based on multiple-point interaction by shrinkable gels. Science. 1999, 286, 1543-1545.

98. Ito K, Chuang J, Alvarez-Lorenzo C, Watanabe T, Ando N, Grosberg AY. Multiple point adsorption in a heteropolymer gel and the Tanaka approach to imprinting: experiment and theory, Prog. Polym. Sci. 2003, 28, 1489-1515.

99. Basavaraja C, Park DY, Choe YM, Park HT, Zhao YS, Yamaguchi T, Huh DS. Dependence of molecular recognition for a specific cation on the change of the oxidation state of the metal catalyst component in the hydrogel network. Bull. Korean Chem. Soc. 2007, 28(5), 805-810.

100. Haruki M, Konnai Y, Shimada A, Takeuchi H. Molecularly imprinted polymer-assisted refolding of lysozyme. Biotechnol. Prog. 2007, 23, 1254-1257.

101. Alvarez-Lorenzo C, Concheiro A. Molecularly imprinted polymers for drug delivery. J. Chromatogr. B. 2004, 804, 231-245.

102. Sellergren B, Allender CJ. Molecularly imprinted polymers: A bridge to advanced drug delivery. Adv. Drug Deliv. Rev. 2005, 57, 1733-1741.

103. Allender CJ, Richardson C, Woodhouse B, Heard CM, Brain KR. Pharmaceutical applications for molecularly imprinted polymers. Int. J. Pharm. 2000, 195, 39-43.

104. Cunliffe D, Kirby A, Alexander C. Molecularly imprinted drug delivery systems. Adv. Drug Deliv. Rev. 2005, 57, 1836-1853.

105. Bawa R, Siegal RA, Marasca B, Karel M, Langer R. An explanation for the controlled release of macromolecules from polymers. J. Controlled Release. 1985, 1, 259-267.

106. Peppas NA, Bures P, Leobandung W, Ichikawa H. Hydrogels in pharamaceutical formulations. Eur. J. Pharm. Biopharm. 2000, 50, 27-46.

107. Brazel CS, Peppas NA. Modeling of drug release from swellable polymers. Eur. J. Pharm. Biopharm. 2000, 49, 47-58.

108. Peppas NA. Hydrogels in Medicine and Pharmacy, Vol II & III, CRC Press, Boca Raton, FL, 1987.

109. Lin CC, Metters AT. Hydrogels in controlled release formulations: network design and mathematical modeling. Adv. Drug Deliv. Rev. 2006, 58, 1379-408.

110. Tahara K, Yamamto K, Nishihata T. Overall mechanism behind matrix sustained release tablets prepared with hydroxypropyl methylcellulose 2910. J. Controlled Release. 1995, 35, 59-66.

111. Lee ES, Kim SW, Cardinal JR, Jacobs H. Drug release from hydrogel devices with rate controlling barriers. J. Membr. Sci. 1980, 7, 293-303.

112. Lee PI. Novel approach to zero-order drug delivery via immobilized non-uniform drug distribution in glassy hydrogels. J. Pharm. Sci. 1984, 73, 1344-1347.

113. Hiratani H, Alvarez-Lorenzo C. The nature of backbone monomers determines the performance of imprinted soft contact lenses as timolol drug delivery systems. Biomaterials. 2004, 25, 1105–1113.

114. Ali M, Horikawa S, Venkatesh S, Saha J, Hong JW, Byrne ME. Zero-order therapeutic release from imprinted hydrogel contact lenses within in vitro physiological ocular tear flow. J. Controlled Release. 2007, 124, 154-162.

115. Ali M, Byrne ME. Challenges and solutions in topical ocular drug-delivery systems. Expert Rev. Clin. Pharmacol. 2008, 1, 145-161.

116. Alvarez-Lorenzo C, Hiratani H, Concheiro A. Contact Lenses for Drug Delivery. Am. J. Drug Deliv. 2006, 4(3), 131-151.

117. Paul G, Steuernagal S, Koller H. Non-covalent interactions of a drug molecule encapsulated in a hybrid silica gel, Chem. Commun. 2007, 5194-5196.

118. Bogershausen A, Pas SJ, Hill AJ, Koller H. Drug release from self-assembled inorganic-organic hybrid gels and gated porosity detected by positron annihilation lifetime spectroscopy, Chem. Mater. 2006, 18, 664-672.

119. Bodhibukkana C, Srichana T, Kaewnopparat S, Tangthong N, Bouking P, Martin GP, Suedee R. Composite membrane of bacterially-derived cellulose and molecularly imprinted polymer for use as a transdermal enantioselective controlled-release system of racemic propranolol. J. Control. Release. 2006, 113, 43-56.

120. Suedee R, Seechamnanturakit V, Canyuk B, Ovatiarnporn C, Martin GP. Temperature sensitive dopamine-imprinted (N,N-methylene-bis-acrylamide cross-linked) polymer and its potential application to the selective extraction of adrenergic drugs from urine. J. Chromatogr. A. 2006, 1114, 239-249.

121. Aburto J, Mendez-Orozco A, LeBorgne S. Hydrogels as adsorbents of organosulphur compounds currently found in diesel. Chemical Engineering and Processing. 2004, 43, 1587-1595.

122. Silvestri D, Cristallini C, Ciardelli G, Giusti P, Barbani N. Molecularly imprinted bioartifical membranes for the selective recognition of biological molecules. Part 2: Release of components and thermal analysis. J. Biomater. Sci. Polymer Edn. 2005, 16, 3, 397-410.

123. Tokuyama H, Naohara S, Fujioka M, Sakohara S. Preparation of molecular imprinted thermosensitive gels grafted onto polypropylene by plasma-initiated graft polymerization, Reactive and Functional Polymers. 2008, 68, 182-188.

124. Tokuyama H, Kanazawa R, Sakohara S. Equilibrium and kinetics for temperature swing adsorption of a target metal on molecular imprinted thermosensitive gel adsorbents, Separation and Purification Technology. 2005, 44, 152-159.

125. Suedee R, Srichana T, Martin GP. Evaluation of matrices containing molecularly imprinted polymers in the enantioselective-controlled delivery of β-blockers. J. Control. Release. 2000, 66, 135-147.

126. Jiang Z, Yu Y, Wu H. Preparation of CS/GPTMS hybrid molecularly imprinted membrane for efficient chiral resolution of phenylalanine isomers, Journal of Membrane Science. 2006, 280, 876-882.

127. Takatsy A, Sedzik J, Kilar F, Hjerten S. Universal method for synthesis of artificial gel antibodies by the imprinting approach combined with a unique electrophoresis technique for detection of minute structural differences of proteins, viruses, and cells (bacteria):Ia. Gel antibodies against proteins (transferrins), J. Sep. Sci. 2006, 29, 2802-2809.

128. Takatsy A, Sedzik J, Kilar F, Hjerten S. Universal method for synthesis of artificial gel antibodies by the imprinting approach combined with a unique electrophoresis technique for detection of minute structural differences of proteins, viruses, and cells (bacteria):II. Gel antibodies against virus (Semliki Forest Virus), J. Sep. Sci. 2006, 29, 2810-2815.

129. Bacskay I, Takatsy A, Vegvari A, Elfwing A, Ballagi-Pordany A, Kilar F, Hjerten S. Universal method for synthesis of artificial gel antibodies by the imprinting approach combined with a unique electrophoresis technique for detection of minute structural

differences of proteins, viruses, and cells (bacteria):III. Gel antibodies against cells (bacteria), Electrophoresis. 2006, 27, 4682-4687.

130. Karmalkar RN, Kulkarni MG, Mashelkar RA. Pendent chain linked delivery systems: II. Facile hydrolysis through molecular imprinting effects, Journal of Controlled Release. 1997, 43, 235-243.

131. Hirayama K, Sakai Y, Kameoka K. Synthesis of polymer particles with specific lysozyme recognition sites by a molecular imprinting technique, Journal of Applied Polymer Science. 2001, 81, 3378-3387.

132. Zhao K, Cheng G, Huang J, Ying X. Rebinding and recognition properties of protein-macromolecularly imprinted calcium phosphate/alginate hybrid polymer microspheres, Reactive and Functioanl Polymers. 2008, 68, 732-741.

133. Lotierzo M, Henry OYF, Piletsky S, Tothill I, Cullen D, Kania M, Hock B, Turner APF. Surface plasmon resonance sensor for domoic acid based on grafted imprinted polymer. Biosens. Bioelectron. 2004, 20, 145–152.

134. Haupt K, Mosbach K. Molecularly imprinted polymers and their use in biomimetic sensors, Chem. Rev. 2000, 100, 2495-2504.

135. Henry O, Cullen DC, Piletsky SA. Optical interrogation of molecularly imprinted polymers and development of MIP sesnors: A review, Bioanalytical Chemistry. 2005, 382, 4, 947-956.

136. Lavine BK, Westover DJ, Kaval N, Mirjankar N, Oxenford L, Mwangi GK. Swellable molecularly imprinted polyN-(N-propyl)acrylamide particles for detection of emerging organic contaminants using surface plasmon resonance spectroscopy. Talanta. 2007, 72, 1042-1048.

137. Miyata T, Jige M, Nakaminami T, Uragami T. Tumor marker-responsive behavior of gels prepared by biomolecular imprinting. Proc. Natl. Acad. Sci. U. S. A. 2006, 103, 1190-1193

138. Hu X, Li G, Huang J, Zhang D, Qiu Y. Construction of self-reporting specific chemical sensors with high sensitivity. Adv. Mater. 2007, 19, 4327-4332.

139. Hu XB, Li GT, Li MH, Huang J, Li Y, Gao YB, Zhang YH. Ultrasensitive specific stimulant assay based on molecularly imprinted photonic hydrogels. Adv. Funct. Mater. 2008, 18, 575-583.

140. Ehrick JD, Stokes S, Bachas-Daunert S, Moschou EA, Deo SK, Bachas LG, Daunert S. Chemically tunable lensing of stimuli-responsive hydrogel microdomes, Adv. Mater. 2007, 19, 4024-4027.

141. Matsui J, Akamatsu K, Hara N, Miyoshi D, Nawafune H, Tamaki K, Sugimoto N. SPR sensor chip for detection of small molecules using molecularly imprinted polymer with embedded gold nanoparticles. Anal. Chem. 2005, 77, 4282-4285.

Table 2.1: Responsive, Intelligent Imprinted Hydrogels

Stimuli Sensitivity/Trigger	Functional Monomers/ Oligomers (Crosslinker)	Stimuli Sensitive Monomers	Crosslinking Amount (%), Template, Solvent	Characterization of Binding Parameters	Cycles	Reference
pH	Acryloylamylose inclusion complex (MBA)	AA	Low (<1%), Bisphenol-A, Water	At higher degrees of substitution of acryloyl-amylose, enhanced binding was observed. As pH increased template binding decreased as network swelled. IP bound 2.5*x* NIP.	Yes-3 cycles. Reversibility gradually decreased due to hydrolysis of ester bonds of inclusion complex.	[69]
	Semi-IPN -PVA (MW 70,000-80,000)/AA (trihydroxymethyl propane glycidol ether)	AA	Moderate (33%); MMTCA; DMSO/water (1:1)	At acidic conditions (pH 2 and 4), hydrogen bonding predominate to promote absorption while at pH 7 and 9 stereo shape effect becomes important.	No	[62]
Temperature	MAA (EGDMA)	NIPA	Low (8.7%); 4-aminopyridine; DMF	IP bound ~2.2*x* NIP in shrunken state.	Yes- 3 cycles Nearly equal amount bound after each cycle with 85% release.	[89]
	MAA (EGDMA)	NIPA	Low (12.5%), L-pyroglutamic acid, Methanol	IP bound ~2.5*x* NIP in shrunken state.	No	[88]
	MAA/ AM (MBA; EGDMA)	MBA	High, Dopamine HCl, Methanol/Water (4:1)	Imprinting factor increased as temperature increased and gel shrinks. It peaked at 35°C after which it decreased due to increased non specific binding.	No	[120]
pH/ Temperature	TBA, AM, Maleic Acid, (MBA)	TBA	Low (<1%); BSA; Methanol/ Water (1:1)	Max binding at pH 5. Binding increased with template increase in formulation (at 8.63 weight % binding nearly 5*x* that of NIP). As temperature increases, gel shrinks and binds less template (however still more than corresponding NIP)	No	[86]
Light	MAPASA (Various MBA sizes)	MAPASA	High (83%); Paracetamol; DMF/Water	Long crosslinker means high photoisomerization and low binding strength (2C~5 times 8C). N,N`–hexylene-bis-acrylamide (6C) is optimal crosslinker. NIP not photoregulated.	Yes – 3 Cycles. Decrease in release and uptake (29.1% decrease by third cycle) explained by deformation of receptors.	[90]

Template, Temperature, Salt Concentration	MAA/AM (MBA)	NIPA	Low (1.4%), Lysozyme, Tris-HCl Buffer (pH 7.0)	IP shrinks with Lys concentration. Binding in IP increases with temperature and salt concentration which decreases gel swelling (max at 20mM NaCl after which ionic interactions dominate to reduce binding; little binding at 100mM)	No	[87]
Template	AM/MAA/ DMAEM (MBA)	--	Low, Lysozyme, Tris-HCl Buffer (pH 7.0)	IP for native lysozyme promotes folding of denatured lysozyme. NIP does not promote folding.	No	[100]
	Poly(AM-g-Con A)/AM (MBA)	--	Low, α-fetoprotein; Phosphate buffer (pH 7.4)	α-fetoprotein (AFP) provides a recognition link between Con-A and antibody on differing polymer chains. When AFP is in solution, Con-A and anti-AFP are bound together by AFP which leads to shrinking of the gel.	No	[137]
	MAA/NNPA (MBA)	--	Low (5.5%), Theophylline, acetonitrile	IP swells with theophylline concentration but is unaffected by caffeine. NIP does notrespond to either molecule.	No	[136]
	MAA (EGDMA)	--	Moderate (~20%), Bovine serum albumin, anhydrous ethanol	Albumin causes hydrogel swelling in IP and not NIP. Excellent selectivity between template and lysozyme were demonstrated in competitive binding experiments.	No.	[138]
	AA (MBA)	NIPA	Low (4.7%), Dopamine, DMSO	Swelling on analyte binding that is demonstrated to be reversible.	Yes. Increasing concentrations of template are studied.	[141]

Note: For brevity, notable responsive imprinted gels references are missing for ions [45, 92-94, 98-99] and small molecules [44, 95-97]. When appropriate, crosslinking % was calculated and is equivalent to (100% x (mole crosslinking monomer/(mole crosslinking monomer and all other monomers))).Abbreviations: AA: Acrylic Acid; AFP: α-fetoprotein; AM: Acrylamide; BSA: Bovine Serum Albumin; DMAEM: 2-(dimethylene amino)ethyl methacrylate; DMF- Dimethylformamide; DMSO: dimethyl sulfoxide; EGDMA: Ethylene Glycol Dimethacrylate; IP: Imprinted Polymer; IPN: interpenetrating network; Lys: Lysozyme; MAA: Methacrylic Acid; MAPASA: 4-[(4-methacryloyloxy)phenylazo]benzenesulphonic acid; MBA-N,N–methylene-bis-acrylamide; MMTCA: 1-(4-methoxyphenyl)-5-methyl-1,2,3-triazol-4-carboxylic acid; NIP: Non-Imprinted Polymer; NIPA- N–isopropylacrylamide; NNPA N-(N-propyl)acrylamide; PVA: poly(vinyl alcohol); VA: Vinyl Acetate; TBA: N-tert-Butylacrylamide.

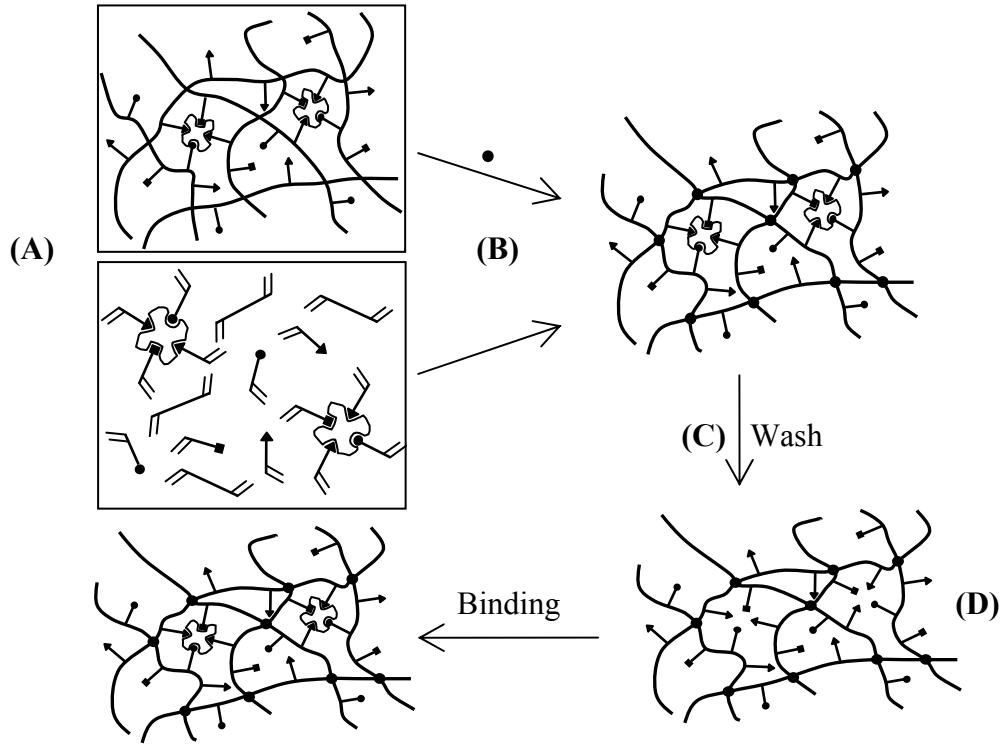

Figure 2.1: Macromolecular Memory within Crosslinked Hydrogels. (A) depicts **s**elf-assembly of template-monomer complexes within the pre-polymerization solution. This can be in the form of monomeric species or oligomers/polymers that have pendant double bonds or are reacted to other chains by another molecule (●). (**B)** depicts formation of an idealized network structure (with or without solvent) while (**C)** depicts the wash step where template is removed. (**D)** shows a macromolecular network with recognition sites consisting of functional chemistry on differing polymer chains.

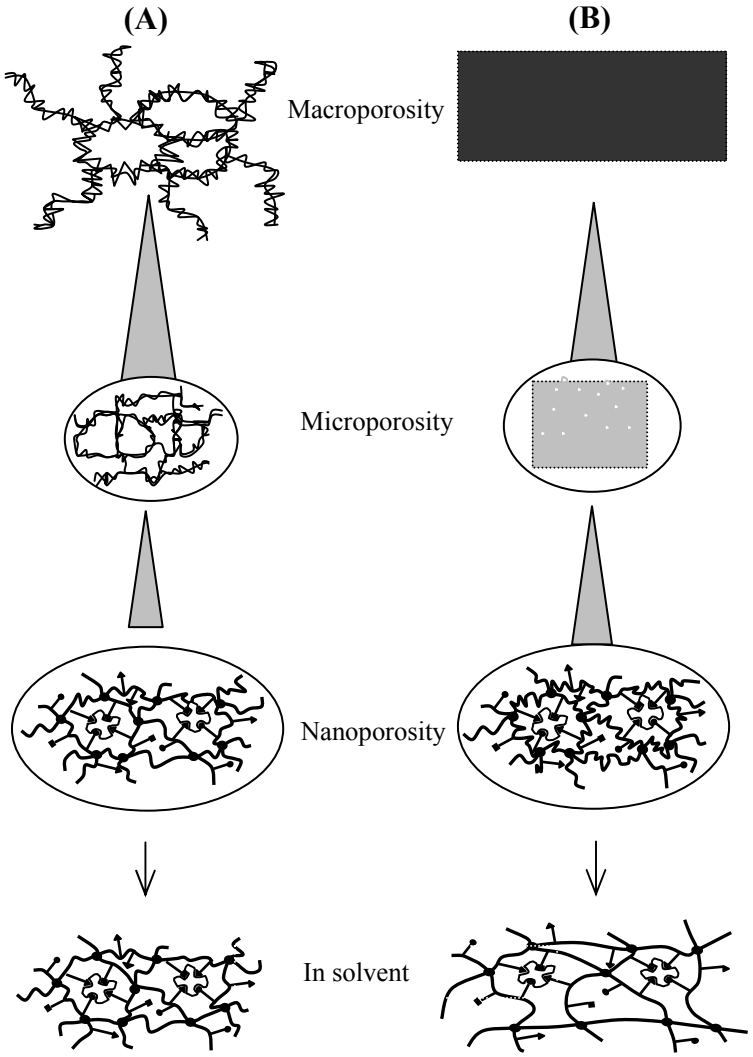

Figure 2.2: Porosity within Imprinted Hydrogels. For **i**mprinted gels prepared in solvent **(A)** the polymer will contain significant macro- and microporosity. Template transport will be primarily related to the porosity and tortuosity within the polymer, as in conventional hydrogels. For imprinted gels prepared without solvent **(B)**, the polymer will not typically exhibit macro and micro-porosity and will have small pores that approach the size of the template. Once solvated, the mesh size or the free volume within the polymer chains and the imprinting effect will influence template transport.

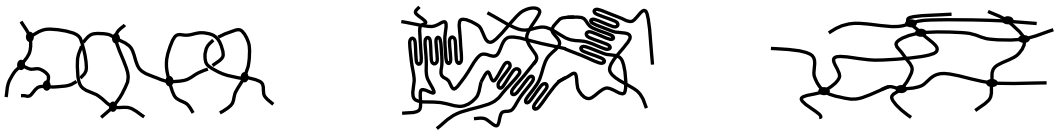

(A) **(B)** **(C)**

Figure 2.3: Types of Crosslinking in Polymer Networks. (A) Permanent physical entanglements; **(B)** Microcrystalline regions incorporating various chains; **(C)** Covalent or non-covalent bonds.

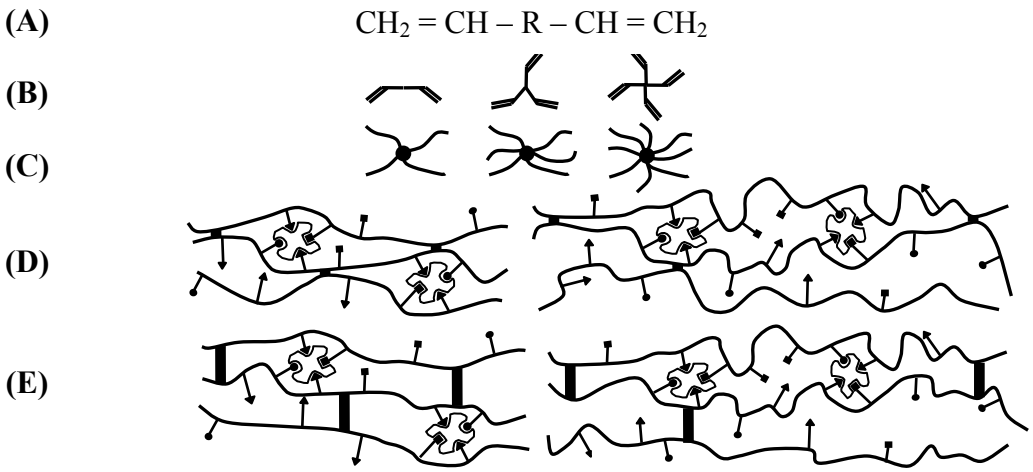

Figure 2.4: Variations in Covalent Crosslinkers. (A) depicts bifunctional crosslinker where R is the crosslinking bridge. As the length of R increases this will lead to additional flexibility in the hydrogel structure. A bifunctional crosslinking monomer **(B, left)** exhibits a tertrafunctional crosslink **(C, left)** in the gel, a tri-functional crosslinker **(B, centre)** exhibits a hexafunctional crosslink **(C, centre)**, and a tetra-functional crosslinker **(B, right)** exhibits an octafunctional crosslink **(C, right)** within the polymer gel. Gels prepared with small bifunctional crosslinking monomer at moderate concentration **(D, left)** and low concentration **(D, right)** are represented in **(D)** while those with longer bifunctional crosslinking monomer (larger R) at moderate concentration **(E, left)** and low concentration **(E, right)** are represented in **(E)**. Structures have increasing flexibility moving top to bottom with the most flexible structure on the bottom right. If the functional monomer is grafted to the polymer chain (i.e., branched, dangling functional chain), it can also have segment flexibility.

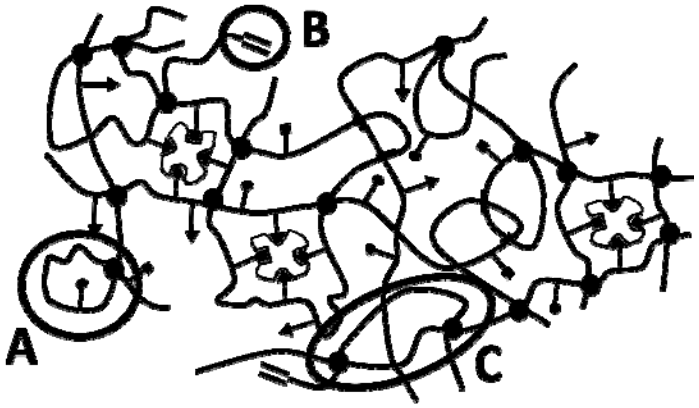

Figure 2.5: Network Imperfections in Imprinted Crosslinked Polymer Networks. A non ideal network is shown where **(A)** represents primary cycles **(B)** represents pendant double bonds and **(C)** represents secondary cycles.

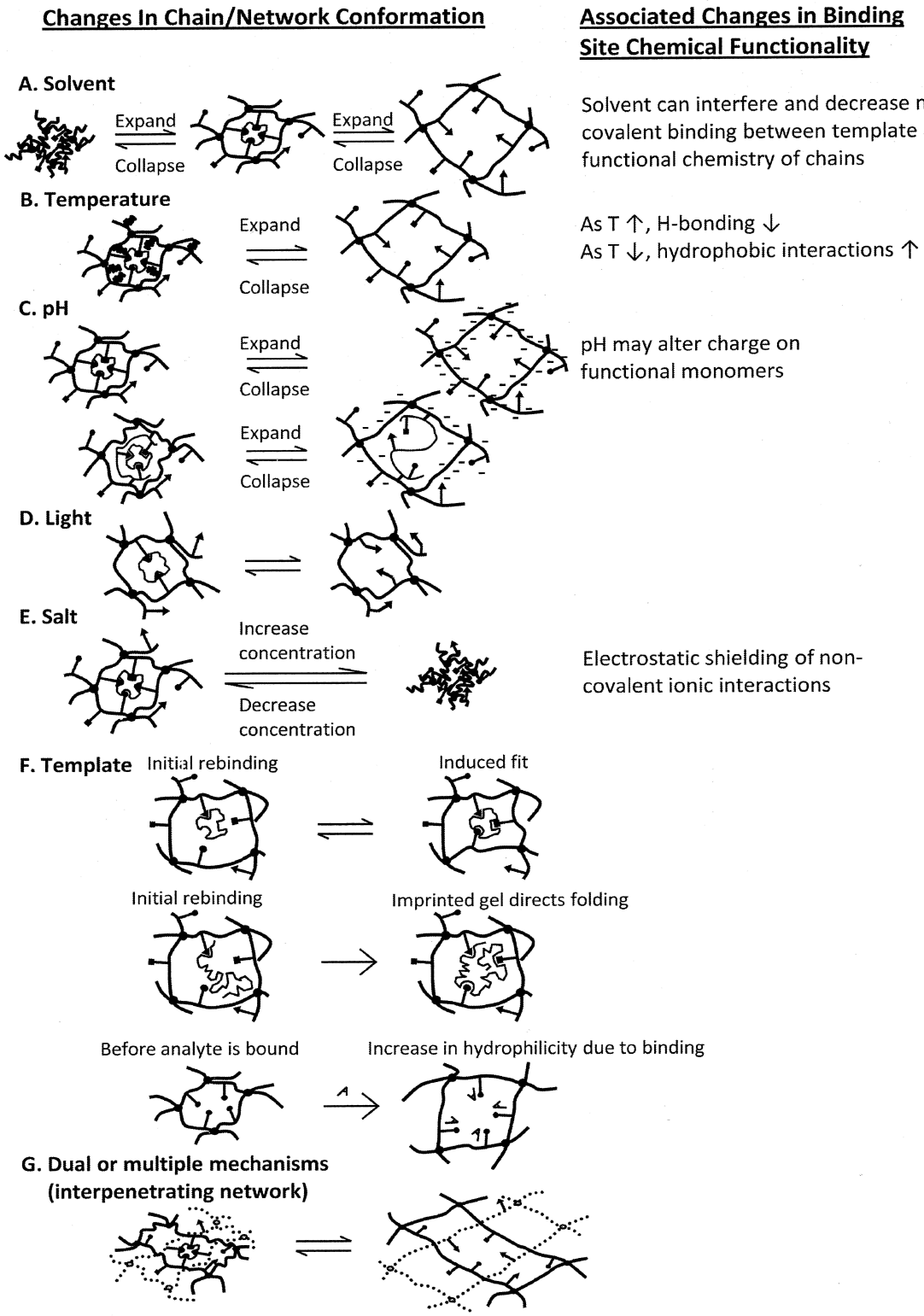

Figure 2.6: Modulatory Mechanisms within Responsive Imprinted Hydrogel Networks. Changes can occur in the chain/network conformation **(left)** and also in the binding site functional groups **(right)** leading to template recognition or release. **(A)** shows solvent-sensitive

imprinted network. The gel can collapse or expand depending on the polymer-solvent interaction. In a good solvent, the polymer chains will be solvated and the network will expand. In a poor solvent, the chains will prefer to be in close proximity to each other and the network will collapse. (**B)** shows temperature-sensitive imprinted network. Temperature sensitive groups along the polymer chains aggregate as they become more hydrophobic, with increase in temperature, leading to collapse of the polymer network [88-89, 120]. (**C)** shows pH-sensitive imprinted network. As groups along the polymer ionize (acrylic acid groups ionize at pH above ~4.5), the chains become more hydrophilic and also exhibit charge repulsion, leading to swelling and disrupting of the binding cavity. This has been demonstrated using a covalently attached amylose inclusion complex that is altered in conformation due to the movement of the network chains [62]. If the chain monomers are cationic, the gel expands as pH is decreased. (**D)** shows light-sensitive imprinted network. Light affects the conformation of functional monomers disrupting complexation [90]. (**E)** shows salt-sensitive imprinted network. As salt concentration is increased [87], the NIPA-based network collapses due to a dehydration mechanism due to destabilization of water molecules clustered around the isopropyl group. (**F)** shows template-sensitive imprinted network As template binds, the imprinted network shrinks to accommodate the template [87] and also has been demonstrated to depend on concentration of template [95]. Other methods have included imprinted gels that swell with binding of template [136] and biomolecular methods using lectin and antibody chains that complex as glycoprotein enters the network [137]. Imprinted networks have also assisted in the folding of protein [100]. (**G)** shows. dual mechanisms or interpenetrating imprinted networks. Using networks with differing stimuli-sensitivities that are physically entagled, template binding and recognition can be further controlled [62].

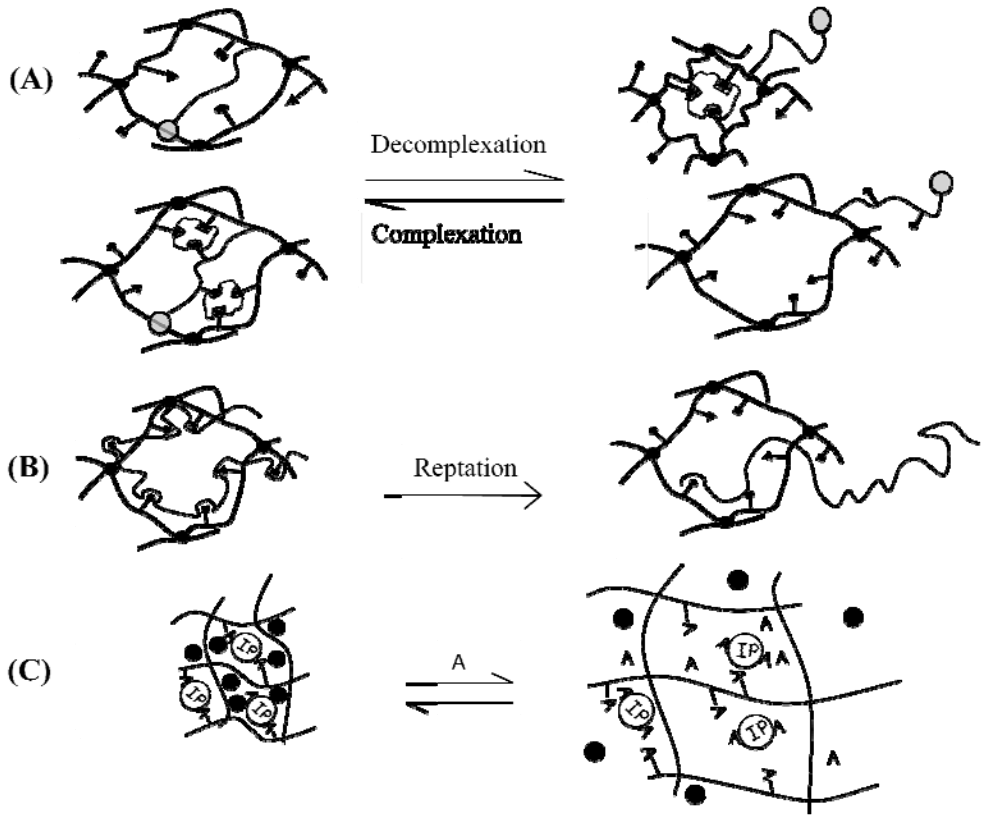

Figure 2.7: Future Modulatory Template Release of Imprinted Hydrogels. A grafted chain that reversibly complexes with group on other chains can create imprinted gels that turn recognition on and off **(A)**. This grafted chain can also have functionality that can non-covalently bind with the template. Disruption of the complex may lead to disruption of the binding site. The transport of long molecular weight molecules can be also be controlled by imprinting mechanisms **(B)**. While the size of the macromolecule and its conformation as well as the polymer mesh size will influence release, imprinting will lead to an additional level of control to delay release or turn release on and off. An imprinted polymer particle, covalently attached or bigger than network mesh, can be used as effective crosslinks in a polymer gel that has pendent attached template to the polymer chains **(C)**. When free template enters the gel, the gel will expand.

CHAPTER 3: CHARACTERIZATION OF IMPRINTED POLYMER GELS

Analysis of template binding and structural parameters of imprinted polymer gels is crucial to properly characterize and understand macromolecular recognition. In order to assess structural and recognition/transport property relationships, additional experiments and theoretical analysis is needed. The sections below provide a basis for characterizing imprinted polymer structures.

3.1 Determination of Template Binding Parameters

Imprinting effectiveness can be determined by assessment of the binding parameters of template binding affinity (i.e., the equilibrium association or dissociation constant between the ligand molecule and the network), capacity of loading (i.e., the maximum ligand bound per mass or volume of polymer) and selectivity (i.e., the ability to differentiate between the ligand and other molecules). Compared to highly crosslinked imprinted networks, weakly crosslinked gels can remove most of the template before rebinding experiments. Proper template washing procedures and verification of template removal is very important in the analysis of binding parameters. Binding characterization can be incorrect if post-polymerization washing of template is not verified.

Binding affinity is a measure of how well the template molecule is attracted to the macromolecular binding site or how well a ligand is held to the receptor site formed between the macromolecule chains. The equilibrium dissociation constant, K_d, or equilibrium association

constant, K_a, provide a quantitative measure of this level of attraction. Ligands with low K_d or high K_a values bind tightly to the receptor and have high affinity. Conversely, high K_d and low K_a values are indicative of weak template binding.

Template affinity and loading capacity can be estimated from equilibrium binding isotherms analyzing template bound versus the equilibrium template concentration. At a particular binding concentration, the amount of template bound or template partition/distribution coefficients have been used. It is common knowledge that imprinting leads to a distribution of binding sites of varying affinity. The distribution has been demonstrated in a number of systems to be bi-modal, but affinity distribution models have been successfully applied [1-2] and better approximate the heterogeneity of binding cavities within imprinted networks. Analysis has been conducted in a number of ways using theoretical or empirical based binding isotherms. Care must be taken when applying the best isotherm based on the fit of the data but also on the inherent assumptions in the underlying equations, especially if a theoretical is used.

Imprinted networks have been analyzed via limiting slope Scatchard analysis [3], Langmuir isotherms [4-7], Freundlich isotherms [5-6, 8], bi-[9-10] and tri-[11] Langmuir isotherms, and Langmuir-Freundlich isotherms [10]. Recently, isothermal titration calorimetry has thermodynamically verified differences in the binding enthalpy of template within imprinted and non-imprinted gels [4]. Using this microcalorimetric method, the binding mechanism can be elucidated with quantification of the enthalpic and entropic contributions during the binding event [12]. This technique has also been used to determine the optimum monomer template ratio [13]. We direct the reader to the following review which classifies typical dissociation constants of molecularly imprinted polymers and those of common classes of receptor-ligand interactions [14].

Selectivity, α, can be determined by a ratio of the equilibrium association or dissociation constants between two molecules (one which differs from the template in chemical functionality, orientation of chemical functionality, or physical size).

$$\propto = \frac{K_{a,template\ molecule}}{K_{a,template\ analog}} \qquad 3.1$$

In the last six years, there has been a substantial increase in the number imprinted polymer gels displaying template selectivity. For a list of papers describing imprinted gels displaying selectivity refer to Table 3.1. In most polymer gel imprinted networks, selectivity has been most commonly evaluated as the ratio of the loading capacities or partition/distribution coefficients of the template to the template analog in the gel. Also, most papers in the field, whether highly or weakly crosslinked imprinted structures, do not provide a competitive challenge of various molecules including the template.

Demirel et al. [15] describe a polymer gel with N-tert-butylacrylamide and maleic acid as functional monomers interacting with bovine serum albumin as template. Acrylamide was used to form the backbone while N,N`-methylene-bis-acrylamide served as the crosslinking monomer. The selectivity of the gels increased as the template percentage in the formulation increase. A maximum selectivity of 4.2 was reached at 8.63 weight% of template whereas the non-imprinted gel was unselective (with a value of 0.9).

Similarly selectivities were demonstrated by Hawkins et al. [16], Liu et al. [17] and others [18-19]. Liu and coworkers determined selectivity on the distribution coefficients of the template (L-pyroglutamic acid) and analog molecules in separate binding experiments. Three template analogues were used (2-pyrrolidone, L-proline, pyrrolidone), and imprinted gels exhibited selectivities of 2.5, 3.0, and 5.1, respectively. The poly(AM-co-MBA) prepared by Hawkins and

coworkers bound more than 90% of the template (Bovine Hemoglobin) while rejecting nearly 80% of the template analogs (cytochrome C and myoglobin).

Larger molecules such as viruses [20-21] and DNA [22] have been imprinted and these networks have demonstrated selectivity. For example, fragments of DNA were imprinted and electrophoresis experiments with a cocktail of fragments revealed decreased migration of template within the imprinted gel. Also, most analogues, that only differed by a few base pair substitutions, did not demonstrate decreased migration.

Notably, Fazal and Hansen [23] have shown that the differing binding capacities of poly(allylamine hydrochloride) imprinted networks crosslinked with epichlorohydrin are correlated with the octanol/water partition coefficients. Their gels were prepared in a manner similar to the original papers that highlighted selective recognition [24-25], but multiple templates were used (D-glucose-6-phosphate monobarium salt, D-glucose, L-glucose, barium hydrogen phosphate and D-gluconamide) to prepare five different imprinted gels. All gels showed preferential binding for glucose and the selectivities were reasonably similar irrespective of the template used.

These results illustrate that better analysis must be conducted when performing selectivity studies. It is recommended that “reverse selectivity” experiments be carried out where the selectivity of analog imprinted polymers towards the template is measured. This emphasizes selective imprinting and eliminates the effect of preferential binding of the template to the networks via non-specific interactions. Some other important steps that may affect the results include the selection of the template analog and the verifying of template removal post-polymerization. Insufficient washing results in the reported binding values being lower than the

actual values due to residual template present before the rebinding step. Also, it is also recommended that template octanol/water partition coefficients be calculated, which are not presented for the majority of systems in the literature.

However, some groups do carry out additional experiments in the form of competitive challenge [4-5, 26-27] and reverse selectivity [23, 28]. For example, Chen et al. [28] have shown excellent results for lysozyme recognition in polymer gels. Not only are seven different template analogs used to perform competitive selectivity studies, but lysozyme and cytochrome c are used to create two separate imprinted gels in addition to the non-imprinted polymer gels. Both imprinted gels selectively bound the template with lysozyme imprinted gels exhibiting selectivities of 2.5 and 5. Xia and coworkers [5] have also demonstrated competitive selectivity experiments of hemoglobin imprinted semi-interpenetrating polymer gel networks. Kimhi and Bianco-Peled [4] also carried out reverse selectivity and competitive binding experiments between the lysozyme and cytochrome c, demonstrating selectivity of lysozyme imprinted gels.

3.2 Structural Characterization of Imprinted Gels

There have been some excellent reviews characterizing polymer gel structures. We direct the reader to the following references [28-29]. Structural assessment of imprinted polymer gels can be achieved by analysis of the following related parameters: the polymer volume fraction in the swollen state (i.e., the amount of water absorbed by the gel), the average molecular weight between two adjacent crosslinking or junction points, and the average correlation distance between two adjacent crosslinking or junction points (i.e., the average mesh size or free space between the macromolecular chains available for transport).

Factors such as the extent or degree of crosslinking in the network, the size and flexibility of the crosslinking monomer, and the type of chemical groups that comprise the polymer chains, both functional that non-covalently interact with the template and those that do not, primarily affect the swelling and mesh structure of imprinted polymer gel structures. Typically, higher crosslinked imprinted gels have a tighter mesh structure and swell to a lesser extent than weakly crosslinked gels. Imprinted gels containing more hydrophilic moieties tend to swell more than gels containing hydrophobic groups, which will minimize their chain exposure to aqueous solvent.

Equilibrium swelling and rubber elasticity theories have been used to characterize the structural parameters of polymer gels. Flory-Rehner theory states that a crosslinked polymer gel in equilibrium is subject to two opposing forces, the thermodynamic force of mixing and the elastic, restrictive force of the polymer chains [30-31]. At equilibrium, the total Gibbs free energy is zero and these two forces are equal as *Equation 3.2* denotes.

$$\Delta G_{total} = \Delta G_{elastic} + \Delta G_{mixing} \qquad 3.2$$

Differentiating *equation 3.2* with respect to the number of solvent molecules, while keeping the temperature and pressure constant, will yield an equivalent equation in terms of chemical potential. At equilibrium, the chemical potential of the solvent outside and inside the gel must be equal. The change in chemical potential due to elastic restrictive forces of the polymer chains can be determined from the theory of rubber elasticity [31], and the change in chemical potential due to mixing can be expressed using the heat and entropy of mixing. Essentially, this measures the interaction and compatibility of the polymer chains with the solvent molecules. By equating these two contributions, an expression can be written for the determination of the molecular

weight between two adjacent crosslinks of a neutral, non-ionized, imprinted polymer gel prepared without solvent,

$$\frac{1}{M_c} = \frac{2}{M_n} - \frac{\left(\frac{\bar{\vartheta}}{V_1}\right)[\ln(1-\vartheta_{2,s})+\vartheta_{2,s}+\chi_1\vartheta_{2,s}^2}{[(\vartheta_{2,s})^{\frac{1}{3}} - \left(\frac{\vartheta_{2,s}}{2}\right)]} \tag{3.3}$$

where M_c is the average molecular weight between crosslinks, M_n is the average molecular weight of the polymer chains prepared under identical conditions in the absence of crosslinking agent, V_1 is the molar volume of solvent (e.g., V_1 for water is 18.1 cm^3/mol), υ is the specific volume of the polymer (i.e., the reciprocal of density), χ_1 is the Flory polymer-solvent interaction parameter, and $\upsilon_{2,s}$ is the polymer volume fraction in the swollen state. The polymer volume fraction in the swollen state is related to the volume swelling ratio, Q, which can calculated from equilibrium swelling experiments as follows:

$$Q = \frac{1}{\vartheta_{2,S}} = \frac{V_{2,S}}{V_{2,d}} \tag{3.4}$$

where $V_{2,S}$ is the swollen gel volume at equilibrium, $V_{2,d}$ is the volume of the dry polymer, and $\upsilon_{2,S}$ is the polymer volume fraction in the swollen state. The relaxed polymer volume fraction is the volume of the dry polymer divided by the relaxed polymer volume. The volume of the gel in the swollen, relaxed, or dry state can be obtained by using Archimedes buoyancy principle [28].

If the imprinted network is prepared in the presence of solvent, the Peppas and Merrill equation [32] must be used (*equation 3.5*). It is a modification of the Flory-Rehner theory to include the presence of solvent, which modifies the chemical potential due to elastic forces. The molecular weight between adjacent crosslinks in a neutral, imprinted gel prepared in solvent is determined by *equation 3.5*,

$$\frac{1}{\overline{M_c}} = \frac{2}{\overline{M_n}} - \frac{\left(\frac{\bar{\vartheta}}{V_1}\right)[\ln(1-\vartheta_{2,s})+\vartheta_{2,s}+\chi_1\vartheta_{2,s}^2}{\vartheta_{2,r}[(\frac{\vartheta_{2,s}}{\vartheta_{2,r}})^{\frac{1}{3}} - \left(\frac{\vartheta_{2,s}}{2\vartheta_{2,r}}\right)]} \quad 3.5$$

where $v_{2,r}$ represents the polymer volume fraction in the relaxed state. It is defined as a physical property of the polymer immediately after crosslinking before swelling or collapse of the network. If the imprinted network contains a number of ionic moieties, an ionic contribution is added to the expression of chemical potential,

$$\mu_1 - \mu_{1,0} = \Delta\mu_{elastic} + \Delta\mu_{mixing} + \Delta\mu_{ionic}) \quad 3.6$$

where μ_1 is the chemical potential of the solvent in the polymer gel, $\mu_{1,o}$ is the chemical potential of pure solvent, and μ_{ionic} is the ionic contribution term. Equations have been derived for both anionic and cationic gels prepared in the presence of solvent [33, 34]. For anionic, imprinted gels, *equation 3.7* can be used,

$$\frac{V_1}{4I}\left(\frac{\vartheta_{2,s}^2}{\bar{\vartheta}}\right)\left(\frac{K_a}{10^{-pH}-K_a}\right)^2 = \left[\ln(1-\vartheta_{2,s}) + \vartheta_{2,s} + \chi_1\vartheta_{2,s}^2\right]$$

$$+\left(\frac{V_1}{\bar{\vartheta}\overline{M_c}}\right)\left(1-\frac{2\overline{M_c}}{\overline{M_n}}\right)\vartheta_{2,r}\left[\left(\frac{\vartheta_{2,s}}{\vartheta_{2,r}}\right)^{\frac{1}{3}} - (\frac{\vartheta_{2,s}}{2\vartheta_{2,r}}\right) \quad 3.7$$

where ionic strength is I and K_a is the equilibrium constant for the acid. For basic, imprinted gels, the term containing the acid equilibrium constant K_a is replaced by K_b in the numerator and 10^{pH-14}- K_a in the denominator. In networks containing weakly acidic or basic pendent groups, water uptake can result in ionization of pendent groups depending on the solution pH and ionic composition. The gels then act as semi-permeable membranes to the counterions influencing the osmotic balance between the polymer gel and the external solution. The equilibrium degree of swelling increases as the pH of the external solution increases for ionic gels containing weakly acidic pendent groups. The equilibrium degree of swelling increases as the pH decreases for gels

containing weakly basic pendent groups. In an ampholytic gel, containing both acidic and basic groups, the isoelectric pH determines the transitional pH of swelling of the gel. An increase in the ionic content of the gel increases the hydrophilicity leading to faster swelling and a higher equilibrium degree of swelling. Numerous physicochemical parameters contribute to the swelling of ionic polymer gels, including the ionic content, ionization equilibrium considerations, nature of counterions, and nature of the polymer [35-37].

In cases where the swelling of the gel can be influenced by the complexation of multiple chains via multiple non-covalent interactions with the template, we believe that another free energy term must be added to reflect the complexation contribution of multiple polymer chains due to imprinting. While the numerical significance and weight of this contribution has yet to be realized, in theory, multiple, strong, non-covalent interactions, such as those with highly functionalized templates interacting with multiple chains, can lead to less expansion of imprinted networks compared to non-imprinted networks. For imprinted polymer gels that demonstrate template associated swelling differences, the free energy associated with template-chain complexation may need to be included as a term in *equation 3.2*, presented below as *equation 3.8*. Thus, there is now opportunity and need to develop this theoretical framework.

$$G_{Total} = G_{elastic} + G_{mixing} + G_{Imprinting\ complexation} \qquad 3.8$$

The average molecular weight between crosslinks, $\overline{M_C}$ of imprinted polymer gels can be determined from the theory of rubber elasticity [30-31]. For an isotropic, swollen, imprinted polymer gel synthesized without solvent, with a constant deformation volume, *equation 3.9* is valid for short elongation ratios of up to 2:

$$\tau = \left(\frac{RT\vartheta_{2,s}^{\frac{1}{3}}}{\bar{\vartheta}\overline{M_c}}\right)\left(1 - \frac{2\overline{M_c}}{\overline{M_n}}\right)(\alpha - \frac{1}{\alpha^2}) \quad 3.9$$

where τ is the stress, α is the elongation ratio in any direction (final length/initial length), R is the universal gas constant, and T is the absolute temperature.

If, $\overline{M_C} << \overline{M_N}$, $\left(1 - \frac{2\overline{M_c}}{\overline{M_n}}\right) \rightarrow 1$, *equation 3.9* becomes,

$$\tau = \left(\frac{RT\vartheta_{2,s}^{\frac{1}{3}}}{\bar{\vartheta}\overline{M_c}}\right)(\alpha - \frac{1}{\alpha^2}) \quad 3.10$$

Stress-strain data is typically obtained by performing tensile studies on a dynamic mechanical analyzer. Polymer gels can be cut into thin sheets, clamped between the two parallel arms of the dynamic mechanical analyzer and subjected to a linear load until breaking point. Strain values are converted into the elongation function $\left(\alpha - \frac{1}{\alpha^2}\right)$ and the slope can be used to calculate $\overline{M_C}$. If the imprinted gel is prepared in the presence of solvent, *equation 3.11* is used.

$$\tau = \left(\frac{RT\vartheta_{2,s}^{\frac{1}{3}}}{\bar{\vartheta}\overline{M_c}}\right)\left(1 - \frac{2\overline{M_c}}{\overline{M_n}}\right)\left(\alpha - \frac{1}{\alpha^2}\right)(\frac{\vartheta_{2,s}}{\vartheta_{2,s}}) \quad 3.11$$

The space available for diffusion, occurring through the space available between macromolecular chains is regarded as the pore or mesh size. A structural parameter that is often used in describing the size of pores is the correlation length, ξ, which is defined as the linear distance between two adjacent crosslinks [28, 38]. It can be calculated by e*quation 3.12*,

$$\xi = \alpha(\bar{r}_0^2)^{\frac{1}{2}} = \vartheta_{2,s}^{-\frac{1}{3}}(\bar{r}_0^2)^{\frac{1}{2}} \quad 3.12$$

where α is the elongation ratio, which for gels that swell isotropically can be related to the swollen polymer volume fraction, $\upsilon_{2,s}$ as shown. The unperturbed end-to-end distance of the polymer chain between two adjacent crosslinks can be calculated using the following,

$$(\bar{r}_0^2)^{\frac{1}{2}} = l(C_n N)^{\frac{1}{2}} \quad 3.13$$

where C_n is the Flory characteristic ratio or rigidity factor of the polymer, l is the length of the bond along the polymer backbone (e.g., for vinyl polymers equals 1.54 Å), and N is the number of links per chain between crosslinks that can be calculated from *equation 3.14*.

$$N = \frac{2\bar{M}_c}{\bar{M}_r} \quad 3.14$$

where M_r is the molecular weight of repeating units from which the polymer chain is composed. For heteropolymers, this can be a weighted average of the monomers that make up the polymer chains assuming equal reactivity. If reactivity ratios differ greatly, the polymer chains will not reflect the feed composition. In light of recent results demonstrating enhanced network binding properties of multiple, different functional monomers interacting non-covalently with the template [39-40], there is a need to explore differences in reactivity of monomers due to complexation with the template pre-polymerization, which has not been adequately studied to date. Combining equations [28, 38], yields:

$$\xi = \vartheta_{2,S}^{-\frac{1}{3}} \left(\frac{2C_n\bar{M}_c}{M_r}\right)^{\frac{1}{2}} l \quad 3.15$$

The crosslinking density, ρ_x, can be calculated from:

$$\rho_x = \frac{1}{\bar{\vartheta}\bar{M}_c} \quad 3.16$$

These calculations along with one-dimensional transport studies of template and template analogues can fully characterize the structural architecture of imprinted gels. Nitrogen porosimetry experiments or positron annihilation lifetime spectroscopy [41] can complement

gravimetric analysis of gel swelling and can lead to pore size analysis. In template transport applications, such as membrane separation, drug delivery carriers, etc., a proper analysis of structural parameters and their relation to binding parameters and template transport is crucial to the design and understanding of such systems.

3.3 Determination of Template Transport in Imprinted Gels

Mass transfer of the template through the imprinted polymer will depend on a number of structural and physiochemical considerations. For imprinted gels prepared in solvent (i.e., macro or microporous gels), the template diffusion coefficient will be primarily related to the porosity and tortuosity within the polymer, as in conventional polymer gels [28-29]. For polymers with relatively small pores that approach the size of the template and nanoporous polymers (i.e., polymers exhibiting free volume mostly within the polymer chains or with the mesh), the template can experience delayed transport due to steric hindrance of the polymer chains or the 'screening effect' due to the crosslinked structure and the mobility of the polymer chains excluding template. The chains can also increase the frictional drag on the template [42]. Delayed transport can also occur due to the imprinting effect and binding of the template in the binding cavities between the chains [40].

Recently, our group has exploited molecular imprinting methods to delay the transport of drug via interaction of the drug with numerous functional groups organized within the network [40]. The drug's heightened interaction with the memory pockets slowed its transport within the polymer gel despite comparable free volume within the polymer chains for drug transport. One-dimensional permeation studies showed that the gel with maximum incorporated chemical functionality had the lowest diffusion coefficient, which was at least an order of magnitude lower

than all other gels studied. All imprinted networks had significantly lower diffusion coefficients than non-imprinted networks, in spite of comparable mesh sizes and equilibrium polymer volume fractions in the swollen state. It is important to note that no solvent was used in the formulation. Since permeation studies showed different template permeation rates after lag/breakthrough times, we proposed the "tumbling hypothesis", wherein a molecule tumbling through an imprinted network with multiple, organized functionalities and an appropriate mesh size, experiences heightened, transient interactions with memory sites and shows delayed transport kinetics. This could also be partially due to bound template temporarily obstructing free template transport. Thus, the structural plasticity of polymer chains, i.e. the organization of functional groups into memory sites, may be responsible for enhanced loading and extended release.

Template transport depends on the size and chemistry of the template, the macromolecular structure and organization of the network chains (i.e., mesh size or mesh free-volume), the macro/micro porosity (which is reflected in the polymer volume fraction of the gel), and tortuosity of the polymer. Without careful consideration of structure and porosity, transport analysis and the effect of imprinting on template transport cannot be correctly ascertained. Recent work has demonstrated that network mesh structure as well as the micro- and macro-porosity of the polymer can significantly impact the ability to extend drug release via enhanced affinity networks prepared by molecular imprinting [43]. Essentially differences in polymer porosity, which can even exist between imprinted and their corresponding non-imprinted control structures due to the inclusion of template or aggregation of template, can overshadow the contributions of enhanced affinity for the template. It is clear that more study is needed on the design, formation, and understanding of structure- property relationships of such systems. Since

recognition and loading take place between the polymer chains, a smaller polymer volume fraction in the swollen state will decrease template loading capacity. Thus, imprinted polymer gels prepared with solvent will have reduced template binding capacities and demonstrate less 'imprinted' control over the release profile compared to a similar imprinted polymer prepared without solvent.

There are some excellent reviews of mechanisms and models of solute diffusion within polymer gels [42] and a number of references that discuss free-volume [28, 44], hydrodynamic [28, 45], and obstruction [46] theories and models as well as solute-polymer interactions [46-48]. These models can be applied to imprinted polymer gels; however, depending on the porosity, the binding of the template within the polymer chains should be considered and will decrease transport. Thus, considering most theories do not include solute-polymer interactions, there is considerable opportunity to provide a theoretical framework for template diffusion phenomena with imprinted polymer gels. For a list of papers decribing template release/transport in imprinted polymer gels refer to Table 3.2

3.4 References

1. Rampey AM, Umpleby RJ, Rushton GT, Iseman JC, Shah RN, Shimizu KD. Characterization of the imprint effect and the influence of imprinting conditions on affinity, capacity, and heterogeneity in molecularly imprinted polymers using the freundlich isotherm-affinity distribution analysis. Anal. Chem. 2004, 76, 4, 1123-1133.
2. Umpleby II RJ, Bode M, Shimizu KD. Measurement of the continuous distribution of binding sites in molecularly imprinted polymers. Analyst. 2000, 125, 7, 1261-1265.
3. Lubke C, Lubke M, Whitcombe MJ, Vulfson EN. Imprinted polymers prepared with stoichiometric template-monomer complexes: efficient binding of ampicillin from aqueous solutions, Macromolecules. 2000, 33, 5098-5105.
4. Kimhi O, Bianco-Peled H. Study of the interactions between protein-imprinted hydrogels and their templates. Langmuir. 2007, 23, 6329-6335.
5. Xia YQ, Guo TY, Song MD, Zhang BH, Zhang BL. Hemoglobin recognition by imprinting in semi-interpenetrating polymer network hydrogel based on polyacrylamide and chitosan. Biomacromolecules. 2005, 6, 2601-2606.
6. Espinosa-Garcia BM, Argelles-Monal WM, Hernandez J, Felix-Valenzuela L, Acosta N, Goycoolea FM. Molecularly imprinted chitosan-genipin hydrogels with recognition capacity toward o-xylene. Biomacromolecules. 2007, 8(11), 3355-3364.
7. Hiratani H, Alvarez-Lorenzo C. The nature of backbone monomers determines the performance of imprinted soft contact lenses as timolol drug delivery systems. Biomaterials. 2004, 25, 1105–1113.
8. Umpleby RJ, Baxter SC, Bode M, Berch JK, Shah RN, Shimizu KD. Application of the freundlich isotherm in the characterization of molecularly imprinted polymers, Analytica Chimica Acta. 2001, 435, 35-42.

9. Chen Y, Kele M, Quinones I, Sellergren B, Guiochon B. Influence of the pH on the behavior of an imprinted polymeric stationary phase — supporting evidence for a binding site model, Journal of Chromatography A. 2001, 927, 1–17.
10. Li X, Husson SM. Adsorption of dansylated amino acids on molecularly imprinted surfaces: A surface plasmon resonance study. Biosensors and Bioelectronics. 2006, 22, 336-348.
11. Kim H, Kaczmarski K, Guiochon G. Mass transfer kinetics on the heterogeneous binding sites of molecularly imprinted polymers. Chemical Engineering Science. 2005, 60, 5425-5444.
12. Chen W, Chen C, Lin F. Molecular recognition in imprinted polymers: thermodynamic investigation of analyte binding using microcalorimetry, Journal of Chromatography A. 2001, 923, 1-6.
13. Alvarez-Lorenzo C, Yanez F, Barreiro-Iglesias R, Concheiro A. Imprinted soft contact lenses as norfloxacin delivery systems. J. Controlled Release. 2006, 113, 236-244.
14. Hilt JZ, Byrne ME. Configurational biomimesis in drug delivery: molecular imprinting of biologically significant molecules. Adv. Drug Deliv. Rev. 2004, 56, 1599-1620.
15. Demirel G, Ozcetin G, Turan E, Caykara T. pH/temperature-sensitive imprinted ionic poly (N-tert-butylacrylamide-co-acrylamide/maleic acid) hydrogels for bovine serum albumin. Macromolecular Bioscience. 2005, 5, 1032-1037
16. Hawkins DM, Stevenson D, Reddy SM. Investigation of protein imprinting in hydrogel-based molecularly imprinted polymers (HydroMIPs). Anal. Chim. Acta. 2005, 542, 61-65.

17. Liu XY, Guan Y, Ding XB, Peng YX, Long XP, Wang XC, Chang K. Design of temperature sensitive imprinted polymer hydrogels based on multiple-point hydrogen bonding. Macromol. Biosci. 2004, 4, 680-684.
18. Wang B, Liu MZ, Liang R, Ding SL, Chen ZB, Chen SL, Jin SP. MMTCA Recognition by molecular imprinting in interpenetrating polymer network hydrogels based on poly(acrylic acid) and poly(vinyl alcohol). Macromol. Biosci. 2008, 8, 417-425.
19. Gong CB, Lam MHW, Yu HX. The fabrication of a photoresponsive molecularly imprinted polymer for the photoregulated uptake and release of caffeine. Adv. Funct. Mater. 2006, 16, 1759-1767.
20. Bolisay LD, Culver JN, Kofinas P. Molecularly imprinted polymers for tobacco mosaic virus recognition. Biomaterials. 2006, 27, 22, 4165-4168.
21. Bolisay LD, Culver JN, Kofinas P. Optimization of virus imprinting methods to improve selectivity and reduce nonspecific binding, Biomacromolecules. 2007, 8, 3893-3899.
22. Ogiso M, Minoura N, Shinbo T, Shimizu T. Detection of a specific DNA sequence by electrophoresis through a molecularly imprinted polymer. Biomaterials. 2006, 27, 4177-4182.
23. Fazal FM, Hansen DE. Glucose-specific poly(allylamine) hydrogels – A reassessment. Bioorganic & Medicinal Chemistry Letters. 2007, 17, 1, 235-238.
24. Parmpi P, Kofinas P. Biomimetic glucose recognition using molecularly imprinted polymer hydrogels. Biomaterials. 2004, 25, 1969-1973.
25. Wizeman WJ, Kofinas P. Molecularly imprinted polymer hydrogels displaying isomerically resolved glucose binding. Biomaterials. 2001, 22, 1485–91.

26. Wang B, Liu MZ, Liang R, Ding SL, Chen ZB, Chen SL, Jin SP. MMTCA Recognition by molecular imprinting in interpenetrating polymer network hydrogels based on poly(acrylic acid) and poly(vinyl alcohol). Macromol. Biosci. 2008, 8, 417-425.
27. Ogiso M, Minoura N, Shinbo T, Shimizu T. Detection of a specific DNA sequence by electrophoresis through a molecularly imprinted polymer. Biomaterials. 2006, 27, 4177-4182.
28. Peppas NA. (Ed.) Hydrogels in Medicine and Pharmacy. 1987, Volume I: Fundamentals, CRC Press, Boca Raton, FL.
29. Peppas NA, Bures P, Leobandung W, Ichikawa H. Hydrogels in pharamaceutical formulations. Eur. J. Pharm. Biopharm. 2000, 50, 27-46.
30. Flory PJ, Rehner J. Statistical mechanics of cross-linked polymer networks. II Swelling. J. Chem. Phys. 1943, 11, 521-526.
31. Flory PJ. Principles of Polymer Chemistry. 1953, Cornell University Press, Ithaca, NY.
32. Peppas NA, Merrill EW. Crosslinked poly(vinyl alcohol) hydrogels as swollen elastic networks. J. Appl. Polym. Sci. 1977, 21, 1763-1770.
33. Ricka J, Tanaka T. Swelling of ionic gels: quantitiative performance of the Donnan theory. Macromolecules. 1984, 17, 2916-2921.
34. Brannon L, Peppas NA. Equilibrium swelling behavior of pH-sensitive hydrogels. Chem. Eng. Sci. 1991, 46, 715-722.
35. Peppas NA, Khare A. Preparation, structure and diffusional behavior of hydrogels in controlled release. Adv. Drug Deliv. Rev. 1993, 11, 1-35.
36. English AE, Tanaka T, Edelman ER. Polyelectrolyte hydrogel instabilities in ionic solutions. J. Chem. Phys. 1996, 105, 10606-10613.

37. English AE, Tanaka T, Edelman ER. Polymer and solution ion shielding in polyampholytic hydrogels. Polymer. 1998, 39, 5893-5897.
38. Canal T, Peppas NA. Correlation between mesh size and equilibrium degree of swelling of polymeric network. J. Biomed. Mater. Res. 1989, 23, 1183-1193.
39. Venkatesh S, Sizemore SP, Byrne ME. Biomimetic hydrogels for enhanced loading and extended release of ocular therapeutics. Biomaterials. 2007, 28, 717-724.
40. Venkatesh V, Saha J, Pass S, Byrne ME. Transport and structural analysis of molecularly imprinted hydrogels for controlled drug delivery. Eur. J. Pharm. Biopharm. 2008, 69, 852-860.
41. Bogershausen A, Pas SJ, Hill AJ, Koller H. Drug release from self-assembled inorganic-organic hybrid gels and gated porosity detected by positron annihilation lifetime spectroscopy, Chem. Mater. 2006, 18, 664-672.
42. Amsden B. Solute Diffusion within Hydrogels. Mechanisms and Models. Macromolecules. 1998, 31, 8382-8395.
43. Byrne ME, Hilt JZ, Peppas NA. Recognitive biomimetic networks with moiety imprinting for intelligent drug delivery. J. Biomed. Mater. Res. Part A. 2008, 84A, 137-147.
44. Lustig SR, Peppas NA. Solute diffusion in swollen membranes. 9. Scaling laws for solute diffusion in gels. J. Appl. Polym. Sci. 1988, 36, 735-747.
45. Cukier RI. Diffusion of Brownian spheres in semidilute polymer-solutions. Macromolecules. 1984, 17, 252-255.
46. Amsden B. Solute diffusion in hydrogels. An examination of the retardation effect. Polym. Gels Networks. 1998, 6, 13-43.

47. Valente AJM, Polishchuk AY, Burrows HD, Miguel MG, Lobo VMM. Sorption/diffusion behavior of anionic surfactants in polyacrylamide hydrogels: from experiment to modeling. Eur. Polym. J. 2003, 39, 1855-1865.
48. Cheng M, Sun Y. Observation of the solute transport in the permeation through hydrogel membranes by using FTIR-microscopy. J. Membr. Sci. 2005, 253, 191-198.
49. Chen ZY, Hua ZD, Xu L, Huang Y, Zhao MP, Li YZ. Protein-responsive imprinted polymers with specific shrinking and rebinding. J. Mol. Recognit. 2008, 21, 71-77.
50. Kublickas R, Werner C, Jariene G, Voit B, Lasas L. Polyacrylamide gels containing ionized functional groups for the molecular imprinting of human growth hormone. Polym. Bull. 2007, 58, 611-617.
51. Oral E, Peppas NA. Responsive and recognitive hydrogels using star polymers. J. Biomed. Mater. Res. Part A. 2004, 68A, 439-447.
52. Alvarez-Lorenzo C, Hiratani H, Gomez-Amoza JL, Martinez-Pacheco R, Souto C, Concheiro A. Soft contact lenses capable of sustained delivery of timolol. J. Pharm. Sci. 2002, 91, 2182-2192.
53. Hiratani H, Mizutani Y, Alvarez-Lorenzo C. Controlling drug release from imprinted hydrogels by modifying the characteristics of the imprinted cavities. Macromol. Biosci. 2005, 5, 728-733.
54. Singh B, Chauhan N. Preliminary evaluation of molecular imprinting of 5-fluorouracil within hydrogels for use as drug delivery systems, Acta Biomaterialia. 2008, 4, 5, 1244-1254.
55. Paul G, Steuernagal S, Koller H. Non-covalent interactions of a drug molecule encapsulated in a hybrid silica gel, Chem. Commun. 2007, 5194-5196.

56. Puoci F, Iemma F, Muzzalupo R, Spizzirri UG, Trombino S, Cassano R, Picci N. Spherical molecularly imprinted polymers (SMIPs) via a novel precipitation polymerization in the controlled delivery of sulfasalazine, Macromol Biosci. 2004, 4, 22-26.

57. Spizzirri UG, Peppas NA. Structural analysis and diffusional behavior of molecularly imprinted polymer networks for cholesterol recognition. Chem. Mater. 2005, 17, 6719-6727.

58. Cai W, Gupta RB. Molecular-imprinted polymers selective for tetracycline binding. Sep. Purif. Methods. 2004, 35, 215-221.

Table 3.1: Imprinted Gels Displaying Selectivity

Functional Monomers/Oligomers (Crosslinker)	Crosslinking Amount (%), Template, Solvent	Selectivity Assessment (Template Analogues)	Reference(s)
MAA/DEAEM/AM (MBA)	Low (0.9%), Lysozyme, Tris-HCL buffer(pH 7)	Competitive binding at conc. ratios of CyC/template of less than one, IP bound 3.5x more than NIP, for conc. ratios >1 IP bound ~12x more template. Analogue imprinted gel demonstrated more analogue binding than lysozyme. (cytochrome c)	[4]
MAA/AM (MBA)	Low (1.4%), Lysozyme, Tris-HCl buffer (pH 7)	Competitive binding with Lys-IP preferentially bound Lys over CyC (~5*x),* myoglobin (~2.5*x*). The other proteins, unlike the template in size/structure, show very little binding to Lys-IP and NIP. (CyC, myoglobin, BSA, horseradish peroxidase, trypsin inhibitor, Hb)	[49]
TBA/AM/Maleic Acid (MBA)	Low (<1%), Bovine Serum Albumin, Methanol/Water (1:1)	Template/analogue bound ratio increases with template percentage in monomer mix (0.9 for NIP to 4.2 for IP made with 8.63 wt% template) (casein)	[15]
Semi-IPN Chitosan/AM (MBA)	Low (2.4%), Bovine Hemoglobin, Buffered water	Competitive binding distribution coefficient (DC) of IP for template was 83 and too little to be detected for analogue. NIP DC for template was 1.9 and 2.9 for analogue. (bovine serum albumin)	[5]
VDAT/AM (MBA)	Low (2.3%) dsDNA (564 base pair fragment) and verotoxin DNA, Buffered water	Electrophoresis detection experiments with mixed DNA samples, template had decreased migration distance due to hindrance binding in gel. 2 of 3 base pair substitutions with Verotoxin DNA IP did not show decreased migration.	[22]
DEAEM/MAA/AM (MBA)	Low (4.3%), Human growth hormone (22kDa) and dimmer (44kDa), PBS buffer (pH 6.2)	IP for dimer binds monomeric hGH ~2x less than dimeric template. IP for dimer binds trimer ~3x less as dimeric template. Other proteins demonstrate very low binding (0.4-1.5%) (Human growth hormone dimers(44kDa), trimers (66kDa), BSA(66kDa), HSA (66kDa), lysozyme)	[50]
PAA-HCl (MW 15,000) (epichlorohydrin)	Low, Tobacco Mosaic Virus, Water	IP bound 8.8 mg TMV/ g IP, NIP bound 4.2 mg TMV/g NIP. Ratio of binding capacity of TMV/ TNV is ~2 for IP and identical for NIP. TMV is rod shape(300nm length, 18nm diameter) and TNV is icosahedral shape (24nm diameter). (TNV)	[20]
PAA-HCl (MW 15,000) (ethylene glycol diglycidyl ether)	Low, Tobacco Mosaic Virus, Water	IP bound 2.7 mg TMV/ g IP, NIP bound 1.18 mg TMV/g NIP. Ratio of binding capacity of TMV/ TNV is ~7.8 for IP and ~1.8 for NIP. (TNV)	[21]
AM (MBA)	Low (10%), Bovine Hemoglobin, Water	For IP, 90% of template in solution bound as opposed to 20% of analogues (CyC, myoglobin)	[16]
Star PEG polymers/MAA (PEG600DMA)	Low(11% v/v) D-Glucose; Water	Selectivity of ~3.1 is shown for glucose over fructose by the 31 arm polymer (5970 g/mol per arm; 450,000 M_n (g/mol)) while the 75 arm polymer (20,000 g/mol per arm; 624,000 M_n (g/mol)) showed no selectivity. (D-fructose)	[51]
MAA (EGDMA)	Low (12.5%), L-Pyroglutamic Acid Methanol	IP distribution coefficient (DC) for template ~5, 3, 2.5*x* larger than that for corresponding analogues. DC's in NIP similar for all analytes and ~4*x* less than IP for template. (pyrrolidine, L-proline, 2-pyrrolidine)	[17]
Semi-IPN -PVA (MW 70,000-80,000)/AA (trihydroxymethyl propane glycidol ether)	Moderate (33%), MMTCA, DMSO/Water (~1:1)	Competitive binding capacity for MMTCA/ riboflavin was ~2.6 and MMTCA/ aspirin was ~10. Note: aspirin is smaller and riboflavin has a different molecular geometry. (aspirin, riboflavin)	[18]

MAPASA (Various MBA sizes)	High (83%), Paracetamol, DMF/Water	As crosslinker increased in length, template binding affinity decreased and capacity increased. Analogues show ~ 10% or less binding compared to 45% for the template. (phenacetin, antifebrin)	[19]

Note: Binding takes place in aqueous solution unless specified. When appropriate, crosslinking % was calculated and is equivalent to (100% x (mole crosslinking monomer/(mole crosslinking monomer and all other monomers))). Abbreviations: AA: Acrylic Acid; AM: Acrylamide; BSA: Bovine serum albumin; CyC: Cytochrome C; DBT: Dibenzothiophene; DBTS: Dibenzothiophene Sulfone; DEAEM: 2-(dimethylamino)ethyl methacrylate; DMF: Dimethylformamide; EGDMA: Ethylene Glycol Dimethacrylate; Hb: Hemoglobin; HAS: Human serum albumin; IP: Imprinted Polymer; IPN: Interpenetrating Network; Lys: Lysozyme; MAA: Methacrylic acid; MAPASA: 4-[(4-methacrylolyoxy)phenylazo] benzenesulfonic acid; MBA: N,N–methylene-bis-acrylamide; MMTCA: 1-(4-methoxyphenyl)-5-methyl-1,2,3-triazol-4-carboxylic acid; NIP: Non-Imprinted Polymer; NIPA: N–isopropylacrylamide; PAA-HCl: Poly(allylamine hydrochloride); PEG: Polyethylene glycol; PEG600DMA: Poly(ethylene glycol)600 dimethacrylate; PVA: Poly(vinyl alcohol); TBA: N-tert-butylacrylamide; TFMAA: 2-(trifluoromethyl)acrylic acid; TRIM: Trimethylolpropane Trimethacrylate; DMDBT: 4,6-dimethyl dibenzothiophene; TNV: Tobacco Necrosis Virus; TMV: Tobacco Mosaic Virus; VDAT: 2-vinyl-4,6-diamino-1,3,5-triazine; VPD: 4-vinylpyridine.

Table 3.2: Imprinted Hydrogel Template Release/Transport

Functional Monomers (Crosslinker)	Crosslinking Amount (%), Template, Solvent	Characterization of Binding Parameters	Characterization of Template Release/Transport	IP Structural/ Swelling Analysis	Reference
HEMA/MAA (EGDMA) **HEMA/MMA (EGDMA)**	Low (0.128%), Timolol, No solvent	HEMA/MAA IPs bind 12 mg/g at pH 5.5, NIPs bind 4 mg/g. HEMA/MMA IPs demonstrate poor binding	90-100% release in 9 hrs	Swelling	[52]
MAA (EGDMA)	Low, Timolol, No solvent	IP demonstrated higher affinity than NIP	Template diffusion coefficients were calculated from template release studies. The diffusion coefficient from IP at certain M/T ratios (16/1, 32/1) 2 orders of magnitude lower than NIP. Lowest IP diffusion coefficient approaching 10^{-10} cm^2/s)	Swelling	[53]
HEMA/ AA/ AM/ NVP (PEG200DMA)	Low (5%), Ketotifen fumarate, No solvent	Most biomimetic IP (AA/ AM/ NVP/HEMA functional monomers) bound 21.3mg/g, with NIP binding 3.4 mg/g (~8x greater than single functional monomer IP)	IP demonstrated delayed release compared to NIP. Most biomimetic, or more functionalized gels exhibited more delayed release compared to less functionalized gels. Most diverse network released 65% of template in 3.5 days and 100% in 5 days.	Swelling	[39]
HEMA/ AA/ AM/ NVP (PEG200DMA)	Low (5%), Ketotifen fumarate, No solvent	Partitioning of template into IP gels composed of multiple functional monomer was ~8x greater than less diverse IPs. Each IP bound more template than corresponding NIP.	One-dimensional transport studies show template diffusion coefficient 2 orders of magnitude lower ($7x10^{-10}$ cm^2/s) in most diverse IP with comparable gel mesh sizes and equilibrium polymer volume fractions. All IP gels had lower template diffusion coefficients than corresponding NIP with comparable mesh sizes.	Swelling & Structural Analysis	[40]
AA or VPD (EGDMA)	Low (1%), Norfloxacin, No solvent	IP loaded more than NIP Highest loading at M/T of 3:1 and 4:1.	IP polymer release extended compared to NIP. IP at M/T 4/1 released 40% template in 24 hrs.	Swelling	[13]
AM; (EGDMA; PEGnDMA)	Variable (80, 67, 30%), Glucose, DMSO	Binding of glucose analogue in water, tighter mesh-sized IP networks demonstrate increased affinity and capacity	No differences between IP and controls, different porosity and mesh structure affected release in water	Swelling	[43]
HEMA/AA (MBA)	Low (~2.5%) 5-fluorouracil, water	IP bound 1.3 mg/g gel and NIP bound 0.7 mg/g gel.	Gels were dried and release evaluated under swelling when placed in water. Template diffusion coefficients calculated from release data indicate 2.3 $x10^{-7}$ cm^2/s with no evidence of imprinting delaying release.	Swelling	[54]
Self-assembled silica and hybrid organo-silica sol-gel	Persantin, Ethanol/water	Drug included in formulation, but no binding information presented	Hydrophobic interactions dominated drug dissolution and release. Polar end of drug interacts with hydrophilic SiOH groups	Pore Size	[41, 55]
MAA (EGDMA)	Moderate (57%), Sulfasalzine, Acetonitrile/Toluene (77/23 vol %)	None reported	IP particle release slower than NIPs. NIPs release 100 % and IPs release 80 % in 5 hours. Average IP and NIP particle sizes are different.	No	[56]
MAA (EGDMA)	Moderate and High (44% & 77%), cholesterol, THF; THF/DMSO; THF/water; THF/water/salt	Higher crosslinked structures had higher binding compared to NIP (maximum at 77% was ~ 13 times)	Transport of template into gel for up to 1500 minutes. IP had lag time in binding.	Swelling & Structural Analysis	[57]

MAA (EGDMA)	Moderate and High (50-90%), Tetracycline	Range with highest partition coefficient (80% crosslinked) of 107.4 and 3.84 mg/g; IP partition coefficients 3-5 times higher than controls. 50% crosslinked gels bound 2.19mg/g template.	IP shows slower release kinetics. However, only 20% released at 8 hrs with no further release	No	[58]

Note: Adapted from reference [32]. We direct the reader to reference [32] for a list that contains additional entries of transport or release of template from highly crosslinked, rigid networks. When appropriate, crosslinking % was calculated and is equivalent to (100% x (mole crosslinking monomer/(mole crosslinking monomer and all other monomers))). Abbreviations: AA: acrylic acid; AM: acrylamide; DMF: dimethylformamide; DMSO: Dimethyl Sulfoxide; EGDMA: ethylene glycol dimethacrylate; HEMA: 2-hydroxyethylmethacrylate; IP: imprinted polymer; MAA: methacrylic acid; MBA- N,N–methylene-bis-acrylamide;MMA: methyl methacrylate; M/T: Monomer template ratio; NAA: N-acryloyl-alanine polymer; NIP: non-imprinted polymer; NVP: N-vinyl 2-pyrrolidinone; PEG200DMA: poly(ethylene glycol)200 dimethacrylate; THF: Tetrahydrofuran; VPD: 4-vinylpyridine.

CHAPTER 4: CONTROLLING POLYMER STRUCTURE USING LIVING RADICAL POLYMERIZATION

4.1 Introduction

Radical polymerization is one of the most versatile chemical reactions as it allows for the conversion of a wide variety of vinyl monomers into polymeric materials. The extremely high reactivity of the radicals provides great versatility and tolerance of a wide variety functional groups during polymerization allowing for the use of a broad spectrum of monomers and additives at various reaction conditions [1-2]. Unfortunately, this high reactivity also results in a large number of undesirable side reactions resulting in significant branching as well as a loss of control of the molecular weight and tacticity of the polymer [3-5]. Living radical polymerization promises better control over these parameters.

The heterogenous structures produced by free radical polymerization (FRP) are due to the drastic difference between the slow initiation rate of the radicals and the subsequent fast propagation and termination of the radicals. This results in an unbalanced growth of polymer chains dictated by the concentration of monomers around the growing radicals. As a result, polymers prepared using free radical polymerization typically display a broad molecular weight distribution. The speed of the free radical polymerization reaction combined with the heterogeneity of the reaction environment result in non-stereospecific addition of the vinyl monomers to the propagating radical chain. This results in a predominance of atactic polymers being formed. The tacticity of a polymer is an important determinant in its mechanical, thermal

and electrical properties. For example, the lower critical solution temperature (LCST) of N-isopropyl acrylamide (NIPAM) polymers in water is governed by their tacticity. An increase in the isotacticity of NIPAM results in decreased LCST so much so that polymers with isotacticity greater than 70% are insoluble [6]. As a result, early applications of radical polymerization were to create cheap polystyrene and polyethylene polymers for low strength applications. However, the promise of a simple, versatile, economical process combined with a growing demand for polymeric materials has fueled research in overcoming problems associated with high polydispersity and atacticity.

In this chapter, techniques to achieve control over molecular weight as well as tacticity in polymers formed using free radical polymerization are discussed. First, the role of functional moieties and interacting solvents in the formation of heterogeneity in polymers is discussed in detail by analyzing the effect of their presence on the free radical polymerization reaction. The resultant heterogeneity in polymers formed as well as the negative impact on their properties is also discussed. This is especially relevant to the field of molecular imprinting of polymers where polymer networks with molecular memory for template molecules are created. Molecularly imprinted polymers demonstrate poorer binding and transport characteristic due to the heterogeneity in the polymer networks formed using free radical polymerization. Next, we discuss some novel techniques which may alleviate the problem of heterogeneity in polymer networks. Living radical polymerization has been successfully used to control the molecular weight of polymer chains and is a promising solution for eliminating network imperfections in crosslinked polymers by controlling the rate of chain growth during polymerization reaction. In addition, the use of stereospecific polymerization to improve the tacticity of polymers is

examined. Lastly, the improvements in properties of imprinted polymer networks, specifically, the binding and transport characteristics will be detailed.

4.2 Effect of Interacting Species on Free Radical Polymerization

Free radical polymerization reactions, as described earlier, are generally very fast reactions driven by the reactivity of the carbon radicals. One of the side effects of the high reactivity of the carbon radical is an increased sensitivity to functional moieties present during radical polymerization. This includes functional groups substituted on the vinyl monomers as well as other interacting species, such as solvents, salts and template molecules used for molecular imprinting. The presence of interacting species during polymerization affects the polymerization reaction. As a result, the properties of the polymer networks formed are also affected. A variety of interacting species can, thus, be introduced into the pre-polymerization solution to modify the properties of the resultant polymer networks. The molecular imprinting technique exploits this attribute to create polymer networks with improved binding and transport characteristics for a template molecule.

4.2.1 Effect of Solvents

Solvents are often used in crosslinked polymer networks to improve porosity, swelling characteristics, and molecular transport through the polymer. The use of solvents is especially useful for highly crosslinked gels where using a high concentration of short crosslinking monomers results in rigid networks with very poor swelling characteristics. Early investigations into the effect of solvents on polymerization reactions were inconclusive because the solvents tended to be very similar to the monomers in size and functionality. However, with the use of solvents that actively interact with the reacting species a change in the propagation constant (k_P), which is a measure of the rate of propagation, was observed. In fact, the interaction between

various species during polymerization can affect not only the stereoselectivity and regioselectivity of monomer addition but also monomer reactivity.

The rate of propagation of the macroradical is governed by its mobility and flexibility in solution. As a result, as the intra and inter molecular interactions around a macroradical are varied, the polymer chain length and tacticity are affected. For example, a solvent that interacts with a macroradical provides increased stability to the growing macroradical, resulting in improved stereo specificity and monodispersity. It has also been demonstrated that solvents such as benzyl alcohol, dimethylsulfoxide, N-methylpyrrolidone and others resulted in significantly increased k_P values for styrene and methyl methacrylate polymerization reactions [7-9].

The effect of solvent interaction with the propagating radical often dictates the properties of the polymer formed. As a result, careful selection of a solvent is necessary to eliminate undesirable reaction products. When used strictly as a porogen it is important to minimize solvent interaction with monomer and the propagating radical.

4.2.1.1 Effect of Polar Solvents

Polar solvents are especially effective at changing the reactivites of polar monomers. Polymerization studies of MAA [10] and NVP [11] showed a tenfold increase in the k_P values as the solvent concentration was increased to 60wt%. As described earlier, the determining factor here is the mobility of the propagating radical. In this instance, hydrogen bonding between the carbonyl group on the propagating radical and the monomer/solvent affects the rotational mobility of the macroradical. The macroradical participates in inter as well as intramolecular hydrogen bonding. The intramolecular hydrogen bonding hinders the reptation of the macroradical. The solvent molecules, in this case water, are much smaller than the monomers

allowing them to compete better with the intramolecular hydrogen bonding. This results in higher k_P values. Lewis acids of metal salts demostrate similar behavior forming co-ordinate bonds with the carbonyl groups in polar monomers [12-14]. Bamford et al. [14] were the first to demonstrate that the presence of a Li ion during polymerization of acrylonitrile resulted in increased rate of polymerization and consequently higher molecular weight polymers. The degree of ionization is another important factor affecting the propagation constant. An increase in the degree of ionization has been demonstrated to decrease k_p values in dilute solutions [15-16]. However, as the concentration of monomer is increased, the influence of the degree of ionization decreases significantly.

4.2.1.2 Effect of Non-Polar Solvents

Inert solvents can also affect the rate of polymerization as long as there is a significant difference in the size of the monomer and solvent molecules. In solution polymerization, solvent and monomer molecules compete to be in position to react with the propagating macroradical. If the solvent molecule is larger than the monomer molecule, the local monomer concentration around the reactive chain end increases since the smaller monomer can diffuse to the active site more readily. This results in higher k_p values. Conversely, if the solvent molecule is smaller, the local monomer concentration is lower than the overall concentration resulting in lower k_p values. The effect of a non-interacting solvent is most prominent in dilute solutions. When the monomer concentration is increased, this effect is muted.

4.2.2 Effect of Other Interacting Species

Lewis acids of metal salts have also been used to achieve greater control over the stereospecificity of polymers. Relatively small quantities of meitnerium triflate have been shown to achieve great control over the tacticity of acrylamide and methacrylamide polymers [17-19].

The Lewis acid of meitnerium triflate interacts strongly with the amide groups on the monomers during polymerization to form higher proportions of isotactic polymers. Similarly, scandium triflate was used to achieve syndiotactic poly(methyl methacrylate) (PMMA) polymers [20]. This is consistent with previous results where the complexation of Lewis acids with polar conjugated monomers has been shown to lead to alternating cross-propagation [21].

4.2.2.1 Molecular Imprinting and Free Radical Polymerization

Molecular imprinting is a technique used to create macromolecular memory for a template molecule within a polymer network. It is based on a specific interaction between the template molecule and one or more monomers to form a template-monomer complex which is incorporated into the polymer network and results in enhanced template binding in the polymer network. Molecular imprinting has traditionally been associated with highly crosslinked polymer networks due to the decreased flexibility of the polymer chains. The lower flexibility was hypothesized to aid the creation of template specific memory due to the retention of the shape specificity of the polymer chains forming the template complexation site [24-26]. However, recently it has been demonstrated [27-29] to work effectively even in weakly crosslinked polymers with flexible polymer chains. The key to the effective use of molecular imprinting in weakly crosslinked polymers is to strengthen the interaction of the template with the polymer chains by using complementary chemistry rather then shape specificity. Molecular imprinting in weakly crosslinked polymers is, thus, favored by heteropolymer systems. Typically, one type of functional monomer does not provide optimal interactions between the polymer chains and the template (i.e., depending on the chemistry of the template molecule, each functional monomer will have preferred and more energetically favorable interactions with certain chemical groups on the template). Imprinting can organize the incorporation of monomers within the growing

polymer chains in a low energy state conformation that favors multiple point complexation with the template. Increasing the potential for growing polymer chains with template binding complexes to reach a global energy minimum during network formation, will lead to increased memorization of the chain conformation and enhance template binding parameters in both highly and weakly crosslinked polymers. Multiple monomer-template interactions, thus, play a crucial role in forming well-designed imprinted polymers [30]. The strength of the monomer-template complexation would be much stronger in the presence of multiple interacting species and it may thus accommodate the presence of some solvents without demonstrating a significant loss in binding properties.

While the use of heteropolymers systems to induce stronger template complexation is beneficial for better memory creation, it leads to even more heterogeneity in the polymer network formed. The presence of interacting molecules affects the rate of propagation of the polymer radicals and has been demonstrated to result in increased polydispersity in the polymer chains [10-11, 15]. Other reports have shown that the presence of template molecule also affects the tacticity of the polymers formed [22-23]. In crosslinked polymer networks, this would result in greater heterogeneity in the polymer mesh structure as well as a number of imperfections in the network as shown in Figure 4.1. The use of multiple monomers to create better template binding properties only exacerbates this problem by introducing additional heterogeneity into the system The active species in free radical polymerization, the carbon radical, is very reactive towards the C-C double bonds in vinyl monomers resulting in extremely fast propagation and thus a rapid growth of the polymer chains. The carbon radical is also extremely reactive towards other radicals in the polymerization system, resulting in rapid termination via combination or disproportionation. This becomes a significant factor at high monomer conversions. In addition,

the radical undergoes chain transfer reactions by abstracting the hydrogen from C-H bonds in polymers and solvents. This results in undesirable branching in the polymers. Unconjugated monomers, which do not have a stabilizing group, tend to form even more reactive radicals, resulting in some degree of head to head propagation. In the presence of multiple monomers with different reactivites to the propagating radical it becomes even more difficult to control polymer formation. It should be noted that network formation does limit the contribution of the interacting species since the polymer chains tend to lose their mobility drastically as they approach the gelation point.

4.3 Living Radical Polymerization to Control Molecular Weight and Tacticity of Polymer Chains

Living or controlled radical polymerization is a term used to describe a set of polymerization techniques where the chain growth of the polymer is controlled by an extremely fast, reversible activation and deactivation of the reacting species [1-2]. Currently, the most popular living radical polymerization techniques are nitroxide –mediated polymerization (NMP) also known as stable free radical polymerization (SFRP), atom transfer radical polymerization (ATRP) and reversible addition-fragmentation chain transfer (RAFT). As described before, the broad molecular weight distribution associated with free radical polymerization is due to the fast propagation and termination reaction combined with slow initiation of the radicals. During living radical polymerization, the growing radical chain end is reversibly deactivated forming a dormant species. This allows for controlled propagation where all polymer chains grow at nearly the same rate. The key to molecular weight control with all of these techniques lies in the speed of the activation-deactivation process of the reacting species. Molecular weight control can only be achieved when the activation-deactivation process is faster than the propagation rate of the

monomers. Therefore, systems need to be chosen carefully taking into account the reactivities of the monomers.

NMP (Figure 4.2) involves cleaving the C-ON bond using heat to generate a stable aminoxyl or nitroxyl radical and a reactive carbon radical. The carbon radicals undergo controlled propagation to form monodisperse polymer chains. 2,2,6,6-tetramethylpiperidin-N-oxyl (TEMPO) was the primary mediator used as a mediator/ chain transfer agent for NMP, and it was initially used for synthesis of block copolymers [31]. However, the TEMPO based reactions are limited to styrene polymers, and they also require high temperatures (125°C) due to high dissociation energy of the C-ON bond [32]. Recently, several other nitroxides [33-36] have been used to replace TEMPO as the mediator offering greater variety in terms of monomers that can be used. However, a fairly high temperature (around 90°C) is still required for NMP. As a result, NMP is not suitable for polymerization reactions where non-covalent interactions play a significant role in controlling polymer formation.

ATRP, also known as metal-catalyzed radical polymerization, involves the cleavage of the C-X bond by the oxidation of the central metal to form a metal ligand and the active carbon radical [37-38]. Greater control of the polymerization reaction can be achieved by careful selection of the central metal, the associated ligand as well the halogen atom [39-42]. Thus, ATRP offers significant versatility and it can be applied to various vinyl monomers including methacrylates, acrylates, and styrenics, but it is very important that the system be chosen carefully. ATRP can also be used within a fairly wide temperature range from -80°C to 150°C and with a fairly wide selection of solvents including aqueous solvents. However, care must be taken with polar solvents since they may deactivate the metal catalyst by complexation. A newer variation is reverse ATRP where the metal is present in a higher oxidation state while the polymerization is

initiated by a traditional azoinitiator. Reverse ATRP in conjunction with normal ATRP can be used to achieve excellent control to create block copolymer systems.

RAFT is the most recently developed technique [43-44], and it is arguably the most versatile. It is applicable for the polymerization of a wide variety of conjugated and unconjugated vinyl monomers in the presence of organic and polar solvents including aqueous solutions [45-48]. The RAFT mechanism (Figure 4.2) consists of the reversible activation of a C-SC(S)Z group by an active carbon radical to form a dormant species. Dithiocarbonyl compounds provide the reversible chain transfer group while a traditional azoinitiator is used to initiate the polymerization reaction. The greatest advantage of RAFT is that both the dithicarbonyl reagents and the dormant macroradicals are non-reactive to polar and ionic groups. As a result, polymerization reactions where polar species participate significantly are best suited to be used with RAFT. Some examples of stereospecific radical polymerization systems described earlier which need Lewis acids to regulate stereospecific polymer chain growth as well molecularly imprinted polymers, especially if the monomer-template interaction is based on hydrogen bonding or ionic interactions.

The processes described above offer great molecular weight control and there have been reports of reduced heterogeneity in the polymers. However, the polymer chain growth is still predominantly non-stereospecific and the resultant polymers are largely atactic. Hence, additional methods are necessary to control tacticity and molecular weight.

4.3.1 Stereochemical Control in Living Radical Polymerization

Recently, reagents controlling stereospecificity have been introduced into living radical polymerization reactions to achieve combined control of molecular weight and tacticity. ATRP

can be used to carry out these reactions, but RAFT is generally preferred due to its greater stability in the presence of polar and ionic reagents. There are two key factors in achieving simultaneous control of molecular weight and tacticity: the presence of a polar carbonyl group on the vinyl monomers to achieve stereospecific control using polar or ionic solvents, and a lack of interaction between the RAFT agent and the polar solvents. It is very important that neither reagent interfere with the other. This process is applicable to a fairly wide variety of vinyl monomers including amides, acrylamides, methacrylamides and methacrylates among others.

Dual control has been demonstrated for the creation of poly(NIPAM) using RAFT polymerization in the presence of yttrium triflate and methanol/toluene as a solvent [49-50]. The stereospecific control proceeds independent of the RAFT mechanism allowing for the formation of a higher proportion of isotactic poly(NIPAM). However, the presence of the Lewis acid results in an increase in the k_p values as described in section 4.2.2, resulting in a small increase in the observed polydispersity. Similar control can also be achieved for a variety of polymers by using other triflates in conjunction with RAFT [51-53].

Dithiobenzoate mediated RAFT polymerization of PMMA in the presence of scandium triflate resulted in great control of tacticity. However, the molecular weight control was significantly lesser due to interference by the Lewis acid. Conversely, using trithiocarbonate as the RAFT agent instead of dithiobenzoate demonstrated a dramatic improvement in molecular weight control while the isotacticity was maintained [54-55]. This demonstrates the necessity of selecting the right reagents.

Hydrogen bonding has also been demonstrated to offer effective control of stereospecificity in living radical polymerization reaction. Stereospecific control of RAFT mediated

polymerization of N,N-dimethylacrylamide was achieved by the introducing thiourea additives [56]. The strength of the hydrogen bond being weaker than the co-ordinate bond by the triflates resulted in lower isotacticity. However, the molecular weight control of the RAFT process was virtually unaffected resulting in polymers with very low polydispersity indices (1.1-1.3). The weak interaction of hydrogen bonding also necessitated the use of fairly high concentrations of the thiourea additive. In addition, a low temperature (20°C) during polymerization was necessitated due to the tendency of hydrogen bonds to dissociate at high temperatures.

Thus, stereospecific polymer chain growth with molecular weight control can be achieved by using polar reagents and solvents in conjunction with ATRP or RAFT. Greater stereospecific control is achieved by selecting reagents which form strong interactions with the monomer. However, as the strength of the interactions increases, there is a loss of molecular weight control as the polar interactions interfere with the chain transfer mechanism of the living radical polymerization process. Therefore, an optimization of these factors is necessary to balance the stereospecific control versus the molecular weight control to achieve the desired polymer.

4.4 Living Radical Polymerization in Polymer Networks

Living polymerization was introduced as a means to control the molecular weight during the creation of polymer chains. However, this type of reaction can have significant benefits in the production of polymer gels and networks. Consequently, a few researchers have investigated the effect of living polymerization in polymer network formation as well as the formation of highly branched polymers [57-64]. Fukuda et al. [57-59] used TEMPO based NMP to demonstrate that divinyl based crosslinked networks showed delayed gelation, decreased gel fraction in the polymer network as well a significant decrease in microgel regions over conventional free radical polymerization methods. Matyjaszewski et al. [39, 60-61] used ATRP to demonstrate

similar results. In addition, Matyjaszewski and co-workers attempted to determine the change in gel point due to the use of living polymerization. They were able to successfully demonstrate that the gel point in living polymerization reactions is delayed by nearly 70% over that of polymers prepared via conventional free radical polymerization. The relatively slow initiation combined with extremely fast propagation and termination during free radical polymerization typically leads to high heterogeneity in polymer chain growth. Conversely, the characteristic decrease in the rate of propagation observed during living radical polymerization results in a slow and simultaneous growth of polymer chains. In addition, the rapid transfer between active and dormant states of the living radicals allows greater control over the number of active polymer chains resulting in a nearly uniform number of growing polymer chains throughout the polymerization process, even at high monomer conversions. As a result, the intra molecular crosslinking, and microgel formation (Figure 4.3) typically observed with conventional free radical polymerization is absent in living radical polymerization [58].

Recently, RAFT has been used to create amphiphilic polymer networks and highly branched polymers where the decreased rate of propagation allows for the formation of stable, functional amphiphillic species [65]. These networks also demonstrated increased swelling ratios and an increase in the molecular weight between crosslinks. Although these results are promising, more work is needed to demonstrate that the use of living polymerization can lead to more homogenous polymer networks with significantly improved bulk properties. A majority of the recent investigators have focused on the ability of living polymerization to create complex structures within polymer networks.

4.4.1 Living Radical Polymerization to Improve Molecular Imprinting within Polymer Networks

Template binding properties are strongly dependent on the network structure of imprinted polymer networks; hence, it is important to study the details of the polymerization reaction. For example, network structure of free radical polymerizations of multifunctional monomers depends upon monomer/macromer size, flexibility, functionality, the amount of solvent and concentration of monomers and initiators, initiation methods and initiation rate, as well as diffusional constraints of the propagating polymer chains. Conventional free radical polymerization is highly non-ideal and differences in theory and experimental data indicate heterogeneity within the network structure [66-71]. Research work on non-imprinted structures has involved the examination of major variables that control crosslinking polymerization rate, conversions, and final crosslink density. While a lower concentration of crosslinking monomer and lower final conversion will produce less densely crosslinked networks, other factors, such as the pendant double bond reactivity which is based upon monomer size, monomer stiffness, co-monomer ratio, and solvent concentration, significantly affect the structure and heterogeneity of the resulting polymeric network. Typically, a pendant double bond is formed when one end of a crosslinking agent reacts in a polymer chain leaving the other reactive end dangling from the polymer chain and free to react. Primary cyclization (where a radical reacts with the radical on its own propagating chain) and secondary cyclization (where a radical reacts with the radical on secondary chain) (Figure 4.1) do not contribute as crosslinks to the overall structure of the polymer and will reduce the crosslinking density. These lead to more heterogeneous, crosslinked, imprinted networks, which may negatively impact binding effectiveness, decrease the overall material strength, and alter template transport. Reaction conditions such as the type of free radical initiation mechanism and the polymerization temperature have been explored, but more

analysis is needed. Reactions that have controlled temperature have been demonstrated to lead to better imprinted structures and free radical, UV-initiated imprinted polymerizations have been demonstrated to lead to better binding parameters compared to thermally initiated polymerizations due to lower temperature of the system during polymerization. However, the benefits of reduced temperatures gained in the stability of the monomer-template complex can negatively influence the structure of the network since reduced temperatures will decrease reaction rates and monomer conversion.

Another factor which introduces heterogeneity in the polymer network is the difference in the rates of chain propagation and chain relaxation during a free radical polymerization process. Our group [72] was the first to show that reaction analysis of a typical highly crosslinked poly(methacrylic acid-co-ethylene glycol dimethacrylate) molecularly imprinted network revealed low double bond conversion (35 ± 2.3% at 0°C to 54 ± 1.9% at 50°C) due to severely constrained network formation. This work highlighted that the final composition of imprinted polymers does not represent the initial formulation when using significant amounts of short bifunctional crosslinking monomer. Living radical polymerization reactions suppress the rapid propagation reaction allowing it to match more closely the relaxation rate of the growing polymer chains. Thus, the polymer network is formed under more favorable thermodynamic circumstances. Living radical polymerization with a reversible termination reaction can provide much more control over the network structure. It increases the potential for the growing polymer network and template binding complexes to reach a global energy minimum and leads to further memorization of the chain conformation.

Living radical polymerization reactions use reaction intermediates to control the rate of propagation. One of the most popular living polymerization techniques is RAFT polymerization;

where a reversible chain transfer agent combines with a radical to form a stable intermediate. The efficacy of RAFT polymerization lies in the use of photosensitive chain transfer agents which allow the formation of a dynamic controllable equilibrium between the active species, or radicals, and the dormant species. The advantage of RAFT lies in its versatility; it can be used with a variety of monomers at varying conditions. Thus, living polymerization can be combined with other efficient reaction conditions to create more homogenous networks with improved binding and transport properties (Figure 4.4).

4.4.1.1 Living Radical Polymerization in the Creation of Highly Crosslinked Imprinted Networks

Two separate groups reported the use of living radical polymerization in the creation of highly crosslinked imprinted networks in 2006 [73-74]. Boonpangrak et al. [73] used sacrificial covalent imprinting and nitroxide-mediated living radical polymerization (NMP) to produce cholesterol imprinted polymers at a relatively high temperature of 125°C with divinyl benzene as the crosslinker. Template removal was achieved by hydrolyzing the polymers with sodium hydroxide to remove the sacrificial spacer. Using the Scatchard plot they calculated that the binding capacities and affinities for the imprinted polymers. It was found that the cholesterol binding affinity for the high affinity sites in NMP initiated polymers (K_D=4.5 ± 1.2 μM) was much higher than that of BPO initiated polymer (K_D=8.1 ± 2.5μM) while the number of high affinity binding sites was nearly the same. Overall, the NMP initiated polymers were reported to have a 60% higher overall cholesterol loading as compared to the BPO initiated polymers; however, they also reported a 75% increase in template removal by hydrolysis for the NMP initiated polymers which would increase the availability of binding sites post polymerization. They also reported 30% higher BET surface area for the BPO initiated polymers (prepared using

conventional free radical polymerization) as compared to the NMP initiated polymers indicating differences in polymer morphologies.

Our group used non-covalent molecular imprinting based primarily on multiple hydrogen bonds to produce highly crosslinked polymer networks via UV free radical polymerization and iniferter controlled living radical polymerization reaction at 0ºC [72, 74]. Ethyl adenine-9-acetate (EA9A) imprinted polymers were prepared using methacrylic acid (MAA) as the primary functional monomer and ethylene glycol dimethacrylate (EGDMA) as the crosslinker. Molecularly imprinted polymers prepared using non-covalent molecular imprinting are featured more prominently in literature due to their ease of preparation and the versatility of non-covalent molecular imprinting. Imprinted polymers prepared using living radical polymerization demonstrated a 63% increase in binding capacities (calculated using the Frendlich isotherm) (1421 ± 64 μmol/g) as compared to the corresponding polymers prepared via conventional free radical polymerization (862 ± 60 μmol/g) while retaining the average binding affinity and selectivity for the template molecule. The binding affinity values reported in this paper were overall mean values over both high affinity and low affinity binding sites. Both imprinted polymers also had similar final double bond conversions indicating that the increase in binding capacity was not due to a higher incorporation of monomer in the polymer network. In fact, the increase in binding capacity was hypothesized to be attributed to a decrease in kinetic chain length and/or a more narrow dispersity of kinetic chains which leads to increased structural homogeneity with more stability and integrity of more appropriately sized binding sites.

More recently, Sasaki et al. [75] reported using reverse ATRP (rATRP) to create bisphenol A (BPA) imprinted polymers. They used a covalent imprinting technique similar to the one described before. Equilibrium binding isotherms showed that the polymers prepared using

rATRP had nearly twice as much BPA bound as compared to corresponding polymers prepared using FRP. However, there was also a 20% increase in template removal by hydrolysis, which as described above should result in a 20% increase in the number of available binding sites. They also carried out selectivity studies with various template analogs to demonstrate improved shape specificity in polymers prepared using rATRP. BPA binding was shown to have increased two fold while the binding of template analogs showed no appreciable increase resulting in significantly higher selectivity for the template molecule. The polymers prepared using rATRP also showed a large (more than order of magnitude) decrease in the BET surface area and higher swelling when compared to the polymers prepared using FRP indicating that rATRP resulted in more homogenous crosslinking and decreased macroporosity in the polymer networks formed.

Contrary to the previous reports, Zu et al. [76] reported that BPA imprinted polymers prepared using ATRP and rATRP showed reduced binding as compared to conventional FRP polymers. Using Scatchard analysis on the equilibrium binding isotherms of all polymers they found that the ATRP (4.5 μmol/g) and rATRP (4.5 μmol/g) polymers showed nearly 20% decrease in the number of binding sites as compared to FRP polymers (5.4 μmol/g) at similar binding affinities. They also found that that the ATRP and rATRP polymers bound a template analog (hydroquinone) to a higher extent when compared to the FRP polymers indicating a decrease in the selectivity for the template. However, they did report decreases in the BET surface area of ATRP (9%) and rATRP (17%) polymers which were consistent with previous reports. They hypothesized that the anamolous binding characteristics could be explained by faster gelation in the ATRP process as compared to NMP and iniferter controlled processes, however, Sasaki et al. [75] were able to demonstrate improved template binding characteristics using rATRP.

4.4.1.2 Living Radical Polymerization in the Creation of Weakly Crosslinked Imprinted Networks (Gels)

Our group [77] also demonstrated the use of living radical polymerization to prepare weakly crosslinked imprinted gels. Two gel systems were prepared: EA9A imprinted polymers, using MAA and EGDMA, where hydrogen bonding was the primary template-monomer interaction; and diclofenac sodium (DS) imprinted polymers, prepared using diethylaminoethyl methacrylate (DEAEM) as the primary functional monomer, 2-hydroxyethyl methacrylate (HEMA) as the backbone monomer and poly(ethylene glycol 200 dimethacrylate) (PEG200DMA) as the crosslinker, where an ionic interaction was the primary template-monomer interaction. Imprinted polymer gels prepared via LRP were reported to demonstrate 54% increase in template loading capacity (35.4 ± 1.6 μmol/g) over that of the corresponding gels prepared via FRP (23.0 ± 2.0 μmol/g) at similar binding affinities. The EA9A imprinted gels prepared via LRP (38.0 ± 4.0 μmol/g) also showed a 90% increase in template binding capacity over that of the corresponding gels prepared via FRP (20.0 ± 2.0 μmol/g). In addition, release studies showed that imprinting via living radical polymerization extended the template release profile by two fold over the imprinted gels prepared via conventional free radical polymerization and four fold over the non-imprinted gels. In order to gauge the effect of living polymerization on the change in polymer morphology, the theoretical mesh size of the DS imprinted polymer gels was calculated using swelling studies and mechanical analysis. Polymers prepared via LRP (19.7 ± 2.1 Å) reported a 35% decrease in the theoretical mesh size when compared to the corresponding polymer gels prepared via LRP (30.3 ± 1.7 Å). This supported their previous hypothesis that living polymerization results in decreased kinetic chain length in polymer networks.

4.4.1.3 Living Radical Polymerization in the Creation of Imprinted Polymer Microspheres

The creation of imprinted polymer microspheres using LRP is a recent trend which was preceded by the creation of molecularly imprinted core shell particles and the grafting of molecularly imprinted polymers onto inert nanoparticles. The Zhang group [78-79] has shown excellent results combining LRP with precipitation polymerization to achieve improved binding and structural characteristics in imprinted polymer particles. They used RAFT polymerization [78] and iniferter mediated [79] polymerization to create molecularly imprinted polymer (MIP) microspheres using precipitation polymerization. 2,4-Dichlorophenoxyacetic acid (2,4-D) imprinted microspheres were prepared using 4-Vinylpyridine (4-VP) as the primary functional monomer and EGDMA as the crosslinker. The morphology of the microspheres was analyzed by using scanning electron microscopy (SEM). The SEM images showed that the presence of template molecule results in the formation of irregular polymer aggregates while the non-imprinted polymers were visible as uniform microspheres. RAFT polymerization results in the formation of larger polymer microspheres with uniform spherical surfaces for both imprinted and non-imprinted polymers. They reported higher binding capacity per unit surface area in the RAFT polymerized microspheres over the conventionally prepared polymers. Although the increase in the high affinity binding sites was comparatively small, the decrease in the surface area resulted in a significant increase in the high affinity biding site density. The high affinity biding site density of the imprinted microsphere prepared via RAFT (1.4 μmol/m^2) was an order of magnitude higher than that of the corresponding microsphere prepared using FRP (0.13 μmol/m^2).

Xu et al. [80] combined RAFT and precipitation polymerization to create atrazine imprinted polymer microspheres for recovering atrazine from food matrices. They used MAA as the

primary functional monomer for the atrazine template, EGDMA as the crosslinker and acetonitrile as the porogen. SEM images were used to characterize the structure of the polymer microspheres. They found that using RAFT resulted in the formation of uniform spherical particles with rough surfaces containing micropores while conventional precipitation polymerization resulted in irregular MIP aggregates. The results of equilibrium binding experiments showed that the RAFT MIP microspheres demonstrated 2.5 times higher template binding when compared to the corresponding FRP microspheres. Scatchard analysis revealed that template binding capacity and affinity were both nearly doubled simultaneously by using RAFT when compared to the corresponding FRP MIPs. In addition, kinetic binding experiments showed that the RAFT MIPs bound the template faster requiring only one fifth of the time to match the binding capacity of the FRP MIPs. Finally, they demonstrated that using RAFT led to higher recovery of atrazine from lettuce and corn samples. Thus, living polymerization techniques have been demonstrated to result in enhanced binding in a variety of polymeric structures by altering the morphology of the polymeric structures.

4.5 References

1. Moad G, Solomon DH. The Chemistry of Radical Polymerization,2nd ed. : Oxford, U.K.: Elsevier Science, 2006.
2. Matyjaszewski K, Davis TP. Handbook of Radical Polymerization. New York: Wiley-Interscience, 2002.
3. Maunsky J, Klaban J, Dusek K. Vinyl-Divinyl Copolymerization: Copolymerization and Network Formation from Styrene and p- and m-Divinylbenzene. J. Macromol. Sci.-Chem. 1971, A5, 1071-1085.
4. Soper B, Haward RN, White EFT. Intramolecular cyclization of styrene–p-divinylbenzene copolymers. J. Polym. Sci., PartA-1. 1972, 10, 2545-2564.
5. Ulbrich K, Dusek K, Ilavsky M, Kopecek J. Preparation and properties of poly-(N-butylmethacrylamide) networks. Eur. Polym.J. 1978, 14, 45-49.
6. Ray B, Okamoto Y, Kamigaito M, Sawamoto M, Seno K, Kanaoka S, Aoshima S. Effect of Tacticity of Poly(N-isopropylacrylamide) on the Phase Separation Temperature of Its Aqueous Solutions. Polym. J. 2005, 37, 234-237.
7. Olaj OF, Schnoll-Bitai I. Solvent Effects on the Rate Constant of Chain Propagation in Free Radical Polymerization. Monatshefte fur Chemie. 1999, 130,731-740.
8. O'Driscoll KF, Monteiro MJ, Klumperman B. The effect of benzyl alcohol on pulsed laser polymerization of styrene and methylmethacrylate. J. Polym. Sci.,Part A: Polym. Chem. 1997, 35, 515-520.
9. Zammit MD, Davis TP, Willett GD, O'Driscoll KF. The effect of solvent on the homo-propagation rate coefficients of styrene and methyl methacrylate. J. Polym. Sci., Part A: Polym. Chem. 1997, 35, 2311-2321.

10. Beuermann S, Buback M, Hesse P, Lacık I. Free-Radical Propagation Rate Coefficient of Nonionized Methacrylic Acid in Aqueous Solution from Low Monomer Concentrations to Bulk Polymerization. Macromolecules. 2006, 39, 184-193.
11. Stach M, Lacık I, Chorvat D, Buback M, Hesse P, Hutchinson RA, Tang L. Propagation Rate Coefficient for Radical Polymerization of N-Vinyl Pyrrolidone in Aqueous Solution Obtained by PLP−SEC. Macromolecules. 2008, 41, 5174-5185.
12. Banford CH. Alternating Copolymers. In: Cowie JMG, editor. New York: Plenum Press, 1985.
13. Barton J, BorsigE. Complexes in Free-Radical Polymerization. Amsterdam; Elsevier, 1988.
14. Bamford CH, Jenkins AD, Johnston R. Studies in Polymerization. XII. Salt Effects on the Polymerization of Acrylonitrile in Non-Aqueous Solution. Proc. R. Soc. London,Ser. A. 1957, 241, 364-375.
15. Lacık I, Beuermann S, Buback M. PLP-SEC Study into the Free-Radical Propagation Rate Coefficients of Partially and Fully Ionized Acrylic Acid in Aqueous Solution. Macromol. Chem. Phys. 2004, 205, 1080-1087.
16. Beuermann S, Buback M, Hesse P, Kukuckova S, Lacık I. Propagation Kinetics of Free-Radical Methacrylic Acid Polymerization in Aqueous Solution. The Effect of Concentration and Degree of Ionization Macromol. Symp. 2007, 248, 23-32.
17. Isobe Y, Fujioka D, Habaue S, Okamoto Y. Efficient Lewis Acid-Catalyzed Stereocontrolled Radical Polymerization of Acrylamides. J. Am. Chem. Soc. 2001, 123, 7180-7181.

18. Okamoto Y, Habaue S, Isobe Y, Nakano T. Stereocontrol in radical polymerization of acrylic monomers. Macromol. Symp. 2002, 183, 83-88.
19. Okamoto Y, Habaue S, Isobe Y, Suito Y. Stereocontrol using Lewis acids in radical polymerization. Macromol. Symp. 2003, 195, 75-80.
20. Isobe Y, Nakano T, Okamoto Y. Stereocontrol during the free-radical polymerization of methacrylates with Lewis acids. J. Polym. Sci., Part A: Polym.Chem. 2001, 39, 1463-1471.
21. Hirooka M, Yabuuchi H, Iseki J, Nakai I. Alternating copolymerization through the complexes of conjugated vinyl monomers–alkylaluminum halides. J. Polym. Sci.: PartA-1 1968, 6, 1381-1396.
22. Kabanov VA. Polymerization in Organized Media. In: Paleos CM, editor. Philadelphia, PA: Gordon and Breach Science Publishers, 1992. P. 369-454.
23. Tan YY. The synthesis of polymers by template polymerization. Prog. Polym. Sci. 1994, 19, 561-588.
24. Byrne M, Salian V. Molecular imprinting within hydrogels II: progress and analysis of the field. Int. J. Pharm. 2008, 364, 2, 188-212.
25. Ye L, Mosbach K. Molecular imprinting: Synthetic materials as substitutes for biological antibodies and receptors. Chem. Mater. 2008, 20, 859-868.
26. Wulff G, Enzyme-like catalysis by molecularly imprinted polymers. Chem. Rev. 2002, 102, 1-27.
27. Alvarez-Lorenzo C, Hiratani H, Gomez-Amoza JL, Martinez-Pacheco R, Souto C, Concheiro A. Soft contact lenses capable of sustained delivery of timolol. J. Pharm. Sci. 2002, 91, 2182-2192.

28. Venkatesh S, Sizemore SP, Zhang JB, Byrne ME. Therapeutic contact lenses: A biomimetic approach towards tailored ophthalmic extended delivery. Abstr. Pap. Am. Chem. Soc. 2006, 231.
29. Alvarez-Lorenzo C, Yanez F, Barreiro-Iglesias R, Concheiro A. Imprinted soft contact lenses as norfloxacin delivery systems. J. Controlled Release. 2006, 113, 236-244.
30. Venkatesh S, Sizemore SP, Byrne ME. Biomimetic hydrogels for enhanced loading and extended release ofocular therapeutics. Biomaterials. 2007, 28, 717–724.
31. Solomon DH, Rizzardo E, Cacioli P. U.S. Patent 4,581,429, April8, 1986.
32. Georges MK, Veregin RPN, Kazmaier PM, Hamer GK. Narrow molecular weight resins by a free-radical polymerization process. Macromolecules 1993, 26, 2987-2988.
33. Hawker CJ, Bosman AW, Harth E. New Polymer Synthesis by Nitroxide Mediated Living Radical Polymerizations Chem. Rev. 2001, 101, 3661–3688.
34. Studer A, Schulte T. Tin-free radical chemistry using the persistent radical effect: alkoxyamine isomerization, addition reactions and polymerizations. Chem. Soc. Rev. 2004, 33, 267-273.
35. Nielsen A, Braslau R. Nitroxide decomposition: Implications toward nitroxide design for applications in living free-radical polymerization. J. Polym. Sci., Part A: Polym. Chem. 2006, 44, 697-717.
36. Sciannamea V, Jerome R, Detrembleur C. In-Situ Nitroxide-Mediated Radical Polymerization (NMP) Processes: Their Understanding and Optimization. Chem. Rev. 2008, 108, 1104-1126.
37. Waters WA. Vistas in Free-Radical Chemistry. New York: Pergammon Press, 1959.

38. Iqbal J, Bhatia B, Nayyar NK. Transition Metal-Promoted Free-Radical Reactions in Organic Synthesis: The Formation of Carbon-Carbon Bonds. Chem. Rev. 1994, 94, 519-564.
39. Matyjaszewski K, Xia J. Atom Transfer Radical Polymerization. Chem. Rev. 2001, 101, 2921-2990.
40. Kamigaito M, Ando T, Sawamoto M. Metal-catalyzed living radical polymerization: discovery and developments. Chem. Rec. 2004, 4, 159-175.
41. Tsarevsky NV, Matyjaszewski K. "Green" Atom Transfer Radical Polymerization: From Process Design to Preparation of Well-Defined Environmentally Friendly Polymeric Materials. Chem. Rev. 2007, 107, 2270-2299.
42. Ouchi M, Terashima T, Sawamoto M. Precision Control of Radical Polymerization via Transition Metal Catalysis: From Dormant Species to Designed Catalysts for Precision Functional Polymers. Acc. Chem. Res. 2008, 41, 1120-1132.
43. Chiefari J, Chong YK, Ercole F, Krstina J, Jeffery K, Tam PTL, Mayadunne RTA, Meijs GF, Moad CL, Moad G, Rizzardo E, Thang SH. Living Free-Radical Polymerization by Reversible Addition−Fragmentation Chain Transfer: The RAFT Process. Macromolecules. 1998, 31, 5559-5562.
44. Destarac M, Bzducha W, Taton D, Gauthier-Gillaizeau I, Zard SZ. Xanthates as Chain-Transfer Agents in Controlled Radical Polymerization (MADIX): Structural Effect of the O-Alkyl Group. Macromol. Rapid Commun. 2002, 23, 1049-1054.
45. Moad G, Rizzardo E, Thang SH. Living Radical Polymerization by the RAFT Process. Aust. J. Chem. 2005, 58, 379-410.

46. Moad G, Rizzardo E, Thang SH. Radical addition–fragmentation chemistry in polymer synthesis. Polymer. 2008, 49, 1079-1131.

47. Perrier S, Takolpuckdee P. Macromolecular design via reversible addition–fragmentation chain transfer (RAFT)/xanthates (MADIX) polymerization. J. Polym. Sci., Part A: Polym. Chem. 2005, 43, 5347-5393.

48. Barner-Kowollik C. Handbook of RAFT Polymerization. Weinheim, Germany: Wiley-VCH, 2008.

49. Ray B, Isobe Y, Morioka K, Habaue S, Okamoto Y, Kamigaito M, Sawamoto M. Synthesis of Isotactic Poly(N-isopropylacrylamide) by RAFT Polymerization in the Presence of Lewis Acid. Macromolecules. 2003, 36, 543-545.

50. Ray B, Isobe Y, Matsumoto K, Habaue S, Okamoto Y, Kamigaito M, Sawamoto M. RAFT Polymerization of N-Isopropylacrylamide in the Absence and Presence of Y(OTf)3: Simultaneous Control of Molecular Weight and Tacticity. Macromolecules, 2004, 37, 1702-1710.

51. Nuopponedn M, Kalliomaki K, Laukkanen A, Hietala S, Tenhu H. A–B–A stereoblock copolymers of N-isopropylacrylamide. J. Polym. Sci., Part A: Polym. Chem. 2008, 46, 38-46.

52. Hietala S, Nuopponedn M, Kalliomaki K, Tenhu H. Thermoassociating Poly(N-isopropylacrylamide) A−B−A Stereoblock Copolymers. Macromolecules. 2008, 41, 2627-2631.

53. Mori H, Sutoh K, Endo T. Controlled Radical Polymerization of an Acrylamide Containing l-Phenylalanine Moiety via RAFT. Macromolecules. 2005, 38, 9055-9065.

54. Chong YK, Moad G, Rizzardo E, Skidmore MA, Thang SH. Reversible Addition Fragmentation Chain Transfer Polymerization of Methyl Methacrylate in the Presence of Lewis Acids: An Approach to Stereocontrolled Living Radical Polymerization. Macromolecules. 2007, 40, 9262-9271.
55. Rizzardo E, Chen M, Chong B, Moad G, Skidmore MA, Thang SH. RAFT Polymerization: Adding to the Picture. Macromol. Symp. 2007, 248, 104-116.
56. Murayama H, Satoh K, Kamigaito M. Thiourea-Mediated Stereospecific Radical Polymerization of Acrylamides and Combination with RAFT for Simultaneous Control of Molecular Weight and Tacticity. ACS Symp. Ser. 2009, 1024, 49.
57. Ide N, Fukuda T. Nitroxide-Controlled Free-Radical Copolymerization of Vinyl and Divinyl Monomers. Evaluation of Pendant-Vinyl Reactivity. Macromolecules. 1997, 30, 4268-4271
58. Ide N, Fukuda T. Nitroxide-Controlled Free-Radical Copolymerization of Vinyl andDivinyl Monomers. 2. Gelation. Macromolecules. 1999, 32, 95-99
59. Norisuye T, Morinaga T, Miyata Q, Goto A, Fukuda T, Shibayama M. Comparison of the gelation dynamics for polystyrenes prepared byconventional and living radical polymerizations: a time-resolved dynamic light scattering study. Polymer. 2005, 46, 1982–1994
60. Gao H, Min K. Determination of Gel Point during Atom Transfer Radical Copolymerization with Cross-Linker. Macromolecules. 2007, 40, 7763–70.
61. Van Camp W, Gao H, Du Prez F, Matyjaszewski K. Effect of crosslinker multiplicity on the gel point in ATRP. Journal of Polymer Science Part A: Polymer Chemistry. 2010, 48, 2016-2023.

62. Yu Q, Zeng F, Zhu S. Atom Transfer Radical Polymerization of Poly(ethylene glycol) Dimethacrylate. Macromolecules. 2001, 34, 1612-1618.
63. Yu Q, Zhou M, Ding Y, Jiang B, Zhu S. Development of networks in atom transfer radical polymerization of dimethacrylates. Polymer. 2007, 48, 7058–7064.
64. Bannister I, Billingham NC, Armes SP, Rannard SP, Findlay P. Development of Branching in Living Radical Copolymerization of Vinyl and Divinyl Monomers. Macromolecules. 2006, 39, 7483-7492.
65. Krasia TC, Patrickios CS. Amphiphilic Polymethacrylate Model Co-Networks: Synthesis by RAFT Radical Polymerization and Characterization of the Swelling Behavior. Macromolecules. 2006, 39, 2467-2473.
66. Anseth KS, Wang CM, Bowman CN. Reaction behaviour and kinetic constants for photopolymerizations of multi(meth)acrylate monomers. Polymer. 1994, 35, 3243–3250.
67. Anseth KS, Kline LM, Walker TA, Anderson KJ, Bowman CN. Reaction kinetics and volume relaxation during polymerizations of multiethylene glycol dimethacrylates. Macromolecules. 1995, 28, 2491–2499.
68. Anandkumar KR, Anderson KJ, Anseth JW, Bowman CN. Use of "living" radical polymerizations to study the structural evolution and properties of highly crosslinked polymer networks. J. Polym. Sci., Part B: Polym. Phys. 1997, 35, 2297 -2307.
69. Anandkumar KR, Anseth JW, Bowman CN. A study of the evolution of mechanical properties and structural heterogeneity of polymer networks formed by photopolymerizations of multifunctional (meth)acrylates. Polymer. 1998, 39, 12, 2507-2513.

70. Burkoth AK, Anseth KS. MALDI-TOF Characterization of Highly Crosslinked, Degradable Polymer Networks. Macromolecules. 1999, 32, 1438-44.
71. Hutchison JB, Lindquist AS, Anseth KS. Experimental characterization of structural features during radical chain homopolymerization of multifunctional monomers prior to macroscopic gelation. Macromolecules. 2004, 37, 10, 3823-3831.
72. Vaughan AD, Sizemore SP, Byrne ME. Enhancing molecularly imprinted polymer binding properties via controlled/living radical polymerization and reaction analysis. Polymer. 2007, 48, 74-81
73. Boonpangrak S, Whitcombe MJ, Prachayasittikul V, Mosbach K, Ye L. Preparation of molecularly imprinted polymers using nitroxide-mediated living radical polymerization. Biosens Bioelectron. 2006, 22, 349–354.
74. Vaughan AD, Byrne ME. Optimizing recognition characteristics of biomimetic polymer gels via polymerization reaction and crosslinking density analysis. ACS PMSE Preprints. 2006, 94, 762–763.
75. Sasaki S, Ooya T, Takeuchi T. Highly selective bisphenol A—imprinted polymers prepared by atom transfer radical polymerization. Polym. Chem. 2010, 1, 1684-1688.
76. Zu B, Zhang Y, Guo X, Zhang H. Preparation of molecularly imprinted polymers via atom transfer radical "bulk" polymerization. J. Polym. Sci. Part A: Polym. Chem. 2010, 48, 532-541.
77. Vaughan AD, Zhang JB, Byrne ME. Enhancing Therapeutic Loading and Delaying Transport via Molecular Imprinting and Living/Controlled Polymerization. AIChE Journal. 2010, 56, 1, 268-279.

78. Pan G, Zu B, Guo X, Zhang Y, Li C, Zhang H. Preparation of molecularly imprinted polymer microspheres via reversible addition–fragmentation chain transfer precipitation polymerization. Polymer. 2009, 50, 2819–2825.
79. Li J, Zu B, Zhang Y, Guo X, Zhang H. One-pot synthesis of surface-functionalized molecularly imprinted polymer microspheres by iniferter-induced "living" radical precipitation polymerization. Journal of Polymer Science Part A: Polymer Chemistry. 2010, 48, 15, 3217–3228.
80. Xua S, Li J, Chen L. Molecularly imprinted polymers by reversible addition–fragmentation chain transfer precipitation polymerization for preconcentration of atrazine in food matrices. Talanta. 2011, 85, 282–289.

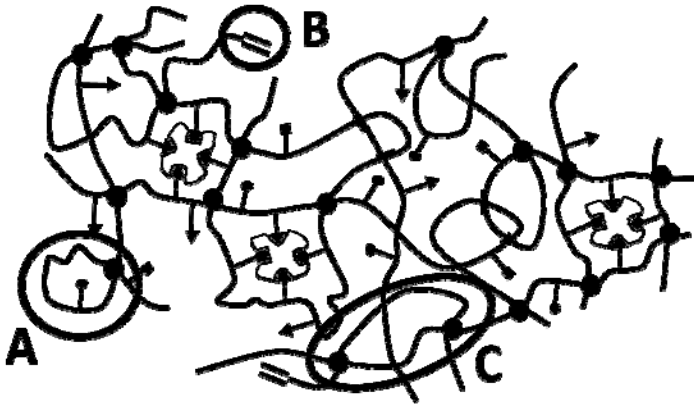

Figure 4.1: Network Imperfections in Imprinted Crosslinked Polymer Networks. A non ideal network is shown where **(A)** represents primary cycles **(B)** represents pendant double bonds and **(C)** represents secondary cycles.

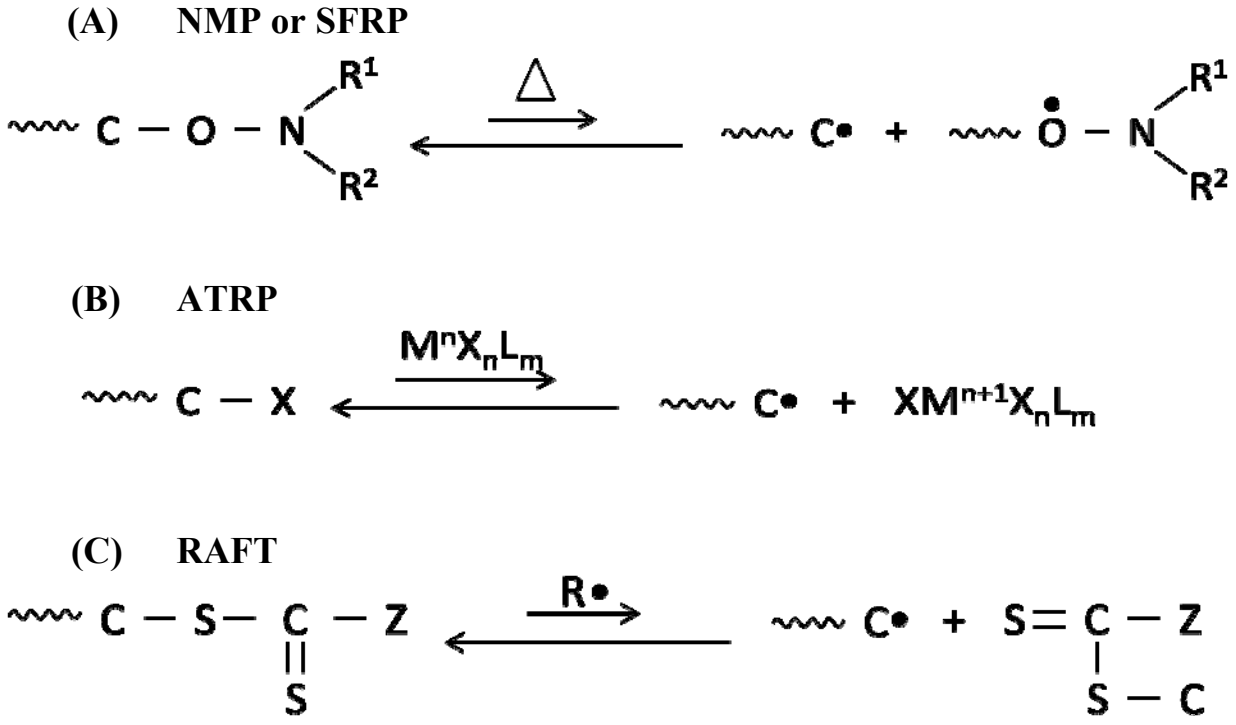

Figure 4.2: Representative Living Radical Polymerization Reactions. Schematics for **(A)** nitroxide mediated polymerization, **(B)** atom transfer radical polymerization and **(C)** reversible addition-fragmentation chain transfer polymerization.

Conventional Radical Polymerization

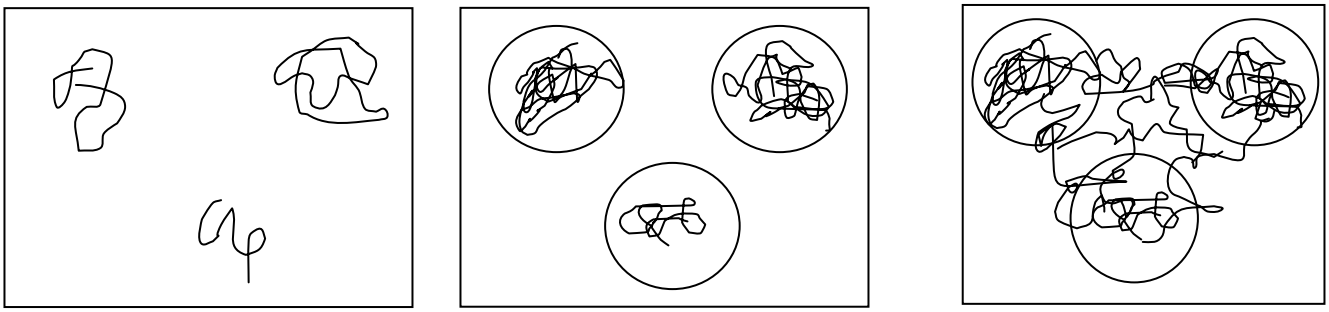

Low Conversion | Moderate Conversion (Microgel formation) | High Conversion (Gelation)

Living Radical Polymerization

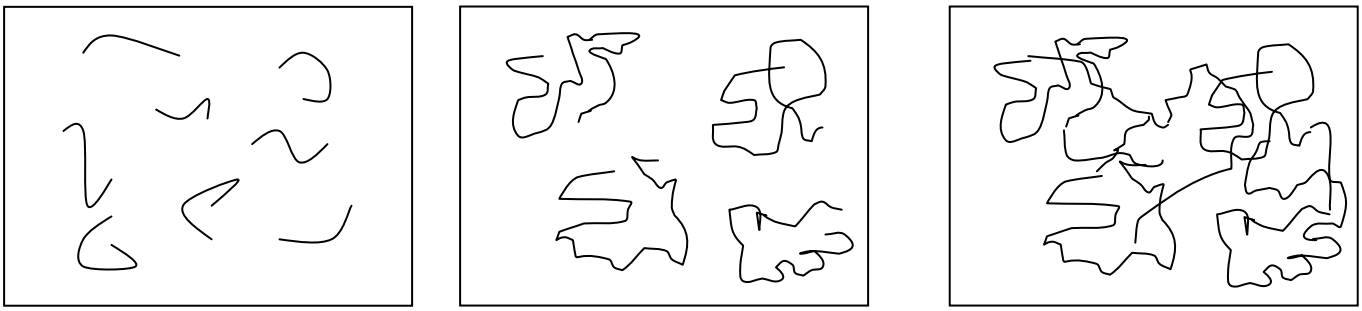

Low Conversion | Moderate Conversion | High Conversion (Gelation)

Figure 4.3: Network Formation in Living versus Conventional Free Radical Polymerization. At low conversion, polymers prepared with CRP grow faster resulting in coiled chains. At moderate conversion intramolecular crosslinking results in microgel formation whereas polymers with LRP do not form microgels due to their slow growth. At high conversion, the microgels in CRP are incorporated into the network forming non-functional areas while the polymers with LRP undergo gelation. Adapted from Ide and Fukuda [58].

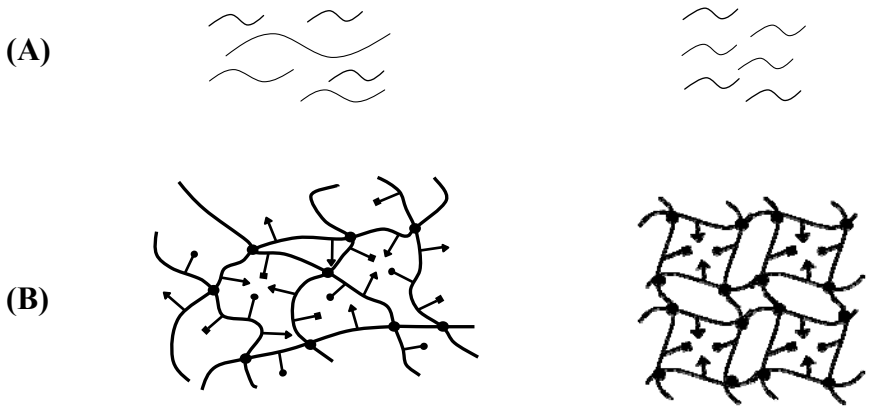

Figure 4.4: Effect of Living Polymerization on Polymer Network Structure. In homo-polymer systems **(A)**, the use of iniferter yields a lower polydispersity of kinetic chains and decreased average chain length. Within crosslinked networks **(B)**, addition of iniferter leads to a more uniform and higher population of appropriately sized imprinted macromolecular cavities for the template. An optimal mesh size, ξ, gives the binding site a better functional configuration which leads to enhanced binding properties.

CHAPTER 5: ENHANCED TEMPLATE BINDING AND IMPROVED NETWORK MORPHOLOGY IN MOLECULARLY IMPRINTED POLYMER NETWORKS PREPARED VIA LIVING RADICAL POLYMERIZATION

5.1 Scientific Rationale

In this chapter, the synthesis and characterization of an imprinted system from the literature is discussed. The ethyl adenine-9-acetate (EA9A) imprinted poly(methacrylic acid-co-ethylene glycol dimethacrylate) poly(MAA-co-EGDMA) network chosen has been studied by multiple investigators and has well documented binding parameters [1-3]. The objective was to alter the reaction parameters and analyze the changes in the macromolecular structure of the polymers and the corresponding impact on the binding capacity and affinity of the polymers.

During polymerization, reaction analysis was used to determine the double bond conversion of the imprinted polymer. In addition, analysis of the reaction signature in the absence of light was used to calculate the kinetic propagation constant for the reaction. Further analysis of the network structure was carried out by estimating the kinetic chain length distribution of the polymer chains between crosslinking points in the imprinted polymer. This was achieved by measuring the kinetic chain length distribution of homopolymers chains created in the absence of crosslinking monomer.

5.2 Introduction

Conventional free radical polymerization (FRP) processes have been the predominant reaction used in the field of molecular imprinting, which produces polymer networks with increased affinity and capacity for a template molecule [1-4]. The popularity of free radical polymerization in this field can be attributed to its versatility: a wide range and combination of monomers with varied functionalities can be used at various reaction conditions. The one drawback to conventional free radical polymerization is the lack of control over chain propagation and termination due to the very high reactivity of the radicals. This results in the formation of polymer networks with heterogeneous structures with various imperfections like primary and secondary cycles; and pendant double bonds [5-6]. The presence of heterogeneity within the network structures of imprinted polymers affects the quality of the binding sites formed within the networks, and results in a broad distribution of binding sites with large proportions of low affinity sites and low overall capacity. Living radical polymerization (LRP) techniques offer the ability to create improved imprinted polymers with more homogeneous network structures and, as a result, better binding parameters. In addition, using living radical polymerization can lead to more control over network structures and a better understanding of their structure-property relationships; however, these reactions are relatively new to the imprinting field and have not been used extensively in molecular imprinting.

Structural evolution of networks prepared via free radical polymerization has been studied [6-10] in some detail, and the mismatch between the rapid chain growth during polymerization and slow chain relaxation of the polymer formed has been understood to introduce structural heterogeneity in polymer networks generated by conventional free radical polymerization. As the polymerization reaction proceeds and the conversion increases the bimolecular termination

reaction between two polymer chains becomes difficult because of diffusional limitations introduced by the difference in rates described above. This results in the Trommsdorff effect or auto-acceleration of the reaction, where an overabundance of carbon radicals results in explosive chain growth and the formation of regions with very highly crosslinked localized microgel domains. Living radical polymerization reaction, by contrast, is a much slower reaction making it thermodynamically favorable to the formation of a more homogeneous polymer network. It replaces the bimolecular termination between polymer chains with a macroradical-iniferter termination reaction which prevents or delays auto-acceleration, forming a more homogenous polymer network. It is important to note that it is still not completely clear how living radical reactions affects the creation of crosslinked polymer networks. However, recent work has attempted to shed light on the matter [11-14]. What the field does know comes from the kinetic study of the polymerization reaction and the analysis of non-crosslinked polymer chains. For example, it is well known that polymers prepared via living radical polymerization have a much narrower polymer chain length distribution with lower polydispersity [10].

The ability of living radical polymerization to control the imprinted network structure was first reported in 2006 by two separate groups, our group and one led by Klaus Mosbach [15-16]. Both groups highlighted the strong potential to enhance binding properties of highly crosslinked imprinted polymer networks using living radical polymerization strategies. Mosbach and co-workers [16], used nitroxide-mediated living radical polymerization (NMP) to produce cholesterol imprinted polymers. The use of NMP necessitated a high reaction temperature of 125°C, and as a result they had to utilize covalent imprinting where the template is associated to the network via a sacrificial covalent bond. They reported an increase in the binding affinity of high affinity binding sites with a small decrease in their binding capacity. Conversely, our group

used non-covalent molecular imprinting to produce highly crosslinked polymer networks via UV initiated, iniferter mediated, radical polymerization at 0ºC [16-17]. Most molecular imprinting relies upon non covalent bonding due to its ease of preparation and versatility. Compared to conventional techniques, living radical polymerization was reported to result in a significant increase in the binding capacity at approximately equivalent average binding affinity while retaining selectivity for the template [18]. This was hypothesized to be attributed to a decrease in kinetic chain length and/or a more narrow dispersity of kinetic chains which leads to increased structural homogeneity with more stability and integrity of more appropriately sized binding sites [18].

Recently, our group was the first to demonstrate the use of living radical polymerization to prepare weakly crosslinked imprinted gels [19]. Significant increases in template loading affinity with large increases in loading for imprinted polymers prepared via living radical polymerization were demonstrated. Release studies showed that imprinting via living radical polymerization extended the template release profile by two fold over the imprinted FRP gels and four fold over the non-imprinted gels.

Meanwhile, Zhang and co-workers have used reversible addition-fragmentation chain transfer (RAFT) polymerization to create MIP microspheres using precipitation polymerization [20]. They reported higher binding capacity per unit surface area in the RAFT polymerized microspheres over the conventionally prepared microspheres. Although the increase in the high affinity binding sites was comparatively smaller, the decrease in the surface area resulted in a significant increase in the high affinity biding site density. More recently, work demonstrating increased enantioselectivity in highly crosslinked imprinted polymers [22] and increased binding in highly crosslinked imprinted polymers [23] using RAFT polymerization was presented at the

6th International Meeting on Molecular Imprinting (MIP2010: The Future of Molecular Imprinting).

Living radical polymerization has been predominantly used in the creation of block copolymers by serial addition of individual monomers. Similarly, it has been used to graft polymer chains and polymer brushes onto existing polymeric networks, including the surface grafting of imprinted films to dormant layers [24-29]. However, the ability of living radical polymerization to control the reaction during the formation of imprinted polymers is largely unexplored. Thus, while living radical polymerization techniques have been used to attach polymer layers onto existing polymeric substrates, its use in altering macromolecular structure and enhancement of template binding parameters is far less common. Thus, the goal of this work, in trying to understand the role, living radical polymerization plays in the creation of imprinted crosslinked polymer networks, is a new direction in the field.

In the work described in this chapter, we exploit living radical polymerization to prepare molecularly imprinted, weakly and highly crosslinked poly(MAA-co-EGDMA) networks, with a chain transfer agent that decays upon UV irradiation into more stable radicals. A significant goal of the work is to study the effect of living radical polymerization on the chain level and begin to explain why the efficiency of the imprinting process is improved using living radical polymerization. The results of this work will be applicable to a majority of imprinted systems in the literature, and improvements in binding parameters will lead to higher applicability of imprinted polymers in novel technologies.

5.3 Materials and Methods

The monomers, methacrylic acid (MAA) and ethylene glycol dimethacrylate (EGDMA), had inhibitors removed via inhibitor removal packing sieves prior to polymerization. The initiator azo-bis(isobutyronitrile) (AIBN), template molecule (EA9A), and chain transfer agent (CTA) (tetraethylthiuram disulfide (TED)) were used as received. Monomers, inhibitor removal packing sieves, initiator, chain transfer agent, and template were purchased from Aldrich (Milwaukee, WI). HPLC grade solvents, acetonitrile and methanol, were used as received from Fisher Scientific (Pittsburgh, PA). Acetonitrile was the polymerization and template rebinding solvent. The polymer wash solvent (to remove template and unreacted monomer) was acetonitrile/methanol at a 4:1 volume ratio. De-ionized (DI) water was used as the mobile phase in the high pressure liquid chromatography (HPLC) system.

5.3.1 Synthesis of Highly Crosslinked Polymers

A typical pre-polymerization solution forming a highly crosslinked poly(MAA-co-EGDMA) imprinted network was made with 2.61 mL EGDMA (13.83 mmol), 0.16 mL MAA (1.88 mmol), 3.96 mL acetonitrile (704.30 mmol), 26.3 mg of AIBN, and 35.4 mg of EA9A. The non-imprinted polymer solution was made exactly in the same manner as the imprinted polymer solution except no template was added. Another poly(MAA-co-EGDMA) imprinted polymer with a higher final double bond conversion was produced by increasing the amount of initiator to 157.6 mg. For creating an imprinted polymer via living radical polymerization, 47.4 mg TED, the CTA, was added to the original formulation while increasing the amount of initiator to 236.4 mg AIBN. The molar ratio of initiator divided by CTA was 8.61. Solutions were placed in a sonicator for several minutes until all solids were dissolved. The temperature of polymerization was carefully controlled (0°C ± 1°C) throughout the exothermic reaction, and the UV free radical

polymerization was conducted using a mercury halide source with a light intensity of 52.5 mW/cm^2 calibrated by a photometer. Oxygen, which is a radical scavenger, was removed by purging the polymerization solution with nitrogen for a period of 15 minutes. The polymerization was carried out via UV-free radical polymerization in a Q-100 differential photo calorimeter (DPC) from TA Instruments (New Castle, Delaware) in a nitrogen atmosphere resulting in a polymer disk with a diameter of 3 mm and a thickness of 1 mm. The DPC allowed strict temperature control within ±1°C. All poly(MAA-co-EGDMA) gels were washed in a modified Soxhlet extraction device to extract the bound template. The Soxhlet extraction device ensured that the disks were immersed in solvent at all times, and the wash was stopped after the template was no longer detected in the effluent. Wash analysis, conducted by performing a mass balance of the template, indicated efficient washing occurred, allowing an accurate comparison between various polymers prepared in this work. The discs were allowed to dry under laboratory conditions at room temperature for 24 hours and then transferred to a vacuum oven (27 in Hg, 33–34°C) for 24 hours until the disc weight change was less than 0.1 wt %. All samples had a reaction signature that was within one standard deviation from the mean to maintain a high degree of quality control for the reaction analysis and resultant polymer networks.

The polymers are named via the preparation reaction (e.g., FRP and LRP denote free radical polymerization and living radical polymerization, respectively) and the final double bond conversion percent. For example, FRP44 denotes a polymer prepared using free radical polymerization with a final double bond conversion of 44%.

5.3.2 Synthesis of Weakly Crosslinked Gels

A typical pre-polymerization solution forming a weakly crosslinked poly(MAA-co-EGDMA) imprinted gel was made with 0.187 mL EGDMA (0.993 mmol), 1.6 mL MAA (18.77 mmol),

18.5 mg of AIBN, and 84.06 mg of EA9A. The non-imprinted polymer solution was made exactly in the same manner as the imprinted polymer solution except no template was added. For creating an imprinted polymer via living radical polymerization, 3.89 mg of TED was added to the original formulation. The molar ratio of initiator divided by CTA was 8.61. Solutions were placed in a sonicator for several minutes until all solids were dissolved. The temperature of polymerization was carefully controlled (14°C ± 1°C) throughout the exothermic reaction, and the UV free radical polymerization was conducted using a mercury halide source with a light intensity of 52.5 mW/cm^2, calibrated by a photometer. Temperatures lower than 14°C resulted in freezing of the pre-polymerization mixture. The UV-free radical polymerization reaction and the washing process is the same as described above for the highly crosslinked polymers.

5.3.3 Synthesis of Poly(MAA) Homopolymer Chains

A typical polymerization solution forming poly(MAA) homopolymer was made with 0.8 mL MAA (9.43 mmol) and 42.03 mg of EA9A. The UV-free radical polymerization reaction was carried out in the DSC exactly as described for the weakly crosslinked polymers above. Poly(MAA) polymers were polymerized in the presence of the template by adding varying amounts of EA9A, calculated based on the desired molar template/monomer ratios, to the pre-polymerization solution. For example, 20.76 mg of EA9A was added to achieve a template/monomer ratio of 0.01 in solution. The polymers were not washed since the template was not bound to the polymers in the absence of a crosslinked network.

5.3.4 Analysis of Kinetic Chain Length of Polymer using GPC

The molecular weight distributions of poly(MAA) homopolymers were characterized by a modified HPLC system (Shimadzu, Columbia, MD) setup to be used for gel permeation chromatography(GPC). The GPC setup consisted of two PL Aquagel size exclusion columns in

series (Varian LLC, Santa Clara, CA), for separation of various molecular weight fractions of the polymer which were detected using a RID10A refractive index detector (Shimadzu, Columbia, MD). DI water was used as the mobile phase for the system. Prior to running the samples, the system was calibrated using narrow molecular weight distribution poly(MAA) standards (Polymer Source Inc., Dorval, Quebec). The poly(MAA) homopolymer obtained after polymerization was dissolved in the mobile phase to achieve a concentration of 1 mg/mL. Poor solubility of poly(MAA) did not allow for the creation of a more concentrated solution. A 50 μL aliquot of the solution was then injected into the system using a Rheodyne (Oak Harbour, WA) 7725(i) manual injection unit. Using the subsequent peaks obtained on the chromatograph, the weight average molecular weight (M_w), the number average molecular weight (M_n) and the polydispersity index (PDI) were calculated, where, the molecular weight (M_i) for a particular weight fraction was described by the x-coordinate of the corresponding point on the chromatograph while the number of chains (N_i) was described by the y-coordinate.

5.3.5 Analysis of Kinetic Parameters

A dark reaction was used to determine the kinetic reaction profile for the poly(MAA-co-EGDMA) gels [7-8]. For each polymerization reaction, the UV light was shut off at a specific time point during the reaction. The rate of polymerization was calculated via reaction analysis using the heat flow vs. time, results from the DPC, average molecular weight of the polymerization solution, and the theoretical heat of reaction. Fractional double bond conversion was determined by dividing the experimental heat of reaction by the theoretical heat of reaction. The experimental heat of reaction was determined by the area under the heat flow versus time curve from the DPC. The termination and propagation constants, k_t and k_p, were calculated from Eqs. 5.1 and 5.2, and the derivation of these equations can be found in Flory [30] or Odian [31].

$$\frac{k_p}{k_t^{0.5}} = \frac{R_p}{[M](f I_o \varepsilon [I])^{0.5}} \quad 5.1$$

where [*M*] is the monomer concentration, the initiator efficiency is *f*, I_o is the light intensity, ε is the extinction coefficient, and [I] is the initiator concentration. The unsteady state equation used to decouple the propagation constant and the termination constant is shown below.

$$k_t^{0.5} = \frac{k_p / k_t^{0.5}}{2(t_1 - t_0)} \left[\frac{[M]_{t=t1}}{R_{p_{t=t1}}} - \frac{[M]_{t=t0}}{R_{p_{t=t0}}} \right] \quad 5.2$$

where t_1 and t_0 are the final and initial times, $[M]_{t=t1}$ and $[M]_{t=to}$ are the corresponding monomer concentrations, respectively, and $Rp_{t=t1}$ and $Rp_{t=to}$ are the rate of polymerization at final and initial times, respectively.

5.3.6 Template Binding Experiments and Analysis of Binding Parameters

After the polymer was washed and dried, template rebinding experiments were carried out in acetonitrile as the rebinding solvent. The procedure for the template rebinding experiments was the same for both highly and weakly crosslinked polymers. Equilibrium binding analysis was determined by placing polymer disks in 200 μL of various concentrations of EA9A in acetonitrile (0.01-2.0 mM solutions). After equilibrium was reached, in approximately 24 hours, a 100 μL aliquot of the solution was taken and absorbance measured at 265 nm using a Biotek UV-Vis spectrophotometer (Biotek Instruments, Winooski, VT). Dynamic binding experiments were carried out to determine the time required to reach equilibrium. Binding parameters for all polymers were calculated by modeling using Langmuir and Freundlich isotherms.

5.4 Results and Discussion

Equilibrium template binding studies of highly and weakly crosslinked poly(MAA-co-EGDMA) polymers highlight enhanced binding parameters and demonstrate improved efficiency of the imprinting process by using living radical polymerization techniques. Tables 5.1 and 5.2, compare the binding affinity and capacity values of highly and weakly crosslinked polymers, respectively. The template binding capacity and affinity, of highly crosslinked gels, calculated using both Langmuir and Freundlich models are shown in Table 5.1 while the capacity and affinity of weakly crosslinked gels are shown in Table 5.2. In addition, the tables also show the values of the coefficient of determination (R^2) for both isotherms.

Both the Freundlich and Langmuir isotherms show considerably good fits for the polymers. Polymers which demonstrated comparable fits between the models tended to be further from the saturation region while polymers where there was a significant difference in the fits tended to be closer to the saturation region of the polymers. The Langmuir-Freundlich isotherm was also used to calculate the binding affinity and capacity values but they are not displayed since the values were close matches to those obtained using the Langmuir isotherm. The binding parameters calculated for the weakly crosslinked gels show a fairly good agreement between the two models. The binding affinity values for the highly crosslinked gels are also fairly consistent between the models. However, the binding capacities, for highly crosslinked polymers, calculated using Freundlich model are significantly higher than those calculated using the Langmuir isotherm, although they exhibit similarities when ratios are taken. The Freundlich model is based on an exponential growth model with multiple layers of template being bound at a specific binding site, assuming the template affinity of the binding site is high enough. In reality, however, these polymers do not exhibit multi-layer binding. In addition, there is a finite

limit to the binding capacity within a polymer whereas the Freundlich isotherm predicts infinitely high binding capacity at infinitely high concentrations. As a result, an analysis of the affinity distribution of binding sites in an approximate region is used to calculate the number of binding sites and the average binding affinity. For a more detailed discussion of how the binding affinities and capacities were calculated the readers are referred to Rampey et al. [32]. In this instance, the Freundlich model overestimates the binding capacity and therefore, the discussion in this chapter is restricted to the binding parameters calculated using the Langmuir isotherm.

Figure 5.1 shows equilibrium binding isotherms for highly crosslinked poly(MAA-co-EGDMA) imprinted and non-imprinted polymers prepared using conventional and living radical polymerization at various final double bond conversions. The imprinted polymer prepared via conventional free radical polymerization with 35% final double bond conversion (FRP35) exhibited a 79% increase in the number of binding sites and a 55% increase in binding affinity over that of the non-imprinted polymer. It is clear from this data that the inclusion of template during the polymerization reaction leads to enhanced template affinity and capacity; strong metrics that indicate molecular imprinting. Imprinted polymers prepared using living radical polymerization (LRP35) showed 64% increase in affinity with a small increase in the number of binding sites when compared to corresponding imprinted polymers prepared via conventional free radical polymerization (FRP35). Thus, living radical polymerization techniques produced significant increases in binding affinity of imprinted polymers without sacrificing the maximum binding capacity. It is important to note that using living radical polymerization in the creation of non-imprinted polymers does not result in a significant increase in either the binding capacity or the affinity. Thus, we can conclude that the living radical polymerization enhances the molecular imprinting process resulting in improved binding properties in molecularly imprinted polymers.

Increasing the final double bond conversion of imprinted polymers prepared via living radical polymerization resulted in an increase in the binding capacity of the polymers. These polymers (LRP44) displayed 4 times the number of binding sites at approximately equivalent affinity when compared to imprinted polymers prepared via conventional free radical polymerization with lower final double bond conversions (FRP35). The importance of this result can be highlighted by looking at the binding parameters of imprinted polymers prepared via conventional free radical polymerization with higher conversions (FRP48). A comparatively smaller 76% increase in the capacity at approximately equivalent affinity was observed when compared to an imprinted polymer with lower conversion (FRP35). Thus, a relatively modest increase in conversion while using living radical polymerization led to a dramatic increase in the binding capacity without resulting in a significant decrease in affinity. Thus, by controlling the double bond conversion, living radical polymerization can be used to increase either the capacity or the affinity of imprinted polymers.

The living radical polymerization technique involves the introduction of chain transfer molecules which combine with the macroradicals to form dormant species. This process allows for the formation of a more thermodynamically favorable network since the decrease in the rate of propagation allows the polymer radicals more time to reorganize to minimize the Gibb's free energy of the system. Using living radical polymerization leads to a delayed transition from the reaction controlled phase to the diffusion controlled phase. Figure 5.2 shows that the propagation phase in a living radical polymerization reaction is extended nearly three times over that in a conventional free radical polymerization reaction. It is important to note that fractional double bond conversions for the polymers shown in Figure 5.2 were not matched. Rather the initial reaction conditions were matched. As a result, living radical polymerization resulted in an

increase in the final fractional double bond conversion. In addition, we hypothesized that the extended propagation phase in living radical polymerization would result in polymer networks with fewer imperfections (like pendant double bonds and, primary and secondary cycles) in the polymer network allowing for higher overall crosslinking.

As in highly crosslinked poly(MAA-co-EGDMA) polymers, weakly crosslinked imprinted polymers prepared using living radical polymerization demonstrated enhancement in template binding parameters (Figure 5.3). Imprinted polymer gels prepared via conventional free radical polymerization demonstrated a 64% increase in binding capacity at nearly double the binding affinity of the non-imprinted gel. This clearly demonstrates the creation of macromolecular memory when a template molecule is present in the pre-polymerization mixture. Macromolecular memory is ideally suited to describe weakly crosslinked imprinted networks due to the significant flexibility in the polymer chains. Imprinted gels prepared using living radical polymerization showed close to 3 times the number of binding sites at the same affinity as the imprinted gels prepared by conventional free radical polymerization. The double bond conversion of the weakly crosslinked gels prepared using conventional free radical polymerization described above was 56%, while the double bond conversion of the gels prepared using living radical polymerization was 59%. An increase in the double bond conversion is expected to result in increased capacity. However, the magnitude of the increase in template binding seen here was much higher than the expected increase due to the increased conversion. Also, the use of living radical polymerization in the creation of weakly crosslinked non-imprinted polymers did not result in any significant improvements in their binding capacity or affinity. This shows that living radical polymerization enhances the creation of macromolecular memory in weakly crosslinked polymer gels.

All the highly crosslinked polymers discussed in this chapter demonstrate a double bond conversion of less than 50% while the weakly crosslinked polymers demonstrate higher conversions. For highly crosslinked polymers, the presence of a high concentration (88%) of short bifunctional crosslinking monomer in the feed constrains the flexibility and mobility of the growing polymer chains resulting in low fractional double bond conversion with a large concentration of pendant double bonds. The fractional double bond conversion reported here is consistent with the values reported in the literature [15, 17]. Conversely, for the weakly crosslinked polymers, the polymer chains are much less constrained and as a result, double bond conversions are higher and the impact of living radical polymerization on the binding parameters may be less pronounced.

Whereas the highly crosslinked polymers prepared using living radical polymerization show a four-fold increase in binding capacity at approximately equivalent affinity over the imprinted polymers prepared using conventional free radical polymerization; the weakly crosslinked gels show a comparatively smaller three fold increase in binding capacity while not showing a significant increase in affinity. However, even for weakly crosslinked gels the improvements introduced by living radical polymerization can have significant application potential, especially in the field of drug delivery [33-38].

It is important to note, that the binding capacity of the weakly crosslinked gels is typically higher than that of the highly crosslinked polymers. This is attributed to an increase in functional groups in the polymer, an increased flexibility of the weakly crosslinked gels allowing for more template capture, as well as more access to available binding sites. However, one must look at non-specific binding and the comparative increase in binding capacity between imprinted and non-imprinted networks to analyze the effect of imprinting more accurately. For instance, the

weakly crosslinked non-imprinted polymer binds more than the highly crosslinked non-imprinted polymer. However, the increase in binding due to imprinting is lower in the weakly crosslinked polymer compared to the highly crosslinked polymer.

Propagation in a free radical polymerization reaction has two stages. The first stage is reaction-controlled where the monomer addition to the growing macroradical is controlled only by the reactivity of the radical. As the reaction proceeds, the concentration of free monomer around the macroradical is depleted and, as a result, the reaction is controlled by the diffusion of the free monomer and the macroradical towards each other. As a result of the unavailability of monomers, many radicals undergo termination. The second (diffusion-controlled) stage is now reached where the termination of the reaction begins to gain importance over the propagation reaction. More homogenous polymer networks result when the propagation phase is extended. Figure 5.4 shows the observed propagation constant versus the double bond conversion for the polymerization reaction to produce the weakly crosslinked gels. In the reaction-controlled stage, the propagation reaction dominates; as a result, the apparent propagation constant stays constant. When the diffusion-controlled stage begins, the contribution of the propagation reaction decreases while that of the termination reaction increases. As a result, when the apparent propagation constant begins to drop, one can assume a transfer from the reaction-controlled to the diffusion-controlled stage. From Figure 5.4, it is clear that living radical polymerization reactions are in the reaction-controlled stage for a greater proportion of the time; approximately 40% of the polymer is formed under the reaction-controlled phase conducive to more homogenous network formation. However, in the case of the conventional free radical polymerization reaction, only 23% of the polymer is formed in the reaction-controlled phase. As a result, even though the final double bond conversion is similar for both reactions, the larger

proportion of polymer formed in the reaction-controlled phase allows the polymer prepared via living radical polymerization to have a more homogenous network overall. It is important to note that the propagation constant for the living radical polymerization reaction is an order of magnitude smaller than that of the conventional free radical polymerization, further extending the time available for the macroradicals to reach minimal free energy states within the polymer network. Figure 5.5 is a similar graph showing the propagation constant for highly crosslinked polymers. As in Figure 5.4, the propagation constant for the living radical polymerization reaction is an order of magnitude smaller than the conventional free radical polymerization reaction. Also, the living radical polymerization reaction appears to be reaction controlled for a majority of the duration (up to a fractional double bond conversion of 32%) whereas the conventional free radical polymerization switches to the diffusion controlled stage relatively quickly (around 12% fractional double bond conversion). Thus, an increase in the crosslinker content results in an early transition to the diffusion-controlled stage. The imprinted polymer prepared via conventional free radical polymerization with a higher initiator concentration stays in the reaction controlled stage for longer (up to 19% double bond conversion).

The discussion above illustrates the effect of living radical polymerization on the kinetics of the polymerization reaction. This analysis can be useful in understanding the effect of living radical polymerization on polymer chain growth and network formation. However, analyzing the polymer chains composing the polymer network would be more beneficial in terms of explaining the role of living radical polymerization in enhancing molecularly imprinting in polymer networks. However, the insolubility of poly(MAA-co EGDMA) polymer networks makes it extremely difficult to analyze their structure directly. As a result, poly(MAA) homopolymers prepared without any crosslinker were used to model the polymer chain growth in crosslinked

systems prior to gelation. Although we expect differences in polymer network formation in crosslinked and uncrosslinked networks, we believe the uncrosslinked polymers can approximate polymer chain growth in crosslinked polymers especially at very low concentrations of the crosslinking monomer.. Thus, the next phase of this work involved the analysis of poly(MAA) chains formed in the presence of template using both conventional and living radical free radical polymerization. Figure 5.6 shows the average molecular weight of poly(MAA) chains as a function of the template/monomer ratio. The template/monomer ratio in the pre-polymer mixture is varied by the addition of increasing amounts of template to the pre-polymerization mixture. As the template concentration increases (increasing template/monomer ratio) the average molecular weight of the corresponding polymer chain decreases. This is an important result as it proves that the decrease in average molecular weight of the polymer chains occurs despite a slight increase in the conversion (Figure 5.7). Therefore, the decrease in average molecular weight cannot be attributed to less monomer being incorporated into the growing chains. Rather at higher template concentrations, there is a tendency of a larger number of comparatively shorter polymer chains to be formed. This may be a result of the diffusional limitations introduced by the presence of the template molecule. The major interaction between the template molecules and the functional monomer is in terms of hydrogen bonds. The template molecules in this case (EA9A) have multiple nucleophilic groups and as a result they can form up to four H-bonds with multiple functional monomer molecules. The resultant template-macromer complexes occupy significantly greater volume as compared to the individual functional monomer molecules and the diffusion of the large and bulky template-macromer complexes becomes a rate limiting step. Thus, we hypothesize that the presence of template causes the polymerization reaction to shift from a reaction-controlled stage to a diffusion-controlled stage earlier than expected.

Living radical polymerization has been demonstrated to extend the propagation period of a polymerization reaction [14]. The active chain transfer radicals combine with polymer radicals to undergo a reversible termination reaction, forming meta-stable species. This results in delayed auto-acceleration and compensates for any diffusional limitation to propagation introduced by the presence of the template molecule. Thus, the addition of chain transfer agent to the pre-polymerization mixture counterbalances the retardation of kinetic chain length of the resultant polymer chains caused by the diffusional limitations presented by an increasing concentration of monomer-template complexes. This is demonstrated in Figure 5.6 where the average molecular weight does not decrease despite an increase in the template concentration. In addition, the longer propagation period combined with the decreased rate of propagation allows the polymer chains to grow uniformly and simultaneously resulting in more monodisperse polymers prepared via LRP as compared to the corresponding polymers prepared via FRP. Figure 5.8 shows the polydispersity index of the poly(MAA) chains as a function of their template concentration. An increase in the template concentration in the pre-polymerization mixture led to a higher polydispersity in the resultant polymer chains. The increased polydispersity can be attributed to the early transition to the diffusion-controlled stage of propagation. Living radical polymerization, however, extends the reaction-controlled stage of propagation negating the effect of the template on the polymerization reaction, leading to a more consistent polydispersity index independent of template concentration in the pre-polymerization solution.

5.5 Conclusions

This work highlights the improved efficiency of the imprinting process achieved by using living radical polymerization techniques on both highly and weakly crosslinked polymers. The use of living radical polymerization techniques resulted in quadrupling of the number of binding

sites in highly crosslinked imprinted polymers; meanwhile, the number of binding sites in weakly crosslinked imprinted gels was tripled by the use of living radical polymerization techniques. It is important to note that the increased binding capacity demonstrated by both the highly, and weakly crosslinked, imprinted polymers prepared via living radical polymerization demonstrated was achieved at similar binding affinities to those of the corresponding imprinted polymers prepared via conventional free radical polymerization. In addition, by adjusting the double bond conversion we can choose to increase either the template binding capacity or affinity of highly crosslinked imprinted polymers, thus, allowing the creation of imprinted polymers with tailorable binding parameters.

Analysis of the polymerization reaction revealed that the observed increase in binding parameters in the highly and weakly crosslinked polymers can be explained by the extension of the reaction-controlled regime during propagation of the macroradical which allows the macroradical more time to achieve a minimal global free energy configuration. The propagation phase in a highly crosslinked system is shown to be extended nearly three times when living radical polymerization is used. For weakly crosslinked system, it is shown that nearly twice the amount of polymer is created in the reaction-controlled regime, when living radical polymerization is used. For uncrosslinked systems, living radical polymerization allows the macroradicals more time to grow which compensates for the decrease in chain length and increase in polydispersity caused by the presence of the template. Thus, living radical polymerization techniques are shown to have extended propagation in polymerization reactions which subsequently resulted in more monodisperse polymer chains and more homogenous polymer networks.

5.6 References

1. Umpleby II RJ, Bode M, Shimizu KD. Measurement of the Continuous Distribution of Binding Sites in Molecularly Imprinted Polymers Analyst. 2000, 125, (7), 1261-1265.
2. Shea KJ, Spivak DA, Sellergren B. Polymer Complements to Nucleotide Bases. Selective Binding of Adenine Derivatives to Imprinted Polymers. J. Am. Chem. Soc. 1993, 115, 8, 3368-3369.
3. Spivak D, Gilmore MA, Shea KJ. Evaluation of Binding and Origins of Specificity of 9-Ethyladenine Imprinted Polymers. J. Am. Chem. Soc. 1997, 119, 19, 4388-4393.
4. Byrne ME, Salian V. Molecular imprinting within hydrogels. II. Progress and analysis of the field. Int. J. Pharm. 2008, 364, 188–212.
5. Anandkumar KR, Anderson KJ, Anseth JW, Bowman CN. Use of "living" radical polymerizations to study the structural evolution and properties of highly crosslinked polymer networks. J. Polym. Sci., Part B: Polym. Phys. 1997, 35, 2297 -2307.
6. Anandkumar KR, Anseth JW, Bowman CN. A study of the evolution of mechanical properties and structural heterogeneity of polymer networks formed by photopolymerizations of multifunctional (meth)acrylates. Polymer. 1998, 39, 12, 2507-2513.
7. Anseth KS, Kline LM, Walker TA, Anderson KJ, Bowman CN. Reaction kinetics and volume relaxation during polymerizations of multiethylene glycol dimethacrylates. Macromolecules. 1995, 28, 2491–2499.
8. Anseth KS, Wang CM, Bowman CN. Reaction behaviour and kinetic constants for photopolymerizations of multi(meth)acrylate monomers. Polymer. 1994, 35, 3243–3250.
9. Burkoth AK, Anseth KS. MALDI-TOF Characterization of Highly Crosslinked, Degradable Polymer Networks. Macromolecules. 1999, 32, 1438-44.

10. Hutchison JB, Lindquist AS, Anseth KS. Experimental characterization of structural features during radical chain homopolymerization of multifunctional monomers prior to macroscopic gelation. Macromolecules. 2004, 37, 10, 3823-3831.
11. Gao H, Miasnikova A, Matyjaszewski K. Effect of Cross-Linker Reactivity on Experimental Gel Points during ATRcP of Monomer and Cross-Linker. Macromolecules. 2008, 41, 7843-7849.
12. Gao H, Min K, Matyjaszewski K. Determination of Gel Point during Atom Transfer RadicalCopolymerization with Cross-Linker. Macromolecules. 2007, 40, 7763-7770.
13. Wang AR, Zhu S. Branching and Gelation in Atom Transfer Radical Polymerization of Methyl Methacrylate and Ethylene Glycol Dimethacrylate. Polym. Eng. Sci. 2005, 45, 720–727.
14. Kannurpatti AR, Lu S, Bunker GM, Bowman CN. Kinetic and Mechanistic Studies of Iniferter Photopolymerizations. Macromolecules. 1996, 29, 7310-7315.
15. Vaughan AD, Byrne ME. Optimizing recognition characteristics of biomimetic polymer gels via polymerization reaction and crosslinking density analysis. ACS PMSE Preprints. 2006, 94, 762–763.
16. Boonpangrak S, Whitcombe MJ, Prachayasittikul V, Mosbach K, Ye L. Preparation of molecularly imprinted polymers using nitroxide-mediated living radical polymerization. Biosens Bioelectron. 2006, 22, 349–354.
17. Vaughan AD, Sizemore SP, Byrne ME. Enhancing molecularly imprinted polymer binding properties via controlled/living radical polymerization and reaction analysis. Polymer. 2007, 48, 74-81.

18. Vaughan AD. Reaction Analysis of Templated Polymer Systems. Doctoral dissertation. 2008, (Doctoral) Dissertation, Auburn University.
19. Vaughan AD, Zhang JB, Byrne ME. Enhancing Therapeutic Loading and Delaying Transport via Molecular Imprinting and Living/Controlled Polymerization. AIChE Journal. 2010, 56, 1, 268-279.
20. Pan G, Zu B, Guo X, Zhang Y, Li C, Zhang H. Preparation of molecularly imprinted polymer microspheres via reversible addition–fragmentation chain transfer precipitation polymerization. Polymer. 2009, 50, 2819–2825.
21. Zu B, Zhang Y, Guo X, Zhang H. Preparation of molecularly imprinted polymers via atom transfer radical "bulk" polymerization, J. Polym. Sci., Part A: Polym. Chem. 2010, 48, 3, 532-541.
22. Halhalli M, Sellergren B. Investigation of the influence of reversible addition fragmentation chain transfer (RAFT) agent on the performance and properties of an L-phenylalanine MIP. In MIP2010: The future of molecular imprinting, Spivak DA, Shea KJ (eds). 2010, New Orleans; 46.
23. Pasetto P, Haupt K. Living/controlled radical polymerization techniques applied to the synthesis of molecularly imprinted polymers In MIP2010: The future of molecular imprinting, Spivak DA, Shea KJ (eds). 2010, New Orleans; 89.
24. Ruckert B, Hall AJ, Sellergren B. Molecularly imprinted composite materials via iniferter-modified supports. J. Mater. Chem. 2002, 12, 2275–2280.
25. Southard GE, Van Houten KA, Murray GM. Soluble and Processable Phosphonate Sensing Star Molecularly Imprinted Polymers. Macromolecules. 2007, 40, 1395-1400.

26. Pan G, Zhang Y, Guo X, Li C, Zhang H. An efficient approach to obtaining water-compatible and stimuli-responsive molecularly imprinted polymers by the facile surface-grafting of functional polymer brushes via RAFT polymerization. Biosens Bioelectron. 2010, 26, 3, 976-982.
27. Wei X, Li X, Husson SM. Surface Molecular Imprinting by Atom Transfer Radical Polymerization, Biomacromolecules. 2005, 6, 1113-1121.
28. Chang L, Li Y, Chu J, Qi J, Li X. Preparation of core-shell molecularly imprinted polymer via the combination of reversible addition-fragmentation chain transfer polymerization and click reaction. Anal. Chim. Acta. 2010, 680, 65-71.
29. Li Y, Li X, Dong CK, Li YQ, Jin PF, Qi JY. Selective recognition and removal of chlorophenols from aqueous solution using molecularly imprinted polymer prepared by reversible addition-fragmentation chain transfer polymerization. Biosens. Bioelectron. 2009, 25, 306–312.
30. Flory PJ. Principles of Polymer Chemistry, 1st ed. 1953, Cornell University Press: Ithaca.
31. Odian G. Principles of Polymerization, 2nd ed. 1981, John Wiley & Sons: New York.
32. Rampey AM, Umpleby RJ, Rushton GT, Iseman JC, Shah RN, Shimizu KD. Characterization of the Imprint Effect and the Influence of Imprinting Conditions on Affinity, Capacity, and Heterogeneity in Molecularly Imprinted Polymers Using the Freundlich Isotherm-Affinity Distribution Analysis. Anal. Chem. 2004, 76, 4, 1123-1133.
33. Venkatesh S, Sizemore SP, Byrne ME. Biomimetic hydrogels for enhanced loading and extended release of ocular therapeutics. Biomaterials. 2007, 28, 717–724.

34. Ali M, Horikawa S, Venkatesh S, Saha J, Hong JW, Byrne ME. Zero-order therapeutic release from imprinted hydrogel contact lenses within in vitro physiological ocular tear flow. J. Controlled Release. 2007, 124, 154–162.
35. Ali M, Byrne ME. Controlled release of high molecular weight hyaluronic acid from molecularly imprinted hydrogel contact lenses. Pharm. Res. 2009, 26, 714–726.
36. Hiratani H, Fujiwara A, Tamiya Y, Mizutani Y, Alvarez-Lorenzo C. Ocular release of timolol from molecularly imprinted soft contact lenses. Biomaterials. 2005, 26, 1293–1298.
37. Alvarez-Lorenzo C, Yanez F, Barreiro-Iglesias R, Concheiro A. Imprinted soft contact lenses as norfloxacin delivery systems. J. Controlled Release. 2006, 113, 236–244.
38. Venkatesh S, Saha J, Pass S, Byrne ME. Transport and structural analysis of molecular imprinted hydrogels for controlled drug delivery. Eur. J. Pharm. Biopharm. 2008, 69, 852–860.

Table 5.1: EA9A Binding Capacities and Affinities of Poly(MAA-co-EGDMA) Polymers prepared with 88% Crosslinking Monomer in Feed

Polymer type (DBC)	K_a Freundlich (mM^{-1})	Q_{max} Freundlich (µmol/g)	R^2 Freundlich	K_a Langmuir (mM^{-1})	Q_{max} Langmuir (µmol/g)	R^2 Langmuir
Non-imprinted (35%)	1.54±0.20	560±38	0.916	2.26±0.20	1.4±0.3	0.981
Living non-imprinted (35%)	1.72±0.34	638±48	0.924	2.37±0.40	1.8±0.4	0.984
FRP35 (35%)	3.12±0.21	776±54	0.739	3.51±0.18	2.5±0.5	0.869
LRP35 (35%)	5.94±0.41	813±62	0.735	5.74±0.31	3.0±0.4	0.852
LRP44 (44%)	2.62±0.12	1421±64	0.963	3.46±0.29	10.8±0.7	0.975
FRP48 (48%)	2.63±0.17	862±60	0.939	3.31±0.33	4.4±0.5	0.978

Table 5.2: EA9A Binding Capacities and Affinities of Poly(MAA-co-EGDMA) Polymers prepared with 5% Crosslinking Monomer in Feed

Gel type (DBC)	K_a Freundlich (mM^{-1})	Q_{max} Freundlich (µmol/g)	R^2 Freundlich	K_a Langmuir (mM^{-1})	Q_{max} Langmuir (µmol/g)	R^2 Langmuir
Non-imprinted (56%)	1.93±0.10	14±3	0.937	1.48±0.15	12.9±2.7	0.993
Living non-imprinted (60%)	2.06±0.14	18±3	0.931	1.61±0.22	15.7±3.1	0.992
FRP (56%)	2.45±0.13	20±2	0.894	2.91±0.19	21.1±2.0	0.967
LRP (59%)	2.21±0.11	38±4	0.924	3.11±0.36	59.4±6.4	0.999

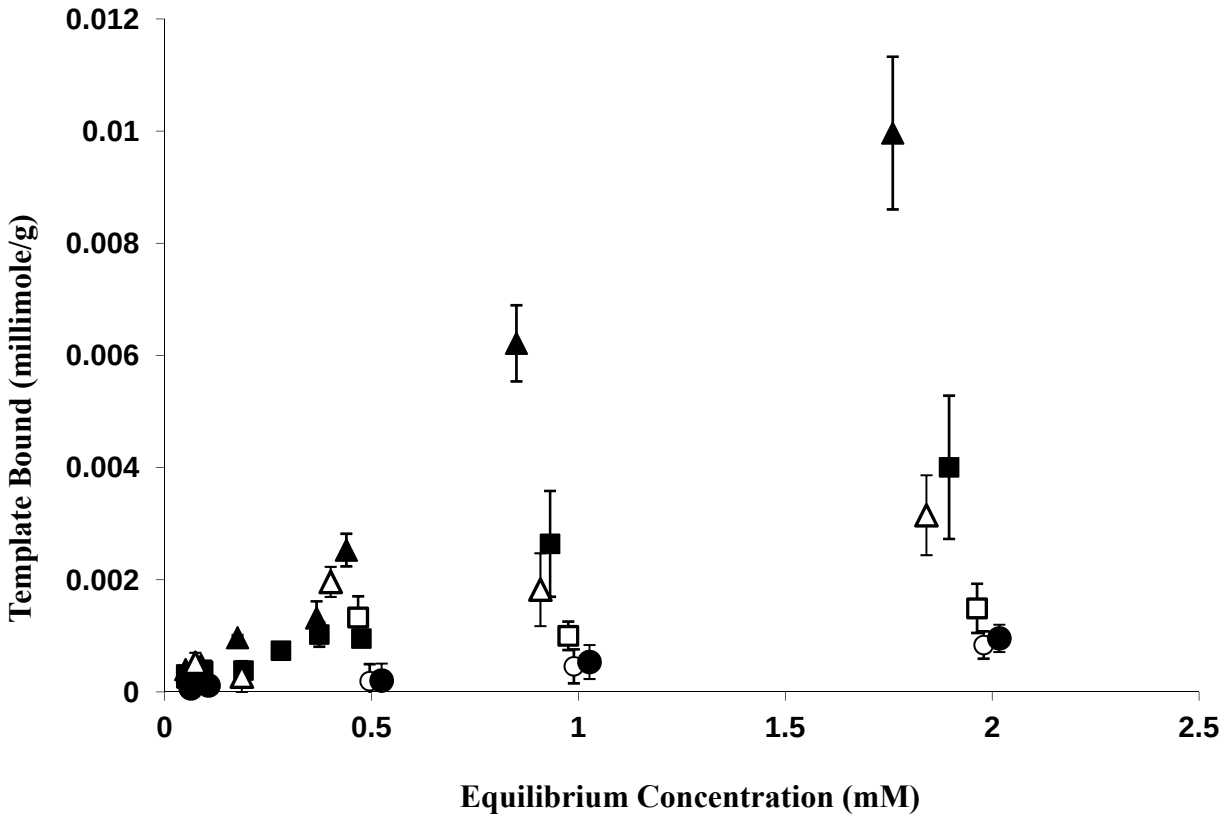

Figure 5.1: Equilibrium Binding Isotherms for EA9A Binding by Highly Crosslinked Imprinted Poly(MAA-co-EGDMA) Networks prepared via FRP and LRP. Poly(MAA-co-EGDMA) imprinted polymers prepared via LRP with 44% double bond conversion (▲), prepared via LRP with 35% double bond conversion (Δ), prepared via FRP with 48% double bond conversion (■), prepared via FRP with 35% double bond conversion (□), and non-imprinted polymers prepared via LRP (●) and FRP (○) are shown here. Error bars represent the standard error (n = 4). LRP leads to significantly higher loading as compared to FRP.

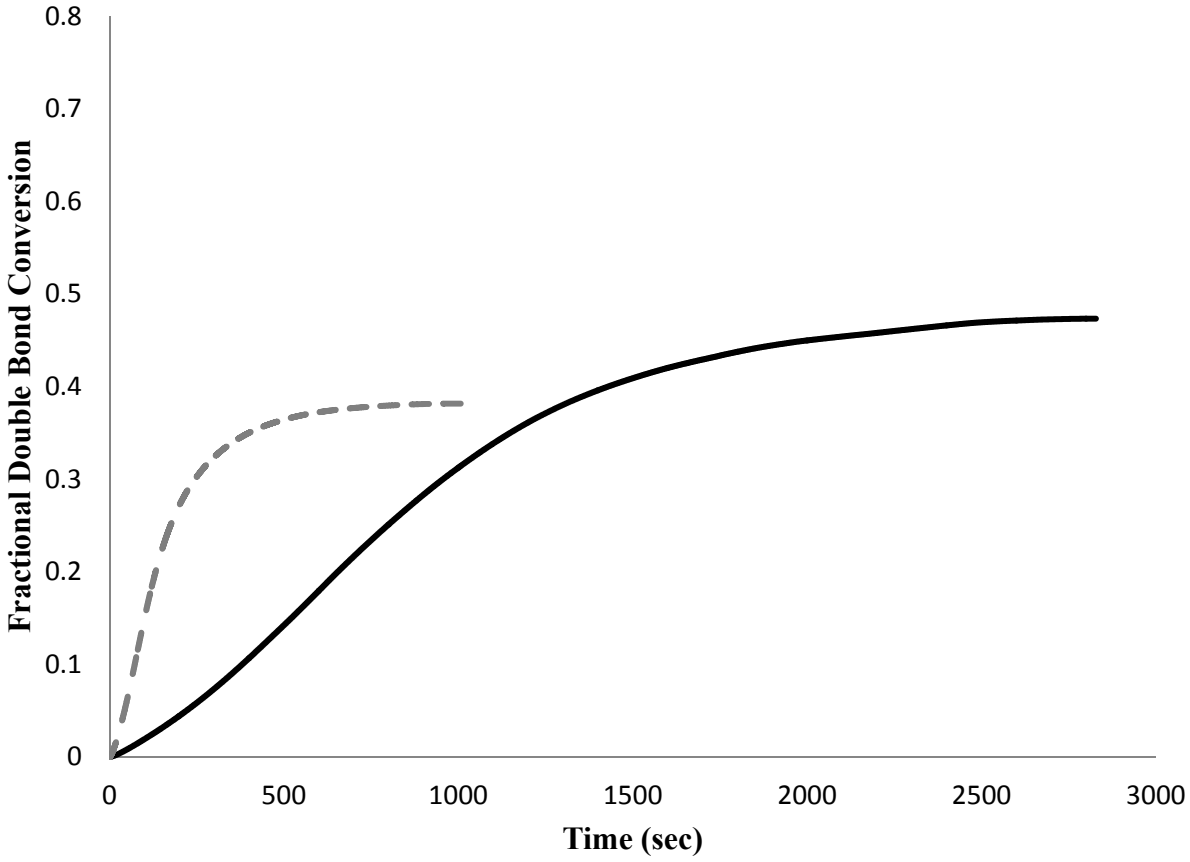

Figure 5.2: Dynamic Double Bond Conversion of Poly(MAA-co-EGDMA) Imprinted Network. Double bond conversion verses time for a typical imprinted polymer synthesized via FRP (---) and LRP (▬). Both polymers had 88% crosslinker in feed and a monomer-template ratio of 11.79. The final double bond conversion reached is 35% for the typical imprinted polymer and 44% for the polymer synthesized via LRP. The propagation phase in LRP is extended nearly three times over FRP.

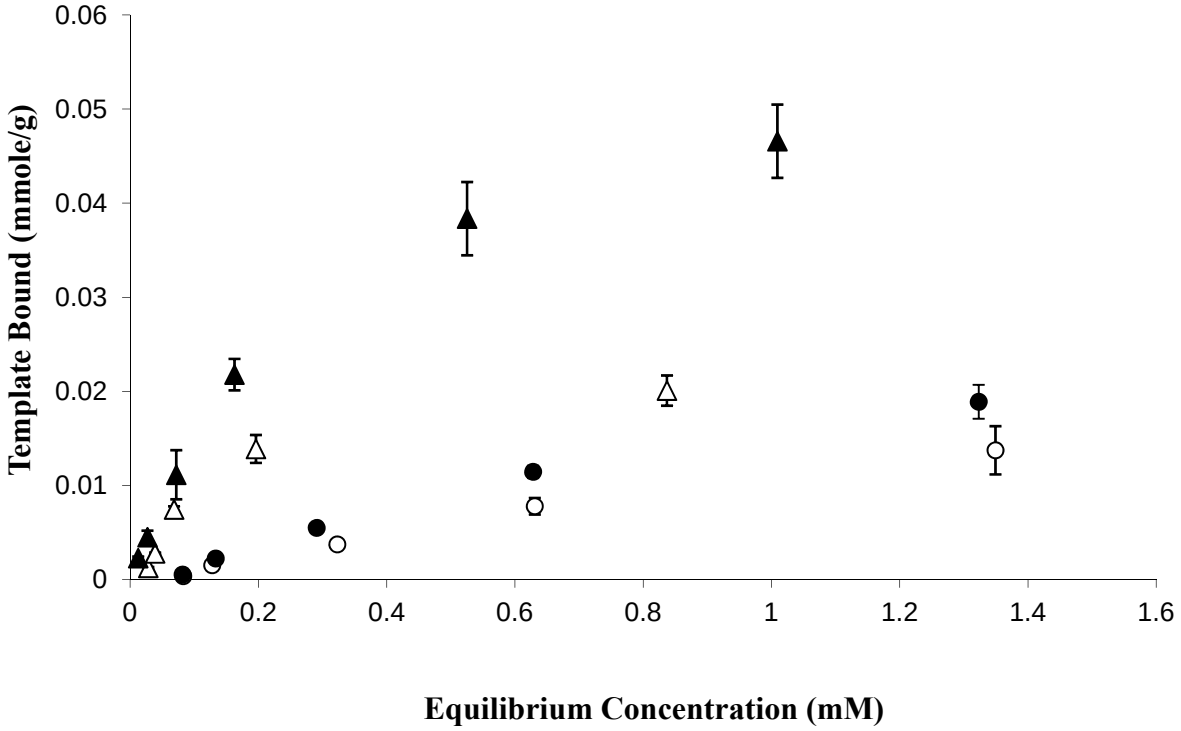

Figure 5.3: Equilibrium Binding Isotherms for EA9A Binding by Weakly Crosslinked Imprinted Poly(MAA-co-EGDMA) Networks prepared via FRP and LRP. Data points represent the non-imprinted poly(MAA-co-EGDMA) gels prepared via FRP(○)and LRP(●),the poly(MAA-co-EGDMA) imprinted gel prepared via FRP (Δ) and LRP (▲). The poly(MAA-co-EGDMA) imprinted gel prepared via LRP has a binding capacity 139% higher than the poly(MAA-co-EGDMA) imprinted gel capacity and 258% higher than the control. Error bars represent the standard error with n=4. LRP leads to tripling of the binding capacity at the same binding affinity.

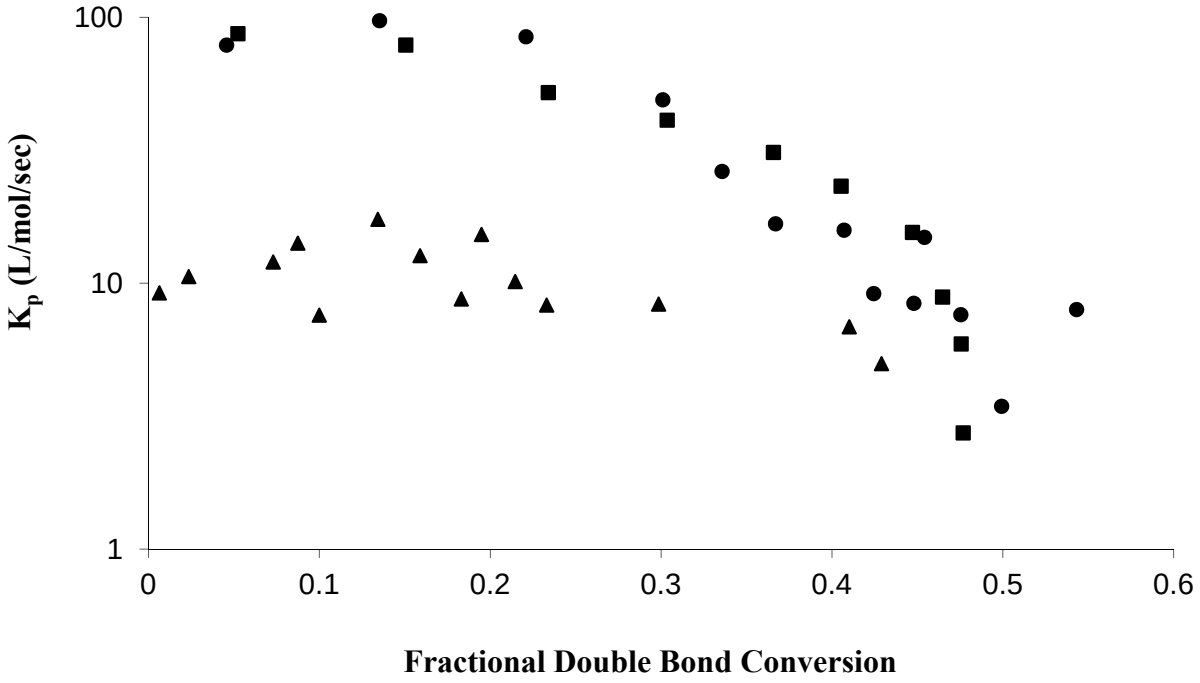

Figure 5.4: Propagation Constant from Kinetic Analysis of Weakly Crosslinked Poly(MAA-co-EGDMA) Formation. The propagation constant for the poly(MAA-co-EGDMA) imprinted (■)and non-imprinted gels (●) synthesized via FRP showed statistically similar trends with respect to the double bond conversion. Chemically controlled propagation mechanism occurs until about 0.23 fractional double bond conversion. Higher conversions have a decrease in propagation indicating diffusion controlled propagation. The imprinted gel prepared via LRP (▲) shows a more constant rate of propagation until a fractional double bond conversion of 0.40 indicating a longer reaction-controlled propagation mechanism.

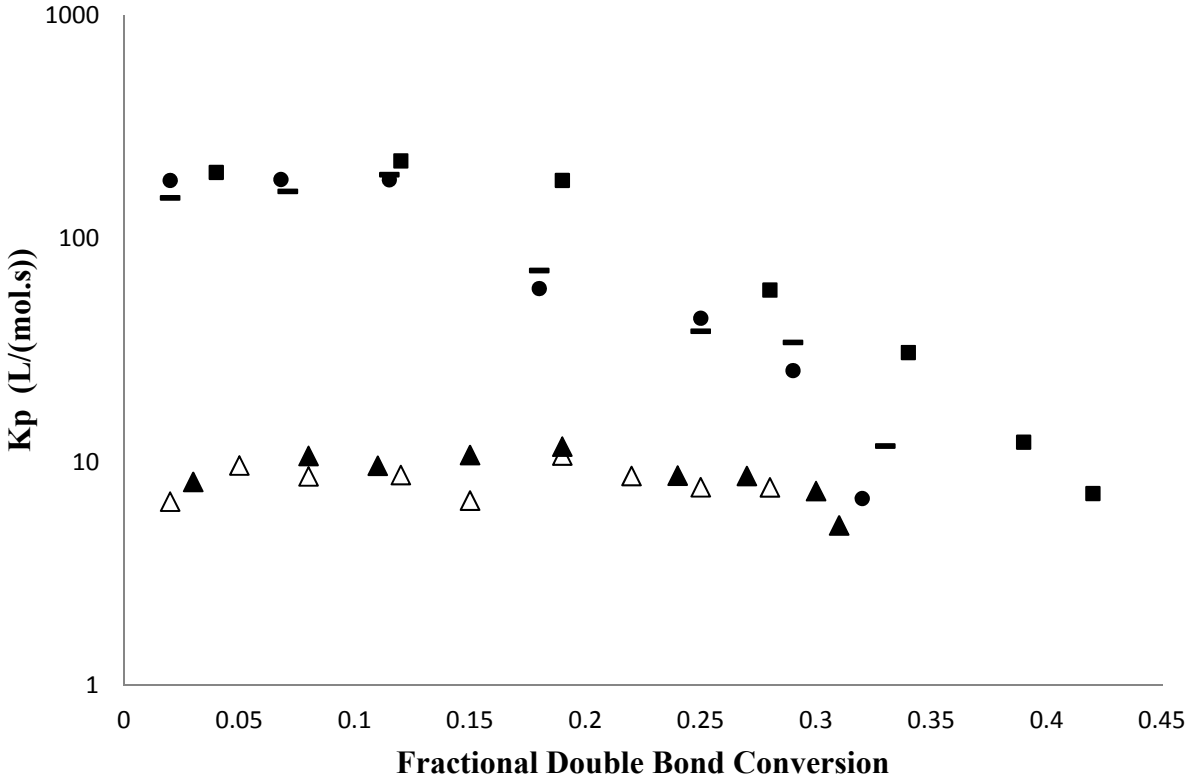

Figure 5.5: Propagation Constant from Kinetic Analysis of Highly Crosslinked Poly(MAA-co-EGDMA) Formation. The propagation constant versus the fractional double bond conversions for poly(MAA-co-EGDMA) imprinted polymers prepared via LRP with 44% double bond conversion (▲), prepared via LRP with 35% double bond conversion (Δ), prepared via FRP with 48% double bond conversion (■), prepared via FRP with 35% double bond conversion (●), and the non-imprinted network via FRP (—) are shown.

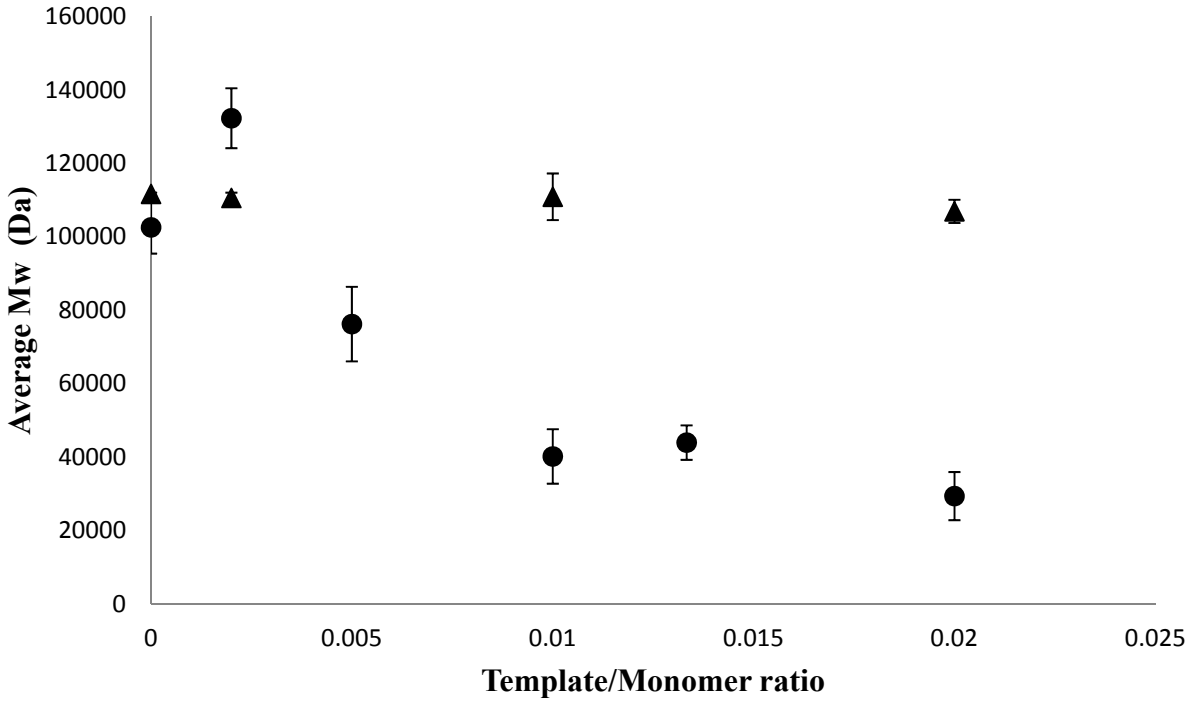

Figure 5.6: Effect of Template Concentration on Kinetic Chain Length of Poly(MAA) Chains. Weight average molecular weight versus template/monomer ratio for poly(MAA) polymers prepared via FRP(●) and LRP (▲) are shown here. Presence of template in the reaction mixture leads to the formation of polymers with shorter chains due to an early transition into the diffusion-controlled regime of propagation. LRP counteracts it by extending the reaction-controlled regime. Error bars represent the standard error with n=3.

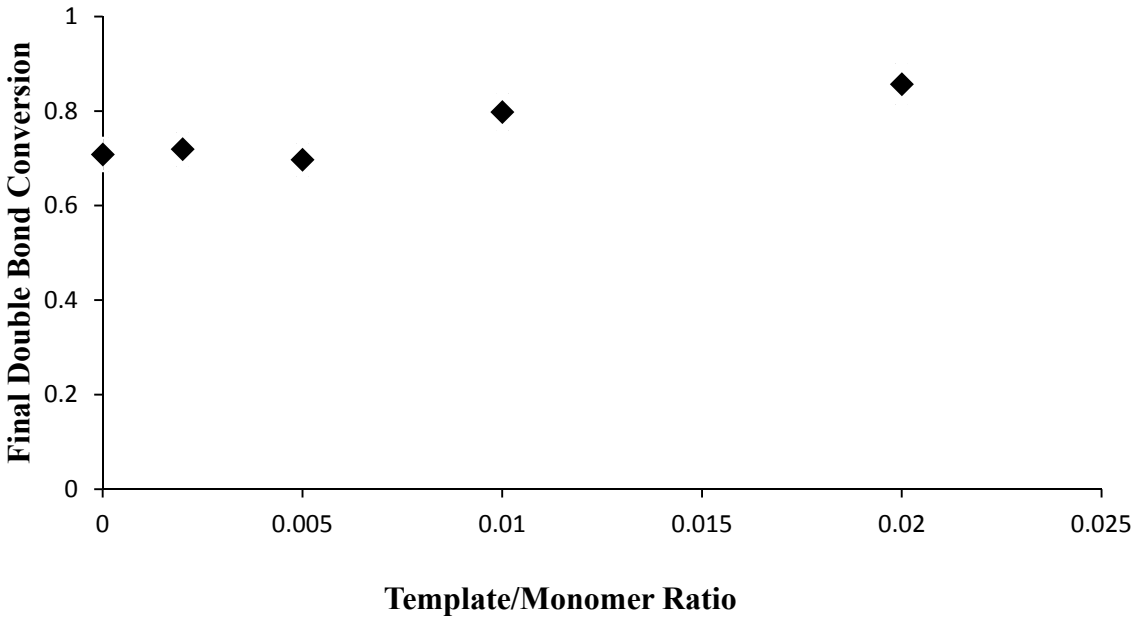

Figure 5.7: Effect of Template Concentration on Double Bond Conversion of Poly(MAA) prepared via FRP. The final double bond conversion of poly(MAA) homopolymers prepared via FRP is presented as a function of the template concentration. A strong correlation is not observed as the final double conversion increases only slightly even at the maximum allowable template concentration.

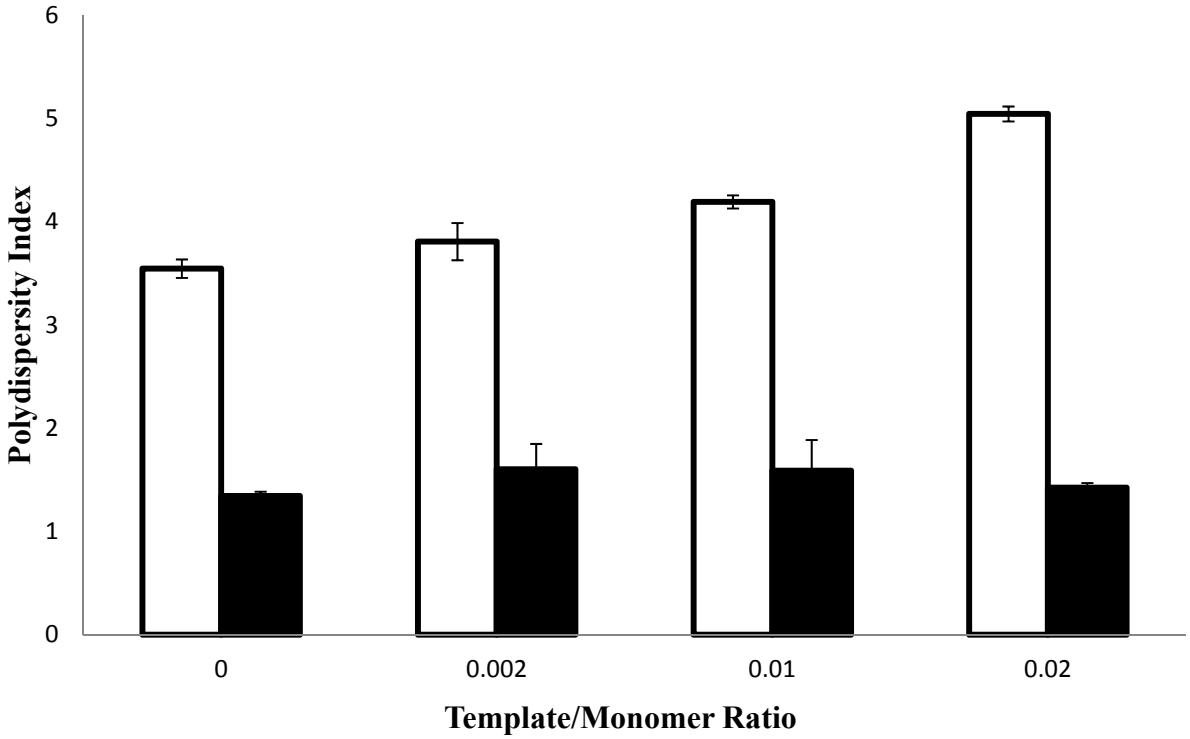

Figure 5.8: Effect of Template Concentration on Polydispersity Index of Poly(MAA) Chains. Polydispersity index of poly(MAA) polymers prepared via FRP (□) and LRP (■) are shown here as a function of the template concentration. Presence of template in the reaction mixture leads to higher polydispersity due to an early transition into the diffusion-controlled regime of propagation. LRP counterbalances it by extending the reaction-controlled regime. Error bars represent the standard error with n=3.

CHAPTER 6: ENHANCING DRUG LOADING IN AND CONTROLLING RELEASE FROM IMPRINTED POLYMERS PREPARED VIA LRP: MANIPULATING TEMPLATE-MONOMER INTERACTION

6.1 Scientific Rationale

In this chapter, the synthesis and characterization of poly(hydroxyethyl methacrylate-co-diethylaminoethyl methacrylate-co-poly(ethyleneglycol200) dimethacrylate) (poly(DEAEM-co-HEMA-co-PEG200DMA)) polymer gels imprinted with diclofenac sodium is discussed. The poly(DEAEM-co-HEMA-co-PEG200DMA) system was chosen because the ionic interaction between the template and functional monomer (FM) is significantly stronger than the hydrogen bonding in the poly(methacrylic acid-co-ethylene glycol dimethacrylate) (poly(MAA-co-EGDMA)) networks. Thus, the effects of variation in the template-monomer interaction should be amplified enough to give observable results. The objective was to analyze the polymer chain growth and network formation, and the corresponding changes to template binding and template transport properties of the polymer gels when the template-monomer interaction was altered. The template-monomer interaction was altered by varying different reaction parameters such as template concentration, functional monomer concentration and presence of solvent during polymerization. Imprinted polymer gels were first synthesized by matching all conditions stated within previously published work [1]. The binding characteristics were determined and

compared to documented literature values in order to ensure the same network was accurately reproduced.

6.2 Introduction

Molecular imprinting is the design of polymer networks that can recognize a given template molecule and bind it preferentially in solution. Selective binding of template molecules combined with stability and cost effectiveness make MIPs attractive for many analytical applications, including catalysis, sensing, solid-phase extraction, chromatography, and binding assays [2-4]. Recently, the potential of molecularly imprinted polymers for new applications in the pharmaceutical field as carriers for drugs, peptides, and proteins has gained increasing attention [5-9]. Imprinted polymers with enhanced affinity for specific molecules could be used as the basis of rate controlled release, triggered or, even, feedback-regulated drug delivery devices [10].

Despite the many attractive attributes of MIPs, wide use of these materials has not been realized. This is primarily because of deficiencies in their binding properties. MIPs, in general, have low average binding affinities and a high degree of binding site heterogeneity. Attempts to improve the binding site heterogeneity have been reported [11], but they come with a decrease in the template binding capacity which is especially detrimental to drug delivery applications. Rational methods of improving the binding characteristics, however, have been limited by a lack of understanding of the synergy between the imprinting process and the polymerization reaction. This is especially true of conventional free radical polymerization (FRP) which is by far the most popular polymerization reaction due to its versatility and economic viability. Unfortunately, FRP gives rise to heterogeneity in the polymer network formed which further exacerbates the binding site heterogeneity observed in molecularly imprinted polymers. Novel techniques like living

radical polymerization (LRP) offer hope in terms of achieving both improved template binding and decreased binding site heterogeneity.

LRP offers the ability to create improved imprinted polymers with more homogeneous network structures [12-13] and, as a result, better binding parameters [1, 14-17]. In addition, using LRP can lead to more control over network structures and a better understanding of their structure-property relationships; however, these reactions are relatively new to the imprinting field and have not been used extensively in molecular imprinting. The first reports of enhanced binding properties in highly cross-linked imprinted polymer networks using LRP were published in 2006 [14-15]. Boonpangrak et al. [14] used covalent imprinting due to the use of a high temperature polymerization reaction while our group [15-16] used UV polymerization which allowed the use of the more favorable non covalent imprinting technique. In addition, our group [1] was the first to demonstrate that using LRP to prepare weakly cross-linked imprinted gels can result in increased template binding capacity and affinity. Pan et al. [17] used reversible addition-fragmentation chain transfer (RAFT) polymerization to create MIP microspheres using precipitation polymerization and they reported higher binding capacity per unit surface area in the RAFT polymerized microspheres over the microspheres prepared via conventional free radical polymerization.

The primary issue with FRP is the mismatch between the rapid chain growth during polymerization and slow chain relaxation of the polymer formed which results in structural heterogeneity in polymer networks generated by FRP [12-13]. As the polymerization reaction proceeds and the conversion increases, the bimolecular termination reaction between two polymer chains becomes difficult because of diffusional limitations. LRP, by contrast, is a much slower reaction making it thermodynamically favorable to the formation of a more homogeneous

polymer network. It replaces the bimolecular termination between polymer chains with a macroradical iniferter termination reaction which prevents or delays auto-acceleration, forming a more homogenous polymer network.

Combining molecular imprinting with LRP has been shown to result in enhanced template binding and delayed release as shown above. However, there has not been an effort to understand the effect of LRP on (a) polymer network structure in imprinted polymer networks and (b) the template binding cavities in the imprinted polymer network. A better understanding of these relationships could lead to the rational design of imprinted polymer networks and gels with the ability to control their template binding and template transport properties. In the work described in this chapter, various reaction parameters, which would affect the template-monomer interaction in the pre-polymerization solution and thus template binding cavities formed in the polymer gels, were altered. The reaction parameters which were varied were the template concentration, functional monomer concentration and solvent content. In addition, all gels were prepared via both FRP and LRP. During the polymerization, reaction analysis was used to determine the double bond conversion of the imprinted polymer. In addition, analysis of the reaction signature in the absence of light was used to calculate the kinetic constants for the reaction. Further analysis of the network structure was carried out by analyzing the growing polymer chains of the imprinted network. Lastly, binding and release studies were carried out to evaluate the template binding and transport properties of the gels. By exploring weakly crosslinked systems, we could analyze the effect of the template concentration on polymer chain growth, in terms of dispersity and molecular weight. In addition, the effect of LRP on the formation of template binding cavities in imprinted networks while varying different reaction

parameters was analyzed. This work will allow much better control of the properties of molecularly imprinted polymers and will result in their broader use in novel technologies.

6.3 Materials and Methods

Poly(ethyleneglycol(200))dimethacrylate (PEG200DMA) was used as received while (diethylaminoethyl)methacrylate (DEAEM) and (hydroxyethyl)methacrylate (HEMA), had inhibitors removed via inhibitor removal packing sieves prior to polymerization. The initiator azo-bis(isobutyronitrile) (AIBN), template molecule (diclofenac sodium (DS)), and chain transfer agent (tetraethylthiuram disulfide (TED)) were used as received. Monomers, inhibitor removal packing sieves, initiator, chain transfer agent, and template were purchased from Aldrich (Milwaukee, WI). HPLC grade solvents, acetonitrile and methanol, were used as received from Fisher Scientific (Pittsburgh, PA). De-ionized (DI) water was the template rebinding solvent, the wash solvent (to remove template and unreacted monomer) as well as the mobile phase in the high pressure liquid chromatography (HPLC) system.

6.3.1 Synthesis of Poly(DEAEM-co-HEMA-co-PEG200DMA) Gels

Poly(DEAEM-co-HEMA- co-PEG200DMA) gels imprinted for DS with a 5% crosslinking percentage were made with 0.336 mL of DEAEM (1.673 mmol), 3.659 mL of HEMA (30.118 mmol), 0.538 mL of PEG200DMA (1.673 mmol), 20 mg of AIBN (0.121 mmol), and 150 mg of DS (0.352 mmol). The solutions were mixed and sonicated until all solids were dissolved. Non-imprinted polymers were prepared similarly except the template was absent. The poly(DEAEM-co-HEMA- co-PEG200DMA) imprinted gel prepared via LRP was synthesized with 4.20 mg of TED (0.014 mmol) and 40 mg of AIBN (0.242 mmol). Solutions were transferred to an MBraun Labmaster 130 1500/1000 Glovebox (Stratham, NH), which provided an inert (nitrogen) atmosphere for free radical UV photopolymerization. Then monomer solutions were pipetted

between two 6" x 6" glass plates coated with trichloromethylsilane (to prevent strong adherence of the polymer matrix to the glass) and separated by 0.25 mm Teflon spacers. The solutions were left uncapped and open to the nitrogen atmosphere until the O_2 levels inside reached negligible levels (<1 ppm) as determined by the attached solid state O_2 analyzer. The polymerization reaction was carried out for 8 minutes for the poly(DEAEM-co-HEMA-co-PEG200DMA) non-imprinted and imprinted gels prepared via FRP, whereas the reaction time was 24 minutes for the polymers prepared via LRP. Separate differential photocalorimetry (DPC) studies revealed exact reaction times. The intensity of light from a UV Flood Curing System (Torrington, CT) was 40 mW/cm2 at 325 V and the temperature within the glovebox was held constant at 25°C. After polymerization, the glass plates were soaked in DI water and the polymers were quickly peeled off the plates and cut into circular discs using a size 10 cork borer (13.5 mm). The gels were washed in a well-mixed 2 L container of DI water for 7 days with a constant 5 mL per minute flowrate of DI water. Absence of detectable drug released from the polymer gel was verified by removing random gels, placing them in fresh DI water with adequate mixing, and sampling the supernatant via spectroscopic monitoring. The discs were allowed to dry under laboratory conditions at a temperature of 20°C for 24 h and then transferred to a vacuum oven (27 in Hg, 33–34°C) for 24 hours until the disc weight change was less than 0.1wt%.

6.3.2 Analysis of Kinetic Chain Length of Polymers

The molecular weight distributions of uncrosslinked polymer chains were characterized by a modified HPLC system (Shimadzu, Columbia, MD) used for gel permeation chromatography(GPC). The GPC setup consisted of two PL Aquagel size exclusion columns in series (Varian LLC, Santa Clara, CA), for separation of various molecular weight fractions of the polymer which were detected using a RID10A refractive index detector (Shimadzu, Columbia,

MD). DI water was used as the mobile phase for the system. Prior to running the samples, the system was calibrated using narrow molecular weight distribution poly(MAA) standards (Polymer Source Inc., Dorval, Quebec). The polymer chains obtained after early termination of polymerization were dissolved in the mobile phase to achieve a concentration of 5 mg/mL. A 50 μL aliquot of the solution was then injected into the system using a Rheodyne (Oak Harbour, WA) 7725(i) manual injection unit. Using the subsequent peaks obtained on the chromatograph, the weight average molecular weight (M_w), the number average molecular weight (M_n) and the polydispersity index (PDI) were calculated, where, the molecular weight (M_i) for a particular weight fraction was described by the x-coordinate of the corresponding point on the chromatograph while the number of chains (N_i)was described by the y-coordinate. Mark – Houwink parameters for poly(HEMA) and poly(MAA) were obtained from the literature [18].

6.3.3 Analysis of Kinetic Parameters

A dark reaction was used to determine the kinetic reaction profile for the poly(DEAEM- co-HEMA- co-PEG200DMA) gels [19-20]. For each polymerization reaction, the UV light was shut off at a specific time point during the reaction. The rate of polymerization was calculated via reaction analysis using the heat flow vs. time from the DPC, average molecular weight of the polymerization solution, and the theoretical heat of reaction. Fractional double bond conversion was determined by dividing the experimental heat of reaction by the theoretical heat of reaction. The experimental heat of reaction was determined by the area under the heat flow versus time curve from the DPC. The termination and propagation constants, k_t and k_p, were calculated from Eqs. 6.1 and 6.2, and the derivation of these equations can be found in Flory [21] or Odian [22].

$$\frac{k_p}{k_t^{0.5}} = \frac{R_p}{[M](f I_o \varepsilon [I])^{0.5}} \qquad 6.1$$

where [*M*] is the monomer concentration, the initiator efficiency is *f*, I_o is the light intensity, ε is the extinction coefficient, and [I] is the initiator concentration. The unsteady state equation used to decouple the propagation constant and the termination constant is shown below.

$$k_t^{0.5} = \frac{k_p/k_t^{0.5}}{2(t_1 - t_0)}\left[\frac{[M]_{t=t1}}{R_{p_{t=t1}}} - \frac{[M]_{t=t0}}{R_{p_{t=t0}}}\right] \quad 6.2$$

where t_1 and t_0 are the final and initial times, $[M]_{t=t1}$ and $[M]_{t=to}$ are the corresponding monomer concentrations, respectively, and $Rp_{t=t1}$ and $Rp_{t=to}$ are the rate of polymerization at final and initial times, respectively.

6.3.4 Template Binding Experiments and Analysis of Binding Parameters

A stock solution of 1 mg/mL of DS was prepared and diluted to five concentrations (0.05, 0.10, 0.15, 0.20, and 0.25 mg/mL). Initial absorbances of each concentration were measured using a Synergy UV–vis spectrophotometer (BioTek Instruments, Winooski, VT) at 276 nm, the wavelength of maximum absorption. After the initial absorbance was taken, a dry, washed poly(DEAEM- co-HEMA- co-PEG200DMA) polymer disk was inserted in each vial and the vials were gently mixed until equilibrium. Separate dynamic studies were performed to assure equilibrium conditions were reached. After equilibrium was reached over a 7-day period, the solutions were vortexed for 10 seconds, and the equilibrium concentrations were measured. A mass balance was used to determine the bound amount of drug within the polymer gel. All gels were analyzed in triplicate, and all binding values are based upon the dry weight of the gel. The Langmuir-Freundlich isotherm was used to determine binding parameters because it gave the best fit to the experimental data.

6.3.5 Dynamic Template Release Studies and Diffusion Coefficient Determination

After binding studies, poly(DEAEM-co-HEMA-co-PEG200DMA) gels, loaded with template at a concentration of 0.25 mg/mL, were placed in 30 ml of DI water which was continuously agitated with an Ocelot orbital shaker(Cheshire, WA) at 375 rpm at 25°C. At various time points, the absorbance of the solution was measured using a Synergy UV–vis spectrophotometer (BioTek Instruments, Winooski, VT) at 276 nm until the concentration did not change more than 1%. At each sample point, the DI water was replaced to maintain infinite sink conditions. Fractional template release profiles were calculated for all polymer gels by taking the amount of template released at specific times, M_t, divided by the maximum amount of DS released during the experiment, M_∞. The fractional template release profile, M_t/M_∞ vs. time, was determined for each gel. Template diffusion coefficients were calculated using Fick's law, which describes one-dimensional planar solute release from gels [23]. For polymer geometries with aspect ratios (exposed surface length/thickness) greater than 10, edge effects can be ignored and the problem can be approached as a one-dimensional process.

6.4 Results and Discussion

Figure 6.1 shows equilibrium binding isotherms for weakly crosslinked poly(DEAEM-co-HEMA-co-PEG200DMA) imprinted and non-imprinted gels prepared using FRP and LRP. Imprinted polymer gels prepared via FRP exhibited higher template binding compared to the corresponding non-imprinted polymer gel. Imprinted polymer gels prepared using LRP exhibited still higher template binding while their corresponding non-imprinted gels matched the template binding demonstrated by non-imprinted polymer gels prepared via FRP. Calculation of binding parameters (Table 6.1) revealed an increase in both the number of binding sites (Q_{max}) and

binding affinity (K_a) in imprinted polymers gels prepared via FRP (K_a=15.7 ± 0.12 mM^{-1}, Q_{max}=16.7 ± 0.64 mg/g) over the corresponding non imprinted polymer gels prepared via FRP (K_a=10.1 ± 0.20 mM^{-1}, Q_{max}=9.6 ± 0.38 mg/g) indicating the successful creation of molecular memory in the imprinted gels. The imprinted gels showed 74% higher binding capacities and 55% higher binding affinities. Similarly, imprinted polymers gels prepared via LRP (K_a=21.7 ± 0.17 mM^{-1}, Q_{max}=23.9 ± 0.60 mg/g) demonstrated 130% increase in the number of binding sites(Q_{max}) and 97% increase in binding affinity over the corresponding non imprinted polymer gels prepared via LRP (K_a=11.0 ± 0.34 mM^{-1}, Q_{max}=10.4 ± 0.48 mg/g). Non-imprinted gels prepared via LRP did not demonstrate a statistically significant enhancement of binding parameters over the non-imprinted gels prepared via FRP indicating LRP enhanced the effect of molecular imprinting on the template binding parameters of the gels. These results were consistent with those reported by our group previously [1].

Figure 6.2 shows the fractional release rate of DS from these polymer gels. Imprinted polymer gels prepared via FRP demonstrated an 81% increase in cumulative mass of drug released as compared to the corresponding non-imprinted gel prepared via FRP which is consistent with increased template binding demonstrated by the imprinted gels. The imprinted gel also exhibited delayed release with 60% of the loaded DS being released in approximately 128 hours whereas the corresponding non-imprinted gel prepared via FRP released 60% of the loaded drug in approximately 78 hours. Despite the slower fractional release rate demonstrated by the imprinted gels, they showed faster absolute drug release rates; for example in the first 48 hours the imprinted gels released an average of 173 μg of DS while the non-imprinted gels released an average of 161 μg of DS. The imprinted polymer gels prepared via LRP further delayed release extending the release to nearly 240 hours for 60% of the loaded drug to transport

out of the gel while the non-imprinted gel prepared via LRP released 60% of the loaded drug in approximately 104 hours. The imprinted gel prepared via LRP showed a 32% increase in cumulative drug released over the imprinted gel prepared via FRP which equated to a 141% increase over the non-imprinted gel prepared via FRP. The non-imprinted gel prepared via LRP did not show a significant increase in the cumulative mass of drug released over non-imprinted gel prepared via FRP. As a result, the non-imprinted gel prepared via LRP demonstrated the slowest absolute drug release rate, releasing an average of 135 μg of DS in the first 48 hours. The imprinted gel prepared via LRP released an average of 148 μg of DS in the first 48 hours indicating that LRP results in a decrease in the absolute drug release rate.

The diffusion coefficient for template transport through the polymer gels was calculated using Fick's Law and the results are shown in Table 6.1. The imprinted gels show decreased coefficients of diffusion when compared to the non-imprinted gels. Also, the LRP gels have smaller diffusion coefficients when compared to their FRP counterparts. When allowed to equilibrate in water the polymer gels prepared via LRP demonstrated lower equilibrium swelling ratios compared to the gels prepared via FRP. In addition, smaller theoretical mesh sizes were observed for gels prepared via LRP (1.98 ± 0.26 nm) when compared with polymer gels prepared via FRP (3.03 ± 0.10 nm). This suggests that LRP results in the formation of a more homogenous crosslinking structure in the imprinted polymer gels.

Propagation in a radical initiated polymerization reaction has two stages, the reaction-controlled stage where monomer addition to the growing macroradical is controlled only by the reactivity of the radical. As the reaction proceeds, the concentration of free monomer around the macroradical is depleted and, as a result, the reaction is controlled by the diffusion of the free

monomer and the macroradical towards each other. As a result of the unavailability of monomers, many radicals undergo termination. The diffusion-controlled stage is now reached where the termination of the reaction begins to gain importance over the propagation reaction. More homogenous polymer networks result when the propagation phase is extended. Figure 6.3 shows the observed propagation constant versus the double bond conversion for the polymerization reaction to produce the weakly crosslinked gels. In the reaction-controlled stage, the propagation reaction dominates, and as a result, the apparent propagation constant stays constant. When the diffusion-controlled stage begins, the contribution of the propagation reaction decreases while that of the termination reaction increases. As a result, when the apparent propagation constant begins to drop, one can assume a transfer from the reaction-controlled to the diffusion-controlled stage. LRP involves the introduction of chain transfer molecules which combine with the macroradicals to form dormant species. This process allows for the formation of a more thermodynamically favorable network since the decrease in the rate of propagation allows the polymer radicals more time to reorganize to minimize the Gibb's free energy of the system. Using LRP leads to a delayed transition from the reaction-controlled phase to the diffusion-controlled phase. In addition, we hypothesized that the extended propagation phase in LRP would result in polymer networks with fewer imperfections in the polymer network, like pendant double bonds and, primary and secondary cycles, allowing for higher overall crosslinking. As a result, even though the final double bond conversion was similar for both reactions, polymer gels prepared using LRP had a more homogenous network because a larger proportion of polymer was formed in the reaction-controlled phase. It is also important to note that the propagation constant for LRP is an order of magnitude smaller than that of FRP, further

extending the time available for the macroradicals to reach minimal free energy states within the polymer network.

The discussion above illustrates the effect of LRP on the kinetics of the polymerization reaction. This analysis can be useful in understanding the effect of LRP on polymer chain growth and network formation. However, analyzing the polymer chains composing the polymer network would be even more useful in terms of explaining the role of LRP in enhancing molecularly imprinting in polymer networks. However, the insolubility of crosslinked polymer gels makes it extremely difficult to analyze their structure directly. Thus, the polymer chains formed in the early stages of polymerization (before gel formation begins) were analyzed using GPC. The polymer chains formed in the initial stages of polymer chains are the building blocks of the polymer networks. Any variations in the polymer chain size as well molecular weight distribution of the chains would be incorporated into the polymer network. Thus, we hypothesize that by analyzing the polymer chains formed before gelation occurs we can approximate the structure and architecture of the polymer network of the gels. Figure 6.4A shows the average molecular weight of the polymer chains as a function of the template/monomer ratio. The template/monomer ratio in the pre-polymer mixture is varied by the addition of increasing amounts of template to the pre-polymerization mixture. As the template concentration increases (increasing T/FM ratio) the average molecular weight of the corresponding polymer chain decreases. This is an important result as it proves that the decrease in average molecular weight of the polymer chains occurs despite the conversion remaining the same. Therefore, the decrease in average molecular weight cannot be attributed to less monomer being incorporated into the growing chains. Rather at higher template concentrations, there is a tendency of a larger number of comparatively shorter polymer chains to be formed. This may be a result of the diffusional

limitations introduced by the presence of the template molecule. Thus, we hypothesize that the presence of template causes the polymerization reaction to shift from a reaction-controlled stage to a diffusion-controlled stage earlier than expected. This is confirmed by Figure 6.3 where the propagation constant for the imprinted polymer gel begins to drop earlier than the propagation constant for the non-imprinted gel.

LRP has been demonstrated to extend the propagation period of a polymerization reaction [24-25]. The active chain transfer radical combines with the polymer radical to undergo a reversible termination reaction, forming a meta-stable species. This results in delayed auto-acceleration and compensates for any diffusional limitation to propagation introduced by the presence of the template molecule. Thus, the addition of a chain transfer agent to the pre-polymerization mixture counterbalances the retardation of kinetic chain length of the resultant polymer chains caused by the diffusional limitations presented by an increasing concentration of monomer-template complexes. This is demonstrated in Figure 6.4A where the average molecular weight does not decrease despite an increase in the template concentration. In addition, the longer propagation period combined with the decreased rate of propagation allows the polymer chains to grow uniformly and simultaneously resulting in more monodisperse polymers prepared via LRP as compared to polymers prepared via FRP. In addition, polymers prepared using LRP show smaller average molecular weights consistent with decreased mesh sizes discussed earlier in the chapter. Figure 6.4B shows the polydispersity index of the polymer chains as a function of the T/FM ratio. An increase in the template concentration in the pre-polymerization mixture led to a higher polydispersity in the resultant polymer chains. The increased polydispersity can be attributed to the early transition to the diffusion-controlled stage of propagation. LRP, however, extends the reaction-controlled stage of propagation negating the effect of the template on the

polymerization reaction, leading to a more consistent polydispersity index independent of template concentration in the pre-polymerization solution. The increased uniformity in the polymer chains manifests itself as increased homogeneity in the polymer network. An increase in the homogeneity in the polymer network means greater availability of binding sites within the polymer gel for the template which could explain the observed improvement in the binding capacity in imprinted polymers due to LRP.

Figure 6.5 compares the average molecular weight and PDI of imprinted polymer gels with varying concentration of functional monomers prepared via FRP and LRP. From Figure 6.5 we can see that an increase in the concentration of functional monomer results in the creation of polymer chains with higher average molecular weight as well as PDI. The use of LRP decreased kinetic chain lengths as well as PDI which is consistent with results described above.

Figure 6.6 compares the average molecular weight and polydispersity index of imprinted polymer gels prepared in the presence of a polar solvent (water) with imprinted polymer gels prepared with no solvent present. We can see that presence of solvent during the creation of imprinted polymers using FRP results in an increase in the kinetic chain length and a decrease in the polydispersity index of polymer chains formed. The increase in the kinetic chain length is consistent with the increase in the observed propagation constant for polymer gels prepared in the presence of solvent. The small, polar water molecule readily associates with the monomer molecules aiding molecular diffusion. The increased propagation constant observed here is consistent with results reported in the literature for non-imprinted polymers [26-27]. The improved molecular diffusion in the polymerization solution may also explain the lower PDI since better transport of the polymer radicals would allow for more uniform growth. The use of LRP resulted in decreases in both the average molecular weight and the PDI which is consistent

with the lower propagation constant and extended polymerization time discussed earlier. It is important to note that LRP overrides the effect of solvent in this case and the presence of solvent during the creation of imprinted polymers via LRP does not have a significant effect on either the average molecular weight or the PDI.

Equilibrium binding isotherms for imprinted polymer gels prepared via FRP and LRP with varying template/functional monomer (T/FM) ratios in the pre-polymerization solution are shown in Figure 6.7. The binding capacity and affinity for all gels were calculated using the Langmuir-Freundlich isotherm and are listed in Table 6.1. From Table 6.1 we can see that both the binding capacity and affinity increase as the T/FM ratio increases to 0.5. The T/FM ratio is the ratio of molar concentrations of the template, DS, and the functional monomer, DEAEM. It is used as a measure of template concentration in the pre-polymerization solution. The T/FM ratio is a very important parameter which affects the strength and abundance of monomer-template complexation in the pre-polymerization solution. This is especially true for systems where multiple non-covalent interactions can be formed between the template and functional monomer. As the T/FM ratio is increased both template binding capacity and the mean template affinity increase since an increase in template concentration results in an increase in the number of specific template binding sites which have higher binding affinities as compared to non-specific binding sites. However, after a certain optimal T/FM ratio as the template concentration is increased further the template affinity begins to decrease [28]. The formation of good high affinity binding sites in systems with multiple non-covalent template-monomer interaction requires the presence of an excess of the functional monomer concentration to ensure all the complexation points on the template are satisfied by functional monomers. As the template concentration is increased the T/FM ratio approaches the stoichiometric ratio and the excess

monomer around a template molecule decreases. As a result, all of the complexation points on the template may not be satisfied resulting in the formation of specific binding sites with lower affinities even while the overall binding capacity may increase. However, the poly(DEAEM-co-HEMA-co-PEG200DMA) gels primarily undergo ionic interactions with DS. The hydrogen bonding sites on DS are satisfied via intramolecular hydrogen bonding [29]. As a result, multi-point complexation is not expected to play a significant role in the formation of the template binding site. Thus, the increased affinity observed with increasing T/FM ratio can be explained by a higher proportion of specific interaction during template rebinding. Conversely since all gels reported in this chapter have functional monomer concentrations higher than the required stoichiometric concentrations a significant decrease in the affinity is not observed at even high T/FM ratios. From Figure 6.7B, one can see that the template loading in the imprinted gels prepared using LRP increase with increasing T/FM ratio. Further, all gels prepared via LRP show an improvement over their corresponding gels prepared via FRP, and the extent of the improvement increases as the template concentration increases. Lastly, the capacity of the FRP gels increases by 23% for FRP1, 74% for FRP2, and 78% for FRP3 over FRP0; whereas the LRP gels show much larger increases of 37% for LRP1, 130% for LRP2, and 144% for LRP3 over LRP0. It is important to note that the use of LRP in non-imprinted gels does not result in a significant improvement in their binding properties.

Figure 6.8 shows fractional release rates from imprinted polymer gels prepared using FRP with varying T/FM ratios (0, 0.1, 0.3, and 0.5) in the pre-polymerization solution. All imprinted gels (T/FM>0) demonstrated delayed release of DS. Also gels with higher T/FM ratio demonstrated slower release of DS. For example, the imprinted gel with T/FM ratio of 0.1 released 60% of the loaded drug in approximately 96 hours while the imprinted gel with a T/FM

ratio of 0.3 took nearly 128 hours to release 60% of the loaded drug. The imprinted gel with T/FM ratio of 0.5 matched the release rate demonstrated by the gel with a T/FM ratio of 0.3. Both gels released nearly the same amount of drug (about 520 μg) through the duration of the study resulting in identical drug elution rates. This is consistent with the binding studies where imprinted gels with a T/FM ratio of 0.3 and 0.5 demonstrated binding capacities and affinities which were identical to within experimental error. This indicates that increasing the template concentration beyond T/FM=0.3 may not result in the creation of additional memory sites.

Figure 6.9 shows the fractional release from the corresponding gels prepared via LRP. These gels demonstrated similar behavior with higher T/FM ratio resulting in delayed release. Interstingly, for these gels increasing the T/FM ratio from 0.3 to 0.5 was shown to result in demonstrable decrease in the fractional release rate indicating synergistic effect between molecular imprinting and LRP resulting in the creation of better memory for the template. In addition, all gels prepared using LRP showed slower fractional release rates when compared with the corresponding gels prepared via FRP. All gels prepared via LRP also demonstrated higher cumulative drug release when compared with the corresponding gels prepared via FRP. Thus, the cumulative drug released in 48 hours was calculated to compare the absolute drug release rates of the various gels. The gels prepared via LRP released an average of 135 μg, 154 μg, 148 μg, and 138 μg in increasing order of T/FM ratio. The corresponding imprinted gels prepared via FRP released 161 μg, 177 μg, 173 μg, and 169 μg of DS in increasing order of T/FM ratio. Thus, gels prepared via LRP demonstrate not only extended drug release but also a lower absolute drug release rate. This can be attributed to smaller mesh sizes in gels prepared via LRP.

Figure 6.10 shows equilibrium binding isotherms for weakly crosslinked polymer gels at varying functional monomer concentrations prepared with and without LRP. It is important to note that the T/FM ratio pre-polymerization mixture is kept at a constant value of 0.3 for all gels. The binding capacity and affinity values are presented in Table 6.1. From Figure 6.10 we can see that the template loading increases significantly as the concentration of functional monomer is increased for both gels prepared via FRP and LRP. It was also noted that gels prepared without the positively charged functional monomer, DEAEM, displayed negligible binding of the drug molecule. This can be explained by the absence of any significant non-covalent interaction sites on the diclofenac ion. As reported in literature [29], although there exist two hydrogen bonding sites, they may satisfy each other by engaging in intramolecular hydrogen bonding. In addition, water being a polar solvent is an excellent solvent for the diclofenac ion negating the possibility of hydrophobic interactions.

Figure 6.11 compares the fractional release rates for the gels with varying functional monomer concentrations (5%, 10%) prepared with LRP and FRP. Due to the negligible drug binding displayed by gels prepared without DEAEM (0% functional monomer), drug release studies were not carried out for these gels. From Figure 6.11, we can see that increasing the functional monomer concentrations results in delayed release of drug molecule from the polymer gels. The imprinted gels with 10% functional monomer prepared using conventional methods release 60% of the loaded drug in approximately 200 hours which is a significantly slower fractional release rate compared to the corresponding imprinted gels with 5% functional monomer which release the same fraction in approximately 128 hours. Similarly, imprinted gels with 10% functional monomer prepared using conventional methods show significantly slower fractional release rates compared to the corresponding imprinted gels with 5% functional

monomer. However, the imprinted gels with 5% functional monomer prepared via LRP show a slower fractional release when compared to imprinted gels with 10% functional monomer prepared using conventional methods. The slower release from a polymer gel prepared via LRP can be explained by the decreased swelling and mesh sizes of the gels. Notably, though, the values obtained are comparable. The closeness of these values signifies the effect of additional binding sites in delaying template transport. Imprinted gels with 10% functional monomer demonstrate more than twice the binding capacity of corresponding imprinted gels with 5% functional monomer. The additional binding sites temporarily capture/bind the template molecule as it tries to elute out of the polymer as indicated by the "tumbling hypothesis" proposed by our group [23]. As the number of binding sites increases, the number of possible temporary binding/capture events a template molecule undergoes before it exits the polymer increase. The high template binding also results in larger amount of cumulative drug released from the polymer. Comparing the absolute release rates; an average of 382 μg of DS is released by an imprinted gel prepared via FRP with 10% functional monomer while the corresponding gel prepared via LRP releases an average of 241 μg of DS in the first 48 hours. The corresponding numbers for the gels with 5% functional monomer are 173 μg and 148 μg for gels prepared via FRP and LRP, respectively. Both sets of gels prepared via LRP demonstrate slower absolute release compared to the corresponding gels prepared via FRP. However, while the absolute release rates of the gels with 5% functional monomer are comparable, the gels with 10% functional monomer demonstrate dramatically slower release rates when LRP was used in their preparation. This can be explained by the difference in drug loading ratios between the gels. The use of LRP for the preparation of gels with 5% functional monomer results in a 43% increase in drug loading while the use of LRP for the preparation of gels with 10% functional monomer

resulted in a more modest increase in drug loading of only 10%. Thus, for gels with 10% functional monomer; the difference in concentration of drug in polymer is less significant, the difference in solvent uptake and mesh size is more significant and the gel prepared via LRP releases the drug much slower. In the case of the gels with 5% functional monomer, the significantly higher drug loading in gels prepared with LRP results in increased drug concentration in the polymer which increases the driving force for drug transport and may explain the observed release rates.

Figure 6.12 compares the equilibrium binding isotherms for gels prepared in the presence of water as a solvent as well as those prepared in its absence. The purpose of this study was to analyze the effect of a small solvent molecule which could alleviate some of the diffusional limitations inherent to late stage bulk polymerization reactions. Thus, a large amount of water was used (50% by weight). All other reaction parameters were maintained identical. The gels prepared in the presence of solvent demonstrated higher template binding. The strong relationship between template loading and functional monomer concentration indicated the possibility of a single ionic bond between the negatively charged diclofenac ion and the positively charged side chains introduced into the polymer gel by DEAEM rather than the creation of a binding cavity. However, the increase in template binding capacity of the gels prepared in the presence of a polar solvent countered the single interaction theory. Water as a polar, protic solvent interferes with the ionic interaction and this should result in lower template binding. However, we observe an increase in template binding capacity suggesting the presence of a well formed binding cavity with more factors stabilizing the template binding than just the primary ionic interaction. The solvent may play a role in aiding the formation of binding sites resulting in higher template binding displayed by the polymer gel.

Figure 6.13 compares the fractional release rates for the gels prepared with (50% by weight) and without solvents via both LRP and FRP. From Figure 6.13, we can see that the presence of solvent during polymerization results in faster release of drug. This is consistent with the increased porosity expected in gels prepared in the presence of solvent. The imprinted gels prepared in the presence of solvent using conventional methods release 60% of the loaded drug in approximately 90 hours which is a significantly faster fractional release rate compared to corresponding imprinted gels prepared in the absence of solvent which release the same fraction in approximately 128 hours. Similarly, the imprinted gels prepared in the presence of solvent via LRP show a faster fractional release when compared to imprinted gels prepared in the absence of solvent via LRP. Lastly, LRP leads to delayed release in solvents prepared with solvents. Comparing the absolute release rates; an average of 295 μg of DS is released by an imprinted gel prepared in the presence of solvent via FRP while the corresponding gel prepared via LRP releases an average of 315 μg of DS in 48 hours. The corresponding numbers for the gels prepared in the absence of solvent are 173 μg and 148 μg for gels prepared via FRP and LRP respectively. Interestingly, the gels prepared via LRP in the presence of solvent demonstrate faster release when compared to the corresponding gels prepared via FRP. This contradicts the results for all the other imprinted gels where the use of LRP resulted in slower absolute release rates. The anomalous behaviour may be explained by the increased porosity in the gels due to the presence of solvents which may negate the effect of structural changes in the gels due to LRP.

6.5 Conclusions

The work in this chapter examined the effects of various reaction parameters on the structure of imprinted gels and subsequently their drug binding and transport properties. It was found that higher template concentrations resulted in increased drug loading and delayed fractional release.

Increase in the concentration of functional monomer showed a similar trend but the magnitude of the increase was significantly higher, indicating the importance of the primary ionic non-covalent interaction to the formation of good imprinting sites. It was also found that the presence of solvent during polymerization resulted in higher drug loading. However, the drug binding affinity was reduced. Drug release from these gels was also much faster which may be attributed to increased porosity in the gels. This work also highlighted the improved efficiency of imprinting in weakly crosslinked polymer gels prepared via LRP. All imprinted poly(HEMA-co-DEAEM-co-PEG200DMA) gels prepared via LRP demonstrated significantly higher drug binding as well as slower drug release rates. It was found that, the use of LRP had a more significant impact than any other reaction parameter. This work was the first to demonstrate that the observed improvement in binding and transport parameters in weakly crosslinked, imprinted polymer gels could be explained by the extension of the reaction-controlled regime during propagation of the macroradical which allows the system to achieve a minimal global free energy configuration. This resulted in shorter more monodisperse polymer chains forming the network which were hypothesized to result in more homogenous networks.

6.6 References

1. Vaughan AD, Zhang JB, Byrne ME. Enhancing Therapeutic Loading and Delaying Transport via Molecular Imprinting and Living/Controlled Polymerization. AIChE Journal. 2010, 56, 1, 268-279.
2. Haupt K, Mosbach K. Molecularly imprinted polymers and their use in biomimetic sensors. Chemical review. 2000, 100, 2495-2504.
3. He Q, Chang X, Wu Q, Huang X, Hu Z, Zhai Y. Synthesis and Applications of Surface-grafted Th(IV)-imprinted Polymers for Selective Solid-phase Extraction of Thorium(IV). Analytica Chimica Acta. 2007, 605, 2, 192-197.
4. Davis ME, Katz A, Ahmad WR. Rational catalyst design via imprinted nanostructured materials. Chem. Mater. 1996, 8, 1820-1839.
5. Byrne ME, Park K, Peppas NA. Molecular imprinting within hydrogels. Adv. Drug Deliv. Rev. 2002, 54, 149-161.
6. Bergmann NM, Peppas NA. Molecularly imprinted polymers with specific recognition for macromolecules and proteins, Progress in Polymer Science. 2008, 33, 3, 271–288.
7. Hilt JZ, Byrne ME. Configurational Biomimesis in Drug delivery: Molecular Imprinting of Biologically Significant Molecules. Advanced Drug Delivery Reviews. 2004, 56, 11, 1599-1620.
8. Byrne ME, Salian V. Molecular imprinting within hydrogels. II. Progress and analysis of the field. Int. J. Pharm. 2008, 364, 188–212.
9. Byrne ME, Hilt JZ, Peppas NA. Recognitive biomimetic networks with moiety imprinting for intelligent drug delivery. J. Biomed. Mater. Res. Part A. 2008, 84A, 137-147.
10. Cunliffe D, Kirby A, Alexander A. Molecularly imprinted drug delivery systems, Advanced Drug Delivery Reviews. 2005, 57, 12, 1836–1853.

11. Umpleby RJ, Rushton GT, Shah RN, Rampey AM, Bradshaw JC, Berch JK, Shimizu KD. Recognition Directed Site-Selective Chemical Modification of Molecularly Imprinted Polymers. Macromolecules. 2001, 34, 24, 8446-8452.
12. Anandkumar KR, Anderson KJ, Anseth JW, Bowman CN. Use of "living" radical polymerizations to study the structural evolution and properties of highly crosslinked polymer networks. J. Polym. Sci., Part B: Polym. Phys. 1997, 35, 2297 -2307.
13. Anandkumar KR, Anseth JW, Bowman CN. A study of the evolution of mechanical properties and structural heterogeneity of polymer networks formed by photopolymerizations of multifunctional (meth)acrylates. Polymer. 1998, 39, 12, 2507-2513.
14. Boonpangrak S, Whitcombe MJ, Prachayasittikul V, Mosbach K, Ye L. Preparation of molecularly imprinted polymers using nitroxide-mediated living radical polymerization. Biosens Bioelectron. 2006, 22, 349–354.
15. Vaughan AD, Byrne ME. Optimizing recognition characteristics of biomimetic polymer gels via polymerization reaction and crosslinking density analysis. ACS PMSE Preprints. 2006, 94, 762–763.
16. Vaughan AD, Sizemore SP, Byrne ME. Enhancing molecularly imprinted polymer binding properties via controlled/living radical polymerization and reaction analysis. Polymer. 2007, 48, 74-81.
17. Pan G, Zu B, Guo X, Zhang Y, Li C, Zhang H. Preparation of molecularly imprinted polymer microspheres via reversible addition–fragmentation chain transfer precipitation polymerization. Polymer. 2009, 50, 2819–2825.

18. Brandrup J, Immergut EH, Grulke EA. Polymer handbook, 4th ed. 1999, John Wiley & Sons: New York.
19. Anseth KS, Kline LM, Walker TA, Anderson KJ, Bowman CN. 1995. Reaction kinetics and volume relaxation during polymerizations of multiethylene glycol dimethacrylates. Macromolecules 28: 2491–2499.
20. Anseth KS, Wang CM, Bowman CN. 1994. Reaction behaviour and kinetic constants for photopolymerizations of multi(meth)acrylate monomers. Polymer 35: 3243–3250.
21. Flory PJ. 1953. Principles of Polymer Chemistry, 1st ed. Cornell University Press: Ithaca.
22. Odian G. 1981. Principles of Polymerization, 2nd ed. John Wiley & Sons: New York.
23. Venkatesh S, Saha J, Pass S, Byrne ME. Transport and structural analysis of molecular imprinted hydrogels for controlled drug delivery. Eur. J. Pharm. Biopharm. 2008, 69, 852–860.
24. Gao H, Miasnikova A, Matyjaszewski K. Effect of Cross-Linker Reactivity on Experimental Gel Points during ATRcP of Monomer and Cross-Linker. Macromolecules. 2008, 41, 7843-7849.
25. Gao H, Min K, Matyjaszewski K. Determination of Gel Point during Atom Transfer Radical Copolymerization with Cross-Linker. Macromolecules. 2007, 40, 7763-7770.
26. Beuermann S, Buback M, Hesse P, Lacık I. Free-Radical Propagation Rate Coefficient of Nonionized Methacrylic Acid in Aqueous Solution from Low Monomer Concentrations to Bulk Polymerization. Macromolecules. 2006, 39, 184-193.
27. Stach M, Lacık I, Chorvat D, Buback M, Hesse P, Hutchinson RA, Tang L. Propagation Rate Coefficient for Radical Polymerization of N-Vinyl Pyrrolidone in Aqueous Solution Obtained by PLP−SEC. Macromolecules. 2008, 41, 5174-5185.

28. Hiratani H, Fujiwara A, Tamiya Y, Mizutani Y, Alvarez-Lorenzo C. Ocular release of timolol from molecularly imprinted soft contact lenses. Biomaterials. 2005, 26, 1293–1298.

29. Ledwidge MT, Draper SM, Wilcock DJ, Corrigan OI. Physicochemical Characterization of Diclofenac N-(2-Hydroxyethyl)pyrrolidine: Anhydrate and Dihydrate Crystalline Forms. Journal of Pharmaceutical Sciences 1996, 85, 1, 16-21.

Table 6.1: Binding Capacities, Affinities and Coefficients of Diffusion for Diclofenac Sodium in Poly(DEAEM-co-HEMA-co-PEG200DMA) Polymer Gels

Polymer type (DBC)	K_a (mM^{-1})	Q_{max} (mg/g)	Diffusion Coefficient (cm^2/s)x10^{13}
Non-imprinted (FRP0) (T/FM=0)	10.1±0.20	9.6±0.38	5.94±0.07
Living non-imprinted (LRP0) (T/FM=0)	11.0±0.34	10.4±0.48	4.56±0.05
Imprinted (FRP1) (T/FM=0.1)	12.8±0.21	11.8±0.54	5.01±0.08
Living imprinted (LRP1) (T/FM=0.1)	13.2±0.41	14.2±0.62	3.42±0.04
Imprinted (FRP3) (T/FM=0.3)	15.7±0.12	16.7±0.64	3.68±0.05
Living imprinted (LRP3) (T/FM=0.3)	21.7±0.17	23.9±0.60	1.84±0.02
Imprinted (FRP5) (T/FM=0.5)	15.4±0.18	17.1±0.41	3.71±0.05
Living imprinted (LRP5) (T/FM=0.5)	19.2±0.25	25.4±0.54	1.62±0.02
Imprinted (10% FM)	21.6±0.38	31.3±0.52	2.49±0.02
Living (10% FM)	25.7±0.40	34.7±0.57	1.37±0.02
Imprinted (50% solvent)	13.3±0.29	20.7±0.33	6.58±0.06
Living (50% Solvent)	13.6±0.30	22.3±0.49	4.81±0.02

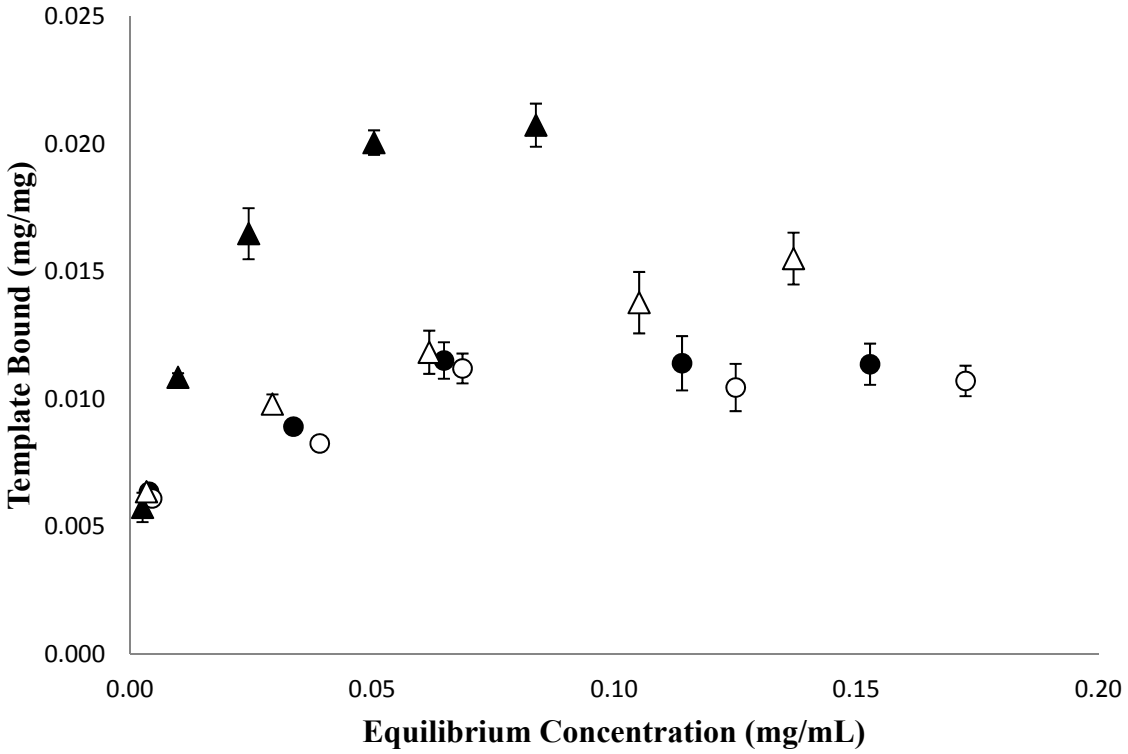

Figure 6.1: Equilibrium Binding Isotherms for Diclofenac Sodium Binding by Weakly Crosslinked Imprinted Poly(DEAEM-co-HEMAco-PEG200DMA) Gels prepared via FRP and LRP. Poly(DEAEM- co-HEMA- co-PEG200DMA) imprinted polymers prepared via LRP (▲), prepared via FRP (Δ) and non-imprinted polymer gels prepared via LRP (●) and FRP (○). Error bars represent the standard error (n = 3). LRP leads to significantly higher loading as compared to FRP.

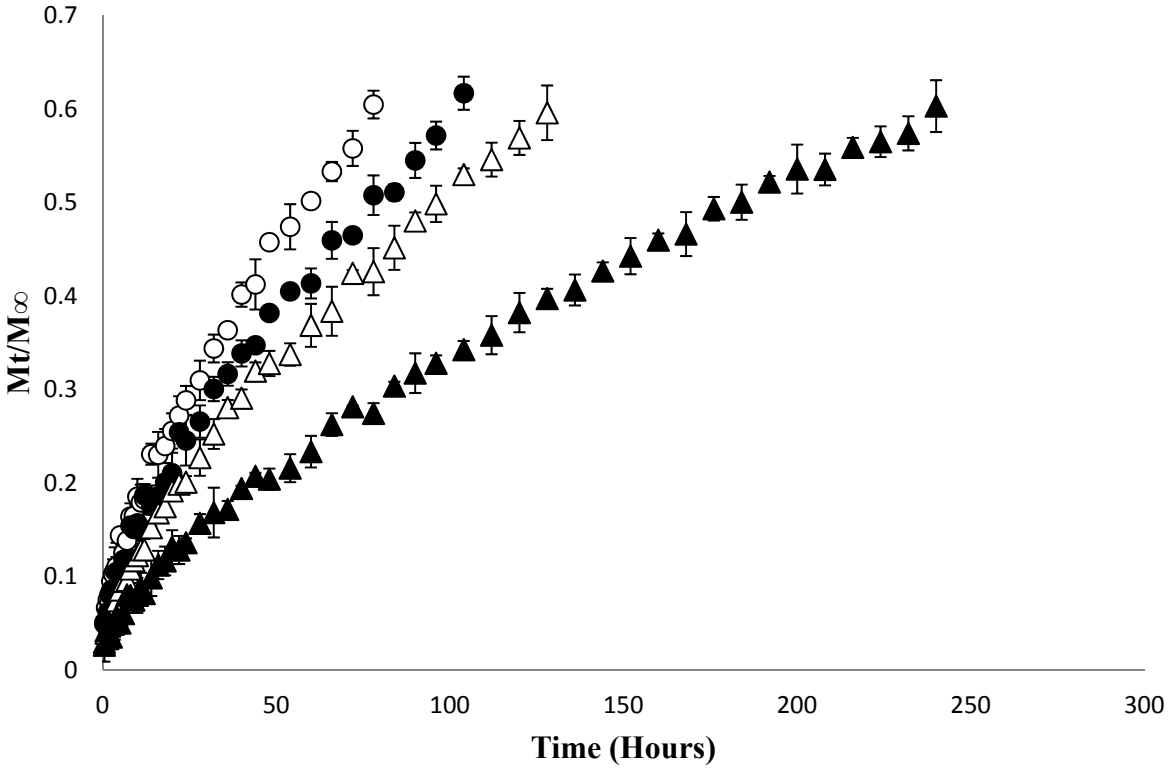

Figure 6.2: Fractional Release of Diclofenac Sodium from Weakly Crosslinked Imprinted Poly(DEAEM-co-HEMA-co-PEG200DMA) Gels in DI Water. Poly(DEAEM-co-HEMA-co-PEG200DMA) imprinted polymers prepared via LRP (▲), prepared via FRP (Δ) and non-imprinted polymer gels prepared via LRP (●)and FRP (○). Error bars represent the standard error (n = 3).

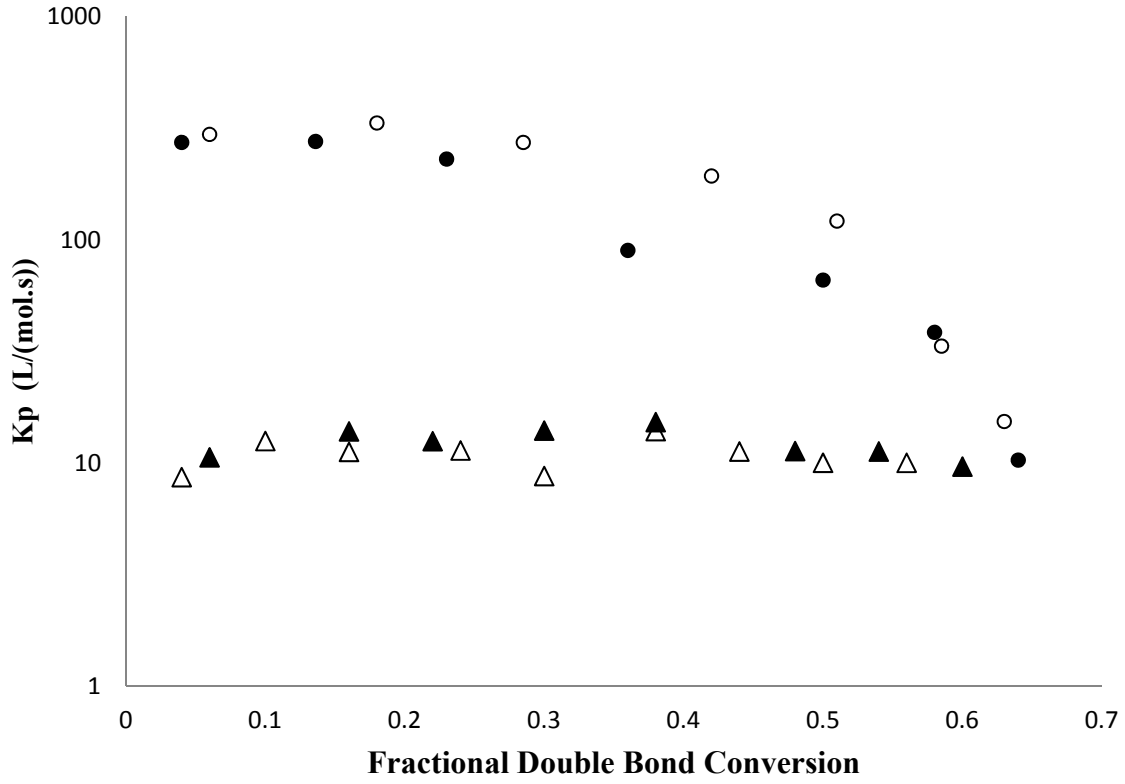

Figure 6.3: Propagation Constant from Kinetic Analysis of Weakly Crosslinked Poly(DEAEM-co-HEMA-co-PEG200DMA) Formation. The propagation constant for the Poly(DEAEM-co-HEMA-co-PEG200DMA) imprinted gel (■) and non-imprinted gel (□) prepared via FRP show similar trends where the propagation constant decreases after initially remaining constant. The imprinted gels decay faster than the non-imprinted gels. The imprinted (▲) and non-imprinted(Δ) gels prepared via LRP show a more constant rate of propagation indicating a longer reaction-controlled propagation mechanism.

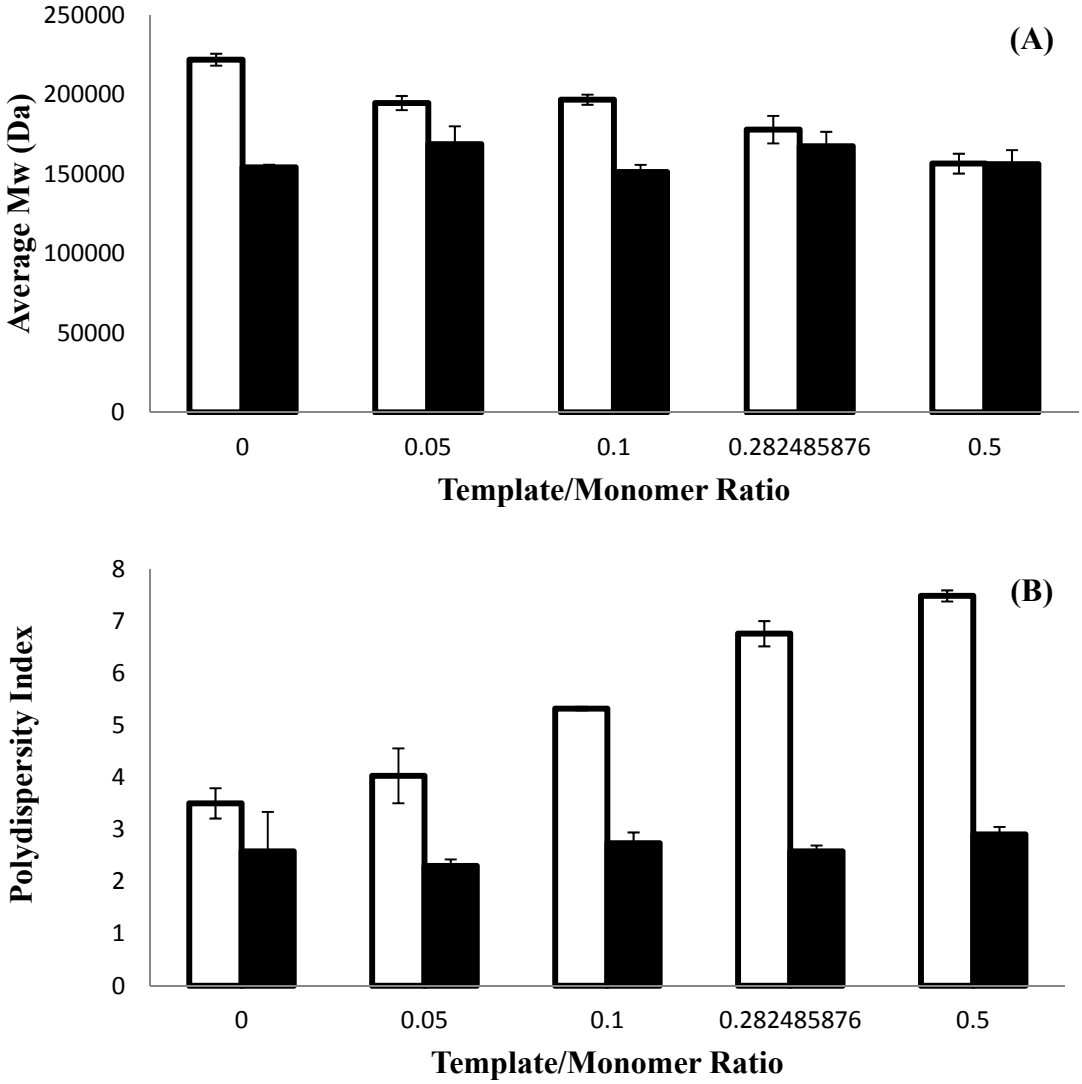

Figure 6.4: Effect of Template Concentration on Kinetic Chain Length and Polydispersity Index of Poly(DEAEM-co-HEMA-co-PEG200DMA) Chains. Weight average molecular weight **(A)** and polydispersity index **(B)** versus template/monomer ratio for pre-gelation Poly(DEAEM-co-HEMA-co-PEG200DMA) chains prepared via FRP (□) and LRP (■) are shown here. Error bars represent the standard error with n=3. Presence of template in the reaction mixture leads to the formation of polymers with shorter chains and higher polydispersity due to an early transition into the diffusion-controlled regime of propagation. LRP counterbalances it by extending the reaction-controlled regime.

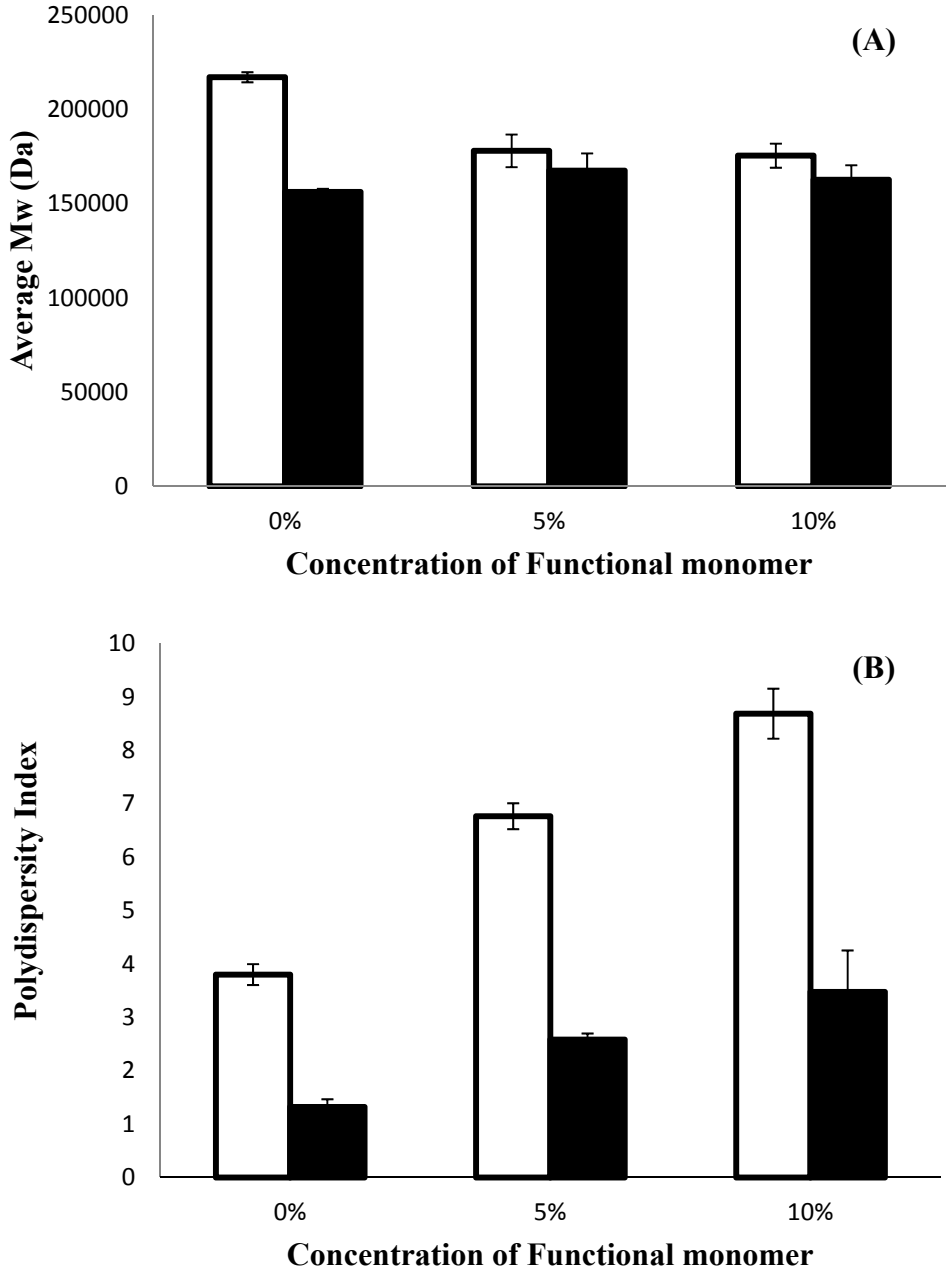

Figure 6.5: Effect of Functional Monomer Concentration on Kinetic Chain Length and Polydispersity Index of Poly(DEAEM-co-HEMA-co-PEG200DMA) Chains. Weight average molecular weight (**A)** and polydispersity index (**B)** versus functional monomer concentraion for pre-gelation Poly(DEAEM-co-HEMA-co-PEG200DMA) chains prepared via FRP (□) and LRP (■) are shown here. Error bars represent the standard error with n=3.

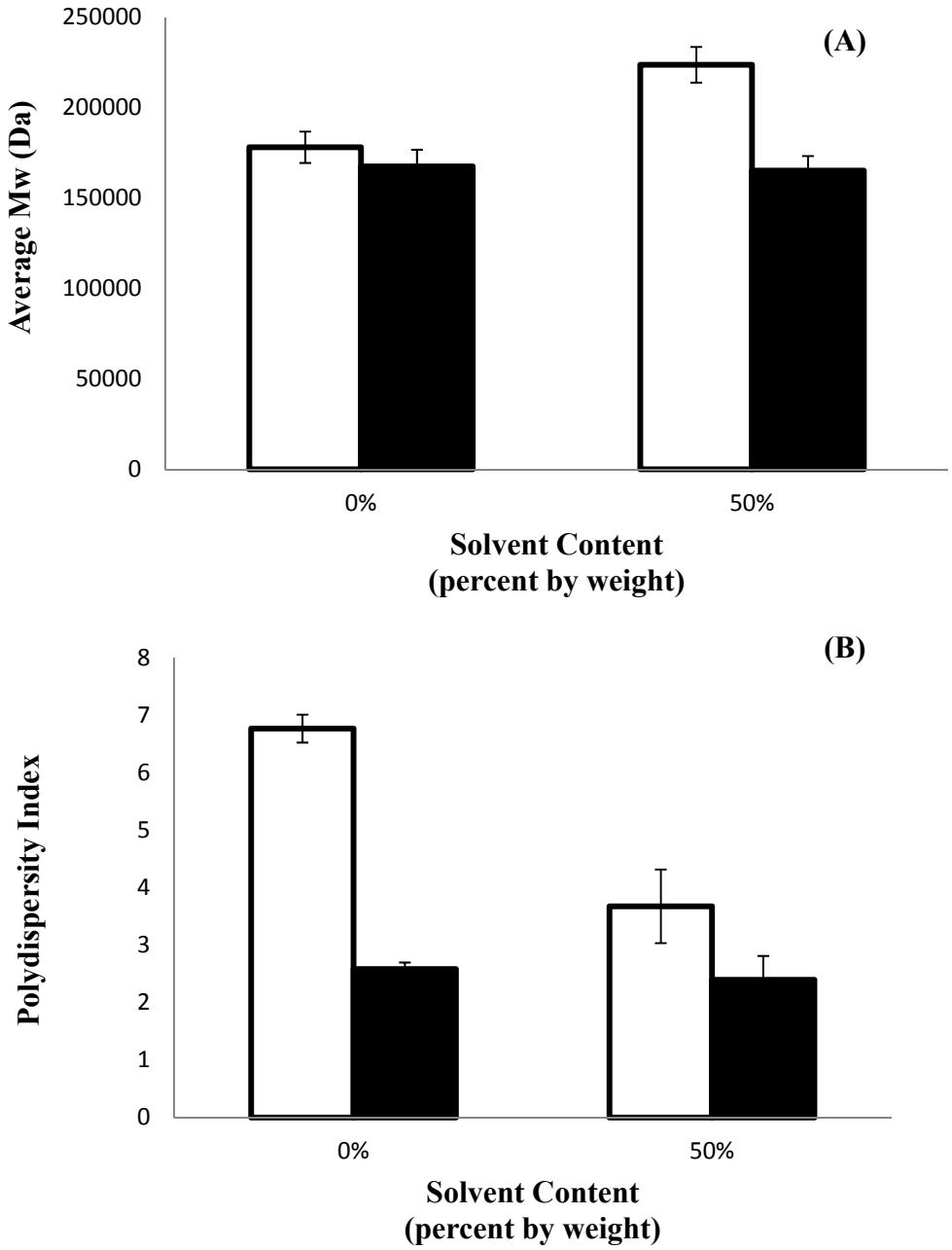

Figure 6.6: Effect of Solvent on Kinetic Chain Length and Polydispersity Index of Poly(DEAEM-co-HEMA-co-PEG200DMA) Chains. Weight average molecular weight (**A)** and polydispersity index (**B)** solvent content during polymerization of Poly(DEAEM-co-HEMA-co-PEG200DMA) chains prepared via FRP (□) and LRP (■) are shown here. Error bars represent the standard error with n=3.

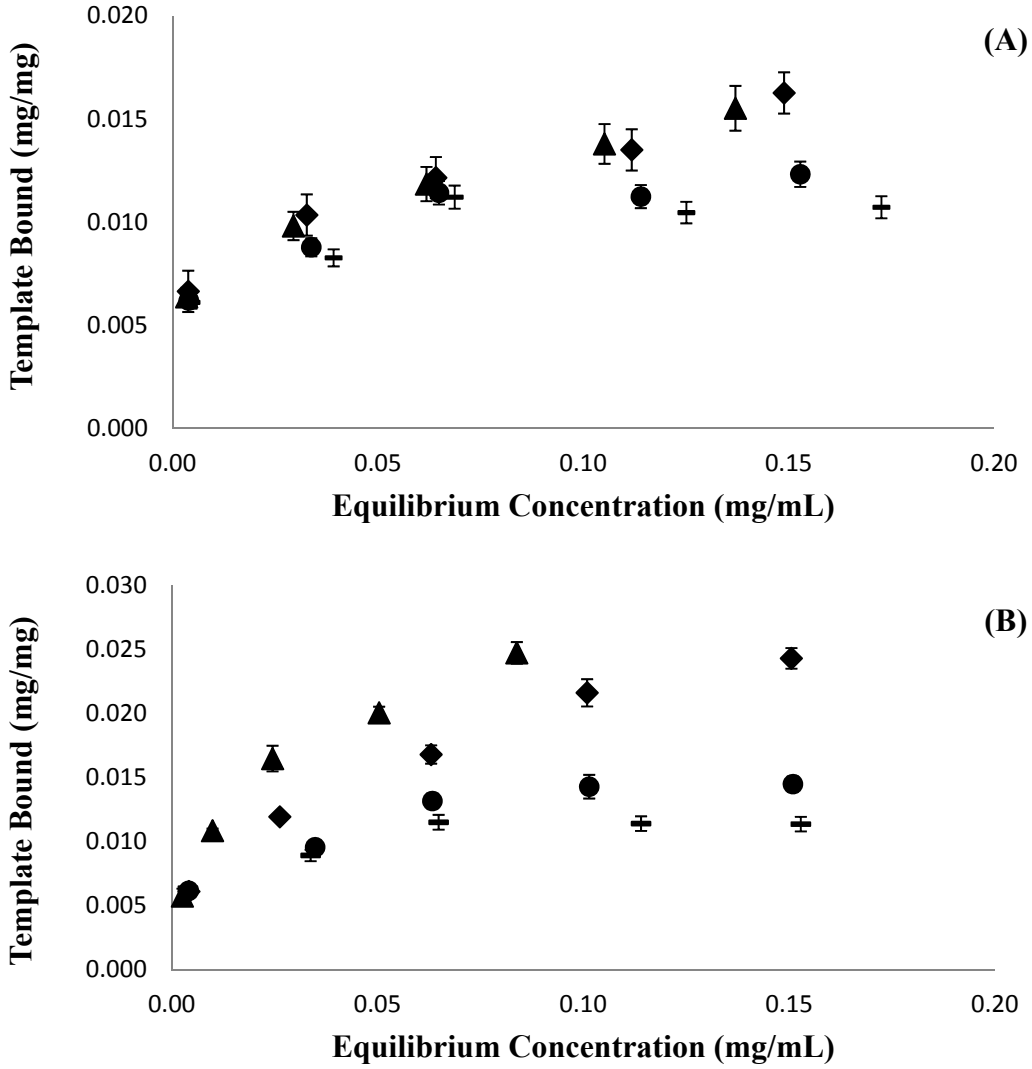

Figure 6.7: Equilibrium Binding Isotherms for Diclofenac Sodium Binding by Weakly Crosslinked Imprinted Poly(DEAEM-co-HEMA-co-PEG200DMA) Gels prepared via (A) FRP and (B) LRP with varying Template Concentration. Data points represent poly(DEAEM-co-HEMA-co-PEG200DMA) gels prepared with varying T/FM ratios: T/FM=0 (—); T/FM=0.1 (●); T/FM=0.3 (▲); T/FM=0.5 (■).Error bars represent the standard error with n=3.

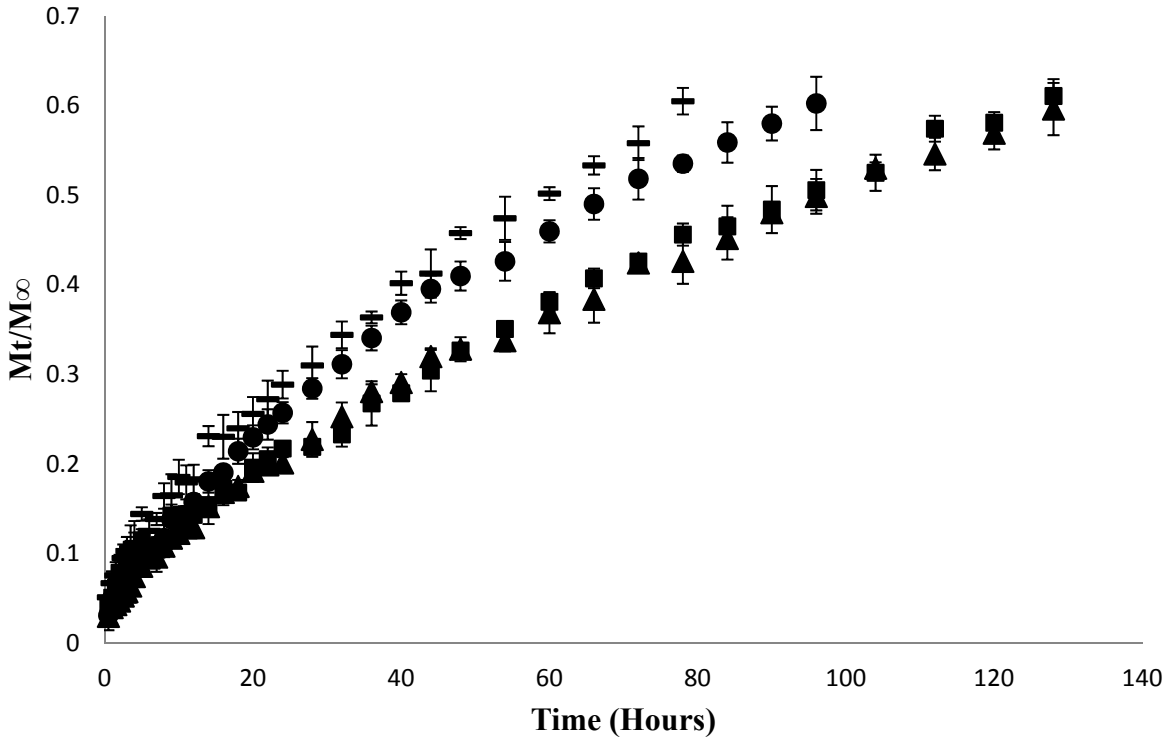

Figure 6.8: Fractional Release of Diclofenac Sodium in DI Water from Weakly Crosslinked Imprinted Poly(DEAEM-HEMA-PEG200DMA) Gels prepared via FRP with varying Template Concentration. Data points represent poly(DEAEM-co-HEMA-co-PEG200DMA) gels prepared with varying T/FM ratios: T/FM=0 (▬); T/FM=0.1 (●); T/FM=0.3 (▲); T/FM=0.5 (■). Error bars represent the standard error with n=3.

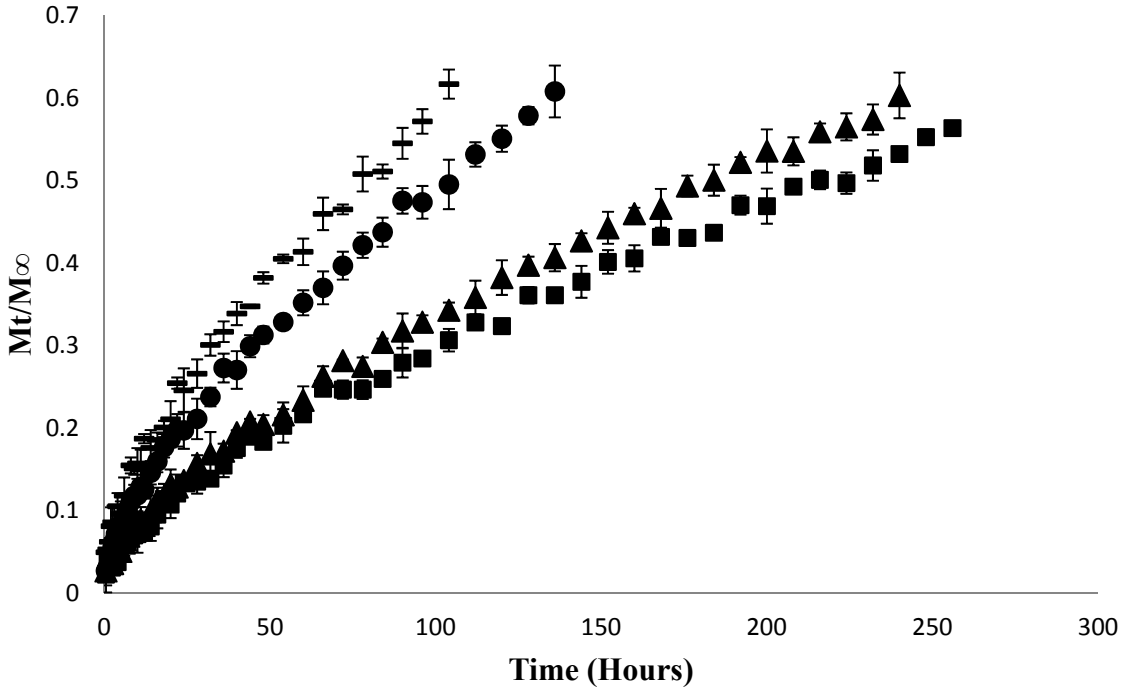

Figure 6.9: Fractional Release of Diclofenac Sodium in DI Water from Weakly Crosslinked Imprinted Poly(DEAEM-co-HEMA-co-PEG200DMA) Gels prepared via LRP with varying Template Concentration. Data points represent poly(DEAEM-co-HEMA-co-PEG200DMA) gels prepared with varying T/FM ratios: T/FM=0 (▬); T/FM=0.1 (●); T/FM=0.3 (▲); T/FM=0.5 (■). Error bars represent the standard error with n=3.

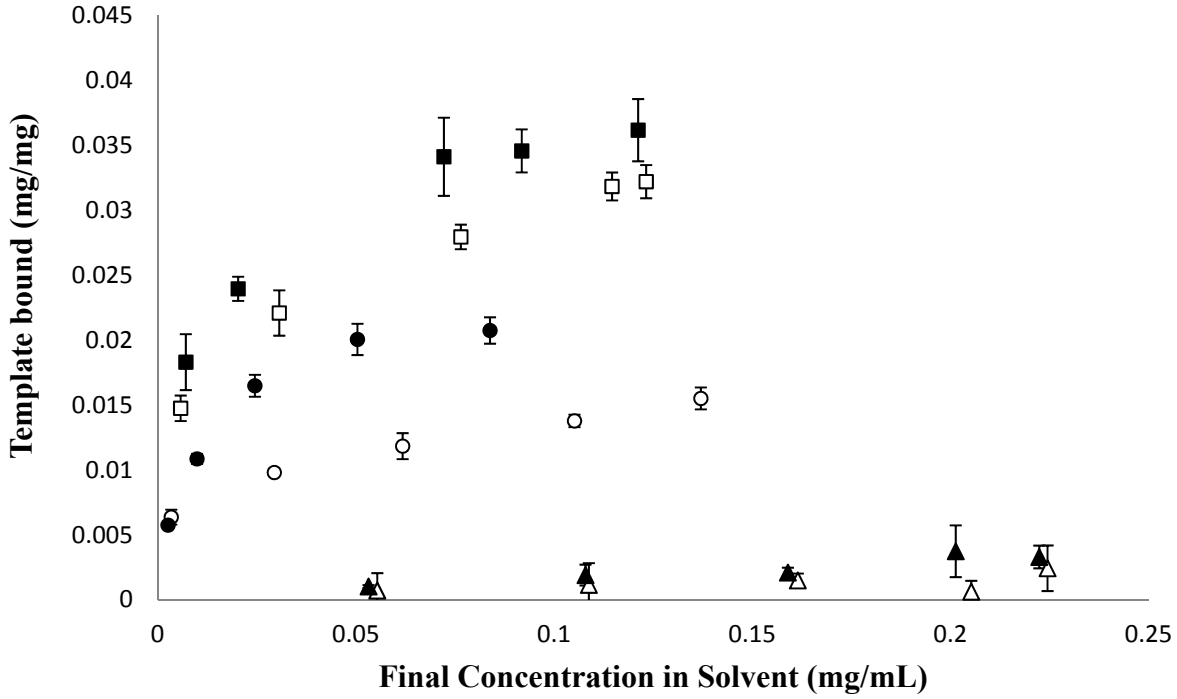

Figure 6.10: Equilibrium Binding Isotherm for Diclofenac Sodium Binding by Weakly Crosslinked Imprinted Poly(DEAEM- co-HEMA- co-PEG200DMA) Gels prepared via FRP and LRP with varying Functional Monomer Concentration. Data points represent poly(DEAEM-co-HEMA-co-PEG200DMA) gels prepared with varying FM concentrations: 0% FM (▲,Δ); 5% FM (●,○); and 10% FM (■,□). Closed symbols (■,●,▲) represent gels prepared via LRP while open symbols (□,○,Δ) represent gels prepared via FRP. Error bars represent the standard error with n=3.

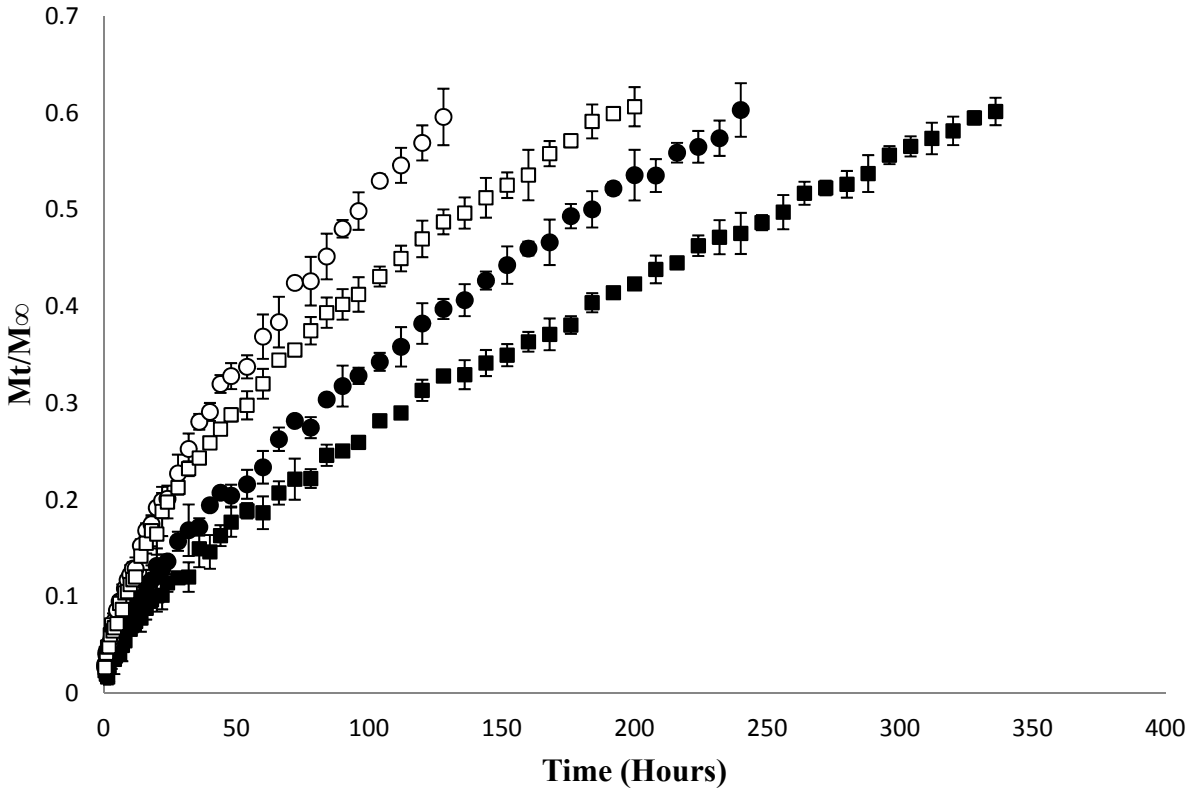

Figure 6.11: Fractional Release of Diclofenac Sodium in DI Water from Weakly Crosslinked Imprinted Poly(DEAEM-HEMA-PEG200DMA) Gels prepared via FRP and LRP with varying Functional Monomer Concentration. Data points represent poly(DEAEM-co-HEMA-co-PEG200DMA) gels prepared with FM concentrations: 5% FM (●,○); and 10% FM (■,□).Closed symbols (■,●) represent gels prepared via LRP while open symbols (□,○) represent gels prepared via FRP. Error bars represent the standard error with n=3.

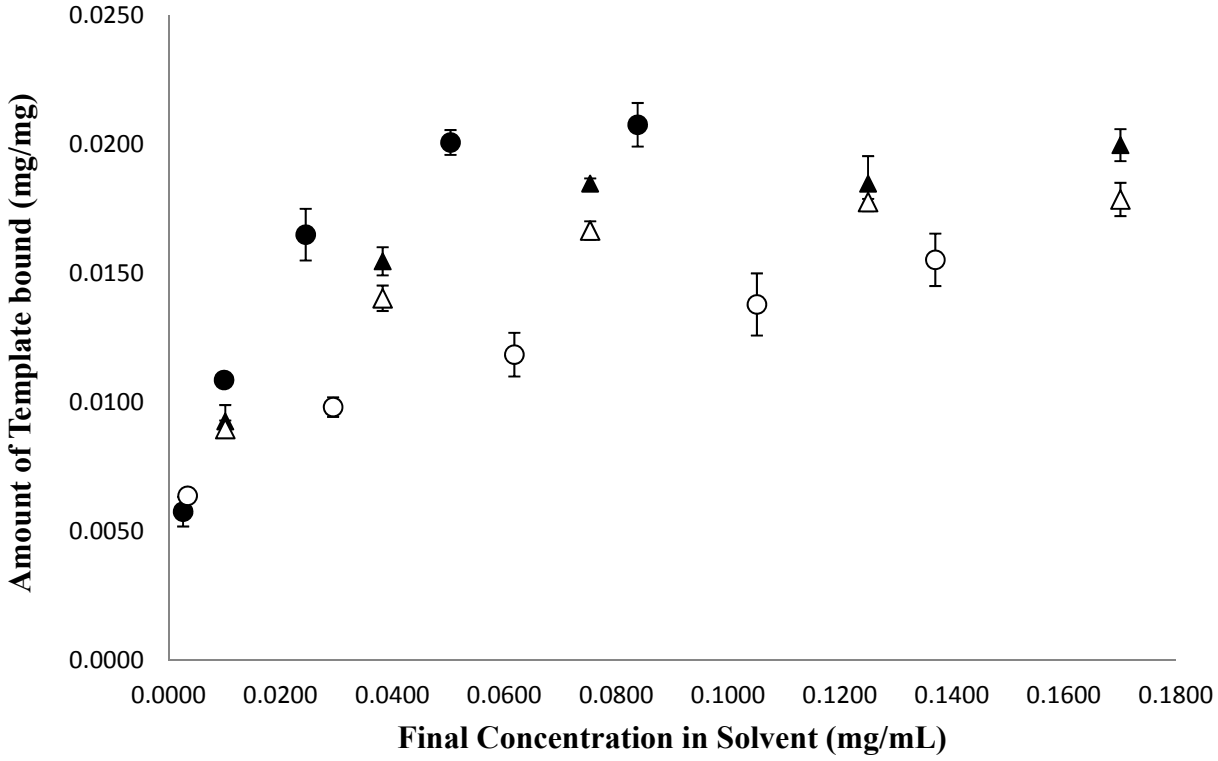

Figure 6.12: Equilibrium Binding Isotherms for Diclofenac Sodium Binding by Weakly Crosslinked Imprinted Poly(DEAEM- co-HEMA- co-PEG200DMA) Gels prepared via FRP and LRP. Data points represent poly(DEAEM-co-HEMA-co-PEG200DMA) gels prepared in the presence (50% by weight) (▲,Δ); and absence of solvent (●,○). Closed symbols (●,▲) represent gels prepared via LRP while open symbols (○,Δ) represent gels prepared via FRP. Error bars represent the standard error with n=3.

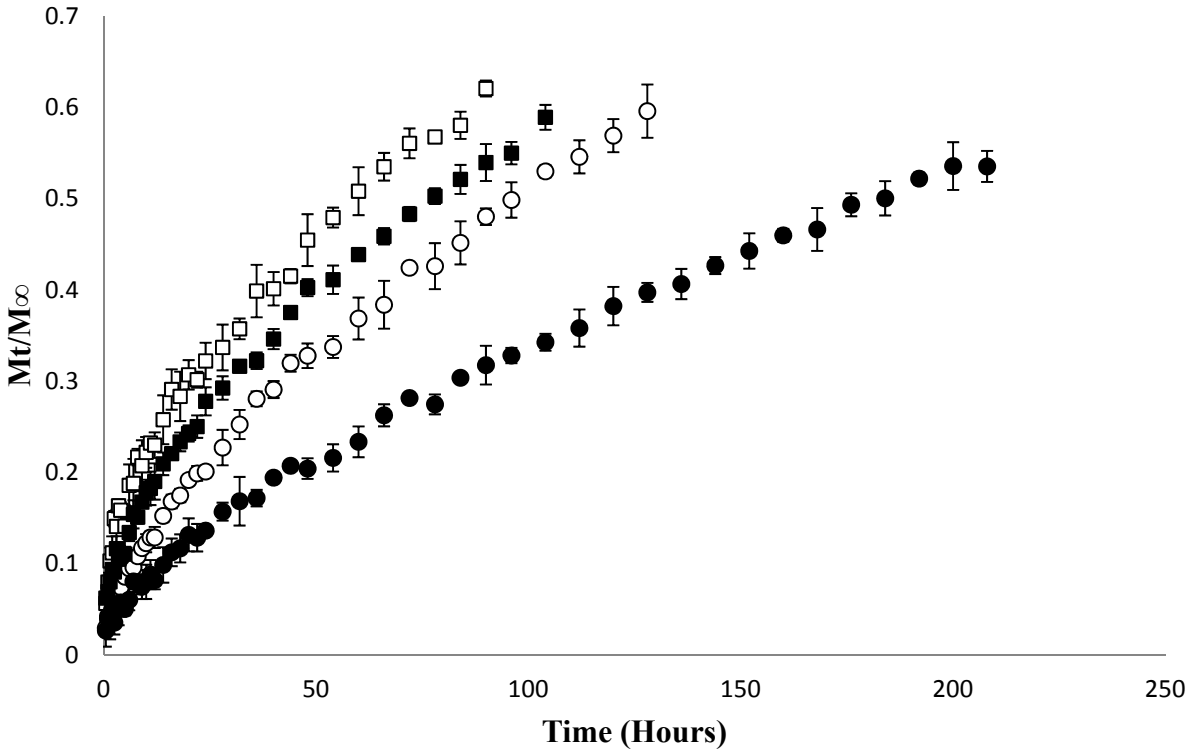

Figure 6.13: Fractional Release of Diclofenac Sodium in DI Water from Weakly Crosslinked Imprinted Poly(DEAEM-HEMA-PEG200DMA) Gels prepared via FRP and LRP. Data points represent poly(DEAEM-co-HEMA-co-PEG200DMA) gels prepared in the presence (50% by weight) (■,□); and absence of solvent (●,○).Closed symbols (■,●) represent gels prepared via LRP while open symbols (□,○) represent gels prepared via FRP. Error bars represent the standard error with n=3.

CHAPTER 7: EFFECT OF CROSSLINKER DIVERSITY ON NETWORK MORPHOLOGY, DRUG LOADING, AND DRUG RELEASE FROM MOLECULARLY IMPRINTED POLYMERS PREPARED VIA LIVING RADICAL POLYMERIZATION

7.1 Scientific Rationale

In this chapter, the synthesis and characterization of imprinted poly(hydroxyethyl methacrylate-co-diethylaminoethyl methacrylate-co-poly(ethyleneglycol200) dimethacrylate) (poly(DEAEM-co-HEMA-co-PEG200DMA)) polymer gels with varying crosslinking monomer lengths and concentrations is discussed. The objective was to analyze the effect of crosslinker diversity on polymer network structure and subsequently the template binding and template transport properties of the polymer gels. The concentration and length of the crosslinking monomer are important factors in determining the strength and the flexibility of the resultant network as well as the stability of the binding cavity formed by the imprinting process. Poly(ethylene glycol(200)dimethacrylate) (PEG200DMA) was chosen as the base crosslinking monomer with 5% molar ratio of crosslinking monomer to total monomer concentration. The concentration was varied by changing the molar ratio of PEG200DMA to 1%, 10% and 50% of the total monomer concentration. The length of the crosslinking monomer was varied by replacing PEG200DMA with ethylene glycol dimethacrylate (EGDMA) and poly(ethylene glycol(400)dimethacrylate) (PEG400DMA). PEG200DMA has a molecular weight of 200 Da and an average of 4.5 ethylene glycol repeating groups between the two vinyl groups.

PEG400DMA has a molecular weight of 400 Da and an average of 9 ethylene glycol repeating groups between the two vinyl groups while EGDMA has a single ethylene glycol group bracketed by vinyl groups. The functional monomer (diethylaminoethyl methacrylate (DEAEM)) concentration (5%) and the template to functional monomer ratio (0.3) were kept constant for all formulations. The change in network structure was analyzed by performing equilibrium swelling studies and dynamic mechanical analysis in addition to the analysis of polymer chain formation using gel permeation chromatography. Template binding and transport properties were also calculated.

7.2 Introduction

Polymer gels are insoluble, crosslinked polymer network structures composed of homo- or hetero-co-polymers, which have the ability to absorb significant amounts of solvent and retain their shape without dissolving. Polymer gels can be deformed and respond as an elastic body. Thus, these solvated polymers are at temperatures above their glass transition, where the amorphous portions of the polymer are in the rubbery state and are flexible. Crosslinks (otherwise known as tie-points or junctions) can be covalent bonds, permanent physical entanglements, non-covalent interactions, or microcrystalline regions incorporating various chains and are primarily responsible for preventing the dissolution of the polymer in solvent [1]. However, crosslinking strategies have primarily included covalent crosslinks with very little work exploiting other methods. For covalent crosslinks, the crosslinker length (i.e, linear size), concentration (i.e., the percent of crosslinking monomer reacted in network or degree of crosslinking) influence imprinting effectiveness. When a dry hydrogel is immersed in a thermodynamically compatible solvent, the solvent movement into the hydrogel polymer chains leads to considerable volume expansion and macromolecular rearrangement depending on the

nature and extent of crosslinking within the network. There have been many excellent reviews characterizing polymer gel structures. We direct the reader to the following references [1-2]. Structural assessment of imprinted hydrogels can be achieved by analysis of the following related parameters: the polymer volume fraction in the swollen state (i.e., the amount of water absorbed by the gel), the average molecular weight between two adjacent crosslinking or junction points, and the average correlation distance between two adjacent crosslinking or junction points (i.e., the average mesh size or free space between the macromolecular chains available for transport). Typically, higher crosslinked imprinted gels have a tighter mesh structure and swell to a lesser extent than weakly crosslinked gels. Equlibrium swelling and rubber elasticity theories have been used to characterize the structural parameters of polymer gels. For a more detailed discussion please refer to chapter 3.

It is well documented that the kinetic chain length of a linear polymer directly impacts its polymerization kinetics and the final mechanical properties of the polymer [3-4]. However, research studies are lacking about the effect of kinetic chain length in crosslinking systems. One reason for the lack of interest is the perceived unlikelihood that kinetic chain length is important in the kinetics of crosslinking systems that quickly form gels of infinite molecular weight. Though it may seem counterintuitive, recent research has shown that chain length does have a measurable effect on the polymerization kinetics of multi-functional methacrylates. It has been shown that chain length dependent termination is important in crosslinking systems. Adding a chain transfer agent to the system or increasing the initiation rate (i.e. decreasing the kinetic chain length) leads to a more mobile reaction environment and more rapid termination rates [5-6]. Additionally, the presence of a chain transfer agent alters the chemical identity of the radical fragment that begins a polymer chain. In chain transfer dominated systems, the initiator

fragments are not responsible for initiating the majority of chains. Rather, the chain transfer agent fragment will reinitiate and begin a new polymer chain. In the presence of small amounts of chain transfer agent it is unlikely that the chemical identity of this beginning fragment has any significant impact on the polymer properties or the network formation. Thus, the effect of chain transfer, even in these systems, is primarily on the kinetic chain length distribution. As the double bond conversion increases and reaction diffusion controlled termination begins to dominate the kinetics, the effect of kinetic chain length on the polymerization kinetics diminishes. The studies illustrate that the kinetics of multi-functional methacrylate systems are significantly impacted by chain length and the termination environment is dominated by the more mobile radical species present in the system [5-6].

One of the most important considerations in effective template recognition is to maintain the binding cavity produced via differing polymer chains close to the state when the original imprint was formed (i.e., close to the relaxed state of the polymer). In other words, the swollen or collapsed polymer volume at equilibrium must not be too different from the relaxed polymer volume fraction. The thermodynamic compatibility of the polymer chains and solvent as well as the number of crosslinking points within the network determines the nature and extent of this transition. The expansion of polymer chains increases the free volume available for template transport, but it can decrease the effectiveness of the imprinting site created by multiple polymer chains. Equilibrium is reached when the swelling force is counterbalanced by the retractive force due to crosslinking points in the network structure. Variations in network structure itself have been demonstrated to influence template binding and control the size of the imprinted cavities [7-12]. For example, maximizing crosslinker content has been shown to improve selectivity of MIPs [13-14].

In the work presented in this chapter, we alter the crosslinking junction by varying the concentration and length of the crosslinking monomer and evaluate the effect on the properties of the polymer gel. In addition, all gels were prepared via both conventional free radical polymerization (FRP) and living radical polymerization (LRP). During the polymerization, reaction analysis was used to determine the double bond conversion of the imprinted polymer. In addition, equilibrium swelling studies in water (a favorable solvent) were carried out to evaluate the flexibility of the polymer chains composing the gel, and tensile testing was carried out to determine the elasticity of the polymer gels. Using these results, the mesh size of the polymers was calculated. Lastly, binding and release studies were carried out to evaluate the template binding and transport properties of the gels.

7.3 Materials and Methods

PEG200DMA and PEG400DMA were used as received while EGDMA, DEAEM and (hydroxyethyl)methacrylate (HEMA), had inhibitors removed via inhibitor removal packing sieves prior to polymerization. The initiator azo-bis(isobutyronitrile) (AIBN), template molecule (diclofenac sodium (DS)), and chain transfer agent (tetraethylthiuram disulfide (TED)) were used as received. Monomers, inhibitor removal packing sieves, initiator, chain transfer agent, and template were purchased from Aldrich (Milwaukee, WI). HPLC grade solvents, acetonitrile and methanol, were used as received from Fisher Scientific (Pittsburgh, PA). De-ionized (DI) water was the template rebinding solvent, the wash solvent (to remove template and unreacted monomer) as well as the mobile phase in the high pressure liquid chromatography (HPLC) system.

7.3.1 Synthesis of Poly(DEAEM-co-HEMA-co-PEG200DMA) Gels

Poly(DEAEM-co-HEMA- co-PEG200DMA) gels imprinted for DS with a 5% crosslinking percentage were made with 0.336 mL of DEAEM (1.673 mmol), 3.659 mL of HEMA (30.118 mmol), 0.538 mL of PEG200DMA (1.673 mmol), 20 mg of AIBN (0.121 mmol), and 150 mg of DS (0.352 mmol). The solutions were mixed and sonicated until all solids were dissolved. Non-imprinted polymers were prepared similarly except the template was absent. The poly(DEAEM-co-HEMA- co-PEG200DMA) imprinted gel prepared via LRP was synthesized with 4.20 mg of TED (0.014 mmol) and 40 mg of AIBN (0.242 mmol). Solutions were transferred to an MBraun Labmaster 130 1500/1000 Glovebox (Stratham, NH), which provided an inert (nitrogen) atmosphere for free radical UV photopolymerization. Then monomer solutions were pipetted between two 6" x 6" glass plates coated with trichloromethylsilane (to prevent strong adherence of the polymer matrix to the glass) and separated by 0.25 mm Teflon spacers. The solutions were left uncapped and open to the nitrogen atmosphere until the O_2 levels inside reached negligible levels (<1 ppm) as determined by the attached solid state O_2 analyzer. The polymerization reaction was carried out for 8 minutes for the poly(DEAEM-co-HEMA-co-PEG200DMA) control and imprinted gels, whereas the reaction time was 24 minutes for the polymers prepared via LRP. Separate differential photocalorimetry (DPC) studies revealed exact reaction times. The intensity of light from a UV Flood Curing System (Torrington, CT) was 40 mW/cm2 at 325 V and the temperature within the glovebox was held constant at 25°C. After polymerization, the glass plates were soaked in DI water and the polymers were quickly peeled off the plates and cut into circular discs using a size 10 cork borer (13.5 mm). The gels were washed in a well-mixed 2L container of DI water for 7 days with a constant 5 mL per minute flowrate of DI water. Absence of detectable drug released from the polymer gel was verified by removing random gels, placing them in fresh DI water with adequate mixing, and sampling the supernatant via

spectroscopic monitoring. The discs were allowed to dry under laboratory conditions at a temperature of 20°C for 24 hours and then transferred to a vacuum oven (27 in Hg, 33–34°C) for 24 h until the disc weight change was less than 0.1wt%.

7.3.2 Analysis of Kinetic Chain Length of Polymers

The molecular weight distributions of uncrosslinked polymer chains were characterized by a modified HPLC system (Shimadzu, Columbia, MD) used for gel permeation chromatography (GPC). The GPC setup consisted of two PL Aquagel size exclusion columns in series (Varian LLC, Santa Clara, CA), for separation of various molecular weight fractions of the polymer which were detected using a RID10A refractive index detector (Shimadzu, Columbia, MD). DI water was used as the mobile phase for the system. Prior to running the samples, the system was calibrated using narrow molecular weight distribution poly(MAA) standards (Polymer Source Inc., Dorval, Quebec). The polymer chains obtained after early termination of polymerization were dissolved in the mobile phase to achieve a concentration of 5 mg/mL. A 50 μL aliquot of the solution was then injected into the system using a Rheodyne (Oak Harbour, WA) 7725(i) manual injection unit. Using the subsequent peaks obtained on the chromatograph, the weight average molecular weight (M_w), the number average molecular weight (M_n) and the polydispersity index (PDI) were calculated, where, the molecular weight (M_i) for a particular weight fraction was described by the x-coordinate of the corresponding point on the chromatograph while the number of chains (N_i)was described by the y-coordinate. Mark – Houwink parameters for poly(HEMA) and poly(MAA) were obtained from the literature [15].

7.3.3 Analysis of Kinetic Parameters

A dark reaction was used to determine the kinetic reaction profile for the poly(DEAEM- co-HEMA- co-PEG200DMA) gels [16-17]. For each polymerization reaction, the UV light was shut

off at a specific time point during the reaction. The rate of polymerization was calculated via reaction analysis using the heat flow versus time from the DPC, average molecular weight of the polymerization solution, and the theoretical heat of reaction. Fractional double bond conversion was determined by dividing the experimental heat of reaction by the theoretical heat of reaction. The experimental heat of reaction was determined by the area under the heat flow versus time curve from the DPC. The termination and propagation constants, k_t and k_p, were calculated from *Equations. 7.1 and 7.2*, and the derivation of these equations can be found in Flory [18] or Odian [19].

$$\frac{k_p}{k_t^{0.5}} = \frac{R_p}{[M](f I_o \varepsilon [I])^{0.5}} \tag{7.1}$$

where [*M*] is the monomer concentration, the initiator efficiency is *f*, I_o is the light intensity, ε is the extinction coefficient, and [I] is the initiator concentration. The unsteady state equation used to decouple the propagation constant and the termination constant is shown below.

$$k_t^{0.5} = \frac{k_p / k_t^{0.5}}{2(t_1 - t_0)} \left[\frac{[M]_{t=t1}}{Rp_{t=t1}} - \frac{[M]_{t=t0}}{Rp_{t=t0}} \right] \tag{7.2}$$

where $t_1$and t_0 are the final and initial times, $[M]_{t=t1}$ and $[M]_{t=to}$ are the corresponding monomer concentrations, respectively, and $Rp_{t=t1}$ and $Rp_{t=to}$ are the rate of polymerization at final and initial times, respectively.

7.3.4 Template Binding Experiments and Analysis of Binding Parameters

A stock solution of 1 mg/mL of DS was prepared and diluted to five concentrations (0.05, 0.10, 0.15, 0.20, and 0.25 mg/mL). Initial absorbances of each concentration were measured using a Synergy UV–vis spectrophotometer (BioTek Instruments, Winooski, VT) at 276 nm, the

wavelength of maximum absorption. After the initial absorbance was taken, a dry, washed poly(DEAEM- co-HEMA- co-PEG200DMA) polymer disk was inserted in each vial and the vials were gently mixed until equilibrium. Separate dynamic studies were performed to assure equilibrium conditions were reached. After equilibrium was reached over a 7-day period, the solutions were vortexed for 10 seconds, and the equilibrium concentrations were measured. A mass balance was used to determine the bound amount of drug within the polymer gel. All gels were analyzed in triplicate, and all binding values are based upon the dry weight of the gel. The Langmuir-Freundlich isotherm was used to determine binding parameters because it gave the best fit to the experimental data.

7.3.5 Dynamic Template Release Studies and Diffusion Coefficient Determination

After binding studies, poly(DEAEM- co-HEMA- co-PEG200DMA) gels, loaded with template at a concentration of 0.25 mg/mL, were placed in 30 ml of DI water which was continuously agitated with an Ocelot orbital shaker(Cheshire, WA) at 375 rpm at 25°C. At various time points, the absorbance of the solution was measured using a Synergy UV–vis spectrophotometer (BioTek Instruments, Winooski, VT) at 276 nm until the concentration did not change more than 1%. At each sample point, the DI water was replaced to maintain infinite sink conditions. Fractional template release profiles were calculated for all polymer gels by taking the amount of template released at specific times, M_t, divided by the maximum amount of DS released during the experiment, M_∞. The fractional template release profile, M_t/M_∞ vs. time, was determined for each gel. Template diffusion coefficients were calculated using Fick's law, which describes one-dimensional planar solute release from gels [20]. For polymer geometries

with aspect ratios (exposed surface length/thickness) greater than 10, edge effects can be ignored and the problem can be approached as a one-dimensional process.

7.3.6 Swelling Studies and Polymer Specific Volume Determination

After polymerization, three gels of each polymer formulation were taken for dry, swollen, and relaxed specific volume determination experiments. For the dry specific volume determination, gels were placed in the vacuum oven at a temperature and pressure of 30°C 28 inches of Hg vacuum until the weight change was less than 0.1 wt%. Once dry, the gels were then taken out and the dry mass was measured on a Sartorius scale. Afterward, a density determination kit was installed on the Sartorius scale. The mass of the gel was then measured in heptane, a non-solvent (density of 0.684 g/mL at a temperature of 25°C). Once measurements were taken, Archimedes bouyancy principle was used to calculate the density of the dry polymer as shown in *equation 7.3*,

$$\rho_x = \frac{W_a \cdot \rho_h}{W_a - W_h} \tag{7.3}$$

where ρ_x is the density of the sample, W_a is the mass of the sample in air, ρ_h is the density of heptane, and W_h is the weight of the sample in heptane. The specific volume of the polymer was calculated as the reciprocal of density. The experiment was repeated for both the relaxed and swollen gel. The relaxed gel specific volume was calculated directly after the polymerization reaction without any additional solvent being introduced into the gel. The swollen gel specific volume was calculated after the gel reached swelling equilibrium with the solvent for each system. The equilibrium volume swelling ratio Q was calculated with the swollen volume $V_{2,s}$ and the volume of the dry polymer, $V_{2,d}$, (*equation 7.4*).

$$Q = \frac{1}{\vartheta_{2,S}} = \frac{V_{2,S}}{V_{2,d}} \quad 7.4$$

Dynamic swelling studies of select poly(DEAEM-co-HEMA-co-PEG200DMA) gels were performed by measuring the initial gel dry weight to determine the dry mass of polymer. The gel was then placed in a 0.5 mg/mL diclofenac sodium solution (i.e., gel was loading in addition to swelling). The gel was taken out of solution and patted dry with Kimwipes®, and the gel weight measured. After the weight was measured, the gel was placed back in solution to continue swelling. The measurement was repeated once every 5 minutes for the first hour, once every 10 minutes for the second hour, and then every 30 minutes until the gel reached a constant mass which indicated equilibrium.

7.3.7 Mechanical Analysis and Calculation of Mesh Size

Mechanical analysis of imprinted poly(DEAEM-co-HEMA-co-PEG200DMA) gels in the equilibrium swollen state (with DI water as solvent) was performed. Samples of each gel (1 mm x 3 mm x 10 mm strips) were removed and analyzed with a RSA III Dynamic Mechanical Analyzer (DMA), (TA Instruments, New Castle, DE) to obtain stress versus strain. Each experiment was conducted in controlled force mode with a force ramp from 0.001 to 0.3 N. The raw data obtained for each gel is included in the Appendix.

Polymer gel mesh size was calculated via data collected from the static experiments via a DMA and by using the theory of rubber elasticity. The following equation describes the tension of a swollen, un-stretched polymer sample, τ.

$$\tau = \left(\frac{RT\vartheta_{2,S}^{\frac{1}{3}}}{\bar{\vartheta}\overline{M_c}} \right) (\alpha - \frac{1}{\alpha^2}) \quad 7.5$$

where R is the universal gas constant, T is the temperature, υ_e is the effective number of moles of chains in a real network, V is the volume of the swollen polymer, $\upsilon_{2,s}$ is the swollen polymer fraction calculated by polymer dry volume $V_{2,d}$ divided by the polymer swollen volume $V_{2,s}$, and α is the deformation of a network structure by elongation which is equivalent to the stretched length over initial length ($\alpha = L/L_o$). The following equation takes into account the polymer swollen until equilibrium with the solvent, but not prepared in solvent.

$$\tau = \left(\frac{RT\vartheta_{2,s}^{\frac{1}{3}}}{\bar{\vartheta}\overline{M_c}}\right)\left(1 - \frac{2\overline{M_c}}{\overline{M_n}}\right)\left(\alpha - \frac{1}{\alpha^2}\right) \qquad 7.6$$

where $\bar{\upsilon}$ is the specific volume of the polymer in the relaxed state, $\overline{M_N}$ is the number average molecular weight, and $\overline{M}_c$ is the average molecular weight between crosslinks. Taking *equation 7.6* and the fact that the average molecular weight between crosslinks is much smaller than the number average molecular weight (i.e., $\overline{M}_c << \overline{M_N}$) will yield *equation 7.7*.

$$\tau = \left(\frac{RT\vartheta_{2,s}^{\frac{1}{3}}}{\bar{\vartheta}\overline{M_c}}\right)\left(\alpha - \frac{1}{\alpha^2}\right) \qquad 7.7$$

The stress and strain data obtained by the static experiments from DMA was plotted with the α term on the y axis and tension τ on the x axis to obtain the slope which gave the average molecular weight between crosslinks $\overline{M}_c$. To determine the actual mesh size, ξ of the polymer network, the relationship of ξ to $\overline{M}_c$ is needed from Peppas and Barr-Howell.

$$\xi = Q^{1/3}\left(\frac{2C_n\bar{M}_c}{M_r}\right)^{\frac{1}{2}} l \qquad 7.8$$

where Q is the equilibrium volume swelling ratio, C_n is the characteristic ratio for the polymer (obtained from the molar average of the C_n from the homopolymers), and M_r is the effective molecular weight of the repeating unit (determined by a weighted average of the copolymer composition). It is important to note the equilibrium volume swelling ratio, Q, is the swollen volume of the gel divided by the dry volume of the gel or the reciprocal of the swollen polymer volume fraction. The C_n values used in this analysis were for polyethylene glycol dimethacrylate (C_n =3.8), and for the poly(DEAEM-co-HEMA-co-PEG200DMA) a typical average value of the characteristic ratio (C_n = 11) was used [21-24]. The carbon-carbon bond length of the polymer backbone, which is equal to 1.54 Å is represented by length, l.

7.4 Results and Discussion

Figure 7.1 shows equilibrium binding isotherms for imprinted polymer gels with varying amounts of the crosslinking monomer, PEG200DMA, ranging from 1% to 50% of the total monomer content. Figure 7.1A shows polymers prepared via FRP while Figure 7.1B shows polymers prepared via LRP. The binding capacity and affinity for all gels were calculated using the Langmuir-Freundlich isotherm and are listed in Table 7.1. From Table 7.1, we can see that at low concentrations of PEG200DMA (less than 5%) there isn't a statistically significant impact on either the template binding capacity or the binding affinity of the polymer gels. However, as the extent of crosslinking is increased the template binding capacity decreases. Polymer gels prepared via FRP with 10% PEG200DMA in the pre-polymerization solution demonstrate a binding capacity of 11.6 ± 0.22 mg/g which is significantly lower than the binding capacity of corresponding polymer gels with 5% PEG200DMA in feed (Q_{max}=16.7 ± 0.64 mg/g). A similar trend is observed for polymer gels prepared via LRP. The decreased binding may be explained by the decreased flexibility of the polymer chains as the extent of crosslinking is increased.

Conventionally, decreased flexibility in imprinted polymers was assumed to favor binding as it helps maintain the shape of the binding cavity. This is especially true for non-covalently imprinted polymers where the primary interaction between the template and the polymer chains is via hydrogen bonding. Conversely, the primary ionic interaction between the diclofenac ion and the charged ammonium group contributed by DEAEM is considerably stronger and the preservation of the binding cavity is less vital. However, the increased flexibility of polymer chains during polymerization may allow them greater freedom to continue to interact with the template throughout the polymerization reaction which would result in the formation of more binding sites. In addition, at high concentration of crosslinker content, gel formation begins early and may result in the loss of available binding sites.

All polymer gels prepared via LRP demonstrate higher binding capacity as well as affinity when compared with the corresponding polymers prepared via FRP. This is consistent with the observed extension of chain propagation and delayed gel formation discussed in Chapter 6. It is interesting to note that the extent of improvement in the binding capacity increased with increasing crosslinker content. LRP resulted in a 43% increase in template binding capacity for polymers with 5% PEG200DMA while polymers with 10% PEG200DMA demonstrated a 59% increase and polymers with 50% PEG200DMA demonstrated a still higher increase in binding capacity of 102% due to LRP.

Figure 7.2 shows fractional release rates from imprinted polymer gels prepared using FRP with varying amounts of crosslinker (1%, 5%, 10%, 50%) in the pre-polymerization solution. From Figure 7.2 we can see that increasing the crosslinking monomer content results in delayed release of the template. For example, polymers with 1% PEG200DMA in the pre-polymerization solution released 60% of the loaded template in approximately 96 hours while the polymers with

5%, 10% and 50% PEG200DMA released 60% of loaded template in approximately 128 hours, 152 hours, and 168 hours, respectively. In addition to demonstrating slower fractional release, polymers with higher crosslinking content also demonstrated slower absolute release of the template. In the first 48 hours of release, approximately 215 μg, 173 μg, 114 μg and 47 μg of DS was released from polymers with 1%, 5%, 10% and 50% PEG200DMA respectively. The slower release rate from high crosslinked polymers can be attributed to the decrease in the mesh size of the polymers as the number of crosslinking points is increased. Polymers prepared via FRP with 1% PEG200DMA in pre-polymerization solution were calculated to have a mesh size of 4.86 ± 0.32 nm while the corresponding polymers with 50% PEG200DMA were calculated to have a mesh size 1.79 ± 0.19 nm. Although, lower binding of template observed in polymers with higher crosslinker content could also contribute to slower release rates.

Figure 7.3 shows the fractional release from the corresponding gels prepared via LRP. These gels demonstrated similar behavior as the polymers prepared via FRP. Polymers with 1% PEG200DMA in the pre-polymerization solution released 60% of the loaded template in approximately 160 hours while the polymers with 5%, 10% and 50% PEG200DMA released 60% of loaded template in approximately 240hours, 256 hours, and 344 hours, respectively. Its important to note that the use of LRP resulted in significantly decreased fractional release rates. Also, the polymers with higher crosslinker content showed greater extension of release duration. For example, for polymers with 1% PEG200DMA the release duration for 60% of the drug was extended by 67% while for the polymers with 5% and 50% PEG200DMA it was extended by 87.5% and 105%. This trend is consistent with the results observed for the binding capacities. The polymer with 10% PEG200DMA goes against this trend demonstrating only a 69% increase in release duration due to LRP. However, this may be explained by the fact that while the

polymers prepared via FRP shows smaller mesh sizes as the crosslinker content is increased (mesh size decreases from 3.03 ± 0.10 nm to 2.48 ± 0.32 nm); polymers prepared via LRP show similar mesh sizes (mesh size is1.98 ± 0.26 nm for polymers prepared with 5% PEG200DMA and 1.94 ± 0.27 nm for polymers prepared with 10% PEG200DMA). As a result, the higher binding capacity in the polymer with lower crosslinking content becomes a factor. As discussed in Chapter 6, an increase in the number of binding sites in the polymer increases the probability and extent of temporary binding events between the template and the polymer chains, as proposed in the tumbling hypothesis, slowing the elution of template out of the polymer.

Figure 7.4 shows the equilibrium volume swelling ratio of the imprinted gels versus the feed crosslinker content for polymers prepared via FRP as well as LRP. It was observed that increasing the crosslinking content generally resulted in lower equilibrium swelling ratios. The presence of crosslinking points has been demonstrated to constrict the ability of a flexible gel to solvate in a favorable solvent resulting in lower equilibrium swelling ratios. Since water is a favorable solvent for the poly(HEMA-co-DEAEM-co-PEG200DMA) gels these results are consistent with other reported results. The use of LRP also resulted in lower equilibrium swelling ratios. This may indicate better homogeneity in the crosslinking structure of polymers prepared via LRP.

Figure 7.5 compares the average molecular weight and PDI of imprinted polymer gels with varying concentration of crosslinking monomer prepared via FRP and LRP. From Figure 7.5, we can see that an increase in the crosslinker content results in the decrease in the kinetic chain length of the polymers as well as an increase in their PDI. This may be explained by an early transition to gelation during polymerization when the crosslinker content is increased. This is supported by the kinetic data for the polymerization reaction. Use of LRP extends propagation

and delays gelation resulting in simultaneous growth of multiple polymer macroradicals in solution as described in Chapter 5 and 6. The effect of LRP is demonstrated by the decrease in the PDI for the polymer chains. Delayed gelation due to LRP is also supported by the increase in average molecular weight for the polymers with 50% PEG200DMA despite LRP having a significantly lower propagation rate.

Figure 7.6 shows equilibrium binding isotherms for imprinted polymer gels with varying crosslinking monomers, EGDMA, PEG200DMA, and PEG400DMA. The concentration of the crosslinking monomers was maintained constant at 5% of the total monomer concentration. The crosslinking monomers were chosen to vary the length of the chain between the two vinyl ends. PEG200DMA has an average of 4.5 ethylene glycol repeating units (average molecular weight = 200 Da) between the two vinyl groups. PEG400DMA has an average of 9 ethylene glycol repeating units (average molecular weight = 400 Da) between the two vinyl groups while EGDMA has a single ethylene glycol unit between two vinyl groups. Figure 7.6A shows polymers prepared via FRP while Figure 7.6B shows polymers prepared via LRP. The binding capacity and affinity for all gels were calculated using the Langmuir-Freundlich isotherm and are listed in Table 7.1. From Table 7.1, we observe that polymers with PEG200DMA as crosslinker demonstrate the highest template binding capacities (Q_{max}=16.7 ± 0.64 mg/g) when compared with the corresponding polymers with EGDMA and PEG400DMA as crosslinkers ((Q_{max}=10.7 ± 0.27 mg/g and 13.3 ± 0.38 mg/g respectively). This seems counterintuitive to the trend observed in Figure 7.1 where increased chain flexibility was demonstrated to result in higher template binding capacity. A possible explanation may be that the impact of a shorter crosslinker (PEG200DMA) on increased stability of the binding site may be more important than the increased flexibility of polymer chains afforded by longer a crosslinker (PEG400DMA). This is

supported by the increase in binding affinity as the crosslinker length is reduced (K_a= 15.1 ± 0.20 mM^{-1}, 15.7 ± 0.12 mM^{-1}, 16.8 ± 0.43 mM^{-1} for PEG400DMA, PEG200DMA and EGDMA, respectively). Thus, PEG200DMA may be the ideal crosslinker for maximizing binding capacity and affinity. The polymers prepared via LRP showed a similar trend. In addition, all polymers prepared via LRP demonstrated higher binding capacities as well as affinites when compared with the corresponding polymers prepared via FRP.

Figure 7.7 shows fractional release rates from imprinted polymer gels prepared via FRP with different crosslinking monomers, EGDMA, PEG200DMA, and PEG400DMA. From Figure 7.7 we can see that increasing the length of the crosslinker results in faster fractional release of the template. For example, polymers prepared with EGDMA in the pre-polymerization solution released 60% of the loaded template in approximately 152 hours while the polymers with PEG200DMA and PEG400DMA release 60% of loaded template in approximately 128hours and 100 hours, respectively. In addition to demonstrating slower fractional release, polymers with shorter crosslinkers also demonstrated slower absolute release of the template. In the first 48 hours of release, approximately 212 μg, 173 μg and 110 μg of DS was released from polymers prepared with PEG400DMA, PEG200DMA and EGDMA as crosslinkers, respectively. The slower release rate from polymers with EGDMA may be due to their smaller mesh sizes (2.36 ± 0.29 nm). The polymers prepared with PEG200DMA and PEG400DMA, however, demonstrated statistically similar mesh sizes. The difference in release rates was thus more likely due to the higher binding capacity and affinity of the polymer with PEG200DMA.

Figure 7.8 shows the fractional release from the corresponding gels prepared via LRP. These gels demonstrated similar behavior as the polymers prepared via FRP. Polymers with EGDMA in the pre-polymerization solution released 60% of the loaded template in approximately 288

hours while the polymers with PEG200DMA and PEG400DMA release 60% of loaded template in approximately 240 hours and 204 hours, respectively. It's important to note that the use of LRP resulted in significantly decreased fractional release rates. This is consistent with results described earlier in the chapter and may be attributed to the improved binding capacity and affinity of these polymers. However,the lower mesh sizes in polymers prepared via LRP may be a significant factor.

Figure 7.9 shows the equilibrium volume swelling ratio for the imprinted gels prepared via FRP as well as LRP with EGDMA, PEG200DMA and PEG400DMA as the crosslinkers. From Figure 7.9, we can see that increasing the crosslinking length results in an increase in equilibrium swelling ratios. The use of LRP also results in lower equilibrium swelling ratios. This may indicate better homogeneity in the crosslinking structure of polymers prepared via LRP.

Figure 7.10 compares the average molecular weight and PDI of the polymer gels described in Figure 7.9. From Figure 7.10, we can see that polymers with PEG200DMA as crosslinking monomer show the highest kinetic chain lengths. This may be due to the higher reactivities of EGDMA and PEG400DMA as compared to PEG200DMA [25]. The higher reactivity of the crosslinking monomer may result in early transition to gelation as described before. This is exacerbated by the decreased flexibility of the shorter EGDMA resulting in the fastest transition to gelation and as a result the shortest kinetic chain length. LRP is again demonstrated to result in decreased PDI of the polymer chains. As with highly crosslinked PEG200DMA, delayed gelation due to LRP results in an increase in average molecular weight for the polymers with EGDMA as crosslinker, despite LRP having a significantly lower propagation rate.

7.5 Conclusion

The work presented in this chapter examined the effects of crosslinker diversity on the structure of imprinted gels and subsequently their drug binding and transport properties. This was the first recorded attempt to comprehensively examine the effects of crosslinker diversity in imprinted gels prepared via LRP. It was found that an increase in the extent of crosslinking resulted in a decrease in the template binding capacity and release rate of template from the polymer gels. This corresponded with lower equilibrium swelling ratios and smaller mesh sizes of the solvated polymer gels. In addition, a decrease in the kinetic chain length of the polymers pre-gelation as well as an increase in their PDI was observed. This may be explained by an early transition to gelation during polymerization. Increase in the length of the crosslinker resulted in decreased binding affinity and faster release of template from polymer which corresponded with increased equilibrium swelling ratios. All polymer gels prepared via LRP demonstrate higher binding capacity as well as affinity when compared with the corresponding polymers prepared via FRP. The use of LRP also resulted in significantly decreased fractional release rates with the extent of delayed release increasing as crosslinker concentration was increased. The use of LRP also resulted in lower equilibrium swelling ratios and smaller mesh sizes of solvated gels. This combined with the observed decrease in the PDI of pre-gelation polymers may indicate better homogeneity in the crosslinking structure of polymers prepared via LRP.

7.6 References

1. Peppas NA (Ed.) Hydrogels in Medicine and Pharmacy, Volume I: Fundamentals. 1987, CRC Press, Boca Raton, FL.
2. Peppas NA, Bures P, Leobandung W, Ichikawa H, Hydrogels in pharamaceutical formulations. Eur. J. Pharm. Biopharm. 2000, 50, 27-46.
3. Berchtold KA, Lovell LG, Nie J, Hacioglu B, Bowman CN. Polymer. 2001, 42, 4925–29.
4. Berchtold KA, Lovell LG, Nie J, Hacioglu B, Bowman CN. Macromolecules. 2001, 34, 5103–11.
5. Doura M, Aota H, Matsumoto AJ. Polym. Sci., Part A: Polym. Chem. 2004, 42, 2192-99.
6. Doura, M.; Naka, Y.; Aota, H.; Matsumoto, A. Macromolecules 2003, 36, 8477-88.
7. Byrne ME, Hilt JZ, Peppas NA. Recognitive biomimetic networks with moiety imprinting for intelligent drug delivery. J. Biomed. Mater. Res., Part A. 2008, 84A, 137-147.
8. Espinosa-Garcia BM, Argelles-Monal WM, Hernandez J, Felix-Valenzuela L, Acosta N, Goycoolea FM. Molecularly imprinted chitosan-genipin hydrogels with recognition capacity toward o-xylene. Biomacromolecules. 2007, 8, 11, 3355-64.
9. Noss KR, Vaughan AD, Byrne ME. Tailored binding and transport parameters of molecularly imprinted films via macromolecular structure: The rational design of recognitive polymers. J. Appl. Polym. Sci. 2008, 107, 3435-3441.
10. Spizzirri UG, Peppas NA. Structural analysis and diffusional behavior of molecularly imprinted polymer networks for cholesterol recognition. Chem. Mater. 2005, 17, 6719-6727.
11. Djourelov N, Ates Z, Guven O, Misheva M, Suzuki T. Positron annihilation lifetime spectroscopy of molecularly imprinted hydroxyelthyl methacrylate based polymers. Polymer. 2007, 48, 2692-2699.

12. Yamashita K, Nishimura T, Ohashi K, Ohkouchi H, Nango M. Two-step Imprinting Procedure of Inter-penetrating Polymer Network-Type Stimuli-Responsive Hydrogel Adsorbents. Polym. J. 2003, 35, 545-550.
13. Wulff G, Kemmerer R, Vietmeier J, Poll HG. Chirality of vinyl polymers. The preparation of chiral cavities in synthetic polymers, Nouv. J. Chim. 1982, 6, 681–687.
14. Spivak DA, Optimization, evaluation, and characterization of molecularly imprinted polymers. Advanced Drug Delivery Reviews. 2005, 57, 1779–1794.
15. Brandrup J, Immergut EH. Polymer handbook, 3rd ed. 1989, Wiley, New York.
16. Anseth KS, Kline LM, Walker TA, Anderson KJ, Bowman CN. 1995. Reaction kinetics and volume relaxation during polymerizations of multiethylene glycol dimethacrylates. Macromolecules 28: 2491–2499.
17. Anseth KS, Wang CM, Bowman CN. 1994. Reaction behaviour and kinetic constants for photopolymerizations of multi(meth)acrylate monomers. Polymer 35: 3243–3250.
18. Flory PJ. 1953. Principles of Polymer Chemistry, 1st ed. Cornell University Press: Ithaca.
19. Odian G. Principles of Polymerization, 2nd ed. 1981, John Wiley & Sons, New York.
20. Venkatesh S, Saha J, Pass S, Byrne ME. Transport and structural analysis of molecular imprinted hydrogels for controlled drug delivery. Eur. J. Pharm. Biopharm. 2008, 69, 852–860.
21. Hariharan D, Peppas NA. Characterization, Dynamic Swelling Behaviour and Solute Transport in Cationic Networks with Applications to the Development of Swelling-Controlled Release Systems. Polymer. 1996, 37, 1, 149-161.

22. Kavimandan N J, Losi E, Peppas N A. Novel Delivery System Based on Complexation Hydrogels as Delivery Vehicles for Insulin-transferrin Conjugates. Biomaterials. 2006, 27, 20, 3846-3854.
23. Berger J, Reist M, Mayer J M, Felt O, Peppas NA, Gurny R. Structure and Interactions in Covalently and Ionically Crosslinked Chitosan Hydrogels for Biomedical Applications. European Journal of Pharmaceutics and Biopharmaceutics. 2004, 57, 1, 19-34.
24. Lowman AM, Dziubla TD, Bures P, Peppas NA, Sefton MV. Structural and Dynamic Response of Neutral and Intelligent Networks in Biomedical Environmnets. In Advances in Chemical Engineering, Academic Press. 2004, 29, 75-130.
25. Peppas NA, Shahar A, Ward JH, Kinetics of 'living' radical polymerizations of multifunctional monomers. Polymer. 43, 2002, 1745-1752.

Table 7.1: Binding Capacities, Affinities and Coefficients of Diffusion for Diclofenac Sodium in Poly(DEAEM-co-HEMA-co-PEG200DMA) Polymer Gels

Crosslinker (Type of reaction)	K_a (mM^{-1})	Q_{max} (mg/g)	Diffusion Coefficient (cm^2/s)x10^{13}
5% EGDMA (FRP)	16.8±0.43	10.7±0.27	3.64±0.02
5% EGDMA (LRP)	22.4±0.20	20.8±0.26	1.58±0.02
5% PEG400DMA (FRP)	15.1±0.20	13.3±0.38	5.38±0.07
5% PEG400DMA (LRP)	19.3±0.20	16.7±0.41	2.42±0.02
1% PEG200DMA (FRP)	15.3±0.27	17.1±0.43	5.47±0.05
1% PEG200DMA (LRP)	21.6±0.20	24.5±0.38	3.38±0.01
5% PEG200DMA (FRP)	15.7±0.12	16.7±0.64	3.68±0.05
5% PEG200DMA (LRP)	21.7±0.17	23.9±0.60	1.84±0.02
10% PEG200DMA (FRP)	15.1±0.24	11.6±0.22	3.73±0.04
10% PEG200DMA (LRP)	20.1±0.57	18.4±0.69	1.68±0.03
50% PEG200DMA (FRP)	12.0±0.18	6.1±0.27	3.16±0.08
50% PEG200DMA (LRP)	16.2±0.31	12.3±0.18	1.35±0.02

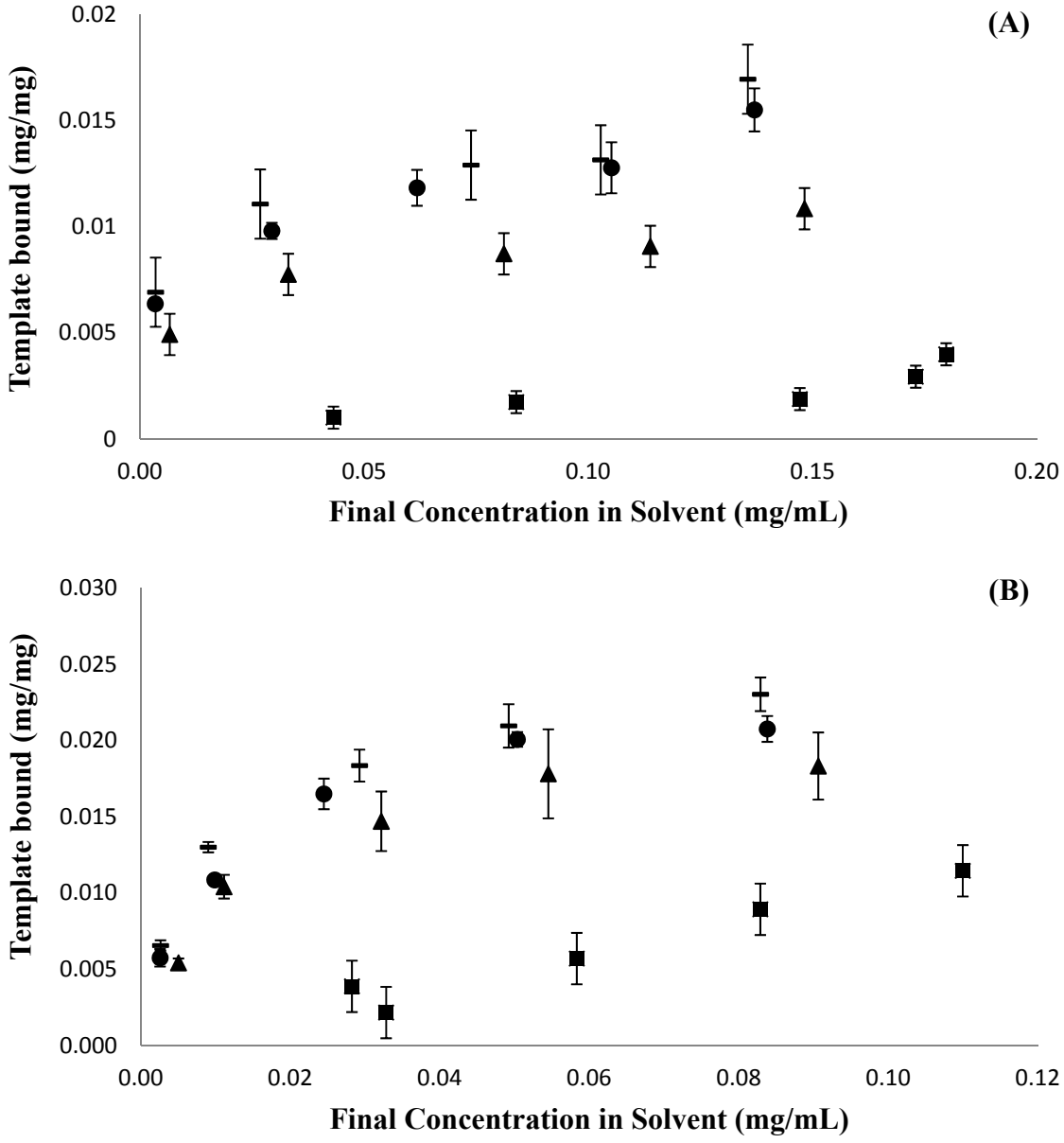

Figure 7.1: Equilibrium Binding Isotherms for Diclofenac Sodium Binding by Imprinted Poly(DEAEM- co-HEMA- co-PEG200DMA) Gels prepared via (A) FRP and (B) LRP with varying Concentrations of Crosslinker. Data points represent poly(DEAEM-co-HEMA-co-PEG200DMA) gels prepared with varying concentrations of crosslinker in feed: crosslinker content=1%(▬); crosslinker content=5%(●); crosslinker content=10%(▲); crosslinker content=50%(■).Error bars represent the standard error with n=3.

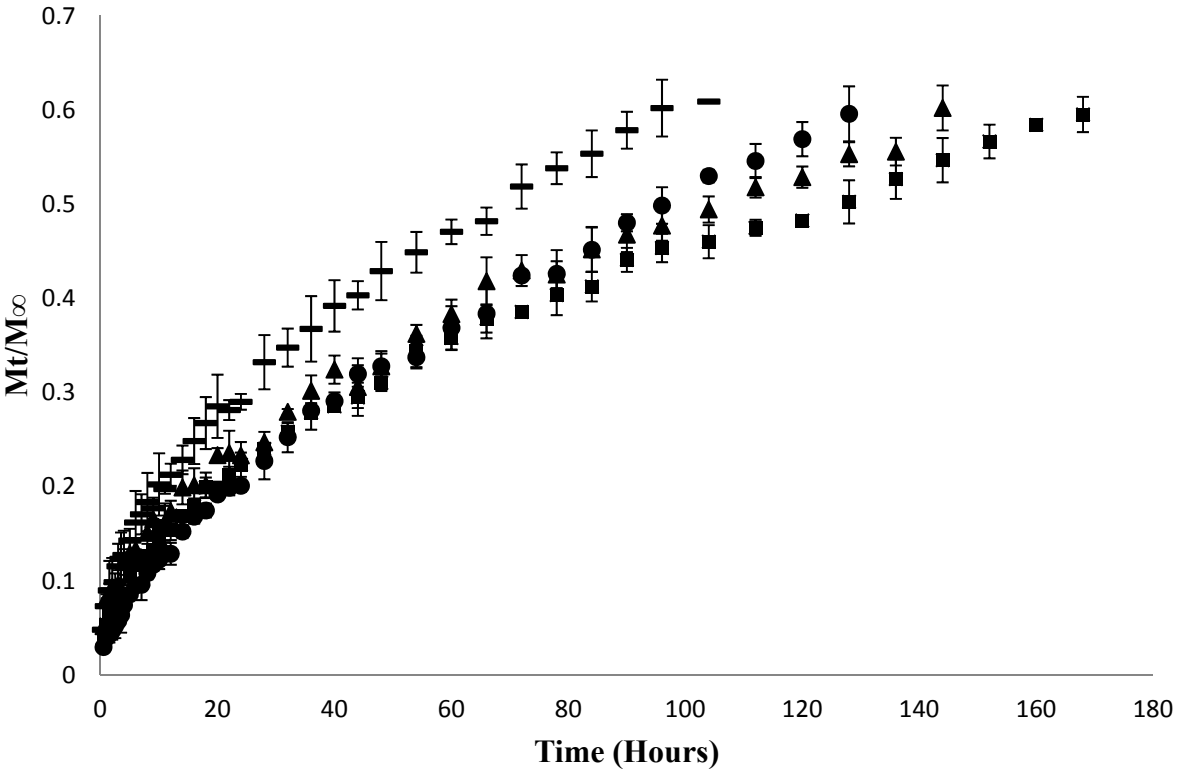

Figure 7.2: Fractional Release of Diclofenac Sodium in DI Water from Imprinted Poly(DEAEM- co-HEMA- co-PEG200DMA) Gels prepared via FRP with varying Concentrations of Crosslinker. Data points represent poly(DEAEM-co-HEMA-co-PEG200DMA) gels prepared with varying concentrations of crosslinker in feed: crosslinker content=1%(▬); crosslinker content=5%(●); crosslinker content=10%(▲); crosslinker content=50%(■).Error bars represent the standard error with n=3.

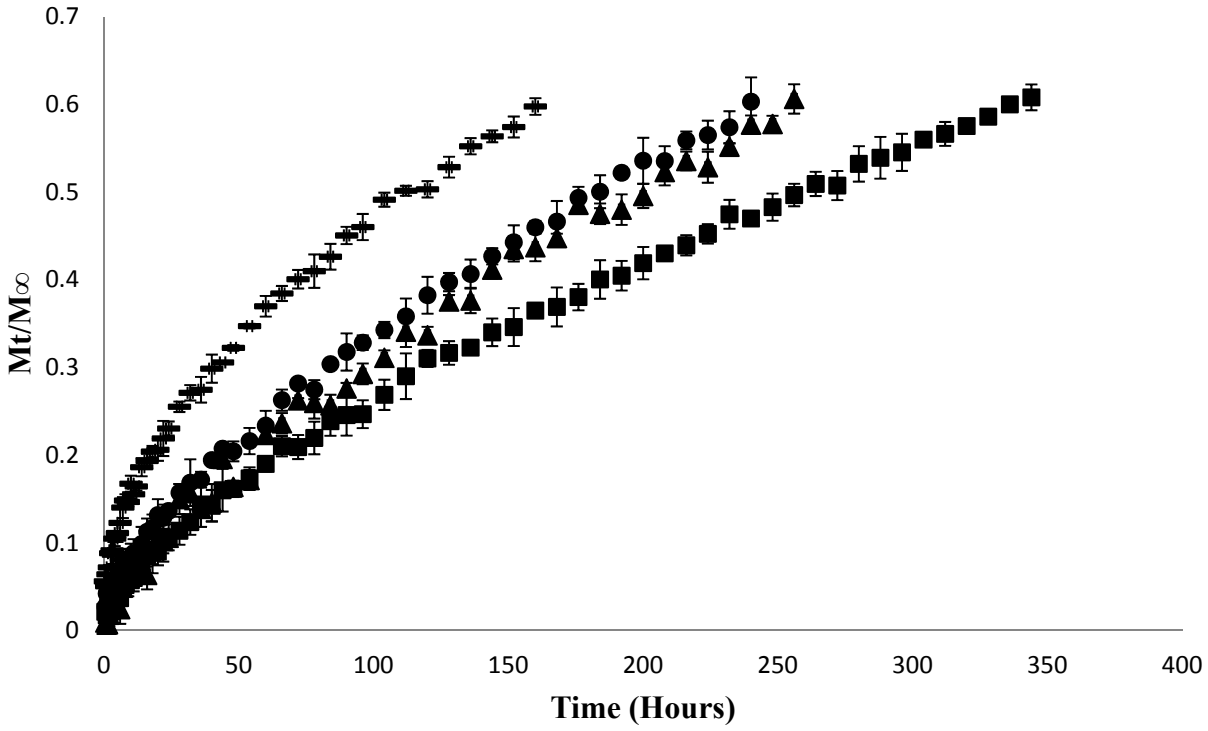

Figure 7.3: Fractional Release of Diclofenac Sodium in DI Water from Imprinted Poly(DEAEM- co-HEMA- co-PEG200DMA) Gels prepared via LRP with varying Concentrations of Crosslinker. Data points represent poly(DEAEM-co-HEMA-co-PEG200DMA) gels prepared with varying concentrations of crosslinker in feed: crosslinker content=1%(▬); crosslinker content=5%(●); crosslinker content=10%(▲); crosslinker content=50%(■).Error bars represent the standard error with n=3.

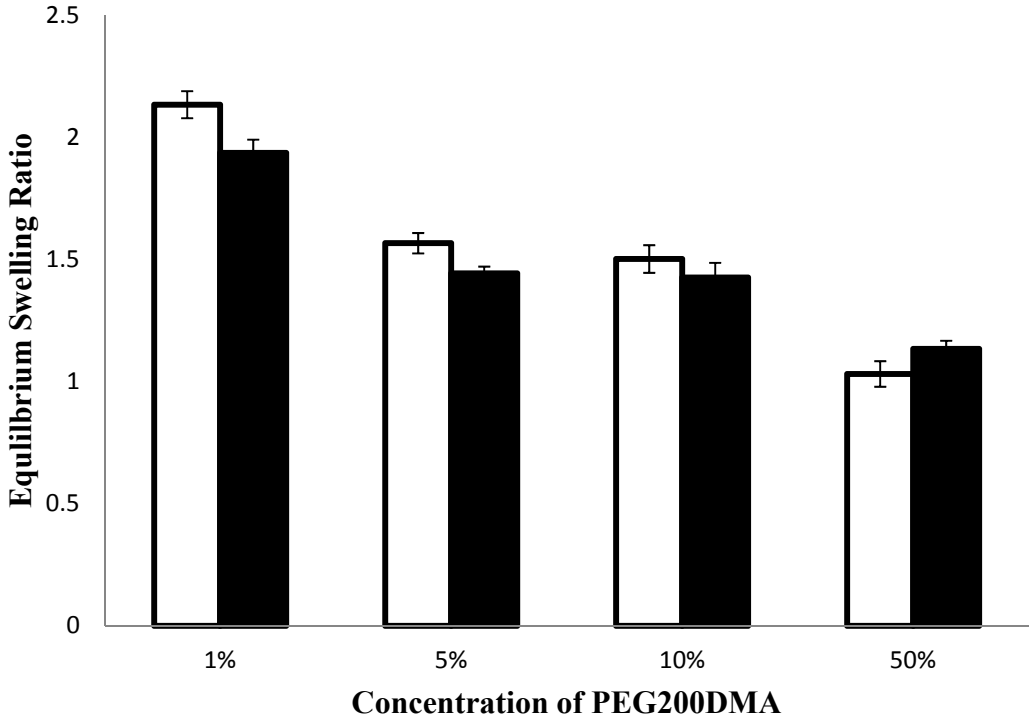

Figure 7.4: Effect of Crosslinking Monomer Concentration on Equilibrium Volume Swelling Ratio of Imprinted Poly(DEAEM- co-HEMA- co-PEG200DMA) Gels prepared via FRP and LRP. Equilibrium volume swelling ratio versus crosslinking monomer concentration for polymers prepared via FRP (□) and LRP (■) are shown here. Error bars represent the standard error with n=3.

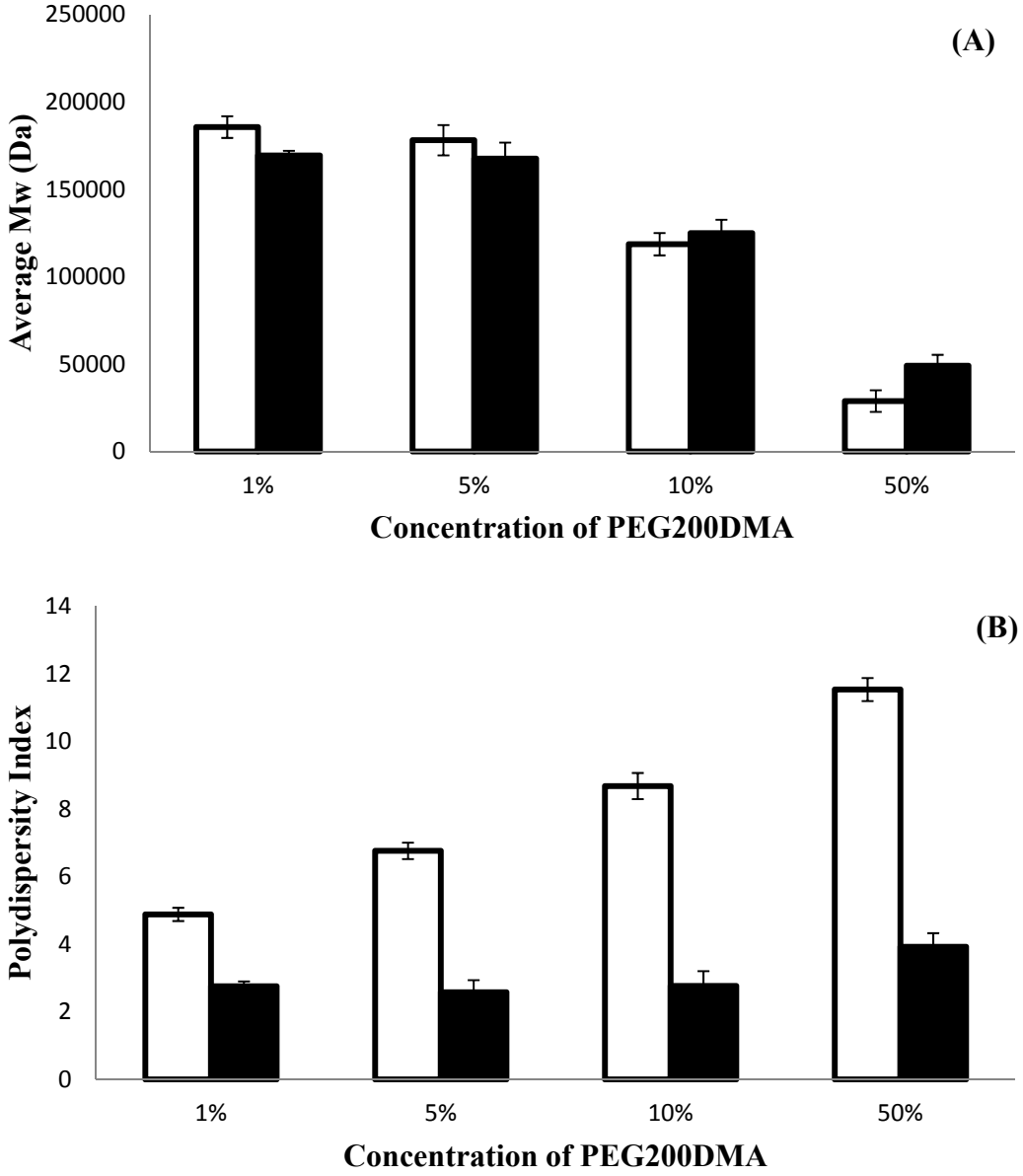

Figure 7.5: Effect of Crosslinking Monomer Concentration on Kinetic Chain Length and Polydispersity Index of Polymer Chains. Weight average molecular weight **(A)** and polydispersity index **(B)** versus functional monomer concentraion for pre-gelation polymers prepared via FRP (□) and LRP (■) are shown here. Error bars represent the standard error with n=3.

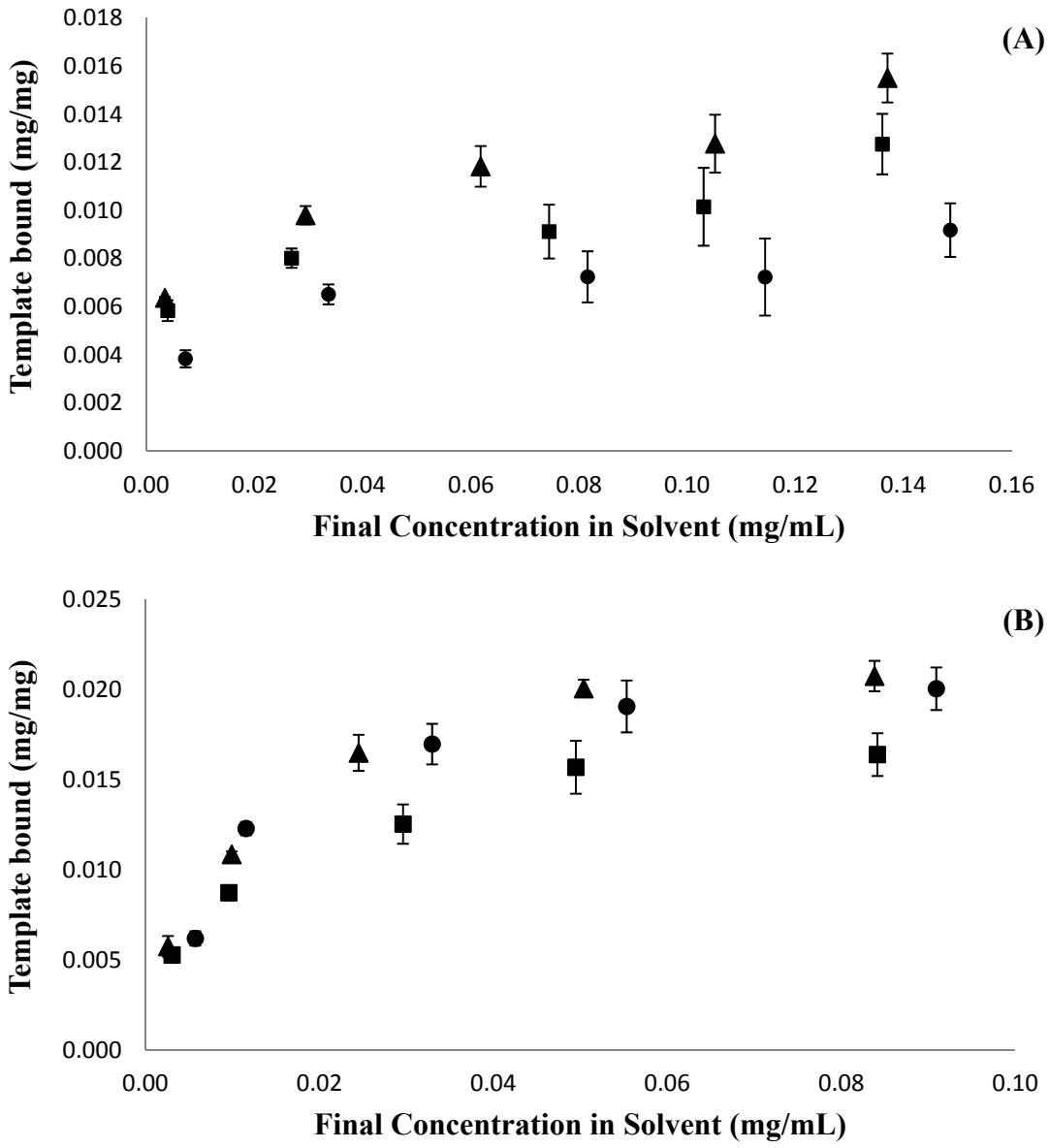

Figure 7.6: Equilibrium Binding Isotherm for Diclofenac Sodium Binding by Imprinted Polymer Gels prepared with Different Crosslinking Monomers via (A) FRP and (B) LRP. Data points represent poly(DEAEM-co-HEMA-co-PEGnDMA) gels prepared with EGDMA (●); PEG200DMA(▲); and PEG400DMA(■) as crosslinking monomers. Error bars represent the standard error with n=3.

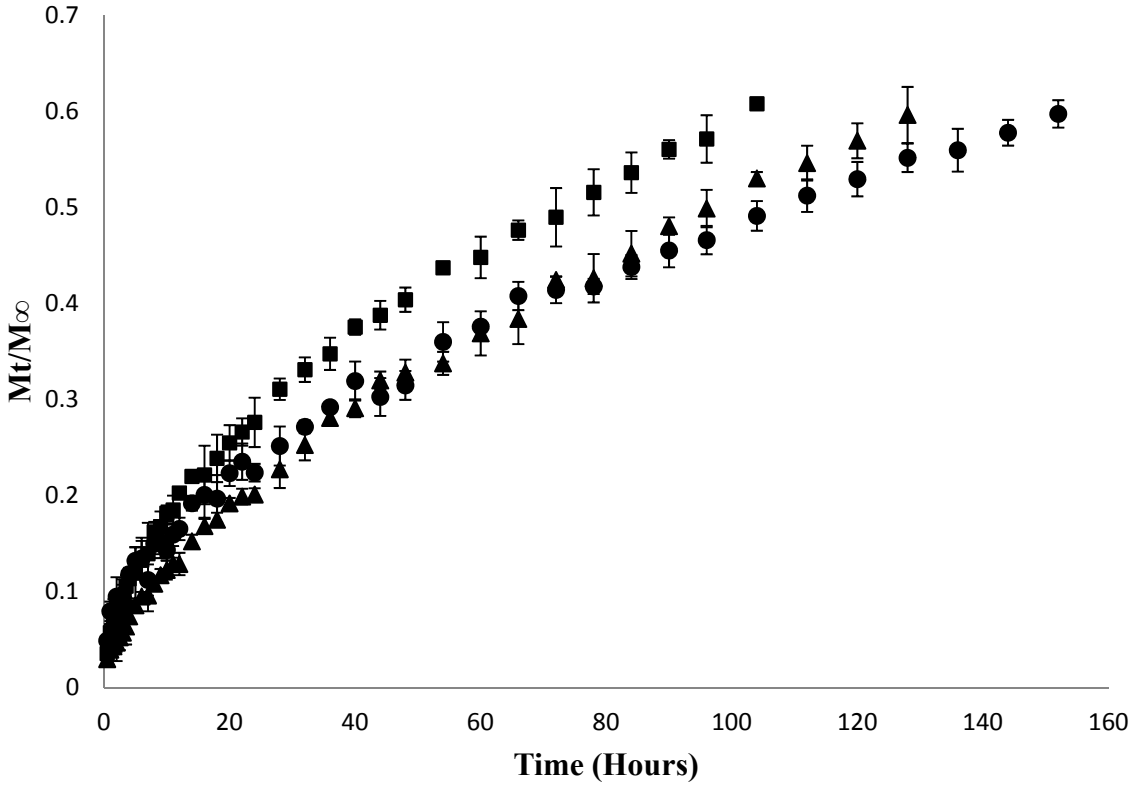

Figure 7.7: Fractional Release of Diclofenac Sodium in DI Water from Imprinted Polymer Gels prepared with Different Crosslinking Monomers via FRP. Data points represent poly(DEAEM-co-HEMA-co-PEGnDMA) gels prepared with EGDMA (●); PEG200DMA(▲); and PEG400DMA(■) as crosslinking monomers. Error bars represent the standard error with n=3.

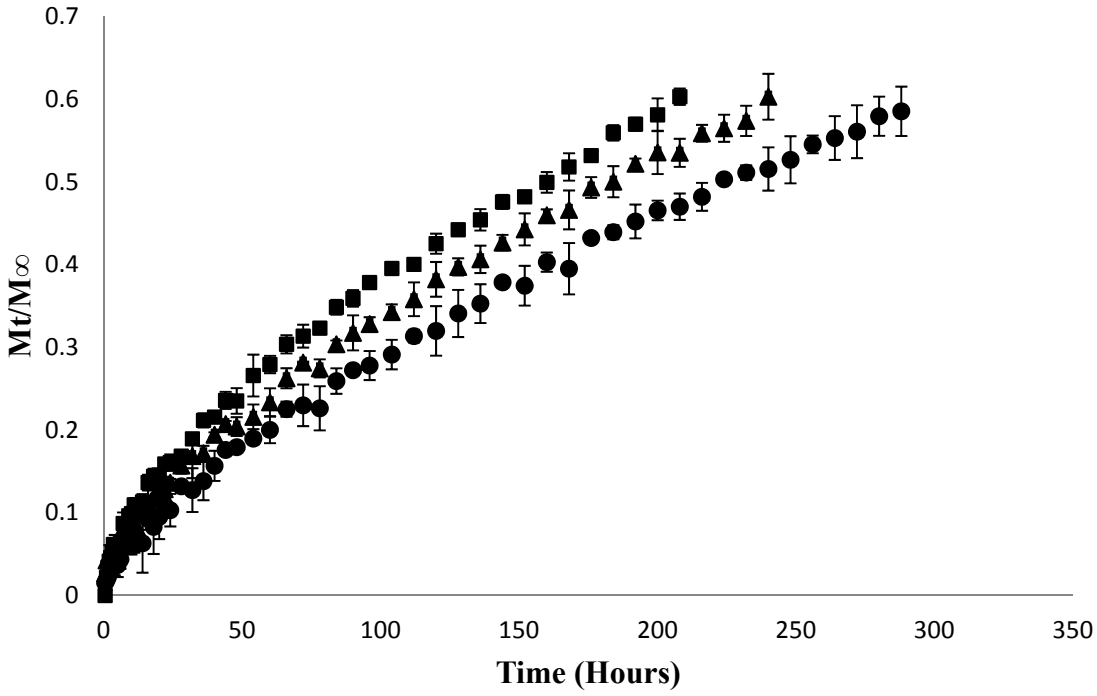

Figure 7.8: Fractional Release of Diclofenac Sodium in DI Water from Imprinted Polymer Gels prepared with Different Crosslinking Monomers via LRP. Data points represent poly(DEAEM-co-HEMA-co-PEGnDMA) gels prepared with EGDMA (●); PEG200DMA(▲); and PEG400DMA(■) as crosslinking monomers. Error bars represent the standard error with n=3.

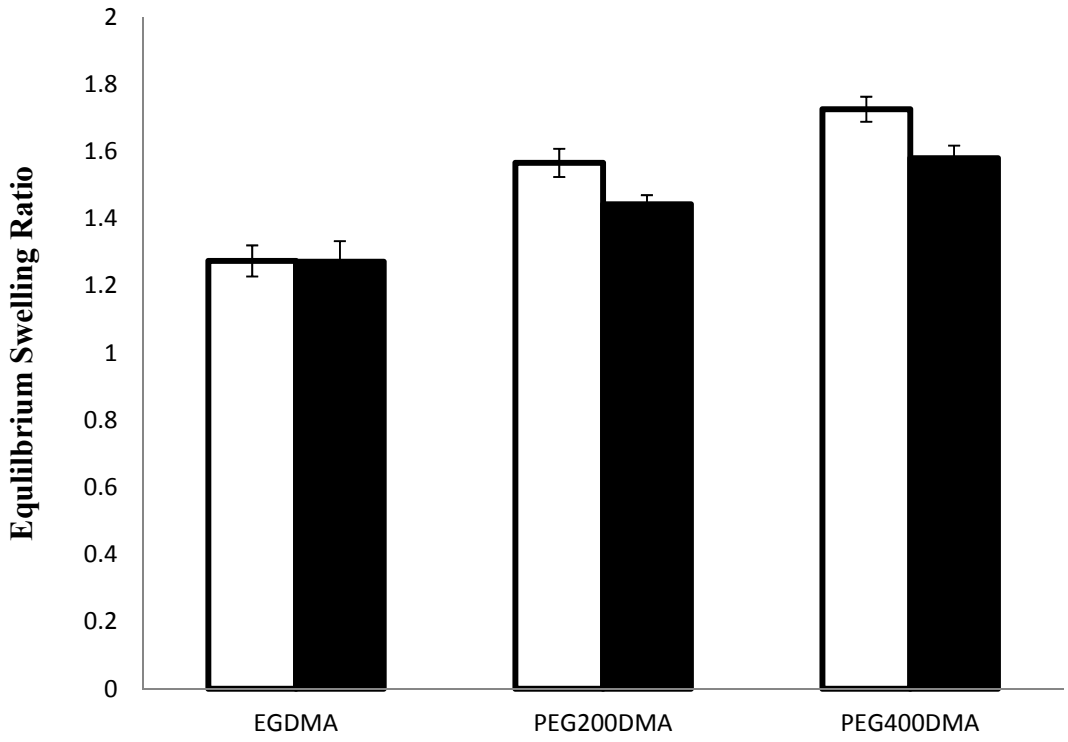

Figure 7.9: Effect of Length of Crosslinking Monomer on Equilibrium Volume Swelling Ratio of Imprinted Poly(DEAEM- co-HEMA- co-PEG200DMA) Gels prepared via FRP and LRP. Equilibrium volume swelling ratio for polymers prepared via FRP (□) and LRP (■) are shown here. Error bars represent the standard error with n=3.

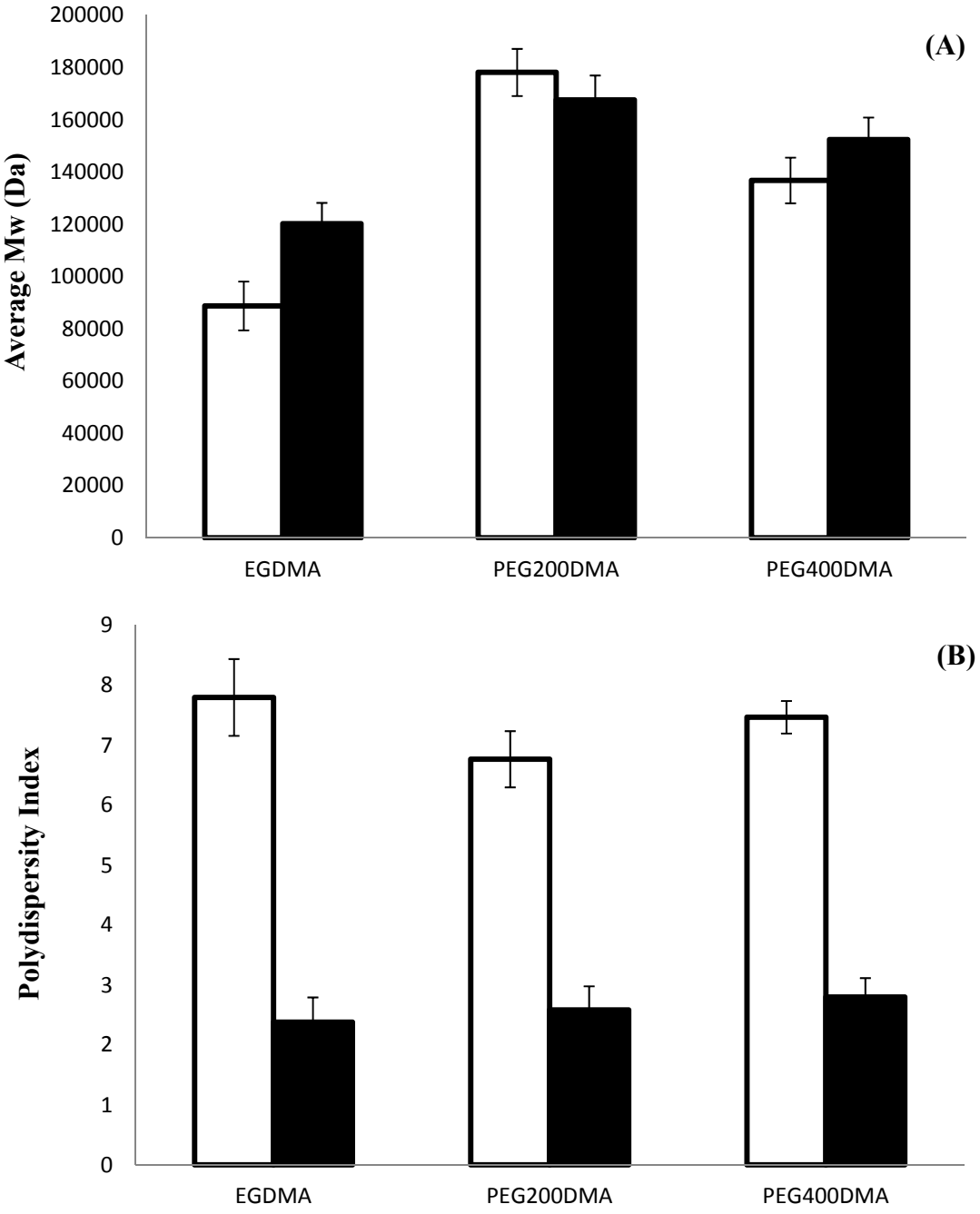

Figure 7.10: Effect of Length of Crosslinking Monomer on Kinetic Chain Length and Polydispersity Index of Polymer Chains. Weight average molecular weight (**A)** and polydispersity index (**B)** for polymers prepared via FRP (□) and LRP (■) are shown here. Error bars represent the standard error with n=3.

CHAPTER 8: CONCLUSIONS

In this work, various poly(hydroxyethyl methacrylate-co-diethylaminoethyl methacrylate-co-poly(ethyleneglycol200) dimethacrylate) (poly(MAA-co-EGDMA)) and poly(hydroxyethyl methacrylate-co-diethylaminoethyl methacrylate-co-poly(ethyleneglycol200) dimethacrylate) (poly(HEMA-co-DEAEM-co-PEG200DMA)) polymers were synthesized by varying feed and reaction parameters. For the first time, the effect of varying different reaction parameters on the polymer network structure as well as polymer chain growth and formation was investigated. Their subsequent effect on the template binding and transport properties of the polymers was also calculated. This work was the first to highlight the improved efficiency of the imprinting process as well as the improvement in polymer network architecture achieved by using living radical polymerization techniques in both highly and weakly crosslinked imprinted polymers.

The use of living radical polymerization (LRP) techniques resulted in quadrupling of the number of binding sites in highly crosslinked imprinted poly(MAA-co-EGDMA) polymers; meanwhile, the number of binding sites in weakly crosslinked imprinted poly(MAA-co-EGDMA) gels was tripled by the use of living radical polymerization techniques. It is important to note that the increased binding capacity demonstrated by both the highly, and weakly crosslinked, imprinted polymers prepared via LRP demonstrated was achieved at similar binding affinities to those of the corresponding imprinted polymers prepared via conventional free radical polymerization (FRP). This ability to create more binding sites without a loss in binding affinity had not been demonstrated previously in imprinted polymers. In addition, by adjusting the

double bond conversion we can choose to increase either the capacity or the affinity in highly crosslinked imprinted polymers, thus, allowing for the first time, the creation of imprinted polymers with tailorable binding parameters. In addition, this work was the first to demonstrate improved imprinting efficiency with the use of LRP over multiple platforms.

Analysis of the polymerization reaction revealed that the observed increase in binding parameters in the highly and weakly crosslinked polymers can be explained by the extension of the reaction-controlled regime during propagation of the macroradical which allows the macroradical more time to achieve a minimal global free energy configuration. The propagation phase in a highly crosslinked system was shown to be extended nearly three times when living radical polymerization was used. For weakly crosslinked system, it was shown that nearly twice the amount of polymer was created in the reaction-controlled regime, when LRP was used. For uncrosslinked systems, LRP allowed the macroradicals more time to grow which compensated for the decrease in chain length and increase in polydispersity caused by the presence of the template. Thus, LRP was shown to have extended propagation in polymerization reactions which subsequently resulted in more monodisperse polymer chains and more homogenous polymer networks. This work was the first to demonstrate the effect of template molecules on polymer chain growth as well as the use of LRP in minimizing the heterogeneity introduced by the presence of template molecules.

Next, the effects of varying reaction parameters which affect monomer-template interaction on the structure of imprinted gels and subsequently their drug binding and transport properties was examined. It was found that higher template concentrations resulted in increased drug loading and delayed fractional release. Increase in the concentration of functional monomer showed a similar trend but the magnitude of the increase was significantly higher. It was also

found that the presence of solvent during polymerization resulted in higher template loading. However, template release from these gels was also much faster which may be attributed to increased porosity in the gels. It was also found that living radical polymerization resulted in improved efficiency of imprinting in weakly crosslinked poly(HEMA-co-DEAEM-co-PEG200DMA) gels. All imprinted poly(HEMA-co-DEAEM-co-PEG200DMA) gels prepared via LRP demonstrated significantly higher drug binding as well as slower drug release rates. It was shown that, the use of LRP had a more significant impact than any other reaction parameter. Analysis of the polymerization reaction revealed that the observed improvement in binding and transport parameters in the weakly crosslinked polymer gels could be explained by the extension of the reaction-controlled regime during propagation of the macroradical which allowed the system to achieve a minimal global free energy configuration. This resulted in shorter more monodisperse polymer chains forming the network which were hypothesized to result in more homogenous networks.

Lastly, the effects of crosslinker diversity on the structure of imprinted gels and subsequently their drug binding and transport properties were examined. It was found that an increase in the extent of crosslinking resulted in a decrease in the template binding capacity and release rate of template from the polymer gels. This corresponded with lower equilibrium swelling ratios and smaller mesh sizes of the solvated polymer gels. In addition, a decrease in the kinetic chain length of the polymers pre-gelation as well as an increase in their PDI was observed. This may be explained by an early transition to gelation during polymerization. Increase in the length of the crosslinker resulted in decreased binding affinity and faster release of template from polymer which corresponded with increased equilibrium swelling ratios. All polymer gels prepared via LRP demonstrate higher binding capacity as well as affinity when compared with the

corresponding polymers prepared via FRP. The use of LRP also resulted in significantly decreased fractional release rates with the extent of delayed release increasing as crosslinker concentration was increased. The use of LRP also resulted in lower equilibrium swelling ratios and smaller mesh sizes of solvated gels. This combined with the observed decrease in the PDI of pre-gelation polymers may indicate better homogeneity in the crosslinking structure of polymers prepared via LRP. This was the first time the effects of crosslinker diversity in imprinted gels prepared via LRP have been demonstrated.

In conclusion, the use of living radical polymerization in the formation of molecularly imprinted polymers was shown to result in significant improvement in the binding and transport properties of the resulting polymers due to improved network architecture of the molecularly imprinted polymers. In addition, the use of living radical polymerization techniques was demonstrated to result in improved morphology and decreased dead polymer regions in crosslinked polymer networks by controlling polymer chain growth. Also, the ability of interacting species, like solvents and template molecules, to alter the polymerization reaction and, as a result, polymer properties was highlighted. Lastly, this work highlights the potential for achieving better control of polymer properties in molecularly imprinted polymers. These developments will contribute to the ability to rationally design imprinted polymers in order to tailor their binding and transport properties. In addition, the demonstrated improvement in polymer network morphology will lead to progress in creating polymeric materials with finely controlled architecture as well as novel commercial polymer products in the future.

APPENDICES

Appendix A

Appendix A is a supplementary data set that was related to the work in the dissertation. The data presented here was obtained as a result of experiments carried out during the course of the doctoral work but was not included in the body of the dissertation.

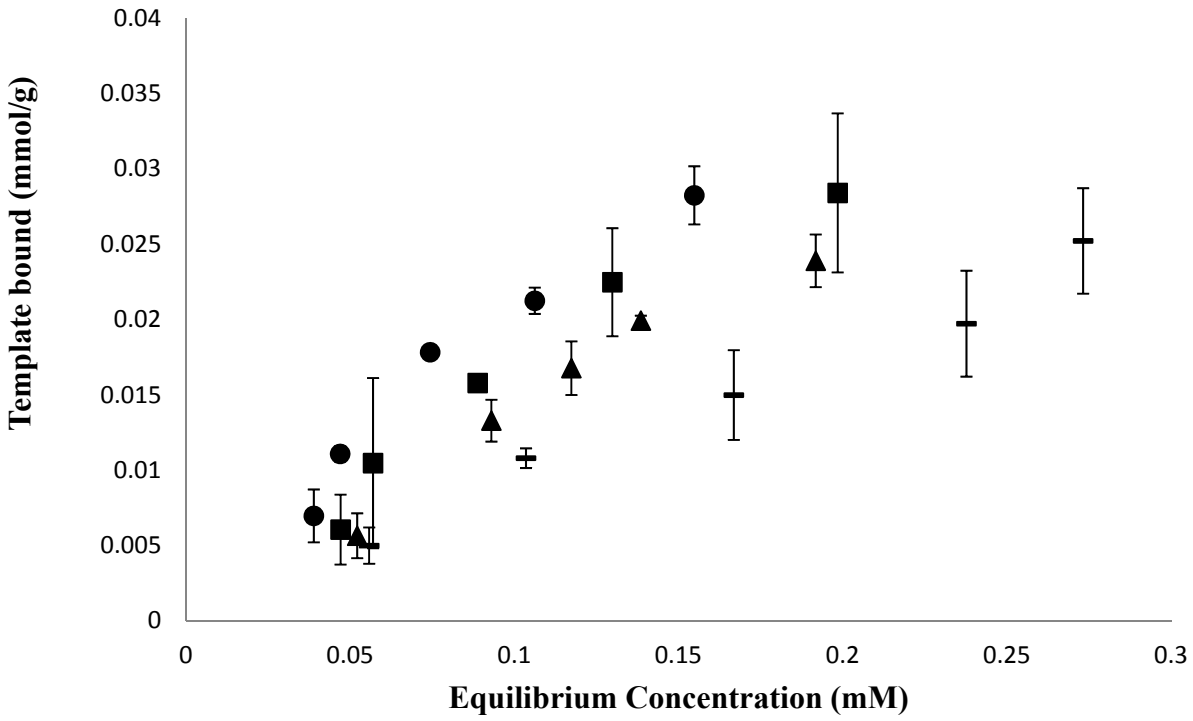

Figure A.1: Equilibrium Binding Isotherm Comparison of Weakly Crosslinked Diclofenac Sodium Imprinted Poly(MAA-co-EGDMA) Gels prepared via Conventional Free Radical Polymerization. Data points represent poly(MAA-co-EGDMA) gels prepared with varying T/M ratios: T/M=0(▬); T/M=0.002(●); T/M=0.005(▲); T/M=0.02(■).
Error bars represent the standard error with n=3.

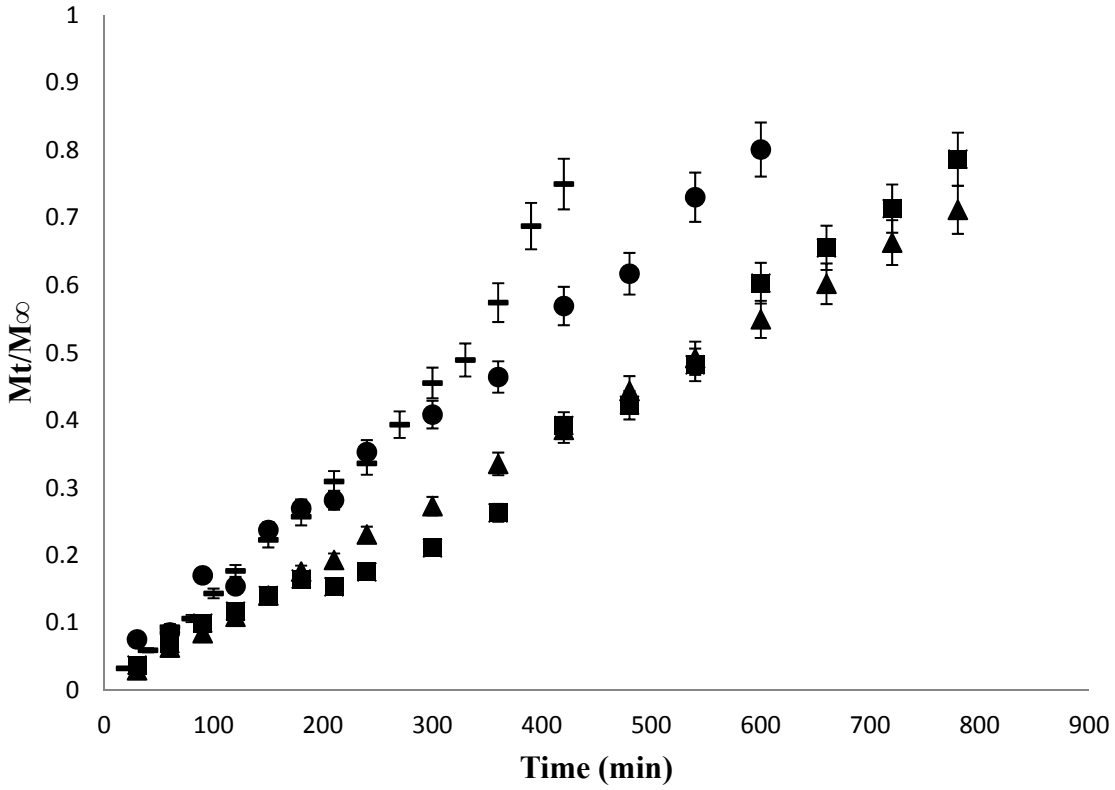

Figure A.2: Comparison of Fractional Release of Diclofenac Sodium in Buffer Solution from Various Weakly Crosslinked Diclofenac Sodium Imprinted Poly(DEAEM-HEMA-PEG200DMA) Gels prepared via Conventional Free Radical Polymerization. Data points represent poly(DEAEM-co-HEMA-co-PEG200DMA) gels prepared with varying T/M ratios: T/M=0(—); T/M=0.1(●); T/M=0.3(▲); T/M=0.5(■).The buffer solution was prepared with 6.78 g/L NaCl, 2.18 g/L NaHCO3, 1.38 g/L KCl, and 0.084 g/L CaCl2_2H2O, and the pH was 8.0. Error bars represent the standard error with n=3.

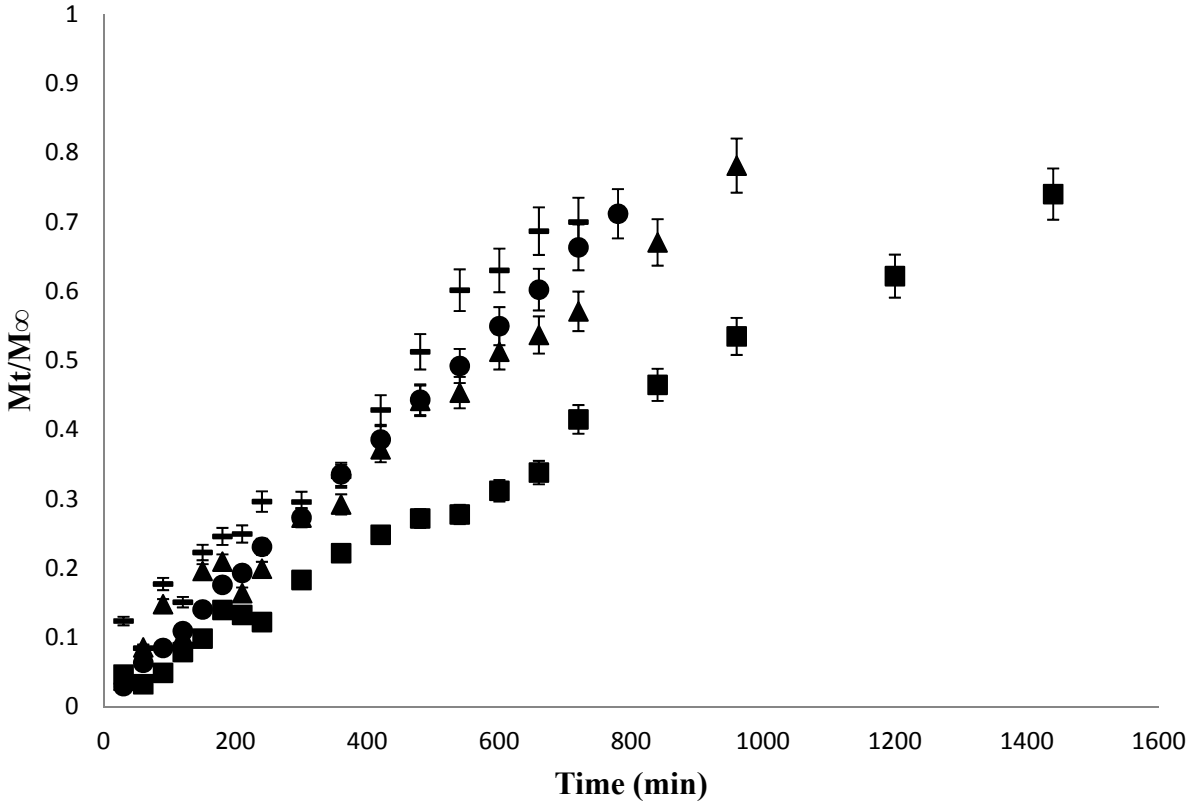

Figure A.3: Comparison of Fractional Release of Diclofenac Sodium in Buffer Solution from Various Weakly Crosslinked Diclofenac Sodium Imprinted Poly(DEAEM-co-HEMA-co-PEG200DMA) Gels prepared via Living Radical Polymerization. Data points represent poly(DEAEM-co-HEMA-co-PEG200DMA) gels prepared with varying T/M ratios: T/M=0(▬); T/M=0.1(●); T/M=0.3(▲); T/M=0.5(■).The buffer solution was prepared with 6.78 g/L NaCl, 2.18 g/L NaHCO3, 1.38 g/L KCl, and 0.084 g/L CaCl2_2H2O, and the pH was 8.0. Error bars represent the standard error with n=3.

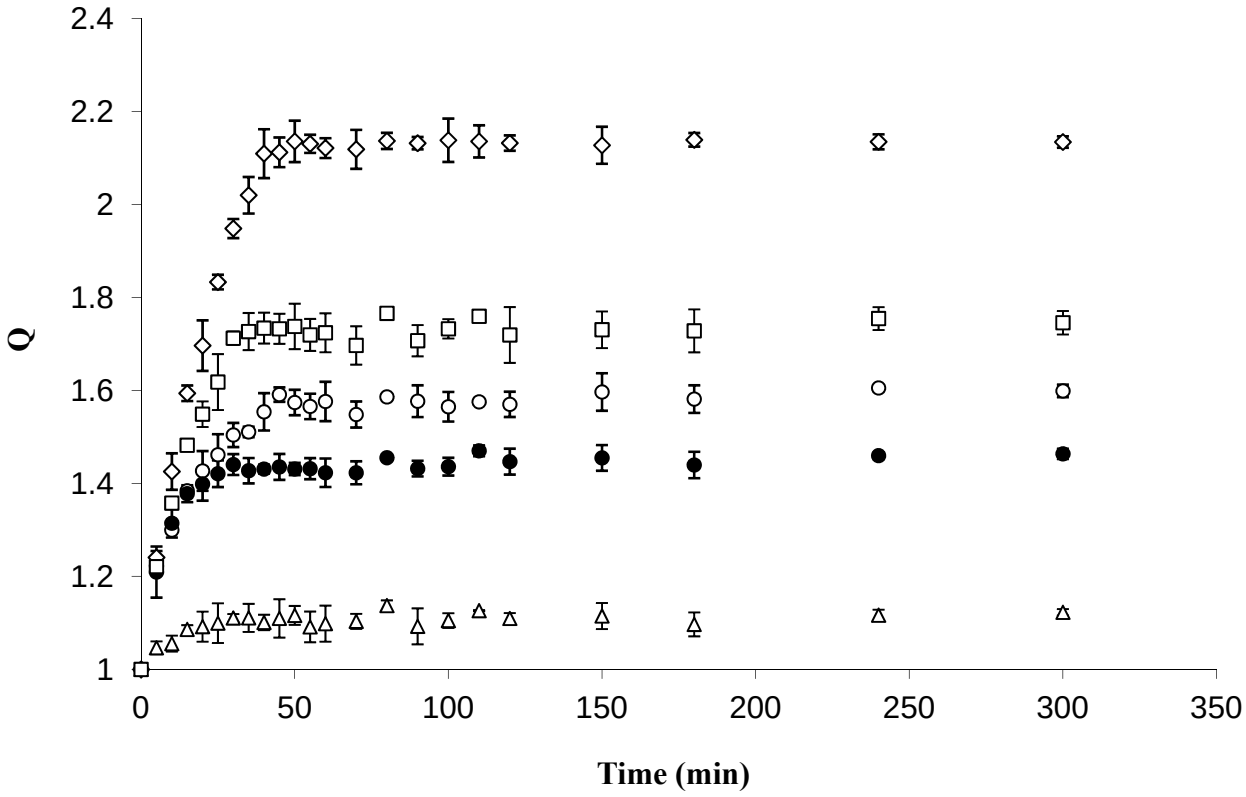

Figure A.4: Comparison of Dynamic Volume Swelling Ratios of Various Crosslinked Diclofenac Imprinted Polymer Gels. Data points represent poly(DEAEM-co-HEMA-co-PEG200DMA) gels prepared via FRP with varying crosslinkers: 1% PEG200DMA (◊); 5% PEG200DMA (○); 50% PEG200DMA (Δ); 5% PEG400DMA (□). Poly(DEAEM-co-HEMA-co-PEG200DMA) gels prepared via LRP with 5% PEG200DMA are represented by (●). Error bars represent the standard error with n=3.

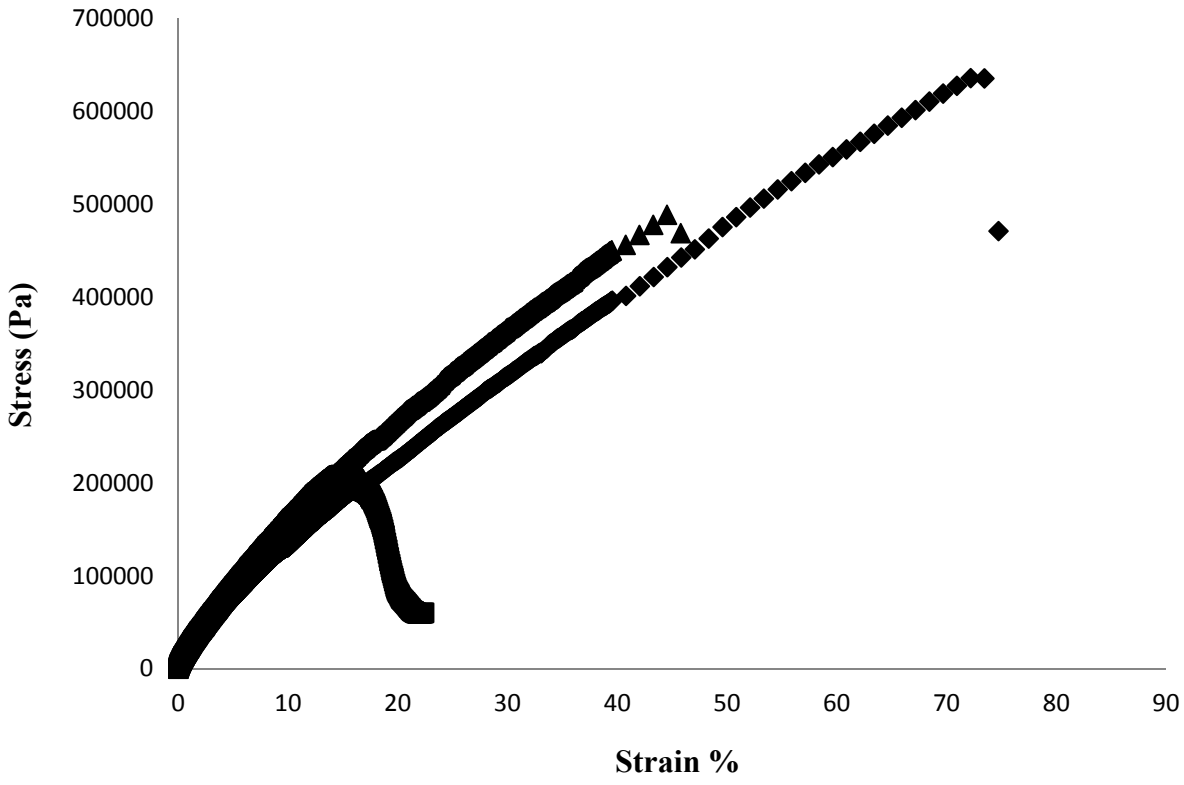

Figure A.5: Raw Stress Vs Strain Data for three poly(DEAEM-co-HEMA-co-PEG200DMA) gels prepared via FRP with 1% PEG200DMA in pre-polymerization solution.

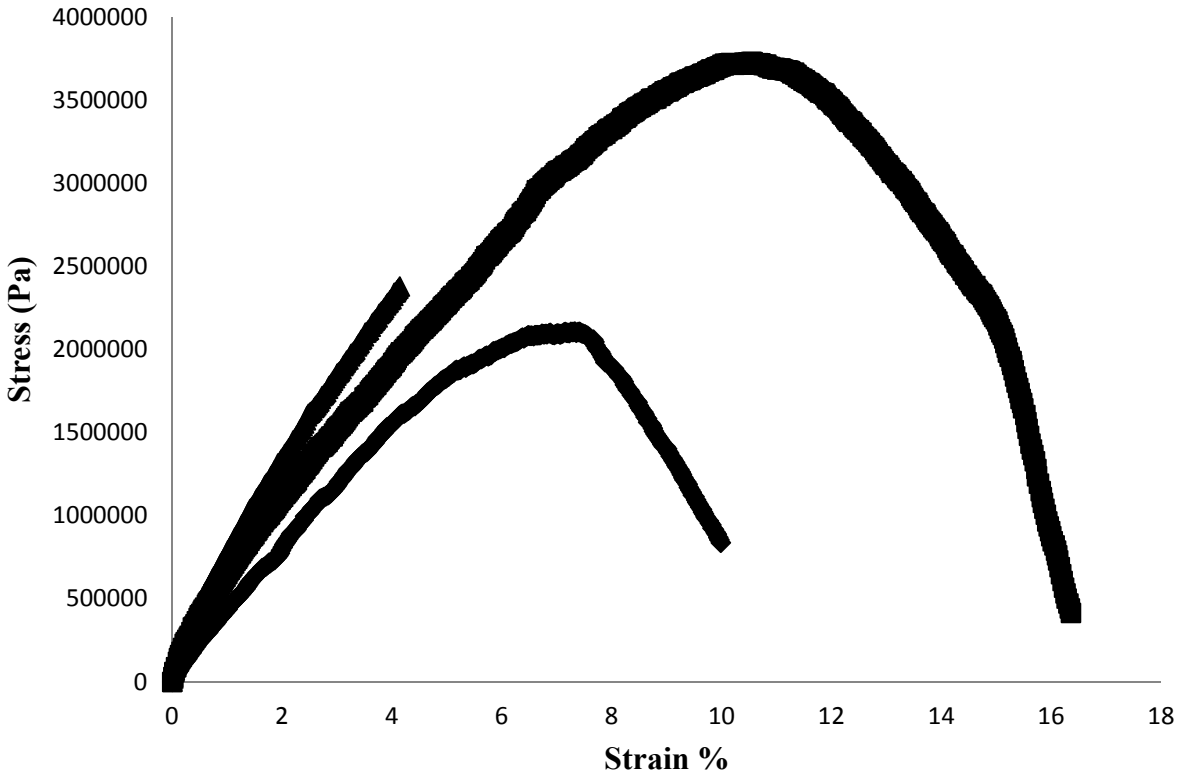

Figure A.6: Raw Stress Vs Strain Data for three poly(DEAEM-co-HEMA-co-PEG200DMA) gels prepared via FRP with 5% PEG200DMA in pre-polymerization solution.

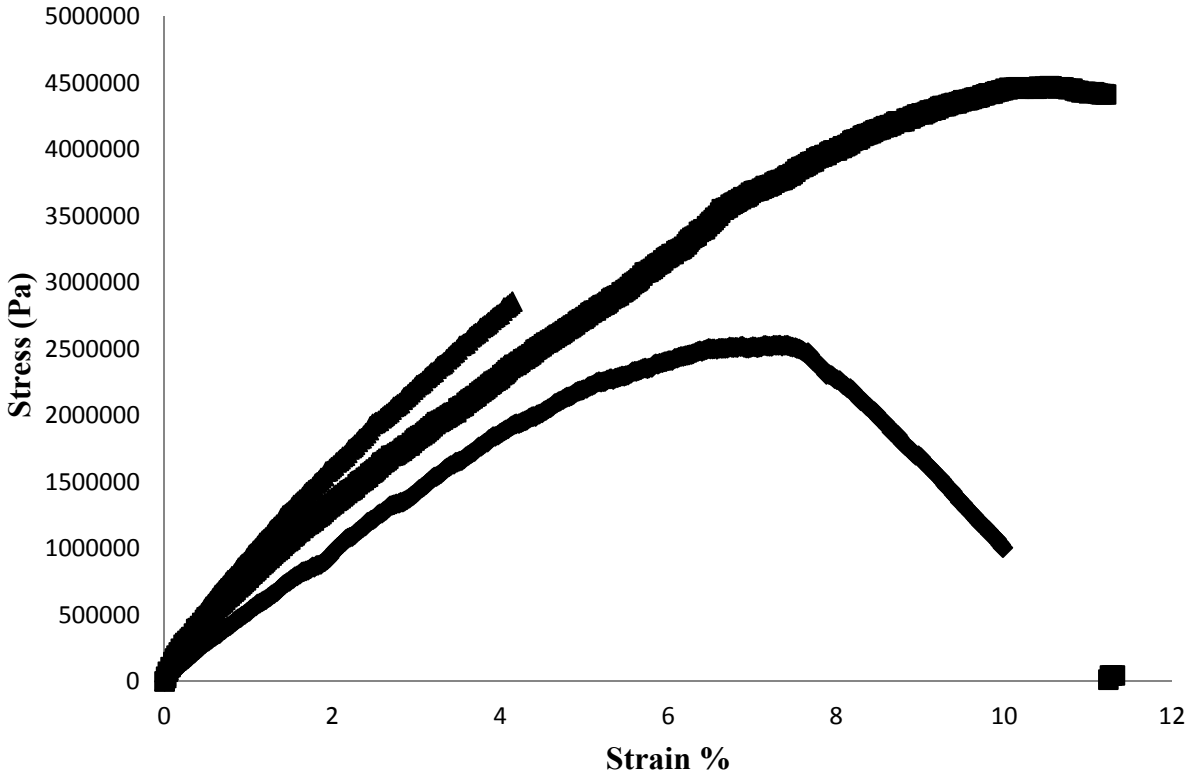

Figure A.7: Raw Stress Vs Strain Data for three poly(DEAEM-co-HEMA-co-PEG200DMA) gels prepared via FRP with 10% PEG200DMA in pre-polymerization solution.

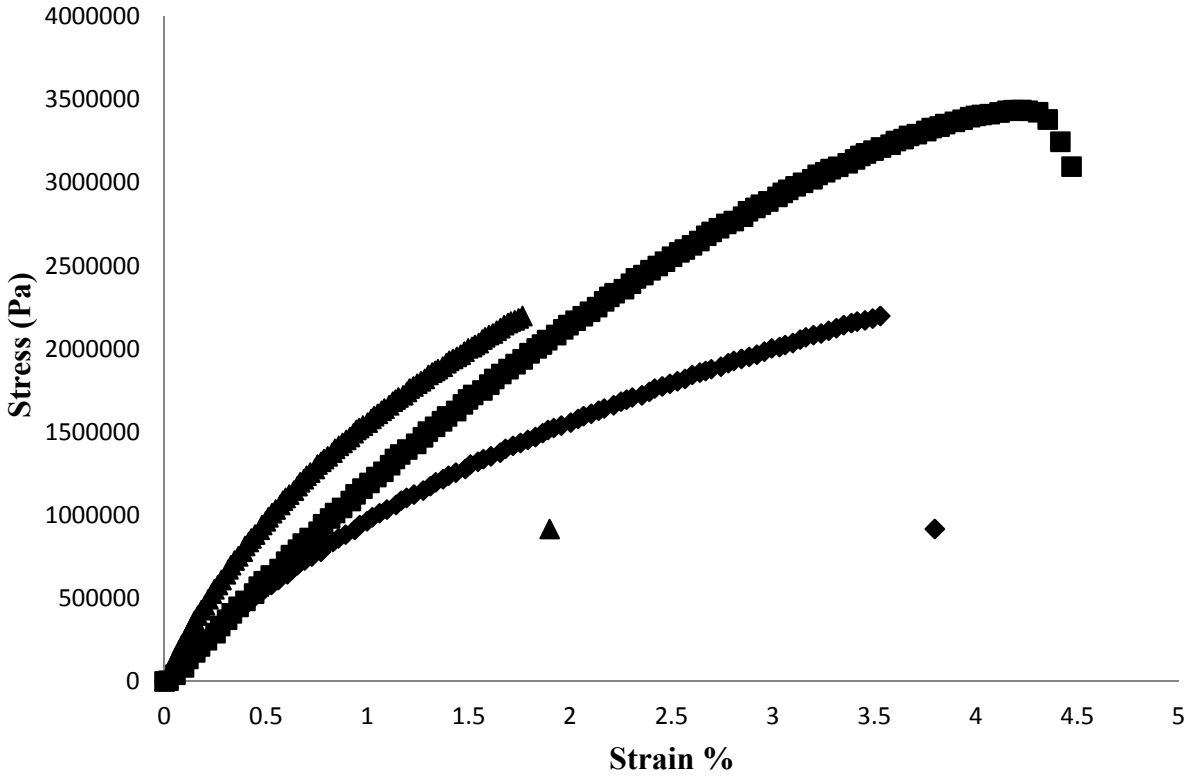

Figure A.8: Raw Stress Vs Strain Data for three poly(DEAEM-co-HEMA-co-PEG200DMA) gels prepared via FRP with 50% PEG200DMA in pre-polymerization solution.

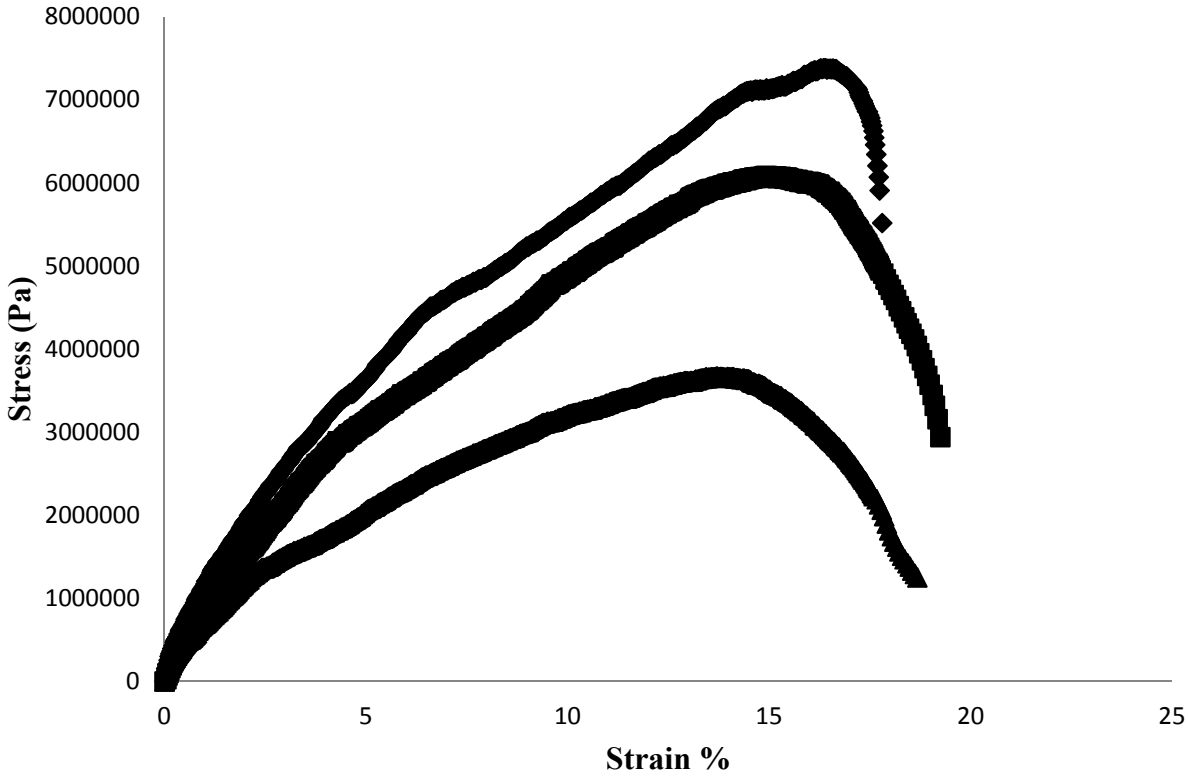

Figure A.9: Raw Stress Vs Strain Data for three poly(DEAEM-co-HEMA-co-PEG200DMA) gels prepared via FRP with 5% EGDMA in pre-polymerization solution.

Figure A.10: Raw Stress Vs Strain Data for three poly(DEAEM-co-HEMA-co-PEG200DMA) gels prepared via FRP with 5% EGDMA in pre-polymerization solution.

Appendix B

In appendix B, the Visual Basic code developed for the calculation of double bond conversion is presented. The Visual Basic code was used to analyze all recognitive polymers presented within this dissertation. The program name is "SAE". The program was designed and developed for the express purpose of analysis of the data obtained from the DPC.

B.1 Program Setup

Procedure for the analysis is in chronological order. Open an Excel workbook containing the Visual Basic program presented in this appendix, press "CTRL-S" to set up the spreadsheet. Second data from the differential photo calorimeter is taken from the Universal Analysis program (TA Instruments, New Castle, DE) and pasted into the first three columns under the cells labeled, Time (sec), Temperature (°C), and Heat Flow (W/g). Third the theoretical heat of reaction must be placed in the cell below the labeled cell heat of reaction, and the average molecular weight of the solution must be placed in the cell below the average molecular weight. It is important to note if any sudden drops in data are observed a correction factor of the exact amount of the drop (10 W/g etc determined from the heat flow just before the drop subtracting the heat flow just after the drop) must be added to the program under the cell light intensity correction. The analysis of the data is done by pressing "CTRL-A". The program to set up and analyze for kinetic parameters is "CTRL-E". Before pressing "CTRL-E", data must be placed within the cells below Delta Time, which is the time after the peak of the reaction for analysis (it normally takes 25 sec for the rate to come to equilibrium after the light shut off time) and Light Shutoff Time (min) which is the time the light is shut off after the beginning of the data collection, respectively. Graphs of the data can be made by pressing "CTRL-G" after the data is analyzed.

B.2 Program Code for "SAE"

```
Sub Setup()
' Setup Macro
" Keyboard Shortcut: Ctrl+s
' Cells.Select
    With Selection
        .HorizontalAlignment = xlGeneral
        .VerticalAlignment = xlBottom
        .WrapText = True
        .Orientation = 0
        .AddIndent = False
        .IndentLevel = 0
        .ShrinkToFit = False
        .ReadingOrder = xlContext
        .MergeCells = False
    End With
    With Selection.Font
        .Name = "Arial"
        .FontStyle = "Regular"
        .Size = 8
        .Strikethrough = False
        .Superscript = False
        .Subscript = False
        .OutlineFont = False
        .Shadow = False
        .Underline = xlUnderlineStyleNone
        .ColorIndex = xlAutomatic
    End With
    Selection.Rows.AutoFit
    Selection.Columns.AutoFit
Cells(1, 1) = "Heat of Reaction J/mole"
Cells(1, 2) = "MW avg"
Cells(1, 3) = "Intensity Heat Flow W/g"
Cells(1, 4) = "Rp Max (sec-1)"
Cells(1, 5) = "Final Conversion"
Cells(1, 6) = "Temperature ( °C)"
Cells(1, 7) = "TimeRpmax"
Cells(1, 8) = "Conversion RpMax"
Cells(1, 9) = "program kmax"
Cells(1, 10) = "Total Polymerization Time (min)"
Cells(1, 11) = "kmax override"
Cells(1, 12) = "Total  Time Data Taken (sec)"
Cells(1, 13) = "Time for Kinetic Time Analysis (min) "
Cells(1, 14) = "Light Intesity Correction"
Cells(3, 1) = "Time (sec)"
Cells(3, 2) = "Temperature (°C)"
```

```
Cells(3, 3) = "Heat Flow (W/g)"
Cells(3, 4) = "Actual Heat Flow (W/g)"
Cells(3, 5) = "Rp (sec-1)"
Cells(3, 6) = "Time"
Cells(3, 7) = "Conversion"
Cells(3, 9) = "rpsum"
Cells(3, 12) = "rp initial"
Cells(3, 13) = "rp final"
Cells(11, 10) = "Kinetic Rp Max (sec-1)"
Cells(11, 11) = "Kinetic Final Converion"
Cells(11, 12) = "Temperature (°C)"
Cells(11, 13) = "Kinetic Time Rpmax"
Cells(11, 14) = "Kinetic Conversion RpMax"
End Sub
Sub Analyze()
' Analyze Macro
' Keyboard Shortcut: Ctrl+a
Dim x As Double
Dim y As Double
Dim z As Double
Dim i As Double
Dim j As Double
Dim k As Double
Dim time As Double
Dim temp As Double
Dim heatflow As Double
Dim avgmw As Double
Dim heatofreaction As Double
Dim lightintensity As Double
Dim rp As Double
Dim rpnew As Double
Dim correctedheatflow As Double
Dim hf As Double
Dim hfnew As Double
Dim rpold As Double
Dim kmax As Double
Dim rpinitial As Double
Dim rpfinal As Double
Dim rpsum As Double
Dim conversion As Double
Dim finalconversion As Double
Dim rpmax As Double
Dim rpmaxold As Double
Dim rpmaxnew As Double
Dim polyrxtime As Double
Dim kmaxoveride As Double
```

```
Dim timerpmax As Double
Dim initialdatapoint As Double
Dim finaldatapoint As Double
Dim numberofpoints As Double
Dim conversionrpmax As Double
Dim lightintensitycorrection As Double
Dim ii As Double
lightintensitycorrection = Cells(2, 14)
ii = 4
Do While Cells(ii, 1) > 0
initialdatapoint = Cells(4, 1)
finaldatapoint = Cells(ii, 1)
ii = ii + 1
Loop
 numberofpoints = ii - 4
heatofreaction = Cells(2, 1)
avgmw = Cells(2, 2)
kmax = numberofpoints
lightintensity = Cells(kmax, 3)
Cells(2, 3) = lightintensity
Cells(2, 9) = kmax
i = 4
j = 1
k = 0
time = 0
rp = 0
rpnew = 0
hf = 0
hfnew = 0
rpinitial = 0
rpfinal = 0
rpsum = 0
rpmax = 0
rpold = 0
rpmaxold = 0
rpmaxnew = 0
timerpmax = 0
temp = Cells(3000, 2)
Cells(2, 6) = temp
converionrpmax = 0
Do While k < kmax
hfnew = Cells(i, 3) - (lightintensity + lightintensitycorrection)
If hfnew < 0 Then Cells(i, 4) = hf
If hfnew > 0 Then hf = hfnew
Cells(i, 4) = hf
rpold = rp
```

```
rpnew = Cells(i, 4) * avgmw / heatofreaction
If rpnew < 0 Then rp = rp
If rpnew > 0 Then rp = rpnew
Cells(i, 5) = rp
Cells(i, 6) = time
If rp = rpold Then time = time
If rp > rpold Then time = time + 0.2
If rp < rpold Then time = time + 0.2
If time = 0.2 Then rpinitial = rp
Cells(4, 12) = rpinitial
rpfinal = rp
Cells(4, 13) = rpfinal
rpsum = rpsum + rp
Cells(i, 9) = rpsum
i = i + 1
k = k + 1
Loop
k = 0
i = 4
Do While (k < kmax)
If Cells(i, 6) = 0 Then conversion = 0
If Cells(i, 6) > 0 Then conversion = (time * (rpinitial + rpfinal + 2 * Cells(i, 9))) / (time * 2 *
5)
Cells(i, 7) = conversion
finalconversion = conversion
Cells(2, 5) = finalconversion
k = k + 1
i = i + 1
Loop
k = 0
i = 4
Do While (k < kmax)
rpmaxnew = Cells(i, 5)
If rpmaxnew > rpmax Then rpmax = rpmaxnew
If rpmaxnew < rpmax Then rpmax = rpmax
If rpmaxnew = rpmax Then rpmax = rpmax
Cells(2, 4) = rpmax
i = i + 1
k = k + 1
Loop
i = 4
k = 0
Do While k < kmax
rpmaxnew = Cells(i, 5)
If rpmaxnew = rpmax Then timerpmax = Cells(i, 6)
Cells(2, 7) = timerpmax
```

```
If rpmaxnew = rpmax Then conversionrpmax = Cells(i, 7)
Cells(2, 8) = conversionrpmax
i = i + 1
k = k + 1
Loop
'kinetic section'
        Dim kmaxoverride As Double
        Dim kineticconversion As Double
        kmaxoverride = Cells(2, 13) * 60 * 5
        Cells(2, 11) = kmaxoverride
        i = 4
        k = 0
        rpmaxnew = 0
        rpmax = 0
        kineticconversion = 0
        Cells(12, 12) = temp
        Do While (k < kmaxoverride)
        rpmaxnew = Cells(i, 5)
        If rpmaxnew > rpmax Then rpmax = rpmaxnew
        If rpmaxnew < rpmax Then rpmax = rpmax
        If rpmaxnew = rpmax Then rpmax = rpmax
        Cells(12, 10) = rpmax
        i = i + 1
        k = k + 1
        Loop
        i = 4
        k = 0
        Do While k < kmaxoverride
        rpmaxnew = Cells(i, 5)
        If rpmaxnew = rpmax Then timerpmax = Cells(i, 6)
        Cells(12, 13) = timerpmax
        If rpmaxnew = rpmax Then conversionrpmax = Cells(i, 7)
        Cells(12, 14) = conversionrpmax
        kineticconversion = Cells(i, 7)
        Cells(12, 11) = kineticconversion
        i = i + 1
        k = k + 1
        Loop
        Rows("14:14").RowHeight = 60
    Range("J14").Select
    ActiveCell.FormulaR1C1 = "Rp at Light"
    With ActiveCell.Characters(Start:=1, Length:=11).Font
        .Name = "Arial"
        .FontStyle = "Regular"
        .Size = 8
        .Strikethrough = False
```

```
    .Superscript = False
    .Subscript = False
    .OutlineFont = False
    .Shadow = False
    .Underline = xlUnderlineStyleNone
    .ColorIndex = xlAutomatic
End With
Range("J14").Select
ActiveCell.FormulaR1C1 = "Rp at Light Shutdown"
With ActiveCell.Characters(Start:=1, Length:=20).Font
    .Name = "Arial"
    .FontStyle = "Regular"
    .Size = 8
    .Strikethrough = False
    .Superscript = False
    .Subscript = False
    .OutlineFont = False
    .Shadow = False
    .Underline = xlUnderlineStyleNone
    .ColorIndex = xlAutomatic
End With
Range("K14").Select
ActiveCell.FormulaR1C1 = "Rp at Light Shutdown plus deltatime"
With ActiveCell.Characters(Start:=1, Length:=32).Font
    .Name = "Arial"
    .FontStyle = "Regular"
    .Size = 8
    .Strikethrough = False
    .Superscript = False
    .Subscript = False
    .OutlineFont = False
    .Shadow = False
    .Underline = xlUnderlineStyleNone
    .ColorIndex = xlAutomatic
End With
Range("L14").Select
ActiveCell.FormulaR1C1 = "Conversion at light shutdown"
With ActiveCell.Characters(Start:=1, Length:=28).Font
    .Name = "Arial"
    .FontStyle = "Regular"
    .Size = 8
    .Strikethrough = False
    .Superscript = False
    .Subscript = False
    .OutlineFont = False
    .Shadow = False
```

```
    .Underline = xlUnderlineStyleNone
    .ColorIndex = xlAutomatic
End With
Range("M14").Select
ActiveCell.FormulaR1C1 = "Conversion at Light shutdown plus deltatime"
With ActiveCell.Characters(Start:=1, Length:=40).Font
    .Name = "Arial"
    .FontStyle = "Regular"
    .Size = 8
    .Strikethrough = False
    .Superscript = False
    .Subscript = False
    .OutlineFont = False
    .Shadow = False
    .Underline = xlUnderlineStyleNone
    .ColorIndex = xlAutomatic
End With
Range("N14").Select
ActiveCell.FormulaR1C1 = "Delta time sec"
With ActiveCell.Characters(Start:=1, Length:=10).Font
    .Name = "Arial"
    .FontStyle = "Regular"
    .Size = 8
    .Strikethrough = False
    .Superscript = False
    .Subscript = False
    .OutlineFont = False
    .Shadow = False
    .Underline = xlUnderlineStyleNone
    .ColorIndex = xlAutomatic
End With
Range("o14").Select
ActiveCell.FormulaR1C1 = "Light Shutoff time min"
With ActiveCell.Characters(Start:=1, Length:=10).Font
    .Name = "Arial"
    .FontStyle = "Regular"
    .Size = 8
    .Strikethrough = False
    .Superscript = False
    .Subscript = False
    .OutlineFont = False
    .Shadow = False
    .Underline = xlUnderlineStyleNone
    .ColorIndex = xlAutomatic
End With
Range("J15").Select
```

```
Range("P1").Select
ActiveCell.FormulaR1C1 = "Rp SS Analysis"
With ActiveCell.Characters(Start:=1, Length:=14).Font
    .Name = "Arial"
    .FontStyle = "Regular"
    .Size = 8
    .Strikethrough = False
    .Superscript = False
    .Subscript = False
    .OutlineFont = False
    .Shadow = False
    .Underline = xlUnderlineStyleNone
    .ColorIndex = xlAutomatic
End With
Range("Q1").Select
ActiveCell.FormulaR1C1 = "Time Start min"
With ActiveCell.Characters(Start:=1, Length:=10).Font
    .Name = "Arial"
    .FontStyle = "Regular"
    .Size = 8
    .Strikethrough = False
    .Superscript = False
    .Subscript = False
    .OutlineFont = False
    .Shadow = False
    .Underline = xlUnderlineStyleNone
    .ColorIndex = xlAutomatic
End With
Range("R1").Select
ActiveCell.FormulaR1C1 = "Deltatime min"
With ActiveCell.Characters(Start:=1, Length:=9).Font
    .Name = "Arial"
    .FontStyle = "Regular"
    .Size = 8
    .Strikethrough = False
    .Superscript = False
    .Subscript = False
    .OutlineFont = False
    .Shadow = False
    .Underline = xlUnderlineStyleNone
    .ColorIndex = xlAutomatic
End With
Range("s1").Select
ActiveCell.FormulaR1C1 = "Endtime min"
With ActiveCell.Characters(Start:=1, Length:=9).Font
    .Name = "Arial"
```

```
        .FontStyle = "Regular"
        .Size = 8
        .Strikethrough = False
        .Superscript = False
        .Subscript = False
        .OutlineFont = False
        .Shadow = False
        .Underline = xlUnderlineStyleNone
        .ColorIndex = xlAutomatic
    End With
    Range("Q3").Select
    End Sub

Sub drkrxnanalyze()
' drkrxnanalyze Macro
' Keyboard Shortcut: Ctrl+e
'    Dim lightofftime As Double
    Dim rplightofftime As Double
    Dim rplightouttime As Double
    Dim convlightofftime As Double
    Dim convlightouttime As Double
    Dim drkrxndeltatime As Double
    Dim a As Double
    Dim b As Double
    Dim c As Double
    Dim i As Double
    Dim heatofreaction As Double
    Dim avgmw As Double
    heatofreaction = Cells(2, 1)
    avgmw = Cells(2, 2)
    lightofftime = Cells(15, 15)
    drkrxndeltatime = Cells(15, 14)
    lightofftime = (lightofftime * 60)
    a = 0
    i = 4
    Do While a < (lightofftime - drkrxndeltatime)
    a = Cells(i, 1)
    rplightofftime = Cells(i, 5)
    convlightofftime = Cells(i, 7)
    i = i + 1
    Loop
    Cells(15, 10) = rplightofftime
    Cells(15, 12) = convlightofftime
    b = 0
    i = 4
    Do While b < (lightofftime)
```

```
    b = Cells(i, 1)
    rplightouttime = Cells(i, 3) * avgmw / heatofreaction
    convlightouttime = Cells(i, 7)
    i = i + 1
    Loop
    Cells(15, 11) = rplightouttime
    Cells(15, 13) = convlightouttime
End Sub

Sub Graph()'
' Graph Macro
Shortcut: Ctrl+g
'    Range("P7").Select
    Charts.Add
    ActiveChart.ChartType = xlXYScatter
    ActiveChart.SetSourceData Source:=Sheets("Sheet1").Range("P7")
    ActiveChart.SeriesCollection.NewSeries
    ActiveChart.SeriesCollection(1).XValues = "=Sheet1!R4C6:R18984C6"
    ActiveChart.SeriesCollection(1).Values = "=Sheet1!R4C4:R18984C4"
    ActiveChart.SeriesCollection(1).Name = "=""Heat Flow"""
    ActiveChart.Location Where:=xlLocationAsNewSheet, Name:="Heat Flow vs Time"
    With ActiveChart
        .HasTitle = True
        .ChartTitle.Characters.Text = "Heat Flow"
        .Axes(xlCategory, xlPrimary).HasTitle = True
        .Axes(xlCategory, xlPrimary).AxisTitle.Characters.Text = "Time (sec)"
        .Axes(xlValue, xlPrimary).HasTitle = True
        .Axes(xlValue, xlPrimary).AxisTitle.Characters.Text = "Heat Flow (W/g)"
    End With
    ActiveChart.PlotArea.Select
    Selection.Interior.ColorIndex = xlNone
    ActiveChart.Axes(xlValue).MajorGridlines.Select
    Selection.Delete
    Sheets("Sheet1").Select
    Charts.Add
    ActiveChart.ChartType = xlXYScatter
    ActiveChart.SetSourceData Source:=Sheets("Sheet1").Range("P7")
    ActiveChart.SeriesCollection.NewSeries
    ActiveChart.SeriesCollection(1).XValues = "=Sheet1!R4C6:R18984C6"
    ActiveChart.SeriesCollection(1).Values = "=Sheet1!R4C5:R18984C5"
    ActiveChart.SeriesCollection(1).Name = "=""Rp"""
    ActiveChart.Location Where:=xlLocationAsNewSheet, Name:="Rp vs Time"
    With ActiveChart
        .HasTitle = True
        .ChartTitle.Characters.Text = "Rp"
        .Axes(xlCategory, xlPrimary).HasTitle = True
```

```
    .Axes(xlCategory, xlPrimary).AxisTitle.Characters.Text = "Time (sec)"
    .Axes(xlValue, xlPrimary).HasTitle = True
    .Axes(xlValue, xlPrimary).AxisTitle.Characters.Text = "Rp (sec -1)"
End With
ActiveChart.PlotArea.Select
Selection.Interior.ColorIndex = xlNone
ActiveChart.Axes(xlValue).MajorGridlines.Select
Selection.Delete
Sheets("Sheet1").Select
Charts.Add
ActiveChart.ChartType = xlXYScatter
ActiveChart.SetSourceData Source:=Sheets("Sheet1").Range("P7")
ActiveChart.SeriesCollection.NewSeries
ActiveChart.SeriesCollection(1).XValues = "=Sheet1!R4C6:R18984C6"
ActiveChart.SeriesCollection(1).Values = "=Sheet1!R4C7:R18984C7"
ActiveChart.SeriesCollection(1).Name = "=""Conversion"""
ActiveChart.Location Where:=xlLocationAsNewSheet, Name:= _
    "Conversion vs Time"
With ActiveChart
    .HasTitle = True
    .ChartTitle.Characters.Text = "Conversion"
    .Axes(xlCategory, xlPrimary).HasTitle = True
    .Axes(xlCategory, xlPrimary).AxisTitle.Characters.Text = "Time"
    .Axes(xlValue, xlPrimary).HasTitle = True
    .Axes(xlValue, xlPrimary).AxisTitle.Characters.Text = _
    "Fractional Double Bond Conversion"
End With
ActiveChart.PlotArea.Select
Selection.Interior.ColorIndex = xlNone
ActiveChart.Axes(xlValue).MajorGridlines.Select
Selection.Delete
ActiveChart.Axes(xlValue).Select
With ActiveChart.Axes(xlValue)
    .MinimumScaleIsAuto = True
    .MaximumScale = 1
    .MinorUnitIsAuto = True
    .MajorUnitIsAuto = True
    .Crosses = xlAutomatic
    .ReversePlotOrder = False
    .ScaleType = xlLinear
    .DisplayUnit = xlNone
End With
Sheets("Sheet1").Select
Charts.Add
ActiveChart.ChartType = xlXYScatter
ActiveChart.SetSourceData Source:=Sheets("Sheet1").Range("P7")
```

```
ActiveChart.SeriesCollection.NewSeries
ActiveChart.SeriesCollection(1).XValues = "=Sheet1!R4C6:R18984C6"
ActiveChart.SeriesCollection(1).Values = "=Sheet1!R4C2:R18984C2"
ActiveChart.SeriesCollection(1).Name = "=""Temperature"""
ActiveChart.Location Where:=xlLocationAsNewSheet, Name:="Temp vs Time"
With ActiveChart
    .HasTitle = True
    .ChartTitle.Characters.Text = "Temperature"
    .Axes(xlCategory, xlPrimary).HasTitle = True
    .Axes(xlCategory, xlPrimary).AxisTitle.Characters.Text = "Time (sec)"
    .Axes(xlValue, xlPrimary).HasTitle = True
    .Axes(xlValue, xlPrimary).AxisTitle.Characters.Text = "Temperature °C"
End With
ActiveChart.PlotArea.Select
Selection.Interior.ColorIndex = xlNone
ActiveChart.Axes(xlValue).MajorGridlines.Select
Selection.Delete
Sheets("Conversion vs Time").Select
ActiveChart.Axes(xlCategory).AxisTitle.Select
Selection.Characters.Text = "Time (sec)"
Selection.AutoScaleFont = False
With Selection.Characters(Start:=1, Length:=10).Font
    .Name = "Arial"
    .FontStyle = "Bold"
    .Size = 10
    .Strikethrough = False
    .Superscript = False
    .Subscript = False
    .OutlineFont = False
    .Shadow = False
    .Underline = xlUnderlineStyleNone
    .ColorIndex = xlAutomatic
End With
Sheets("Sheet1").Select
Charts.Add
ActiveChart.ChartType = xlXYScatter
ActiveChart.SetSourceData Source:=Sheets("Sheet1").Range("P7")
ActiveChart.SeriesCollection.NewSeries
ActiveChart.SeriesCollection(1).XValues = "=Sheet1!R4C7:R18984C7"
ActiveChart.SeriesCollection(1).Values = "=Sheet1!R4C5:R18984C5"
ActiveChart.SeriesCollection(1).Name = "=""Rp"""
ActiveChart.Location Where:=xlLocationAsNewSheet, Name:="Rp vs Conversion"
With ActiveChart
    .HasTitle = True
    .ChartTitle.Characters.Text = "Rp"
    .Axes(xlCategory, xlPrimary).HasTitle = True
```

```
        .Axes(xlCategory, xlPrimary).AxisTitle.Characters.Text = _
        "Fractional Double Bond Conversion"
        .Axes(xlValue, xlPrimary).HasTitle = True
        .Axes(xlValue, xlPrimary).AxisTitle.Characters.Text = "Rp (sec -1)"
    End With
    ActiveChart.PlotArea.Select
    Selection.Left = 33
    Selection.Top = 40
    Selection.Interior.ColorIndex = xlNone
    ActiveChart.Axes(xlValue).MajorGridlines.Select
    Selection.Delete
    ActiveWindow.ScrollWorkbookTabs Sheets:=1
    Sheets("Sheet1").Select
End Sub
```

Appendix C

The kinetic parameters for the recognitive system were analyzed in order to find the termination constant (k_t) and propagation constant (k_p). The program name is "KINO". All kinetic constants were analyzed by this program. The program was developed and designed to collect and analyze the data from the dark reaction analysis presented in Chapter 5. The first step was to take the data from the DPC and analyze the data with the program "SAE" presented in Appendix B. After the data has been analyzed with the program "SAE", the kinetic parameters for the data set can be calculated via the program "KINO".

C.1 Program Setup and Use

The first step is to take each excel file for the dark reaction and rename them as 1, 2, 3, 4, etc. Chonological order is important in the renaming of the Excel files. The second step is to open up a workbook containing the Visual Basic program "KINO". The third step is to open up the program file and edit the location of the data. Default location is found within the code within the subroutine kineticgetdata line 19. Insert the location of the data in the "C:\Documents and Settings\vds0001\My Documents\Vishal's\Research Work\Data\Jan 2010 - Kinetic Analysis" by replacing the file name. Fourth step is to open up a new workbook. Press "CTRL+K" which sets up the Excel spreadsheet. Step five is to insert the values under the labled cells for monomer concentration steady state (Monomer Concentration SS), feed crosslinking, light intensity value in Einstiens (Io), initiator concentration, and the initiator extinction coefficient. Once these values are inputted the operator may press "CTRL+I" this opens up all the workbooks in the data form until done. An error message may pop up at this point. To correct this error the operator must go back to line 18 of the subroutine kineticgetdata and change the value of 14 to the required number of files to be analyzed. Step six is to press "CTRL-N" which analyzes the data

and gives values in the labeled columns for the kinetic constants of propagation and termination. Step seven is to press “CTRL-O” to create the graphs of the data. This completes the analysis program.

C.2 Program Code for “KINO”

```
Sub kineticsetup()
' kineticsetup Macro
' Keyboard Shortcut: Ctrl+k
    Rows("1:1").RowHeight = 51.75
    Rows("1:1").Select
    With Selection
        .HorizontalAlignment = xlGeneral
        .VerticalAlignment = xlBottom
        .WrapText = True
        .Orientation = 0
        .AddIndent = False
        .IndentLevel = 0
        .ShrinkToFit = False
        .ReadingOrder = xlContext
        .MergeCells = False
    End With
    Range("A1").Select
    ActiveCell.FormulaR1C1 = "Rp at Light shut down"
    With ActiveCell.Characters(Start:=1, Length:=21).Font
        .Name = "Arial"
        .FontStyle = "Regular"
        .Size = 10
        .Strikethrough = False
        .Superscript = False
        .Subscript = False
        .OutlineFont = False
        .Shadow = False
        .Underline = xlUnderlineStyleNone
        .ColorIndex = xlAutomatic
    End With
    Range("B1").Select
    ActiveCell.FormulaR1C1 = "Rp at Light out plus deltatime"
    With ActiveCell.Characters(Start:=1, Length:=30).Font
        .Name = "Arial"
        .FontStyle = "Regular"
        .Size = 10
        .Strikethrough = False
        .Superscript = False
```

```
    .Subscript = False
    .OutlineFont = False
    .Shadow = False
    .Underline = xlUnderlineStyleNone
    .ColorIndex = xlAutomatic
End With
Range("C1").Select
ActiveCell.FormulaR1C1 = "Conversion at light shut down"
With ActiveCell.Characters(Start:=1, Length:=29).Font
    .Name = "Arial"
    .FontStyle = "Regular"
    .Size = 10
    .Strikethrough = False
    .Superscript = False
    .Subscript = False
    .OutlineFont = False
    .Shadow = False
    .Underline = xlUnderlineStyleNone
    .ColorIndex = xlAutomatic
End With
Range("D1").Select
ActiveCell.FormulaR1C1 = "Conversion at light out plus deltatime"
With ActiveCell.Characters(Start:=1, Length:=38).Font
    .Name = "Arial"
    .FontStyle = "Regular"
    .Size = 10
    .Strikethrough = False
    .Superscript = False
    .Subscript = False
    .OutlineFont = False
    .Shadow = False
    .Underline = xlUnderlineStyleNone
    .ColorIndex = xlAutomatic
End With
Range("E1").Select
Columns("D:D").ColumnWidth = 10
Columns("C:C").ColumnWidth = 10.57
ActiveCell.FormulaR1C1 = "Delta time"
With ActiveCell.Characters(Start:=1, Length:=10).Font
    .Name = "Arial"
    .FontStyle = "Regular"
    .Size = 10
    .Strikethrough = False
    .Superscript = False
    .Subscript = False
    .OutlineFont = False
```

```
    .Shadow = False
    .Underline = xlUnderlineStyleNone
    .ColorIndex = xlAutomatic
End With
Range("E1").Select
ActiveCell.FormulaR1C1 = "Delta time sec"
With ActiveCell.Characters(Start:=1, Length:=14).Font
    .Name = "Arial"
    .FontStyle = "Regular"
    .Size = 10
    .Strikethrough = False
    .Superscript = False
    .Subscript = False
    .OutlineFont = False
    .Shadow = False
    .Underline = xlUnderlineStyleNone
    .ColorIndex = xlAutomatic
End With
Range("F1").Select
ActiveCell.FormulaR1C1 = "Time light Shut off"
With ActiveCell.Characters(Start:=1, Length:=19).Font
    .Name = "Arial"
    .FontStyle = "Regular"
    .Size = 10
    .Strikethrough = False
    .Superscript = False
    .Subscript = False
    .OutlineFont = False
    .Shadow = False
    .Underline = xlUnderlineStyleNone
    .ColorIndex = xlAutomatic
End With
Range("H1").Select
ActiveCell.FormulaR1C1 = "Monomer Conc SS"
With ActiveCell.Characters(Start:=1, Length:=15).Font
    .Name = "Arial"
    .FontStyle = "Regular"
    .Size = 10
    .Strikethrough = False
    .Superscript = False
    .Subscript = False
    .OutlineFont = False
    .Shadow = False
    .Underline = xlUnderlineStyleNone
    .ColorIndex = xlAutomatic
End With
```

```
Range("J1").Select
ActiveCell.FormulaR1C1 = "Feed Crosslinking"
With ActiveCell.Characters(Start:=1, Length:=16).Font
    .Name = "Arial"
    .FontStyle = "Regular"
    .Size = 10
    .Strikethrough = False
    .Superscript = False
    .Subscript = False
    .OutlineFont = False
    .Shadow = False
    .Underline = xlUnderlineStyleNone
    .ColorIndex = xlAutomatic
End With
Range("K1").Select
ActiveCell.FormulaR1C1 = "kp/kt^.5 ss"
With ActiveCell.Characters(Start:=1, Length:=11).Font
    .Name = "Arial"
    .FontStyle = "Regular"
    .Size = 10
    .Strikethrough = False
    .Superscript = False
    .Subscript = False
    .OutlineFont = False
    .Shadow = False
    .Underline = xlUnderlineStyleNone
    .ColorIndex = xlAutomatic
End With
Range("L1").Select
ActiveCell.FormulaR1C1 = "Io"
With ActiveCell.Characters(Start:=1, Length:=2).Font
    .Name = "Arial"
    .FontStyle = "Regular"
    .Size = 10
    .Strikethrough = False
    .Superscript = False
    .Subscript = False
    .OutlineFont = False
    .Shadow = False
    .Underline = xlUnderlineStyleNone
    .ColorIndex = xlAutomatic
End With
Range("M1").Select
ActiveCell.FormulaR1C1 = "Initiator Concentration"
With ActiveCell.Characters(Start:=1, Length:=23).Font
    .Name = "Arial"
```

```
    .FontStyle = "Regular"
    .Size = 10
    .Strikethrough = False
    .Superscript = False
    .Subscript = False
    .OutlineFont = False
    .Shadow = False
    .Underline = xlUnderlineStyleNone
    .ColorIndex = xlAutomatic
End With
Range("N1").Select
ActiveCell.FormulaR1C1 = "Initiator extinction coefficient"
With ActiveCell.Characters(Start:=1, Length:=32).Font
    .Name = "Arial"
    .FontStyle = "Regular"
    .Size = 10
    .Strikethrough = False
    .Superscript = False
    .Subscript = False
    .OutlineFont = False
    .Shadow = False
    .Underline = xlUnderlineStyleNone
    .ColorIndex = xlAutomatic
End With
Range("H2").Select
Range("O1").Select
ActiveCell.FormulaR1C1 = "Rp SS"
With ActiveCell.Characters(Start:=1, Length:=5).Font
    .Name = "Arial"
    .FontStyle = "Regular"
    .Size = 10
    .Strikethrough = False
    .Superscript = False
    .Subscript = False
    .OutlineFont = False
    .Shadow = False
    .Underline = xlUnderlineStyleNone
    .ColorIndex = xlAutomatic
End With
Range("P1").Select
ActiveCell.FormulaR1C1 = "Conv ss"
With ActiveCell.Characters(Start:=1, Length:=7).Font
    .Name = "Arial"
    .FontStyle = "Regular"
    .Size = 10
    .Strikethrough = False
```

```
        .Superscript = False
        .Subscript = False
        .OutlineFont = False
        .Shadow = False
        .Underline = xlUnderlineStyleNone
        .ColorIndex = xlAutomatic
    End With
    Range("Q1").Select
    ActiveCell.FormulaR1C1 = "Time"
    With ActiveCell.Characters(Start:=1, Length:=4).Font
        .Name = "Arial"
        .FontStyle = "Regular"
        .Size = 10
        .Strikethrough = False
        .Superscript = False
        .Subscript = False
        .OutlineFont = False
        .Shadow = False
        .Underline = xlUnderlineStyleNone
        .ColorIndex = xlAutomatic
    End With
    Range("Q2").Select
    Range("G1").Select
    ActiveCell.FormulaR1C1 = "kt^.5 uss"
    With ActiveCell.Characters(Start:=1, Length:=9).Font
        .Name = "Arial"
        .FontStyle = "Regular"
        .Size = 10
        .Strikethrough = False
        .Superscript = False
        .Subscript = False
        .OutlineFont = False
        .Shadow = False
        .Underline = xlUnderlineStyleNone
        .ColorIndex = xlAutomatic
    End With
    Range("G2").Select
End Sub
Sub kineticgetdata()
'
' kineticgetdata Macro
' Keyboard Shortcut: Ctrl+i
Dim filename As String
Dim filenumber As Double
filenumber = 1
Dim i As Double
```

```
    i = 4
    Dim col As String
    Dim row As String
    Dim numcol As Integer
    Dim numrow As Integer
    Dim where As String
    Do While filenumber <> 14
    filename = " C:\Documents and Settings\vds0001\My Documents\Vishal's\Research
Work\Data\Jan 2010 - Kinetic Analysis " & filenumber & ".xls"
        Workbooks.Open filename:=filename
       Range("J15:O15").Select
       Selection.Copy
       ActiveWindow.Close
       col = Chr(Asc("A"))
       numrow = i
       where = col & numrow
       Range(where).Select
       ActiveSheet.Paste
       With Selection.Font
          .Name = "Arial"
          .Size = 8
          .Strikethrough = False
          .Superscript = False
          .Subscript = False
          .OutlineFont = False
          .Shadow = False
          .Underline = xlUnderlineStyleNone
          .ColorIndex = xlAutomatic
       End With
       Range("A3").Select
       i = i + 1
       filenumber = filenumber + 1
       Loop
       End Sub
    Sub ssandussanalysis()
    '
    ' ssandussanalysis Macro
    ' Keyboard Shortcut: Ctrl+n
    Dim rpss As Double
    Dim convss As Double
    Dim monconc As Double
    Dim iniconc As Double
    Dim iniext As Double
    Dim io As Double
    Dim kpktss As Double
    Dim i As Double
```

```
Dim j As Double
Dim k As Double
Dim timeuss As Double
Dim prob As Double
prob = 1 / (Cells(2, 8) + 1)
iniext = Cells(2, 14)
iniconc = Cells(2, 13)
monconc = Cells(2, 8)
io = Cells(2, 12)
i = 4
j = 0
timeussa = 1
timeuss = 1
Do While timeuss > 0
    rpss = Cells(i, 1)
    convss = Cells(i, 3)
    monconc = monconc * (1 - (prob * convss))
    iniconc = iniconc * (1 - (prob * convss))
    kpktss = rpss / (monconc * Abs((io * iniext * iniconc) ^ 0.5))
    Cells(i, 11) = kpktss
    timeuss = Cells(i, 6)
    i = i + 1
    Loop
Dim rpto As Double
Dim rpti As Double
Dim mto As Double
Dim mti As Double
Dim convo As Double
Dim convi As Double
Dim kpktsss As Double
Dim deltat As Double
Dim a As Double
Dim b As Double
Dim c As Double
Dim ktuss As Double
Dim kp As Double
a = 4
b = 0
timeuss = 1
Cells(3, 7) = "kt^.5)"
Cells(3, 8) = "kp"
Cells(3, 12) = "kt/kp"
Cells(3, 13) = "kt"
Do While timeuss > 0
   rpto = Cells(a, 1)
   rpti = Cells(a, 2)
```

```
    convo = Cells(a, 3)
    convi = Cells(a, 4)
    mto = monconc * (1 - (prob * convo))
    mti = monconc * (1 - (prob * convi))
    kpktsss = Cells(a, 11)
    deltat = Cells(a, 5)
    If rpto = 0 Then ktuss = 0
    If rpto > 0 Then ktuss = (kpktsss / (2 * deltat)) * ((mti / rpti) - (mto / rpto))
    Cells(a, 7) = ktuss
    kp = ktuss * kpktsss
    Cells(a, 8) = kp
    If kp = 0 Then kp = 1
   Cells(a, 12) = (ktuss * ktuss) / kp
   Cells(a, 13) = (ktuss * ktuss)
   timeuss = Cells(a, 6)
   a = a + 1
Loop
End Sub
Sub Macro3()
'
' Macro3 Macro
' Keyboard Shortcut: Ctrl+o
    Charts.Add
    ActiveChart.ChartType = xlXYScatter
    ActiveChart.SetSourceData Source:=Sheets("Sheet1").Range("A1:Q16"), PlotBy _
        :=xlRows
    ActiveChart.SeriesCollection(1).Delete
    ActiveChart.SeriesCollection(1).Delete
    ActiveChart.SeriesCollection(1).Delete
    ActiveChart.SeriesCollection(1).Delete
    ActiveChart.SeriesCollection(1).Delete
    ActiveChart.SeriesCollection(1).Delete
    ActiveChart.SeriesCollection(1).Delete
    ActiveChart.SeriesCollection(1).Delete
    ActiveChart.SeriesCollection(1).Delete
    ActiveChart.SeriesCollection(1).Delete
    ActiveChart.SeriesCollection(1).Delete
    ActiveChart.SeriesCollection(1).Delete
    ActiveChart.SeriesCollection(1).Delete
    ActiveChart.SeriesCollection(1).Delete
    ActiveChart.SeriesCollection(1).Delete
    ActiveChart.SeriesCollection.NewSeries
    ActiveChart.SeriesCollection(1).XValues = "=Sheet1!R4C3:R16C3"
    ActiveChart.SeriesCollection(1).Values = "=Sheet1!R4C13:R16C13"
    ActiveChart.SeriesCollection(1).Name = "=""kt vs conversion"""
    ActiveChart.Location where:=xlLocationAsObject, Name:="Sheet1"
```

```
With ActiveChart
    .HasTitle = True
    .ChartTitle.Characters.Text = "kt vs conversion"
    .Axes(xlCategory, xlPrimary).HasTitle = True
    .Axes(xlCategory, xlPrimary).AxisTitle.Characters.Text = _
    "Fractional Conversion"
    .Axes(xlValue, xlPrimary).HasTitle = True
    .Axes(xlValue, xlPrimary).AxisTitle.Characters.Text = "kt (L/(mole-sec))"
End With
ActiveChart.PlotArea.Select
Selection.Interior.ColorIndex = xlNone
ActiveChart.Axes(xlValue).MajorGridlines.Select
Selection.Delete
ActiveWindow.Visible = False
Range("J18").Select
Charts.Add
ActiveChart.ChartType = xlXYScatter
ActiveChart.SetSourceData Source:=Sheets("Sheet1").Range("J18")
ActiveChart.SeriesCollection.NewSeries
ActiveChart.SeriesCollection(1).XValues = "=Sheet1!R4C3:R16C3"
ActiveChart.SeriesCollection(1).Values = "=Sheet1!R4C8:R16C8"
ActiveChart.SeriesCollection(1).Name = "=""kp vs conversion"""
ActiveChart.Location where:=xlLocationAsObject, Name:="Sheet1"
With ActiveChart
    .HasTitle = True
    .ChartTitle.Characters.Text = "kp vs conversion"
    .Axes(xlCategory, xlPrimary).HasTitle = True
    .Axes(xlCategory, xlPrimary).AxisTitle.Characters.Text = _
    "Fractional Conversion"
    .Axes(xlValue, xlPrimary).HasTitle = True
    .Axes(xlValue, xlPrimary).AxisTitle.Characters.Text = "kp (L/(mole-sec))"
End With
ActiveChart.PlotArea.Select
Selection.Interior.ColorIndex = xlNone
ActiveChart.Axes(xlValue).MajorGridlines.Select
Selection.Delete
ActiveWindow.Visible = False
Range("M20").Select
Charts.Add
ActiveChart.ChartType = xlXYScatter
ActiveChart.SetSourceData Source:=Sheets("Sheet1").Range("M20"), PlotBy:= _
    xlColumns
ActiveChart.SeriesCollection.NewSeries
ActiveChart.SeriesCollection(1).XValues = "=Sheet1!R4C3:R16C3"
ActiveChart.SeriesCollection(1).Values = "=Sheet1!R4C12:R16C12"
ActiveChart.SeriesCollection(1).Name = "=""ktkp vs conversion"""
```

```
    ActiveChart.Location where:=xlLocationAsObject, Name:="Sheet1"
    With ActiveChart
        .HasTitle = True
        .ChartTitle.Characters.Text = "kt to kp vs conversion"
        .Axes(xlCategory, xlPrimary).HasTitle = True
        .Axes(xlCategory, xlPrimary).AxisTitle.Characters.Text = _
        "Fractional Conversion"
        .Axes(xlValue, xlPrimary).HasTitle = True
        .Axes(xlValue, xlPrimary).AxisTitle.Characters.Text = "kt over kp"
    End With
    ActiveChart.PlotArea.Select
    Selection.Interior.ColorIndex = xlNone
    ActiveChart.Axes(xlValue).MajorGridlines.Select
    Selection.Delete
    ActiveChart.ChartTitle.Select
    Selection.Characters.Text = "kt to kp vs conversion"
    Selection.AutoScaleFont = False
    With Selection.Characters(Start:=1, Length:=22).Font
        .Name = "Arial"
        .FontStyle = "Regular"
        .Size = 12
        .Strikethrough = False
        .Superscript = False
        .Subscript = False
        .OutlineFont = False
        .Shadow = False
        .Underline = xlUnderlineStyleNone
        .ColorIndex = xlAutomatic
    End With
    ActiveChart.ChartArea.Select
End Sub
```